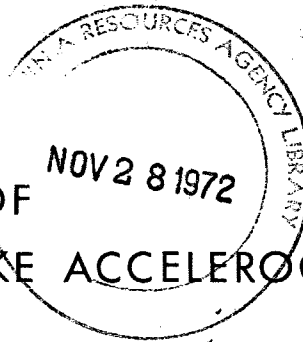


CALIFORNIA INSTITUTE OF TECHNOLOGY

2
EARTHQUAKE ENGINEERING RESEARCH LABORATORY

ANALYSES OF STRONG MOTION EARTHQUAKE ACCELEROGRAMS



VOLUME IV - FOURIER AMPLITUDE SPECTRA
PART A - ACCELEROGRAMS IIA001 THROUGH IIA020

Reports EERL 72-100

A REPORT ON RESEARCH CONDUCTED UNDER A
GRANT FROM THE NATIONAL SCIENCE FOUNDATION

PASADENA, CALIFORNIA

AUGUST 1972

CALIFORNIA INSTITUTE OF TECHNOLOGY
EARTHQUAKE ENGINEERING RESEARCH LABORATORY

ANALYSES
OF
STRONG MOTION EARTHQUAKE ACCELEROGRAMS

Volume IV - Fourier Amplitude Spectra
Part A - Accelerograms IIA001 through IIA020

EERL 72-100

A Report on Research Conducted Under a Grant
from the National Science Foundation

Pasadena, California
August 1972

Abstract

This is the first volume of a series presenting Fourier amplitude spectra for earthquake ground motions and for structural response accelerations. An introduction summarizes Fourier spectrum techniques in earthquake engineering as a background to the use of the data. For each earthquake accelerogram, two spectrum plots are given - a Fourier amplitude spectrum versus frequency on a linear scale, and a log-spectrum, log-frequency plot. In the series, Fourier amplitude spectra will be given for all corrected accelerograms, including building response measurements. For buildings for which simultaneous basement and upper floor accelerograms are available, building transfer functions are also plotted. The earthquakes in Volume IV, Part A, match the uncorrected accelerogram data of Volume I, the corrected accelerogram data of Volume II, and the response spectrum plots of Volume III.

TABLE OF CONTENTS

	<u>Page</u>
Preface	1
Fourier Spectra	3
Introduction to Plots of Fourier Amplitude Spectra	39
Earthquake Data	41
Plots of Fourier Amplitude Spectra	43
List of EERL Reports Available from NTIS	164

PREFACE

The present report is the first part of the fourth volume of data on strong-motion earthquake accelerograms which was initiated in 1969 with the first volume of digitized and plotted records. Since that time, several additional parts of Volume I "Uncorrected Digitized and Plotted Data" have been issued, and the first parts of Volume II "Corrected Accelerograms and Integrated Ground Velocities and Displacements" and Volume III "Response Spectrum Curves" have appeared.

This volume presents calculated Fourier spectrum curves for all significant strong-motion accelerograms including measurements in structures as well as at ground sites. To establish the nomenclature and methods used and to offer examples of applications to various problems of earthquake engineering and strong-motion seismology, an extensive introduction has been prepared. This elementary introduction should also serve as a basic summary of background information for users of the data.

As the conclusion of this extended program of data processing draws near, I should like to pay a special tribute to the excellent backup that the project received at every stage from the Willis H. Booth Computing Center at the California Institute of Technology. Without the unusually fine facilities provided by the center, and the very extensive assistance of the staff, in particular the generous time and effort spent by Mrs. Edith P. Huang, a project of this scope would have been impossible to carry out.

It is also a pleasure to acknowledge again the very important contributions of Dr. Mihailo D. Trifunac. Without his devoted attention to every detail of the project the results would have been much longer in appearing and much less complete in form.

D. E. Hudson

Earthquake Engineering Research Laboratory
California Institute of Technology

FOURIER SPECTRA

Introduction

Fourier series and Fourier transforms arise in problems dealing with time series analysis and vibration analysis. Apart from simplifying theoretical analysis, Fourier transforms can be used to answer many questions related to the nature of data and are useful in exhibiting the frequency content of the function analyzed.

In Earthquake Engineering and in Strong Motion Seismology, Fourier techniques present one of the most important tools in data processing and analysis. Forced vibration tests (Hudson, 1970) and ambient vibration tests (Trifunac, 1970 a, b) of full scale structures, transfer function properties of structures and soil during strong earthquake ground motion, soil structure interaction (Luco, 1969; Bielak, 1971; Trifunac, 1972), source mechanism studies in Strong Motion Seismology (Trifunac, 1972), response spectrum analysis of the recorded strong ground motion (Hudson, 1962; Hudson et al, 1971) are all directly based on the Fourier transform representation of the recorded or theoretically derived time history of the problem.

In recent years the number of recorded strong-motion accelerograms has significantly increased and more than 500 excellent records are presently available. In order to develop the information on the most important of these records and thus collect and present the basic data for Earthquake Engineering and Strong Motion Seismology, an extensive program of standard data processing has been undertaken by the Earthquake Engineering Research Laboratory of the California Institute of Technology.

The present report, which is the first part (Part A) of the Volume IV series presents the Fourier amplitude spectra of the accelerograms corrected for instrument response and zero baseline in the frequency band from 0.07 to 25 cps (Trifunac, 1970 c; Trifunac et al, 1971). This volume is a logical part of the extensive program designed to present the digitized standard version of the recorded strong-motion accelerograms in the original uncorrected form (Volume I, Hudson et al, 1969), corrected accelerograms (Volume II, Hudson et al, 1971 a) and response spectra of corrected accelerograms (Hudson et al, 1971 b) which constitute Volume III.

Unlike Volume III which presents only the response spectra for accelerograms recorded at the ground level of instrumented buildings or free field stations, Volume IV contains the Fourier amplitude spectra for all corrected accelerograms including building installations. Furthermore, for the building sites for which additional accelerograms are available at intermediate and top floors, Volume IV presents the building transfer function properties based on these records. It may be noted that this latter information is of fundamental value for both experimental and theoretical analysis of the dynamic properties of these and similar structures.

Fourier Transform

Given a signal $x(t)$, real or complex, we can form the integral

$$X(f) = \int_{-\infty}^{\infty} x(t) e^{-2\pi i f t} dt \quad (1)$$

where the upper case $X(f)$ represents the frequency domain function, the lower case $x(t)$ is the time domain function, f is frequency and $i = \sqrt{-1}$.

If the integral represented by (1) exists for every real value of f , it defines the Fourier transform $X(f)$ of the signal $x(t)$. A sufficient, although not necessary, condition for the existence of $X(f)$ is the square integrability of $x(t)$ in the Lebesgue sense. This restriction is in general much broader than it need be for most practical applications. For example, the sine and cosine functions, although not absolutely square integrable, possess well defined Fourier transforms.

If $x(t)$ is a function composed of sinusoids of varying amplitude and phase, it can be expressed as

$$x(t) = \sum_{n=1}^m A_n \cos(2\pi f_n t + \varphi_n),$$

and its transform is

$$X(f) = \sum_{n=1}^m \frac{A_n}{2} \left[\delta(f-f_n) e^{i\varphi_n} + \delta(f+f_n) e^{i\varphi_n} \right] \quad (2)$$

where $\delta(f)$ denotes the Dirac delta function. The delta function of Equation (2) cannot be physically measured because of the limited record time lengths involved. This will be discussed in more detail in the section on "leakage".

The function $x(t)$ can be recovered from $X(f)$ by the inverse formula

$$x(t) = \int_{-\infty}^{\infty} X(f) e^{2\pi i f t} df \quad (3)$$

Equation (3) gives $x(t)$ for every point at which it is continuous. If $x(t)$ is discontinuous at $t=t_0$ then the integral in (3) equals the average of $x(t_0^+)$ and $x(t_0^-)$. If therefore we assume that

$$x(t) = (x(t^+) + x(t^-))/2,$$

then (3) will be true for all t . Since the signals encountered in the field of Earthquake Engineering are real functions of time, the real part of $X(f)$ is an even function and the imaginary part of $X(f)$ is an odd function. The even part of $x(t)$ and the even (real) part of $X(f)$ are cosine transforms of each other; while the odd part of $x(t)$ and the imaginary (odd) part of $X(f)$ are negative sine transforms of each other. Further, if $x(t)$ and $X(f)$ constitute a transform pair, then $x(-t)$ and $X(-f)$ also constitute a transform pair, $X(-f)$ being equal to $X^*(f)$, the complex conjugate of $X(f)$.

The transform $X(f)$ is used in characterizing linear systems and in identifying the frequency content of the continuous time function $x(t)$.

1. Discrete Time Series and Sampling Theorem. Digital data collected during an earthquake can be thought of as related to a hypothetical continuous function $x(t)$ defined for all t by the equation

$$x(i) = \int_{-\infty}^{\infty} \delta(t-i\Delta t)x(t) dt, \quad i=0, \dots, N-1, N \quad (4)$$

In order to study how well the sequence $\{x(i)\}$ represents the function $x(t)$, we invoke the sampling theorem. The theorem states that if Δt is the sampling interval and if the function is band limited to frequencies less than $\frac{1}{2\Delta t}$ cycles/sec, then $x(t)$ can be reconstructed uniquely. The theorem gives an approximate answer to a real life problem since the assumptions involved are not generally true.

Stated more generally, the sampling theorem (Papoulis, 1968) says that if $x(t)$ is a band limited signal with transform $X(f)$ such that $X(f)=0$ for $|f| \geq f_1$ and

$$x(t) = \int_{-f_1}^{f_1} X(f) e^{2\pi i f t} df,$$

then $x(t)$ can be uniquely determined from its values, $x(n\Delta t)$, at a sequence of equidistant points $t=n\Delta t$ (where $n=-\infty, \dots, -1, 0, 1, \dots, \infty$) provided $\Delta t \leq \frac{1}{2f_1}$. In fact if $f_2 = \frac{1}{2\Delta t}$ and f_0 is any number between f_1 and $2f_2 - f_1$, that is $f_1 \leq f_0 \leq 2f_2 - f_1$, then $x(t)$ can be expressed as

$$x(t) = \sum_{n=-\infty}^{\infty} x(n\Delta t) \frac{\sin 2\pi f_0 (t-n\Delta t)}{2\pi f_2 (t-n\Delta t)} \quad (5)$$

It may be noted that the theorem is valid for an infinite sequence $\{x(n)\}$. In particular if $f_0 = f_2 = B$ where B is the band width

$$x(t) = \sum_{n=-\infty}^{\infty} x(n\Delta t) \left\{ \frac{\sin 2\pi B (t-n\Delta t)}{2\pi B (t-n\Delta t)} \right\} \quad (6)$$

The theorem breaks down at the frequency $B = \frac{1}{2\Delta t}$ when applied there. Consider the sinusoid

$$x(t) = \sin (2\pi f t + \psi)$$

Assuming $f = B = \frac{1}{2\Delta t}$

$$x(t) = \sin \left(\frac{\pi t}{\Delta t} + \psi \right) \quad (7)$$

If the function represented by (7) is sampled at equidistant points $t=n\Delta t$, we shall have

$$x(n) = \sin (n\pi + \psi) = (-1)^n \sin \psi$$

Hence given only the sequence $\{x(n)\}$ it would be impossible to get back to $x(t)$. Further if $\psi=0$, $x(n)\equiv 0$ for all n and the information would be totally lost.

2. Frequency Resolution. Since the Fourier transform is a tool to study the frequency content of a time signal, one of the problems that arises as a consequence is the possibility of distinguishing two frequencies close to each other in a given continuous time limited signal.

Hence, if for example

$$x(t) = A[\cos 2\pi f_1 t + \cos 2\pi f_2 t], \quad -\infty < t < \infty \quad (8)$$

and

$$d(t) = \begin{cases} 1 & |x| < \frac{T}{2} \\ \text{otherwise} \end{cases}$$

taking

$$y(t) = x(t) \cdot d(t),$$

$$Y(f) = X(f) * D(f)$$

$$Y(f) = \frac{A}{2} \left[\sin \frac{\pi T(f-f_1)}{(f-f_1)} + \sin \frac{\pi T(f-f_2)}{(f-f_2)} \right] + \frac{A}{2} \left[\frac{\sin \pi T(f+f_1)}{f+f_1} + \frac{\sin \pi T(f+f_2)}{f+f_2} \right] \quad (9)$$

Thus the transform consists of two terms like $\left(\frac{\sin x}{x}\right)$ centered at frequencies f_1 and f_2 . The problem of resolving them is then similar to the Rayleigh problem in optics. Using Rayleigh criteria, if $\Delta f = (f_1 - f_2)$ and $\Delta f = \frac{1}{2T}$ the two sinusoids are just resolved; if $\Delta f = \frac{1}{T}$ the two sinusoids are well resolved. Thus, if f_1 and f_2 are separated by $\frac{1}{T}$ cycles/sec or more then they can be easily resolved.

3. Discrete Fourier Transform. Using (1) we have for a signal $x(t)$

such that

$$\begin{aligned} x(t) &= x(t), \quad 0 \leq t \leq T \\ &= 0 \quad \text{otherwise} \end{aligned}$$

$$X(f) = \int_0^T x(t) e^{2\pi i f t} dt \quad -\infty < f < \infty.$$

From the theory of Reimann integration,

$$\int_0^T g(t) dt = \lim_{r \rightarrow \infty} \frac{T}{r} \sum_{j=0}^{r-1} g\left(\frac{T}{r} j\right)$$

Approximating Equation (1) so as to be used for the problem when the sampling rate is finite we have

$$X(j) = \frac{T}{N} \sum_{k=0}^{N-1} x(k\Delta t) \exp\left(-2\pi i \frac{jk}{N}\right) \quad (10)$$

$$= \Delta t \sum_{k=0}^{N-1} x(k\Delta t) \exp\left(-2\pi i \frac{jk}{N}\right) \quad (11)$$

Equation (11) could also have been directly obtained had we taken the transform of the function

$$x_{\text{sampled}}(t) = \sum_{k=0}^{N-1} x(t) \delta(t - k\Delta t) \quad (12)$$

The discrete Fourier transform pair (for $T=1$) is then defined as follows

$$X(j) = \frac{1}{N} \sum_{k=0}^{N-1} x(k) e^{-2\pi i \frac{jk}{N}} \quad (13a)$$

$$x(k) = \sum_{j=0}^{N-1} X(j) e^{2\pi i \frac{jk}{N}} \quad (13b)$$

In (13a) and (13b) $x(k)$ and $X(j)$ stand for $x(k\Delta t)$ and $X(jf_0)$ respectively. That is, the true frequency is the product of j and f_0 and true time is the product of k and Δt . For the time-domain $0 \leq t \leq T$, the sample period is given by

$$\Delta t = \frac{T}{N}$$

and the fundamental frequency by

$$f_0 = \frac{1}{T}.$$

The importance of the Discrete Fourier Transform (D. F. T.) of a sequence of Nyquist samples lies in the relationship between the D. F. T. and the Fourier transform of a continuous waveform which is represented by the Nyquist samples.

Let $g(t)$ be a continuous band limited waveform whose Nyquist samples $x(k)$ vanish outside $0 \leq t \leq N\Delta t$. Then by the sampling theorem

$$g(t) = \sum_{k=0}^{N-1} x(k) \frac{\sin(\pi(t-k\Delta t)/\Delta t)}{(\pi(t-k\Delta t)/\Delta t)} \quad (14)$$

where Δt is the time spacing between the samples.

A periodic repetition of $g(t)$ can be constructed such that it has identically the same Nyquist samples in the interval $0 \leq t \leq N\Delta t$

$$g_p(t) = \sum_{\ell} \sum_{k=0}^{N-1} x(k) \frac{\sin(\pi(t-k\Delta t-\ell N\Delta t)/\Delta t)}{(\pi(t-k\Delta t-\ell N\Delta t)/\Delta t)} \quad (15)$$

If $G(f)$ is the transform of $g(t)$, then $G(f)$ is exactly specified at discrete

frequencies by the complex Fourier series of $g_p(t)$ (Papaulis, 1968). It is this relationship that makes the D. F. T. so useful in the analysis of discrete time series.

4. Fast Fourier Transform Computations. Algorithms that significantly reduce the time involved in computation of Fourier transforms have been recently used on a broad scale (Cooley and Tukey, 1965). Significant time saving algorithms may be developed when the number of data points N is a nonprime integer. In practice, programing the algorithm for N as a power of two offers special advantages.

To illustrate the derivation of the Fast Fourier Transform algorithm for Equation (13b) (Cooley and Tukey, 1965) a case for $N=2^3$ is considered following the presentation given by Bergland (1969). Replacing $e^{2\pi i/N}$ by W in (13a) and (13b) we get

$$X(j) = \frac{1}{N} \sum_{k=0}^{N-1} x(k) W^{-jk} \quad (16a)$$

and

$$x(k) = \sum_{j=0}^{N-1} X(j) W^{jk} \quad (16b)$$

Since (16a) can be written also in the form

$$X(j) = \frac{1}{N} \sum_{k=0}^{N-1} x(k)^* W^{jk} \quad (16a')$$

where the asterisk indicates the complex conjugate operation. Derivation for the transform (13b) also applies to (16a') and therefore also to (13a) and (16a). That is, by evaluating the expression

$$\hat{X}(j) = \sum_{k=0}^{N-1} A(k)W^{jk} \quad (17)$$

and noting that \hat{X} and A may be interpreted as X^* and x^*/N for the forward transform, and by x and X for the inverse transform, the results can be used to calculate both (16a) and (16b).

For $N=2^3$, i. e., $j=0,1,2,\dots,7$ and $k=0,1,2,\dots,7$ one can represent j and k as binary numbers as follows

$$j = j_2 \cdot 2^2 + j_1 \cdot 2^1 + j_0 \cdot 2^0 \quad (18)$$

and

$$k = k_2 \cdot 2^2 + k_1 \cdot 2^1 + k_0 \cdot 2^0 \quad (19)$$

In (18) and (19) j_2, j_1, j_0, k_2, k_1 , and k_0 can be either 0 or 1. Using Equations (18) and (19) in Equation (17), the latter can be rewritten as follows

$$X(j_2, j_1, j_0) = \sum_{k_0=0}^1 \sum_{k_1=0}^1 \sum_{k_2=0}^1 A(k_2, k_1, k_0) W^{(4j_2+2j_1+j_0)(4k_2+2k_1+k_0)} \quad (20)$$

It may be noted that

$$\begin{aligned} & W^{(4j_2+2j_1+j_0)(4k_2+2k_1+k_0)} \\ &= W^{(4j_2+2j_1+j_0) \cdot 4k_2} \cdot W^{(4j_2+2j_1+j_0) \cdot 2k_1} \cdot W^{(4j_2+2j_1+j_0) \cdot k_0} \end{aligned}$$

Looking individually at these terms on the right-hand side of the above equation it is clear that they can be rewritten in the following form

$$\begin{aligned} W^{(4j_2+2j_1+j_0) \cdot 4k_2} &= \left[W^{8(2j_2+j_1) \cdot k_2} \right] \cdot W^{4j_0 k_2} \\ W^{(4j_2+2j_1+j_0) \cdot 2k_1} &= \left[W^{8j_2 k_1} \right] \cdot W^{(2j_1+j_0) \cdot 2k_1} \end{aligned}$$

$$W^{(4j_2+2j_1+j_0) \cdot k_0} = W^{(4j_2+2j_1+j_0) \cdot k_0}$$

However, since

$$W^8 = [e^{2\pi i/8}]^8 = 1$$

further simplifications are possible

$$W^{(4j_2+2j_1+j_0) \cdot 4k_2} = W^{4j_0 k_2}$$

$$W^{(4j_2+2j_1+j_0) \cdot 2k_2} = W^{(2j_1+j_0) \cdot 2k_1}$$

By using these results in Equation (20) we get

$$\begin{aligned} X(j_2, j_1, j_0) &= \sum_{k_0=0}^1 \sum_{k_1=0}^1 \sum_{k_2=0}^1 A(k_2, k_1, k_0) W^{4j_0 k_2} \cdot W^{(2j_1+j_0) \cdot 2k_1} \cdot W^{(4j_2+2j_1+j_0) \cdot k_0} \end{aligned} \quad (21)$$

If $A_1(j_0, k_1, k_2)$, $A_2(j_0, j_1, k_0)$ and $A_3(j_0, j_1, j_2)$ are next defined as

$$A_1(j_0, k_1, k_0) = \sum_{k_2=0}^1 A(k_2, k_1, k_0) W^{4j_0 k_2} \quad (22)$$

$$A_2(j_0, j_1, k_0) = \sum_{k_1=0}^1 A_1(j_0, k_1, k_0) W^{(2j_1+j_0) \cdot 2k_1} \quad (23)$$

$$A_3(j_0, j_1, j_2) = \sum_{k_0=0}^1 A_2(j_0, j_1, k_0) W^{(4j_2+2j_1+j_0) \cdot k_0} \quad (24)$$

Equation (21) becomes

$$\hat{X}(j_2, j_1, j_0) = A_3(j_0, j_1, j_2) \quad (21')$$

Direct evaluation of Eq. (17) for $N=8$ would require 64 complex multiply-and-add operations. Each of Eqs. (22), (23) and (24) requires $2 \times 8 = 16$ multiply-and-add operations. To calculate (21') by the Fast Fourier Transform algorithm with $N=8$ therefore requires 48 such operations. However the first multiplication in each summation is actually a multiplication by +1 so that the number of operations becomes only 24. Also noting that $W^0 = -W$, $W^1 = W^5$, etc., the number of operations is further reduced to 12. Similar reductions hold for $N=2^m$ and it can be shown that the N^2 operations required for the classical evaluation of the Fourier transform from (16b) by using the Fast Fourier Transform algorithm become proportional to $N \log_2 N$. For example when $N=1024$ this represents a 200 fold reduction of computer operations, resulting in not only a more economical determination of the transform but also a more accurate one.

Sums (22), (23) and (24) are illustrated in Figure 1. The first line corresponds to the sum (22), the second line to (23) and the third line to (24). The fourth line shown in Figure 1 performs the operation of reordering due to the fact that the bits are reversed in Eq. (21'). The numbers at the end of each line indicate the power of W .

5. Accuracy of the Discrete Fourier Transform Computations. Several problems may be encountered when discrete Fourier transforms are calculated. Some of these are briefly discussed in this section.

5.1 Aliasing. It is clear that when sampled data is obtained at intervals of $j\Delta t$, $j=1,2,\dots,N$ a certain loss of information occurs. In fact all direct information is lost for frequencies above what is called the Nyquist frequency $f_N = 1/2\Delta t$. The problem of aliasing thus occurs as a result of

FLOW DIAGRAM OF THE COOLEY-TUKEY FAST FOURIER TRANSFORM
ALGORITHM FOR AN EIGHT-POINT TRANSFORM (AFTER BERGLAND, 1969)

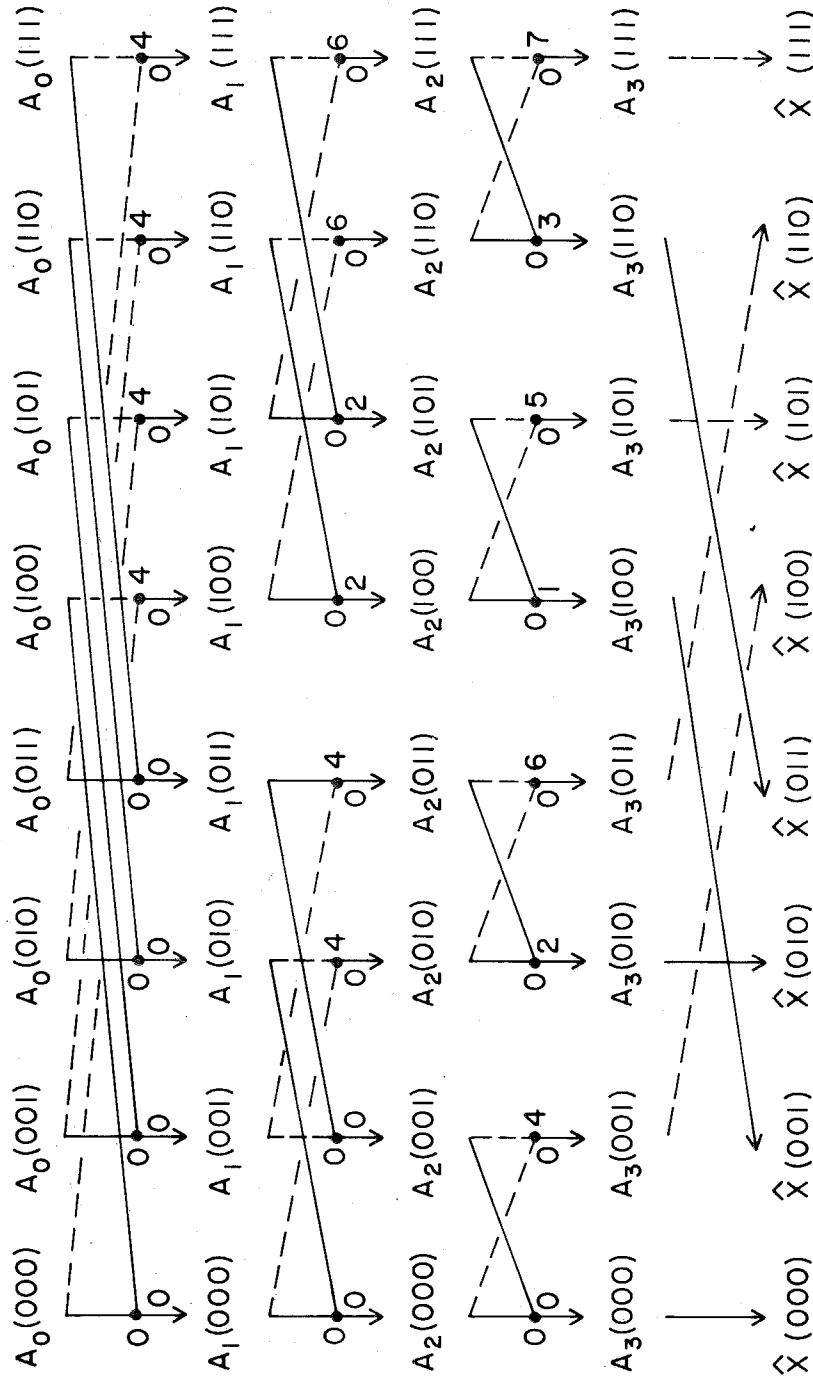


Figure 1

sampling $x(t)$ at equally spaced time intervals Δt and confusing the high frequency content of the original data with lower frequencies (Figure 2a). This can happen when the original data contain frequencies higher than the folding frequency

$$f_f = \frac{1}{2\Delta t} \quad (25)$$

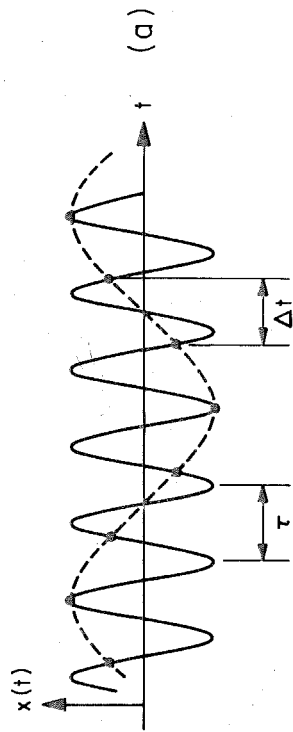
because a wave with a frequency $f = \frac{1}{\tau} > f_f$ appears in the data as a long period wave shown by a dashed line in Figure 2a.

To avoid errors resulting from aliasing one chooses f_f so that it exceeds the maximum frequency present in the data. If f_{\max} is this maximum frequency then the sampling interval should be

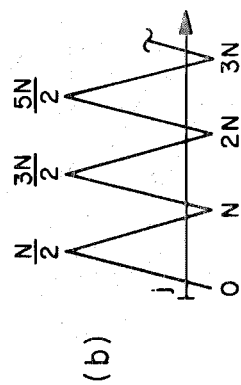
$$\Delta t < \frac{1}{2f_{\max}} \quad (26)$$

The sampling interval for the corrected accelerograms (Hudson et al, 1971 a), which are used to calculate the Fourier amplitude spectra in this report, is $\Delta t = 0.02$ sec and the corresponding folding frequency is $f_f = 25$ cps. Although in some exceptional cases original analog accelerograms may contain frequencies higher than f_f the low-pass filtering effect of the optical digitization process (Trifunac et al, 1971) practically eliminates any possibility for aliasing in the corrected accelerograms. For the accelerograms digitized by an electronic analog-to-digital device, or by some other equivalent procedure, much smaller digitization intervals are required to ensure that the folding frequency is higher than the highest frequency present in the data.

SLOW SAMPLING OF FAST SINE WAVE



FOLDED FREQUENCY AXIS



ALIASES OF THE FREQUENCY $j \frac{2\pi}{T}$

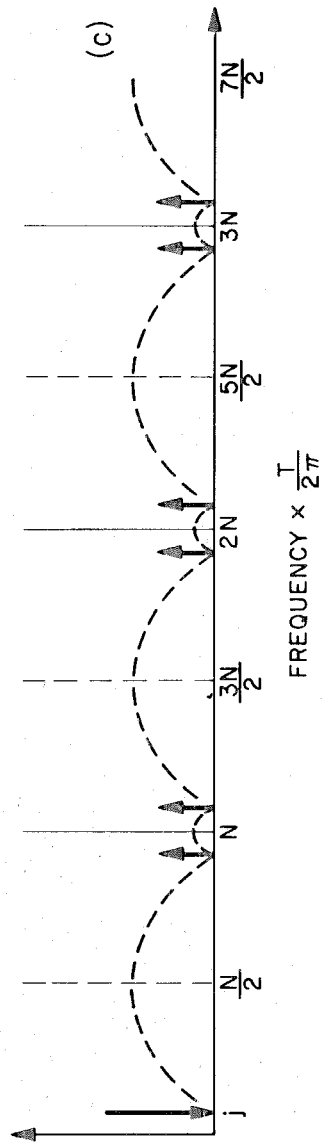


Figure 2

To illustrate the term "folding frequency" a cosine transform

$$X^c(j) = \frac{1}{N} \sum_{k=0}^{N-1} x(k) \cos \frac{2\pi jk}{N} \quad (27)$$

may be considered. We notice that an infinite set of numbers $\{X^c(j), j=0,1,\dots\}$ actually consists of at most $N/2$ different integers. Indeed if j is an integer from 1 to $N/2$, then for any integer ℓ , the following holds for any t in $\{t_0, t_1, \dots, t_N\}$:

$$\left. \begin{aligned} \cos(\ell N + j) \frac{2\pi}{T} t_k &= \cos j \frac{2\pi}{T} t_k \\ \text{and} \\ \cos(\ell N - j) \frac{2\pi}{T} t_k &= \cos j \frac{2\pi}{T} t_k \end{aligned} \right\} \quad (28)$$

In other words given values only at the points t_0, t_1, \dots, t_N a harmonic $\cos m \frac{2\pi t}{T}$, with frequency $m \frac{2\pi}{T}$ cannot be distinguished from a harmonic $\cos j \frac{2\pi t}{T}$ where m and j are related by

$$\left. \begin{aligned} m &= \ell N + j \\ m &= \ell N - j \end{aligned} \right\} \quad (29)$$

To describe the situation we introduce the following terminology; we call the frequency $m \frac{2\pi}{T}$ an alias of the frequency $j \frac{2\pi}{T}$ over the points $t_k = k \frac{T}{N}$ if m and j are related as in (29).

A pictorial representation of aliasing is given in Figures 2b and 2c. The frequencies $j \frac{2\pi}{T}$ are represented on a line running from zero to infinity by the integer j . The aliases for any particular j , shown in Figure 2c by the large downward pointing arrow, are according to (28) all the frequencies $(\ell N \pm j) \frac{2\pi}{T}$ for $\ell=1,2,\dots$ and are shown in Figure 2c

by small arrows pointing upwards. The determination of these aliases can be pictured in the following way. The frequency axis is folded about the multiples of $N/2$ as shown in Figure 2b. The frequency j is then plotted on the folded surface. A horizontal line passing through point j is then pierced through the folded axis. The aliases of j are located at the intersections of this line and the folded frequency axis (Figure 2b). The Figure 2c shows the stretched frequency axis with the above intersections shown with small arrows.

5.2 Uncertainty Principle. If $x(t)$ describes the time behavior of some phenomenon and $X(f)$ is its Fourier transform, it appears that it is impossible to determine $X(f)$ in a narrow frequency band from $x(t)$ in a short time interval and conversely. Or in other words, to precisely determine the frequency a long record time is required, while to determine time precisely a broad frequency band is necessary. This expresses what may be called the "uncertainty principle" in data analysis.

In terms of $x(t)$ and its Fourier transform $X(f)$, the uncertainty principle can also be stated in the following way. Suppose that $x(t)$ is normalized so that

$$\int_{-\infty}^{\infty} x^2(t) dt = 1$$

Then from Parseval's theorem there follows

$$\int_{-\infty}^{\infty} |X(f)|^2 df = 1$$

If one chooses

$$T_0 \equiv \left[\int_{-\infty}^{\infty} t^2 x^2(t) dt \right]^{1/2} \quad (30)$$

as a measure of the spread of $x(t)$ about the origin $t = 0$ and

$$\Omega_0 \equiv \left[\int_{-\infty}^{\infty} f^2 |X(f)|^2 df \right]^{1/2} \quad (31)$$

as a measure of the spread of $X(f)$ about its origin $f=0$, then it can be shown (e. g., Bendat, 1958) that

$$T_0 \Omega_0 \geq \frac{1}{4\pi}$$

Thus, uncertainty exists between the knowledge of time and frequency.

In actual calculations of the Fourier transforms of the length T of a record $x(t)$, discrete Fourier amplitudes are calculated at the frequencies with uniform spacing Δf . If, for a fixed length T , too small a Δf is selected large fluctuations in the calculated $X(f)$ will occur resulting in a large Ω_0 as required by the uncertainty principle. When this happens the reliability of individual amplitudes of $X(f)$ will be small. Therefore an optimum choice of Δf must be made, for given T , in order to achieve adequate resolution and reliability of individual amplitudes of $X(f)$. For the Fourier amplitude spectra in this report the frequency resolution is always equal to $1/T$, and T is the total duration of an accelerogram record.

5.3 Leakage. For actual calculations based on the time limited measurement $y(t)$ of function $x(t)$ in the time interval T the Fourier transform (1) becomes

$$Y(f) = \int_{-T/2}^{T/2} y(t) e^{-2\pi i f t} dt \quad (32)$$

One can view the finite time series $y(t)$ as the product of a finite length boxcar function

$$d(t) = \begin{cases} 0 & t \leq -\frac{T}{2} \\ 1 & -\frac{T}{2} \leq t \leq \frac{T}{2} \\ 0 & t \geq \frac{T}{2} \end{cases} \quad (33)$$

and an infinite time history $x(t)$. This is shown in Figure 3 where, for example, an infinitely long cosine function $x(t)$ is converted to a time limited function $y(t) = d(t)x(t)$ by such multiplication. The transform (32) can be rewritten then as

$$Y(f) = \int_{-\infty}^{\infty} x(t) d(t) e^{-2\pi i f t} dt \quad (34)$$

Since the products transform into convolutions we have

$$Y(f) = X(f) * D(f) \quad (35)$$

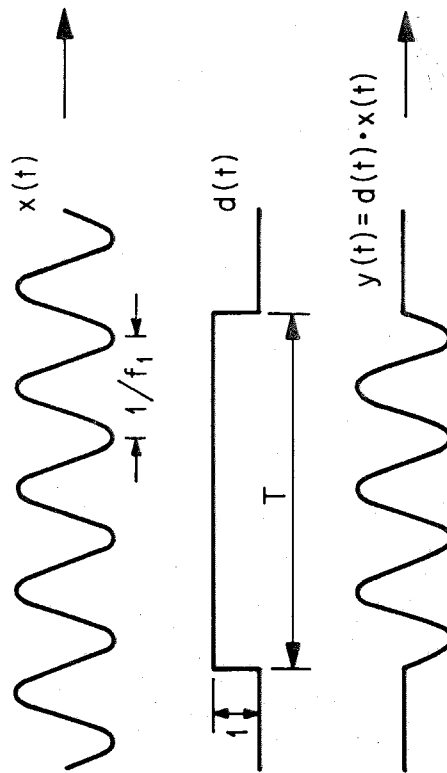
where

$$D(f) = \int_{-T/2}^{T/2} d(t) e^{-2\pi i f t} dt = \frac{\sin \pi f T}{\pi f} \quad (36)$$

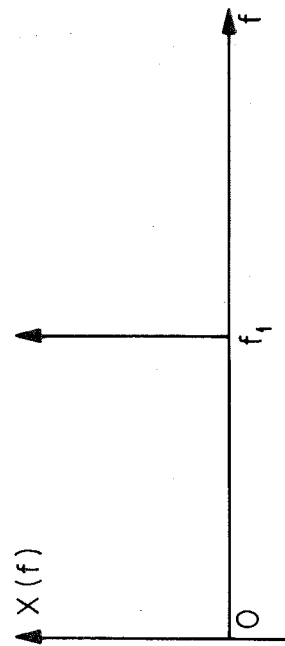
Continuous Fourier transform, for example, of the pure cosine wave $x(t)$ with frequency f_1 (Figure 3) is limited to only one point on the frequency axis and its transform is $X(f) = \delta(f - f_1)$. Since multiplication by $d(t)$ in time domain is equivalent to performing a convolution in the

LEAKAGE EFFECT

RECTANGULAR DATA WINDOW IMPLIED
FOR A FINITE RECORD LENGTH T



FOURIER TRANSFORM OF $x(t)$



FOURIER TRANSFORM OF $y(t)$

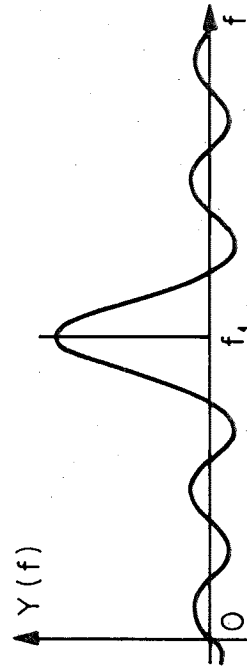


Figure 3

frequency domain, convolving $D(f)$ from (36) with $\delta(f_1)$ has the effect of shifting the central frequency $D(f)$ from zero to f_1 , as shown in Figure 3. The transform of the time limited cosine function (Figure 3) is therefore

$$Y_{\cos}(f) = \frac{\sin \pi(f-f_1)T}{\pi(f-f_1)} \quad (37)$$

The function $Y_{\cos}(f)$ is not localized at the frequency f_1 as $\delta(f_1)$ is but has a series of undesirable side peaks called sidelobes. This spreading effect caused by the finite length of the boxcar function (33) is called "leakage". It might be thought that due to the fact that the actual time history of the ground motion is zero before and after the earthquake applying the boxcar function (33) would therefore not introduce the leakage effect in spectral calculations of earthquake accelerograms. However, since an accelerograph begins to record with a short delay after the first wave arrivals and since it is not always feasible to record or digitize long after the strong ground motion is over, the actual recorded and digitized signals are only part of the total time history.

In order to minimize the leakage effect the time series $y(t)$ is multiplied by a suitable data window having the sidelobes smaller than the rectangular window $d(t)$. A variety of different time windows have been proposed in the literature (Blackman and Tukey, 1958; Welch, 1961; Bingham et al, 1967; and Tukey, 1967). One of the simplest windows, called the Hanning window (after the Austrian meteorologist Julius von Hann), is used for routine Fourier amplitude spectrum calculations in this volume (Blackman and Tukey, 1958). This window $d_c(t)$ has a form of the cosine bell

$$d_c(t) = \begin{cases} 0 & ; t < -\frac{T}{2} \\ \frac{1}{2} \left[1 + \cos \frac{2\pi t}{T} \right] & ; -\frac{T}{2} \leq t \leq \frac{T}{2} \\ 0 & ; t > \frac{T}{2} \end{cases} \quad (38)$$

It can be shown that applying this window in the time domain is equivalent to using the discrete convolution weights $\frac{1}{4}, \frac{1}{2}, \frac{1}{4}$. For the general convolution weights H_k , $k=-M_1, \dots, M_2$ the window function $h(t)$ is obtained from

$$h(t) = \sum_{k=-M_1}^{M_2} H_k e^{i2\pi t k \Delta f} \quad (39)$$

For the Hanning window $M_1=-1$, $M_2=1$ and $H_{-1}=\frac{1}{4}$, $H_0=\frac{1}{2}$ and $H_1=\frac{1}{4}$.

Therefore

$$d_c(t) = \frac{1}{4} \cos 2\pi t \Delta f + \frac{1}{2} + \frac{1}{4} \cos 2\pi t \Delta f \quad (40)$$

Since the resolution for the Fast Fourier Transform calculations is $\Delta f=1/T$ it may be seen that Equation (38) follows immediately from Equation (40).

The standard calculation of the final Fourier amplitude spectrum $|X_i(t)|_{SM}$, $i=1,2,\dots,N/2$, and smoothing those by $\frac{1}{4}, \frac{1}{2}, \frac{1}{4}$ weights in the following way

$$|X_i(f)|_{SM} = \frac{1}{2} |X_i(f)| + \frac{1}{4} \left\{ |X_{i+1}(f)| + |X_{i-1}(f)| \right\} \quad (41)$$

The absolute brackets indicate the modulus of the respective complex quantity.

5.4 Picket-Fence Effect. Each Fourier coefficient in the output of the Fast Fourier Transform algorithm would ideally represent a rectangular

PICKET-FENCE EFFECT

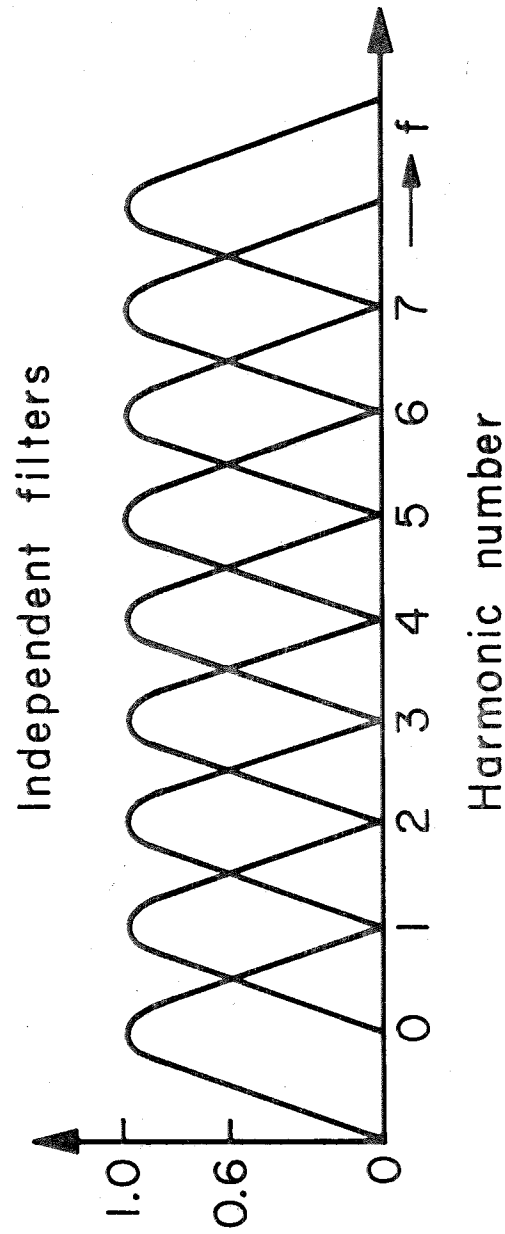


Figure 4

band-pass filter. Actually, due to the leakage effect caused by the multiplication of $x(t)$ by a window $d(t)$, each of these filters is deformed in a function of the same form as $D(f)$ (Equation (36)) but is centered at the frequency of each filter. To illustrate the nature of the output from the Fast Fourier Transform algorithm only the main lobes of these filters are plotted in Figure 4. This means, for example, that an input of the form $e^{i\omega t}$ with a frequency $\omega = \frac{2\pi}{T}n$, where n is an integer, would result in a response of unit amplitude at the n -th harmonic while the amplitudes of all other harmonics would be zero. Thus when n is an integer the picket-fence effect does not take place. For all other frequencies, however, the single frequency signal analyzed is seen by two adjacent filters but in such a way that the amplitudes are lower than one. In the worst case, corresponding to an input frequency $\omega = \frac{2\pi}{T}\left(n + \frac{1}{2}\right)$ where n is an integer, the n and $n+1$ harmonics see the input signal with amplitudes equal to $2/\pi$.

It is possible to reduce the picket-fence problem by the use of an interpolation function or by modification of the Discrete Fourier Transform algorithm, but in practical calculations this problem is not as serious as it might seem from this brief discussion. This is because the signal analyzed is almost never a pure sine or cosine wave but usually has a broad frequency content which covers several or many harmonics. Furthermore, the smoothing of the raw Fourier spectrum amplitudes or equivalently the multiplications of the input signal by a data window other than $d(t)$ (Equation (33)) normally reduces the picket-fence effect by widening the main spectral lobes (Figure 4).

6. Fisher's Test of Significance in Harmonic Analysis. In harmonic analysis of the time series $x(t)$ an inference about the presence of significant frequency components is based on the amplitudes of the corresponding spectral peaks in $|X(f)|$, the Fourier amplitude spectrum of $x(t)$. However, when a set of random numbers with spectrum theoretically known to be constant is subject to spectral analysis, its Fourier amplitude spectrum may indicate amplitudes that are larger for some frequencies than for others. Assuming that the major types of errors, discussed in the previous sections, are negligibly small, this event may be interpreted as a consequence of chance alone.

Statistical reliability of an individual spectral estimate for noise-like signals has been frequently considered in literature (Richards, 1967; Tukey, 1967; Welch, 1967; Bingham et al, 1967; and Parzen, 1968). A particularly useful test for the Fourier spectrum analysis was proposed by Fisher (1929) and successfully used by Nowroozi (1965, 1966) for the analysis of the eigenvibrations of the earth. This test will be summarized here briefly, following its description given by Nowroozi (1967).

Consider a series $x(i)$, $i=1,2,\dots,n$ constituting a random sample from a normally distributed population, and its Fourier series representation

$$x(i) = \frac{a_0}{2} + \sum_{k=1}^m \left\{ a_k \cos \frac{2\pi ki}{n} + b_k \sin \frac{2\pi ki}{n} \right\} \quad (42)$$

where

$$2m+1 = n \quad (43)$$

Harmonic amplitude C_k of the k^{th} harmonic is

$$C_k = (a_k^2 + b_k^2)^{1/2} \quad (44)$$

The probability P that the largest of m ratios

$$\frac{\max_k (C_k^2)}{\sum_{k=1}^m C_k^2} \quad (45)$$

exceeds a parameter g , was found by Fisher (1929) to be

$$P = m(1-g)^{m-1} - \frac{m(m-1)}{2}(1-2g)^{m-1} + \dots + (-1)^{L-1} \frac{m!}{L!(m-L)!} (1-Lg)^{m-1} \quad (46)$$

where L is the largest integer less than $1/g$. It is stated by

Nowroozi (1967) that the error in calculating g from only the first term in (46) is very small. Values of g for hypothetical probabilities $P=0.01, 0.02, 0.05$ and 0.10 calculated from the first term in Eqn. (46) only and for the values of $m=2^N$ where $N=3,4,5, \dots, 13$ are given in Table 1.

In order to examine the accuracy of the first term approximation for given P the values of g were used again in Equation (46). The new value of P , P_0 , was obtained by using all terms in (46), and the errors $\epsilon = \frac{P_0 - P}{P} \cdot 100$ were calculated for each m . For small values of m the errors ϵ are negligible but increase uniformly with increasing m . For the largest value of $m=8192$, given in Table 1, the errors ϵ are listed in the brackets following the assumed P values. From these errors it may be concluded that for all practical purposes the first term approximation in (46) is adequate.

TABLE 1

Values of g for Hypothetical Probabilities

$m = 2^N$	N	P = 0.01 (-0.50%)	P = 0.02 (-1.0%)	P = 0.05 (-2.6%)	P = 0.10 (-4.8%)
8	3	0.615	0.575	0.516	0.465
16	4	0.389	0.360	0.319	0.287
32	5	0.229	0.212	0.188	0.170
64	6	0.130	0.120	0.107	0.0975
128	7	0.0717	0.0667	0.0599	0.0548
256	8	0.0390	0.0364	0.0329	0.0303
512	9	0.0210	0.0197	0.0179	0.0166
1024	10	0.0112	0.0105	0.00966	0.00899
2048	11	0.00596	0.00563	0.00517	0.00484
4096	12	0.00315	0.00298	0.00276	0.00259
8192	13	0.00166	0.00158	0.00146	0.00138

Noting that

$$\sum_{k=1}^m C_k^2 = \frac{2}{2m+1} \sum_{i=1}^n \left[x(i) - \frac{a_0}{2} \right]^2 \quad (47)$$

the test can be applied by calculating the maximum significant amplitude Y , based on the assumption that the data $x(i)$ are random, in the following way

$$Y = \left\{ g_{P=0.05} \frac{2}{2m+1} \sum_{i=1}^n \left[x(i) - \frac{a_0}{2} \right]^2 \right\}^{1/2} \quad (48)$$

Here $g_{P=0.05}$, for $P=0.05$, is arbitrarily selected. Values of g for other probabilities can be read from Table 1. All the spectral peaks which have amplitudes greater than Y are then, in the sense of this test, significant at the 95% confidence level.

A convenient way of applying this test to the Fourier amplitude spectrum of an accelerogram of duration T is to plot a line $C = Y \cdot T/2$ across the plot of Fourier amplitude spectrum versus frequency. In the plots on the subsequent pages this line is identified as the "95 percent confidence level".

Frequency Response Function for a Linear System

An elementary discussion of the computational procedures related to linear systems analysis based on the measured time histories of response is presented in this section. Generally speaking a linear system can be viewed as a device or a process which operates on a time history and changes it in some manner. The most basic description of such a process may be given through the unit impulse function and the convolution integral.

Let $x(t)$ be the input time history and let $y(t)$ be the result of the action of a linear system on $x(t)$. If $x(t) = \delta(t)$ then $y(t) \equiv h(t)$. This is the definition of the impulse response function $h(t)$. That is, if the input to a linear system is a single delta function at time $t=0$ the output of the filter is $h(t)$. The relationship between the general input $x(t)$ and output of a linear system $y(t)$ is then given by

$$y(t) = \int_{-\infty}^{\infty} h(\tau) x(t-\tau) d\tau \quad (49)$$

Equation (49) states that the convolution of $h(t)$ and $x(t)$ gives $y(t)$.

The frequency response function of a linear system is given by the Fourier transform of $h(t)$, that is

$$H(f) = \int_{-\infty}^{\infty} h(t) e^{-2\pi i f t} dt \quad (50)$$

The Fourier transform of an input $x(t)$ is given by

$$X(f) = \int_{-\infty}^{\infty} x(t) e^{-2\pi i f t} dt \quad (51)$$

Taking the Fourier transform of both sides of Equation (49) and using (50) and (51) there follows

$$Y(f) = H(f)X(f) \quad (52)$$

Equation (52) is of great importance in the analysis of linear systems. It states that the Fourier transform of the output is equal to the product of (51), the Fourier transform of the input, and (50) the frequency response function of the linear system.

A simplified representation of the general earthquake engineering problem is schematically shown in Figure 5 (after Duke et al, 1970).

EARTHQUAKE SOURCE - SOIL - STRUCTURE SYSTEM

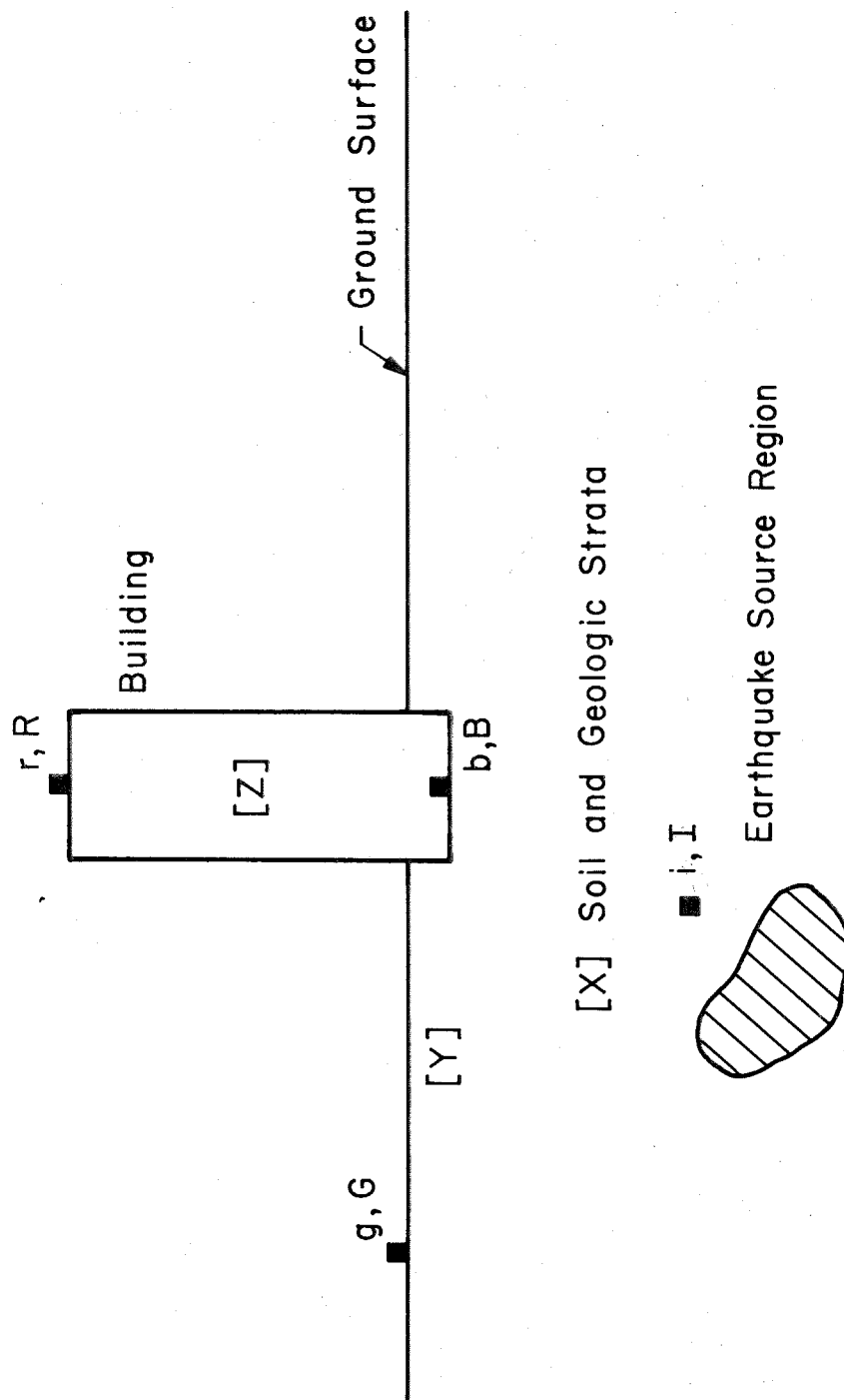


Figure 5

This system consists of three characteristic regions: (1) the region where the earthquake energy is released in the form of elastic waves, (2) the region through which these waves propagate and (3) the structure founded on top or in the second region. During an earthquake or explosion the motion at various points in the system in Figure 5 may be recorded. For illustration purposes it will be assumed here that such records are available at points (i, I), (g, G), (b, B) and (r, R) as shown in Figure 5. The small letter indicates that the time histories $i(t)$, $g(t)$, $b(t)$ and $r(t)$ are available at these points, while the capital letters represent the Fourier transforms $I(f)$, $G(f)$, $B(f)$ and $R(f)$ of these time histories respectively. Then, restricting this discussion to a given horizontal component of motion only, the relationship between the two ends of the system is given by (Duke et al, 1970)

$$R(f) = I(f)[X][Y^H Z^H + Y^\varphi Z^\varphi] \quad (53)$$

where

$[X]$ = horizontal free-field amplification factor, i. e., the frequency response function of the soil and geologic strata
 $[X] = G(f)/I(f)$

Y^H = frequency response function of the soil-structure interaction
 $Y^H = B(f)/G(f)$

Y^φ = ratio of the transform of the rotational basement motion to the transform of the free-field motion

Z^H = frequency response function for the horizontal motion of the structure assuming no rotation of the base

Z^φ = frequency response function of the rotational response of the structure to basement rotation only

$$\frac{R(f)}{G(f)} = Y^H Z^H + Y^\varphi Z^\varphi \quad (54)$$

and

$$\frac{R(f)}{B(f)} = Z^H + Z^\varphi \frac{Y^\varphi}{Y^H} \quad (55)$$

Studies of the general earthquake problem, or of its separate parts, are essentially based on the analysis of the transfer function properties between two points in the system where records of the time history are available. Typically, investigations dealing with soil-structure interactions and the dynamic response of structures during strong earthquake ground motions are all directly or indirectly based on the frequency response functions defined by (54) and (55) respectively.

Frequency response functions ((54) and (55)) can be determined from the recorded accelerograms and will be presented in this series of reports (Volume IV), whenever the appropriate simultaneous recordings are available. This will be limited however only to the amplitude of the transform and the relative phase will be disregarded. The reason for doing so lies in the fact that most accelerographs are triggered independently and, although their relative times can be closely correlated, the accurate knowledge of their relative times, essential only for the calculations of relative phase, is not available.

The objective of this volume will be to systematically collect and present the frequency response functions such as X , Y^H , $Y^H Z^H + Y^\varphi Z^\varphi$ and $Z^H + Z^\varphi (Y^\varphi / Y^H)$ whenever the data for some or all such ratios are available. It will be possible then to compare the experimental and theoretical expressions in order to improve the existing and develop new methods in the field of Earthquake Engineering.

M. D. Trifunac
F. E. Udvardi

Earthquake Engineering
Research Laboratory
California Institute of Technology

REFERENCES

- Bendat, J. S. (1958). Principles and Applications of Random Noise Theory, John Wiley, New York.
- Bergland, G. D. (1969). A Guided Tour of the Fast Fourier Transform, IEEE Spectrum, 6, 41-52.
- Bielak, J. (1971). Earthquake Response of Building-Foundation Systems, Earthquake Engineering Research Laboratory, EERL 71-04, California Institute of Technology, Pasadena.
- Bingham, C., M. D. Godfrey and J. W. Tukey (1967). Modern Techniques of Power Spectrum Estimation, IEEE Trans. Audio and Electroacoustics, AU-15, 56-66.
- Blackman, R. B. and J. W. Tukey (1958). The Measurement of Power Spectra, Dover, New York.
- Cooley, J. W. and J. W. Tukey (1965). An Algorithm for the Machine Calculation of Complex Fourier Series, Math. Comput., 19, 297-301.
- Duke, C. M., J. E. Luco, A. R. Carriveau, P. J. Hradilek, R. Lastrico and D. Ostrom (1970). Strong Earthquake Motions and Site Conditions: Hollywood, Bull. Seism. Soc. Amer., 60, 1271-1289.
- Fisher, R. A. (1929). Test of Significance in Harmonic Analysis, Proc. R. Soc. A, 125, 54-59.
- Grenander, U. and M. Rosenblatt (1957). Statistical Analysis of Stationary Time Series, Chap. 3, John Wiley, New York.
- Hudson, D. E. (1962). Some Problems in the Application of Spectrum Techniques to Strong-Motion Earthquake Analysis, Bull. Seism. Soc. Am., 52, 417-430.
- Hudson, D. E., A. G. Brady and M. D. Trifunac (1969). Strong-Motion Earthquake Accelerograms, Digitized and Plotted Data, Vol. I, Earthquake Engineering Research Laboratory, EERL 69-20, California Institute of Technology, Pasadena.
- Hudson, D. E. (1970). Dynamic Tests of Full-Scale Structures, Chapter 7 in Earthquake Engineering, edited by R. L. Wiegel, Prentice-Hall, Inc., Englewood Cliffs, N. J.

- Hudson, D. E., A. G. Brady, M. D. Trifunac and A. Vijayaraghavan (1971 a). Strong-Motion Earthquake Accelerograms, Corrected Accelerograms and Integrated Velocity and Displacement Curves, Vol. II, Earthquake Engineering Research Laboratory, EERL 71-51, California Institute of Technology, Pasadena.
- Hudson, D. E., M. D. Trifunac and A. G. Brady (1971 b). Strong-Motion Earthquake Accelerograms, Response Spectra, Vol. III, Earthquake Engineering Research Laboratory, EERL 71-80, California Institute of Technology, Pasadena.
- Luco, J. E. (1969). Applications of Singular Integral Equations to the Problem of Forced Vibrations of a Rigid Footing, Ph. D. Thesis, University of California, Los Angeles.
- Nowroozi, A. A. (1965). Eigenvibrations of the Earth after the Alaskan Earthquake, J. Geophys. Res., 70, 5145-5156.
- Nowroozi, A. A. (1966). Terrestrial Spectroscopy following the Rat Island Earthquake, Bull. Seism. Soc. Am., 56, 1269-1288.
- Nowroozi, A. A. (1967). Table for Fisher's Test of Significance in Harmonic Analysis, Geophys. J. R. Astr. Soc., 12, 517-520.
- Papoulis, A. (1968). Systems and Transforms with Applications in Optics, McGraw Hill, New York.
- Parsen, E. (1967). Time Series Analysis Papers, Holden-Day, San Francisco.
- Parsen, E. (1968). Statistical Spectral Analysis (Single Channel Case) in 1968, Tech. Rep. 11, ONR Contract Nonr-225(80) (NR-042-234), Stanford University, Dept. of Statistics, Stanford.
- Richards, P. I. (1967). Computing Reliable Power Spectra, IEEE Spectrum, 4, 83-90.
- Trifunac, M. D. (1970 a). Wind and Microtremor Induced Vibrations of a 22-Story Steel Frame Building, Earthquake Engineering Research Laboratory, EERL 70-01, California Institute of Technology, Pasadena.
- Trifunac, M. D. (1970 b). Ambient Vibration Test of a 39-Story Steel Frame Building, Earthquake Engineering Research Laboratory, EERL 70-02, California Institute of Technology, Pasadena.
- Trifunac, M. D. (1970 c). Low Frequency Digitization Errors and a New Method for Zero Baseline Correction of Strong-Motion Accelerograms, Earthquake Engineering Research Laboratory, EERL 70-07, California Institute of Technology, Pasadena.

- Trifuanc, M. D., F. E. Udwadia and A. G. Brady (1971). High Frequency Errors and Instrument Corrections of Strong-Motion Accelerograms, Earthquake Engineering Research Laboratory, EERL 71-05, California Institute of Technology, Pasadena.
- Trifunac, M. D. (1972). Interaction of a Shear Wall with the Soil for Incident Plane SH Waves, Bull. Seism. Soc. Amer., 62, (in press).
- Tukey, J. W. (1967). An Introduction to the Calculations of a Numerical Spectrum Analysis, in Spectral Analysis of Time Series, edited by Bernard Harris, John Wiley, New York, 25-46.
- Welch, P. D. (1961). A Direct Digital Method of Power Spectrum Estimation, IBM J. Res. Develop., 5, 141-156.
- Welch, P. D. (1967). The Use of the Fast Fourier Transform for the Estimation of Power Spectra: A Method Based on Time Averaging over Short, Modified Periodograms, IEEE Trans. Audio and Electroacoustics, AU-15, 70-73.

PLOTS OF ACCELEROGRAMS AND FOURIER AMPLITUDE SPECTRA

The corrected accelerogram data obtained from the second stage of processing and published in the several parts of Volume II (Hudson et al, 1971a) are retrieved from magnetic tape storage, and by means of the Cooley-Tukey algorithm the Fourier amplitude spectra are calculated.

Details concerning identification are given at the top on each plot. The second line gives the name, date and time of occurrence of the earthquake; the third line is comprised of two labels, the observation station and the component processed. The Roman numeral "IV" in the first identification label indicates that the results pertain to the fourth stage of data processing, i. e., Volume IV of Fourier spectra of accelerogram records already corrected for baseline adjustment and instrument response. The letter "A" following the Roman numerals implies that the processed record belongs to Part A of Volume IV. Volume IV, Part A consists of the Fourier spectra of acceleration for the same records for which the corrected accelerograms are published in Volume II, Part A (Hudson et al, 1971a). The three digit number completing the first label is the Caltech Reference Number for the given earthquake record in Volume I, right-adjusted in a three-digit numerical field. The second label is a string of three numbers separated by periods; the first number gives the year in which the earthquake occurred, the second is the serial number of the record as it was received at the Caltech Earthquake Engineering Research Laboratory during that year, and the last number

indicates whether it was a main event or an aftershock (sequentially numbered, the main event starting from zero). On the linear spectrum plot, the data lying above the 95 percent confidence level may be considered relevant to that degree. The spectra have been plotted up to a frequency of 25 cyc/sec on linear and logarithmic scales, corresponding to the capabilities of the instrumentation and data processing methods used.

The acceleration-time record corresponding to each spectrum plot is reproduced in Volume II, "Corrected Accelerograms".

The spectral data are also stored on magnetic tapes, copies of which will be available on request from the National Information Service for Earthquake Engineering at the California Institute of Technology.

A. Vijayaraghavan
A. G. Brady

Earthquake Engineering
Research Laboratory
California Institute of Technology

EARTHQUAKE DATA

<u>Date & Time</u>	<u>Location</u>	<u>Epicenter</u>	<u>Max. Intensity</u>	<u>Mag.</u>	<u>References (See Below)</u>
May 18, 1940, 2037PST	Imperial Valley	32°44'N, 115°27'W	X	6.3	1, 2, 3
Oct. 7, 1951, 2011PST	Northwest Calif.	40°17'N, 124°48'W	VII		
July 21, 1952, 9453PDT	Kern County	35°00'N, 119°02'W	XI	7.7	4, 5
Mar. 22, 1957, 1144PST	San Francisco	37°40'N, 122°29'W	VII	5.3	6
Apr. 8, 1961, 2323PST	Hollister	36°40'N, 121°18'W	VII	5.6	
Apr. 8, 1968, 1830PST	Borrego Mtn.	33°09'N, 116°08'W	VII	6.5	7, 8

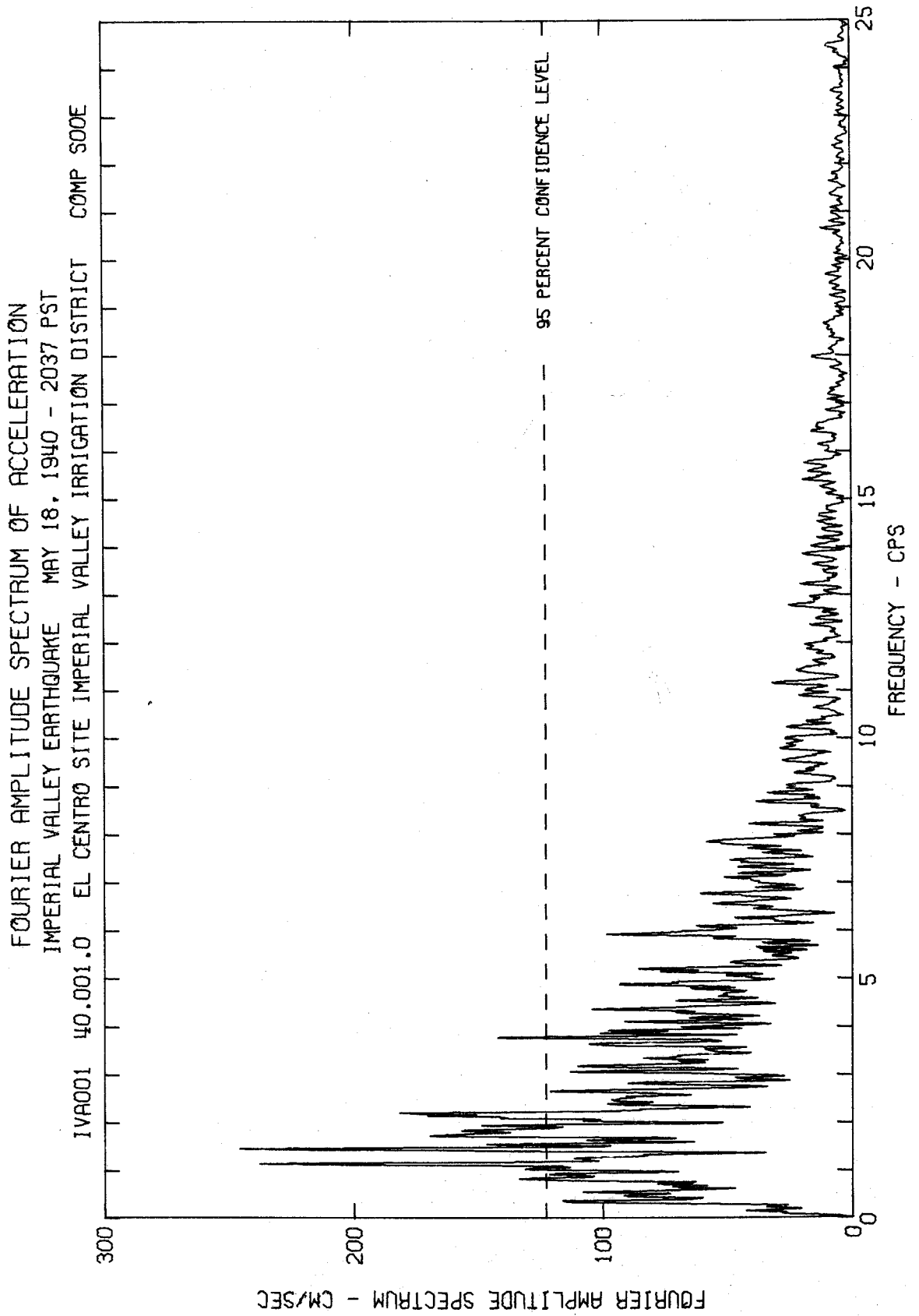
-41-

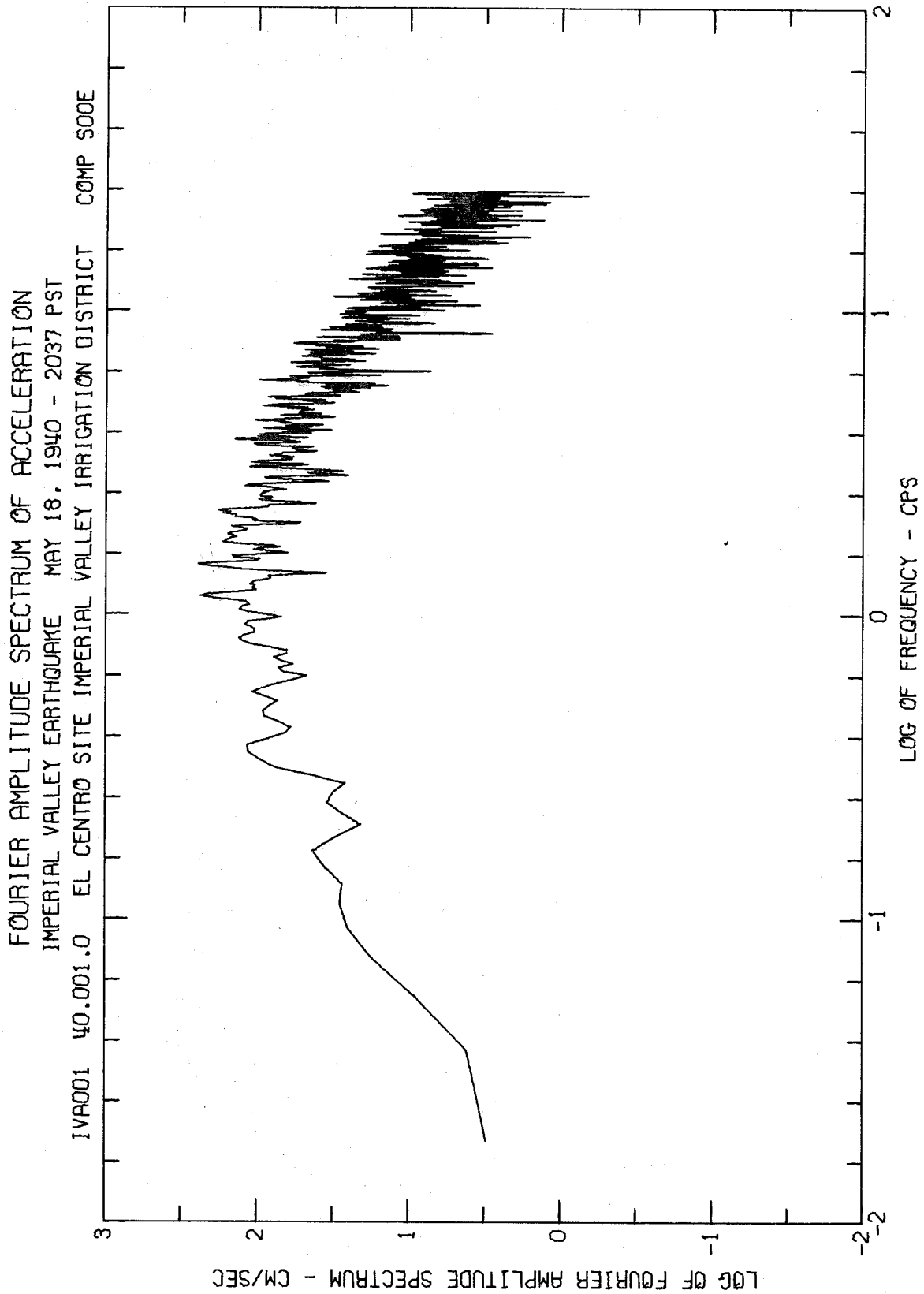
1. Ulrich, F. P., "The Imperial Valley Earthquakes of 1940," BSSA, v. 31, n. 1, January 1941, p. 13-31.
2. Trifunac, M. D. and Brune, J. N., "Complexity of Energy Release During the Imperial Valley, California Earthquake of 1940," BSSA, v. 60, n. 1, February 1970, p. 137-160.
3. Trifunac, M. D., "Response Envelope Spectrum and Interpretation of Strong Earthquake Ground Motion," BSSA, v. 61, n. 2, April 1971, p. 343-356.
4. Steinbrugge, K. V. and Moran, D. F., "An Engineering Study of the Southern California Earthquake of July 21, 1952 and Its Aftershocks," BSSA, v. 44, n. 2B, April 1954.
5. "Earthquakes in Kern County, California During 1952," California Department of Natural Resources, Division of Mines, San Francisco, Bulletin 171, November 1955.

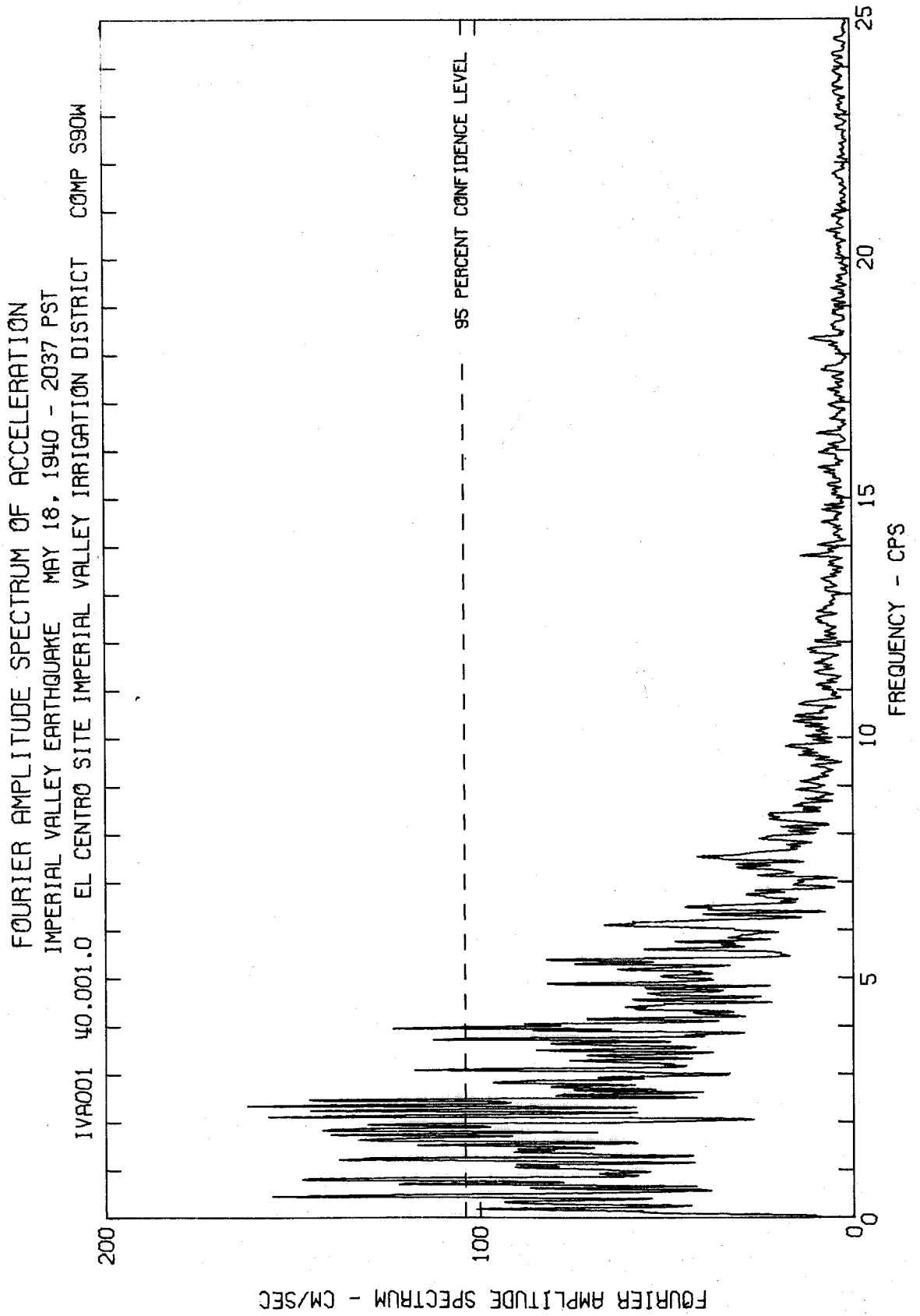
6. "San Francisco Earthquakes of March, 1957," California Division of Mines, Special Report 57, 1959.
7. "Strong Motion Instrument Data on the Borrego Mountain Earthquake of 9 April 1968," Joint Report by the Seismological Field Survey, USCGS, Environmental Science Services Administration, US Department of Commerce, and the Earthquake Engineering Research Laboratory, California Institute of Technology, August 1968.
8. Allen, C. R., et al., "The Borrego Mountain, California, Earthquake of 9 April 1968: A Preliminary Report," BSSA, v. 58, n. 3, June 1968.

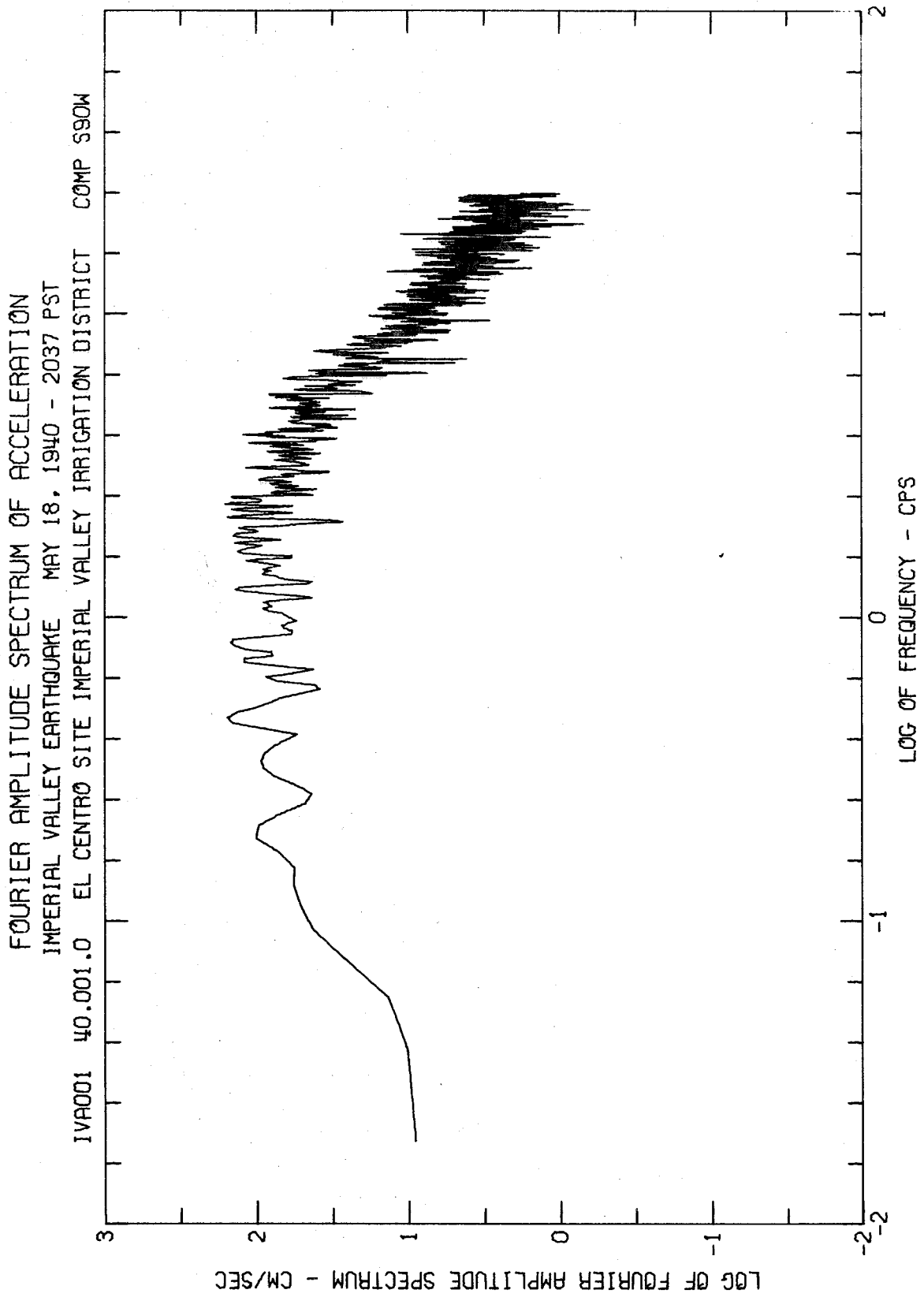
EARTHQUAKE RECORDS CONTAINED IN
VOLUME IV, PART A

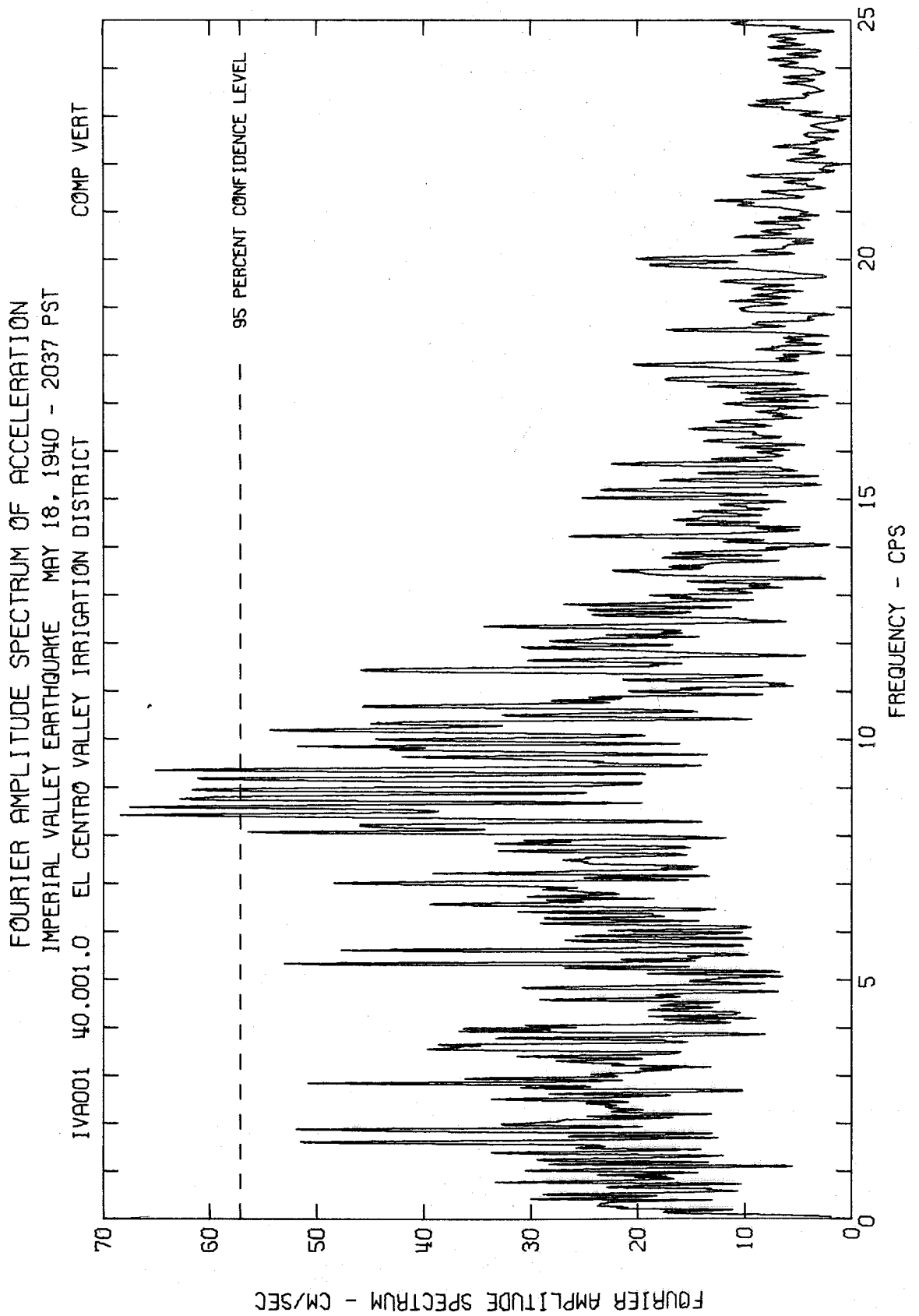
	<u>Page</u>
Imperial Valley Earthquake, May 18, 1940 - 2037 PST IV A001; El Centro, Imperial Valley Irrigation District; S00E, S90W, Vert.	44
Northwest California Earthquake, October 7, 1951 - 2011 PST IV A002; Ferndale City Hall; S44W, N46W, Vert.	50
Kern County Earthquake, July 21, 1952 - 0453 PDT IV A003; Pasadena, Caltech Athenaeum; S00E, S90W, Vert. IV A004; Taft, Lincoln School tunnel; N21E, S69E, Vert. IV A005; Santa Barbara Courthouse; N42E, S48E, Vert. IV A006; Hollywood Storage Basement; S00W, N90E, Vert. IV A007; Hollywood Storage P. E. Lot; S00W, N90E, Vert.	56 62 68 74 80
Eureka Earthquake; December 21, 1954 - 1156 PST IV A008; Eureka Federal Building; N11W, N79E, Vert. IV A009; Ferndale City Hall; N44E, N46W, Vert.	86 92
San Jose Earthquake, September 4, 1955 - 1801 PST IV A010; San Jose, Bank of America, Basement; N31W, N59E, Vert.	98
El Alamo, Baja California Earthquake, February 9, 1956 - 0633 PST IV A011; El Centro, Imperial Valley Irrigation District; S00W, S90W, Vert.	104
El Alamo, Baja California Aftershock, February 9, 1956 - 0725 PST IV A012; El Centro, Imperial Valley Irrigation District; S00W, S90W, Vert.	110
San Francisco Earthquake, March 22, 1957 - 1144 PST IV A013; San Francisco, Southern Pacific Building, Basement; N45E, N45W, Vert. IV A014; San Francisco, Alexander Building, Basement; N09W, N81E, Vert. IV A015; San Francisco, Golden Gate Park; N10E, S80E, Vert. IV A016; San Francisco State Building, Basement; S09E, S81W, Vert. IV A017; Oakland City Hall, Basement; N26E, S64E, Vert.	116 122 128 134 140
Hollister Earthquake, April 8, 1961 - 2323 PST IV A018; Hollister City Hall; S01W, N89W, Vert.	146
Borrego Mountain Earthquake, April 8, 1968 - 1830 PST IV A019; El Centro, Imperial Valley Irrigation District; S00W, S90W, Vert. IV A020; San Diego Light and Power Bldg. ; S00W, N90E, Vert.	152 158



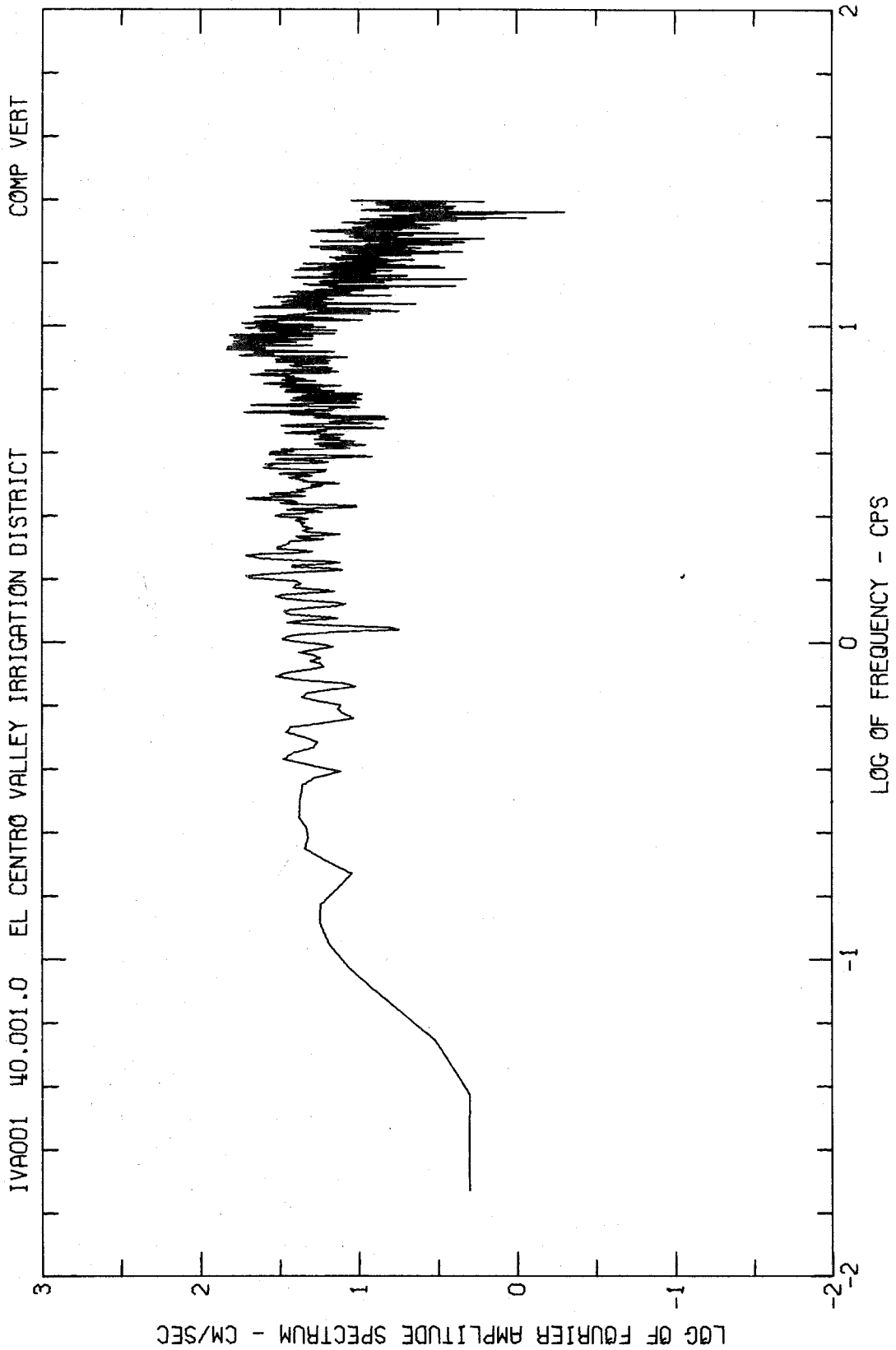




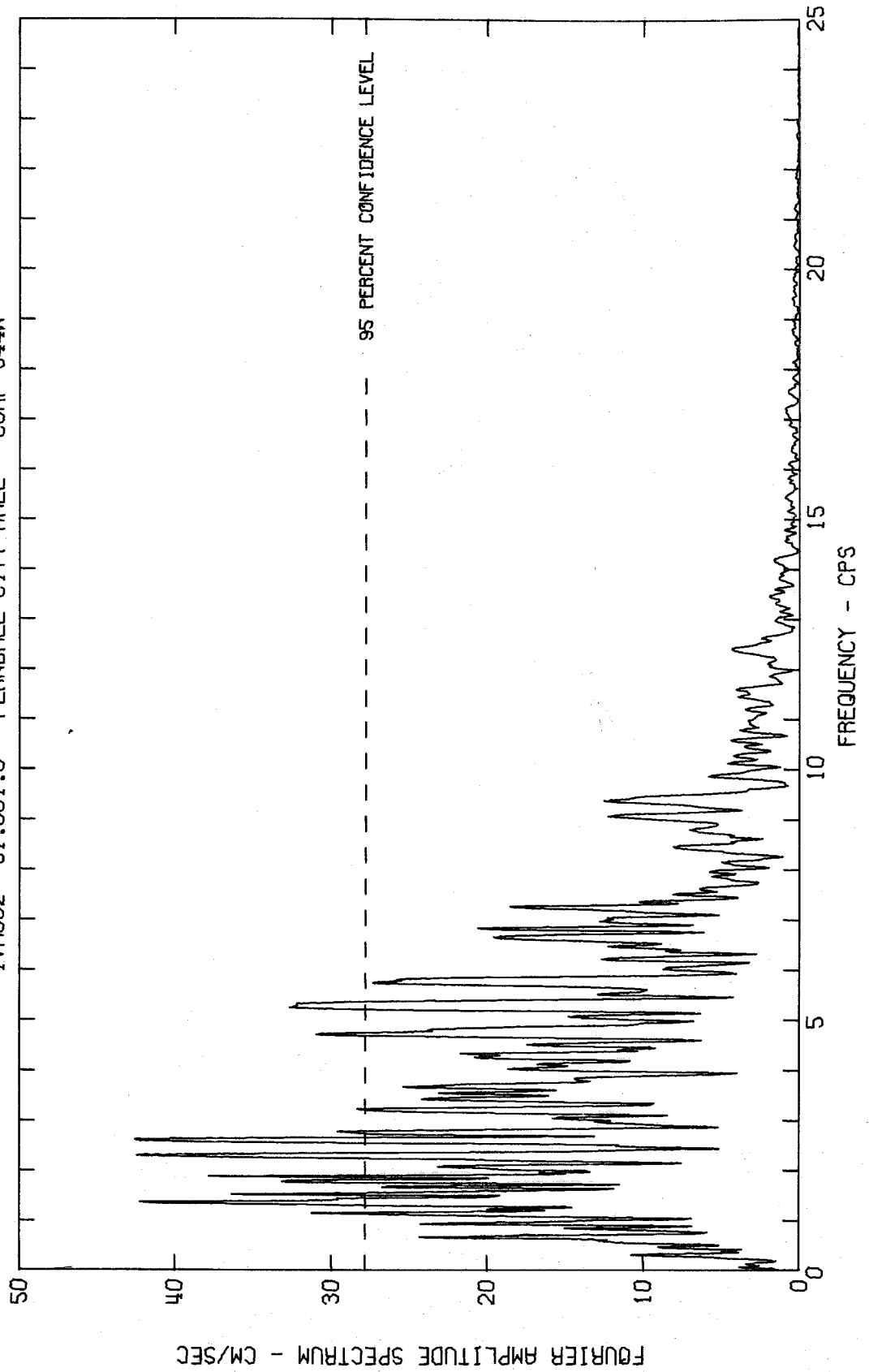




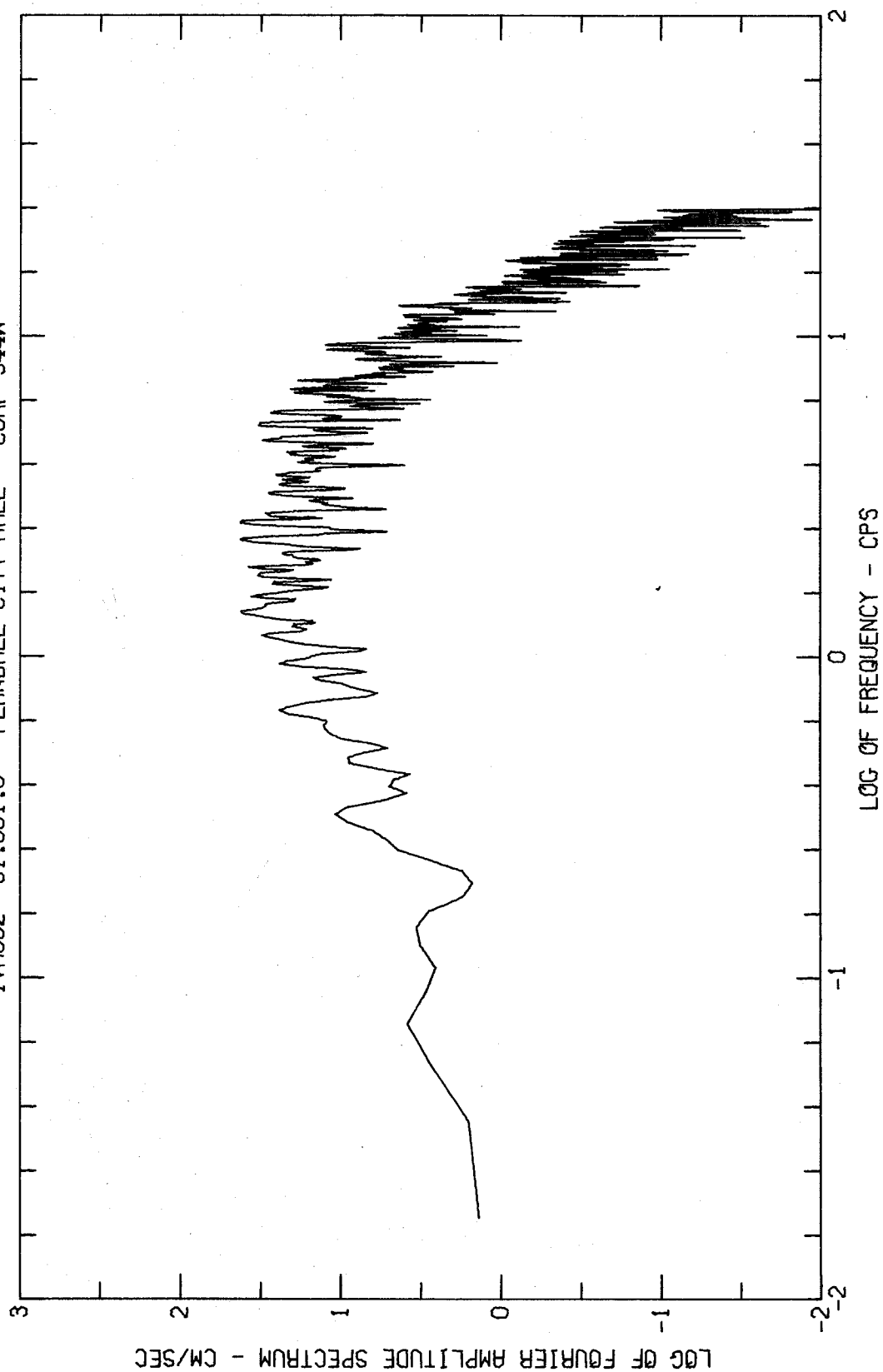
FOURIER AMPLITUDE SPECTRUM OF ACCELERATION
IMPERIAL VALLEY EARTHQUAKE MAY 18, 1940 - 2037 PST
IWA001 40.001.0 EL CENTRO VALLEY IRRIGATION DISTRICT



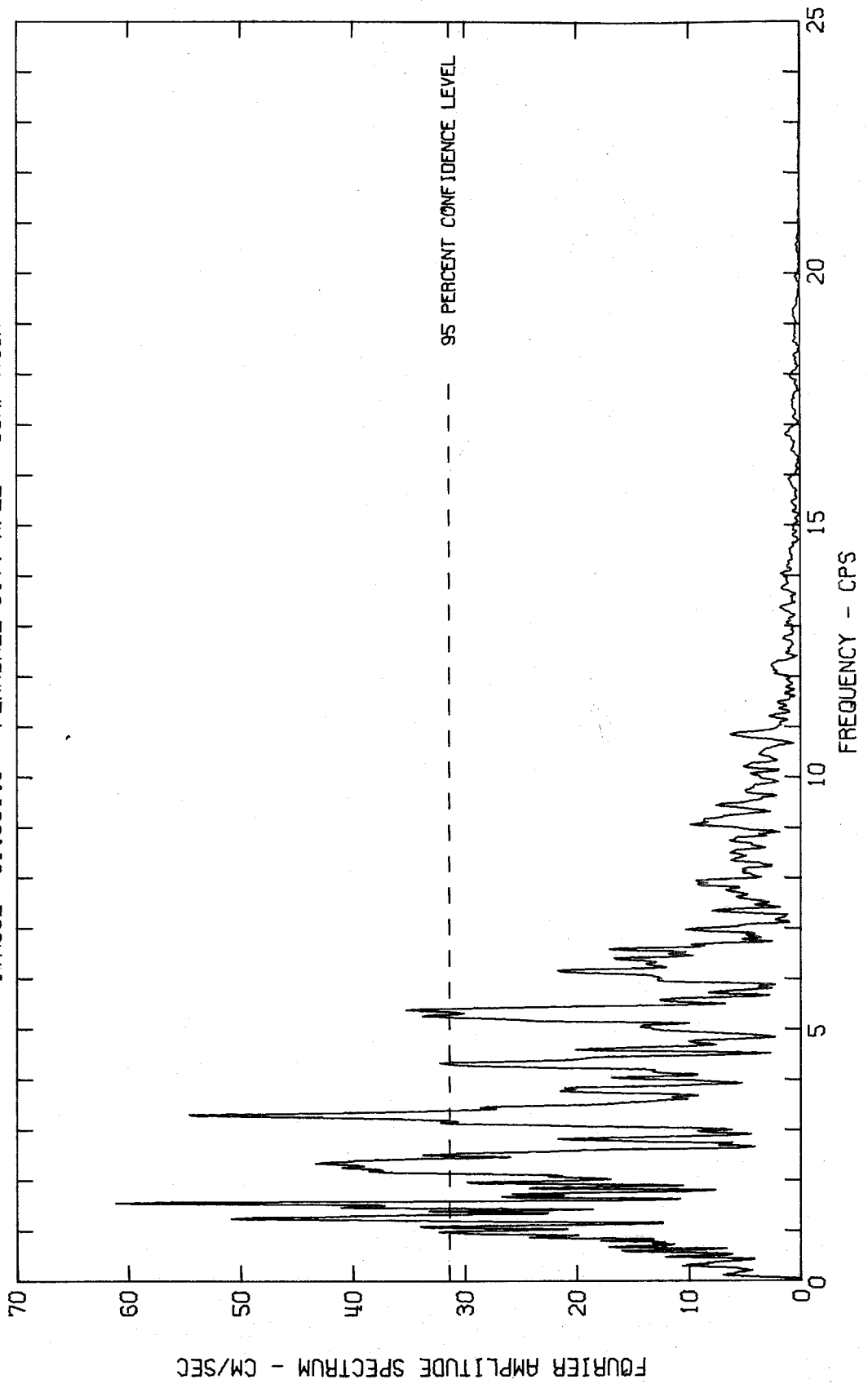
FOURIER AMPLITUDE SPECTRUM OF ACCELERATION
NORTHWEST CALIFORNIA EARTHQUAKE OCT 07, 1951 - 2011 PST
IVAO02 51.001.0 FERNDALE CITY HALL COMP 5444



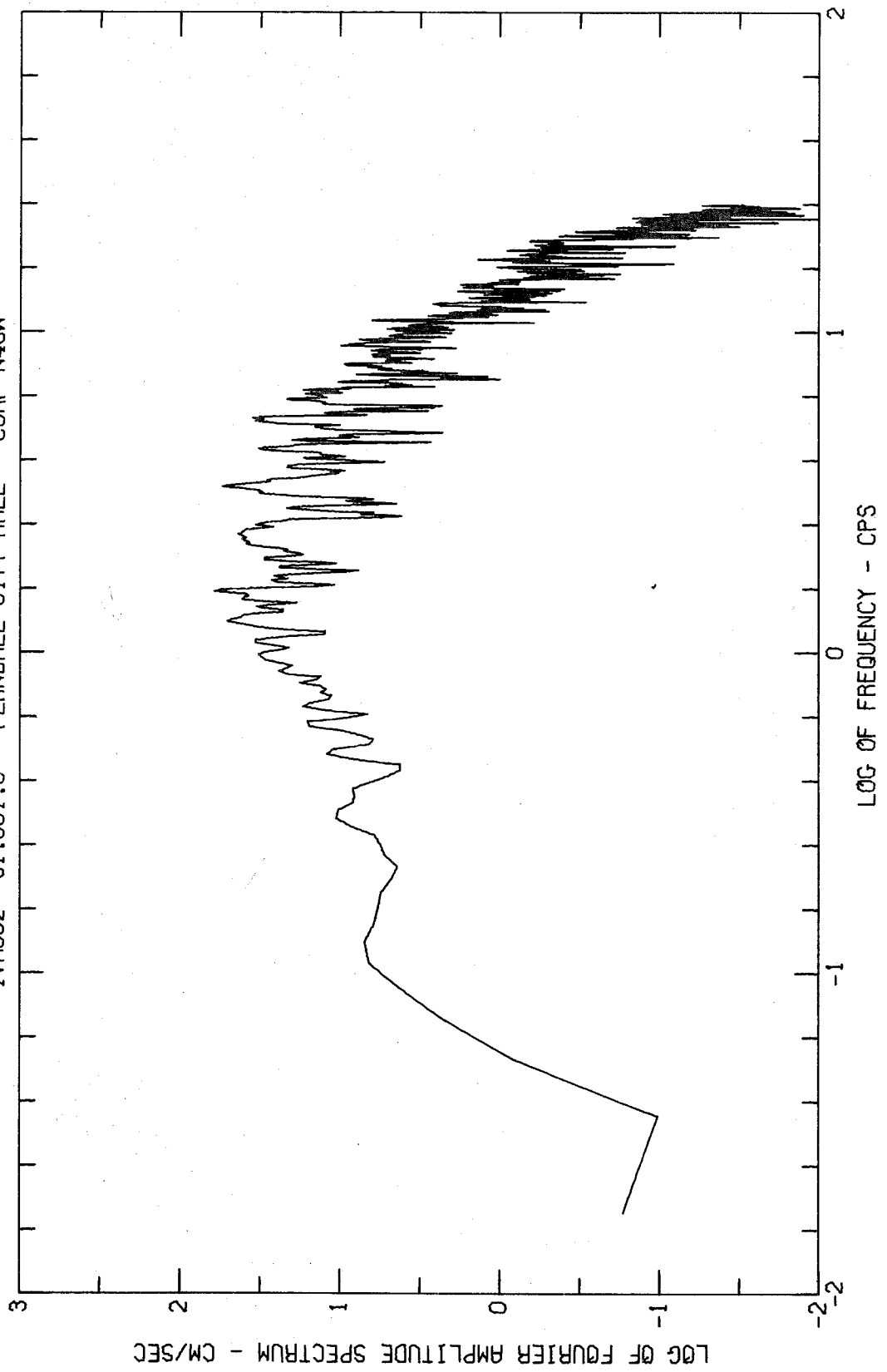
FOURIER AMPLITUDE SPECTRUM OF ACCELERATION
NORTHWEST CALIFORNIA EARTHQUAKE OCT 07, 1951 - 2011 PST
IWA002 51.001.0 FERNDALE CITY HALL COMP S44W



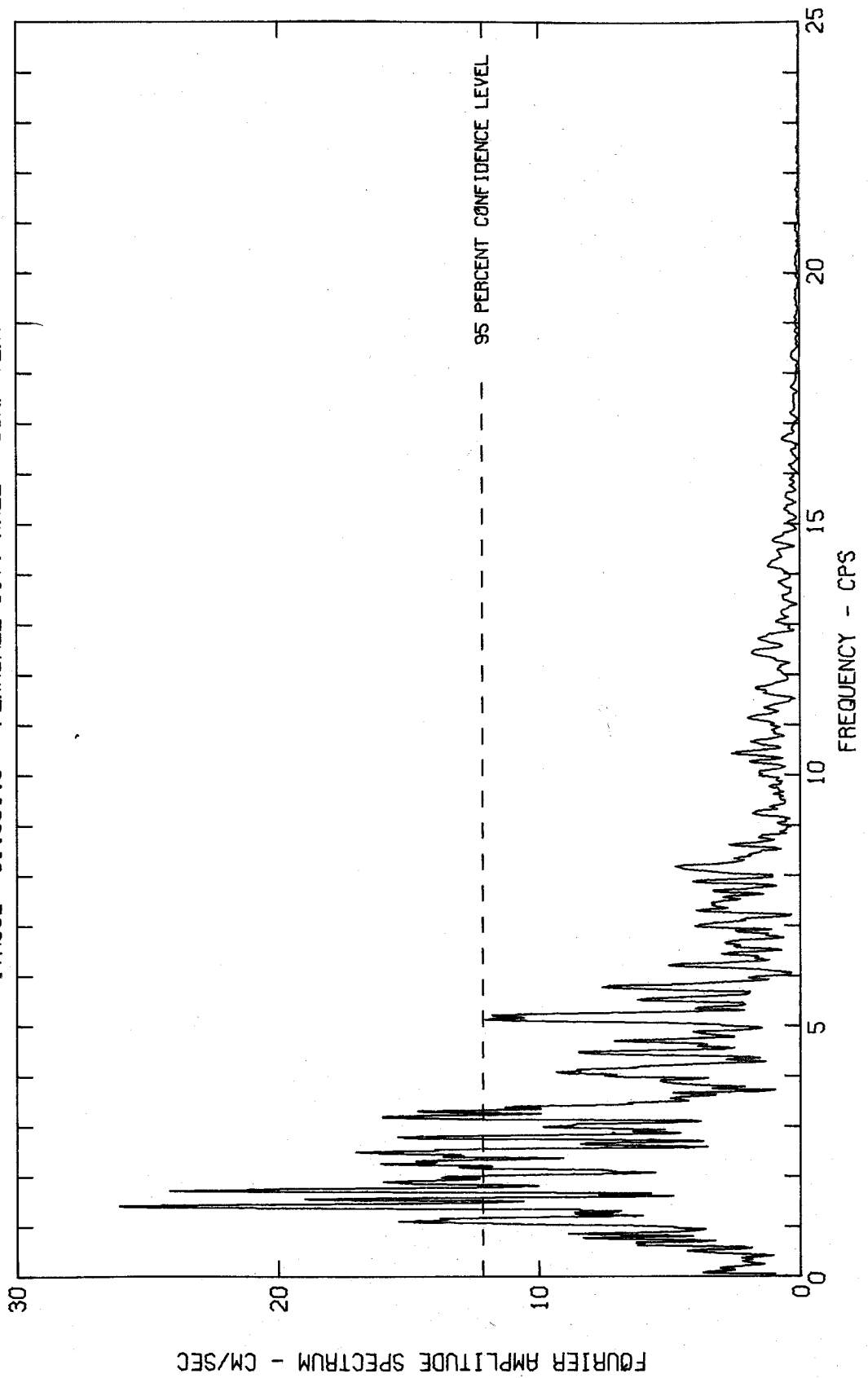
FOURIER AMPLITUDE SPECTRUM OF ACCELERATION
NORTHWEST CALIFORNIA EARTHQUAKE OCT 07, 1951 - 2011 PST
IVA002 51.001.0 FERNDALE CITY HALL COMP N46W



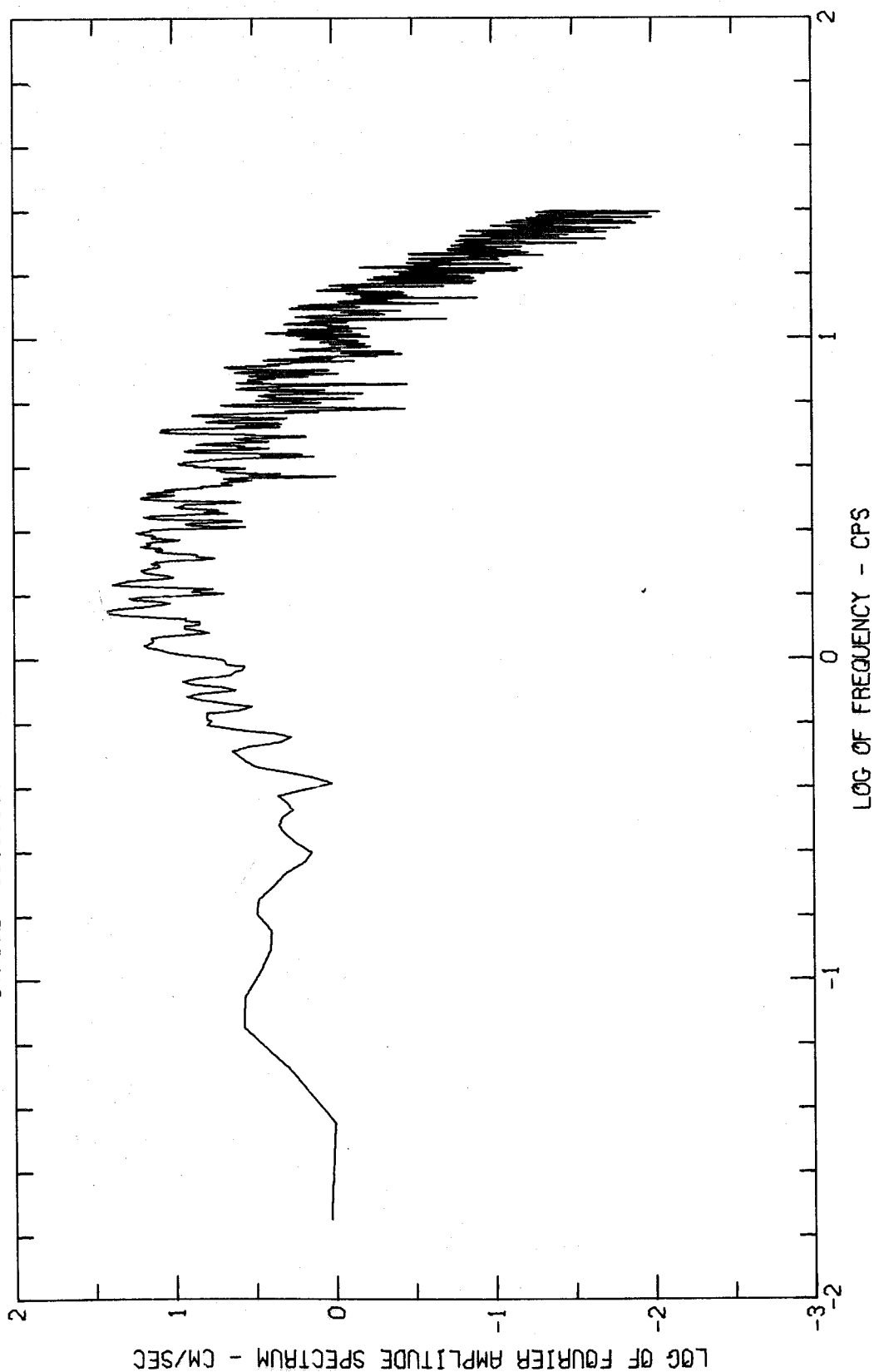
FOURIER AMPLITUDE SPECTRUM OF ACCELERATION
NORTHWEST CALIFORNIA EARTHQUAKE OCT 07, 1951 - 2011 PST
IWA002 51.001.0 FERNDAL CITY HALL COMP N46W



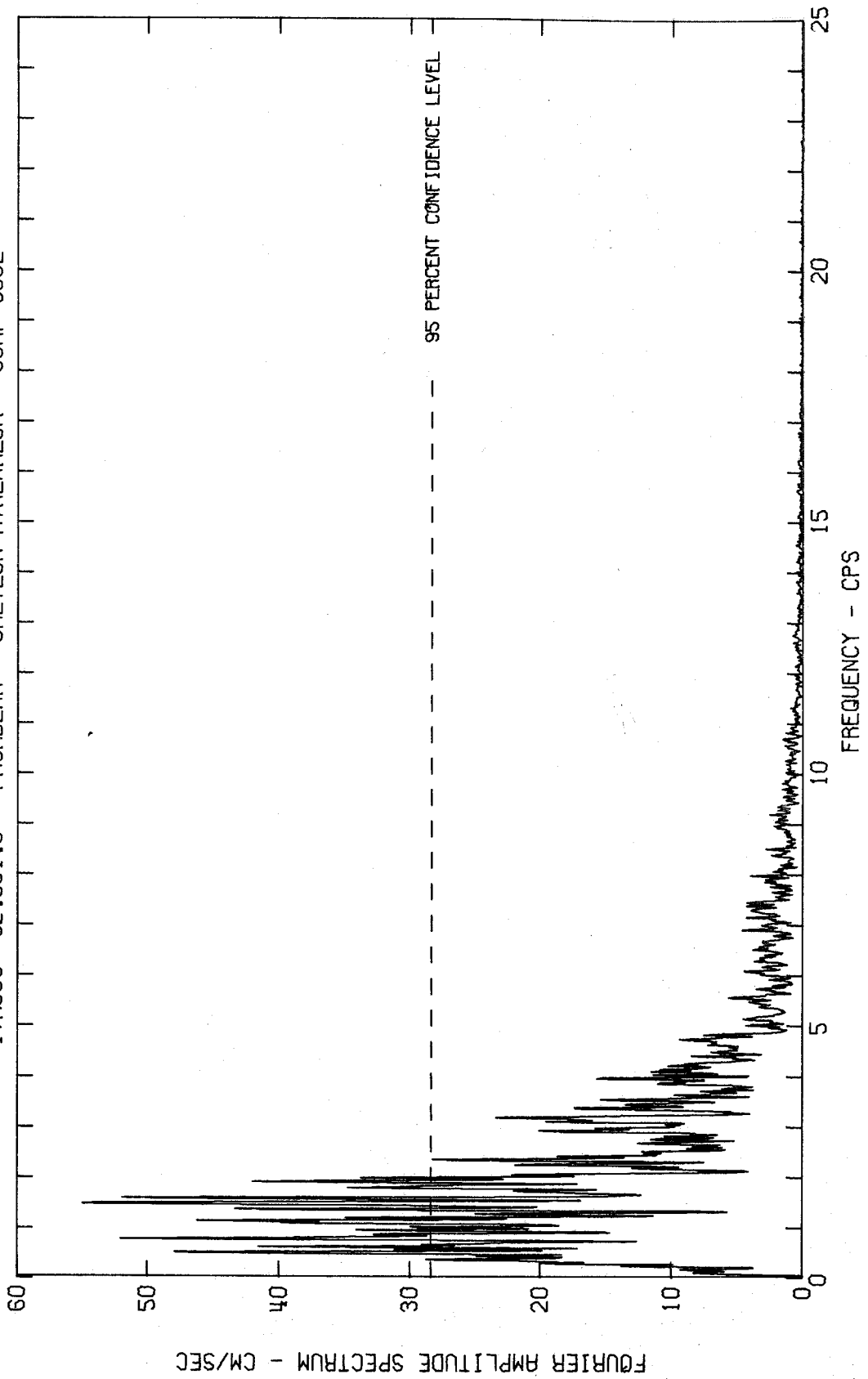
FOURIER AMPLITUDE SPECTRUM OF ACCELERATION
NORTHWEST CALIFORNIA EARTHQUAKE OCT 07, 1951 - 2011 PST
IWA002 51.001.0 FERNDALE CITY HALL COMP VERT



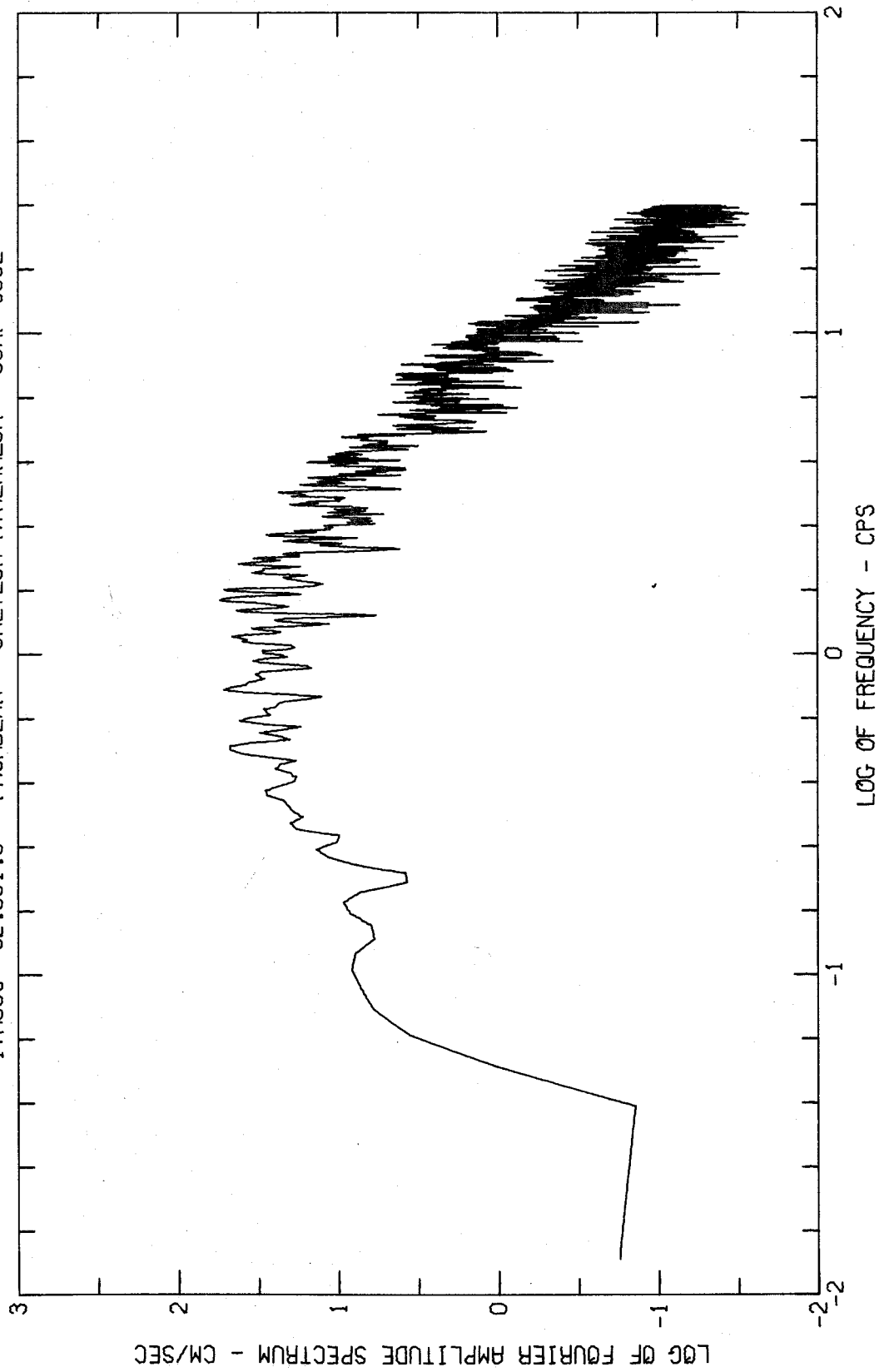
FOURIER AMPLITUDE SPECTRUM OF ACCELERATION
NORTHWEST CALIFORNIA EARTHQUAKE OCT 07, 1951 - 2011 PST
IWA002 51.001.0 FERNDALE CITY HALL COMP VERT



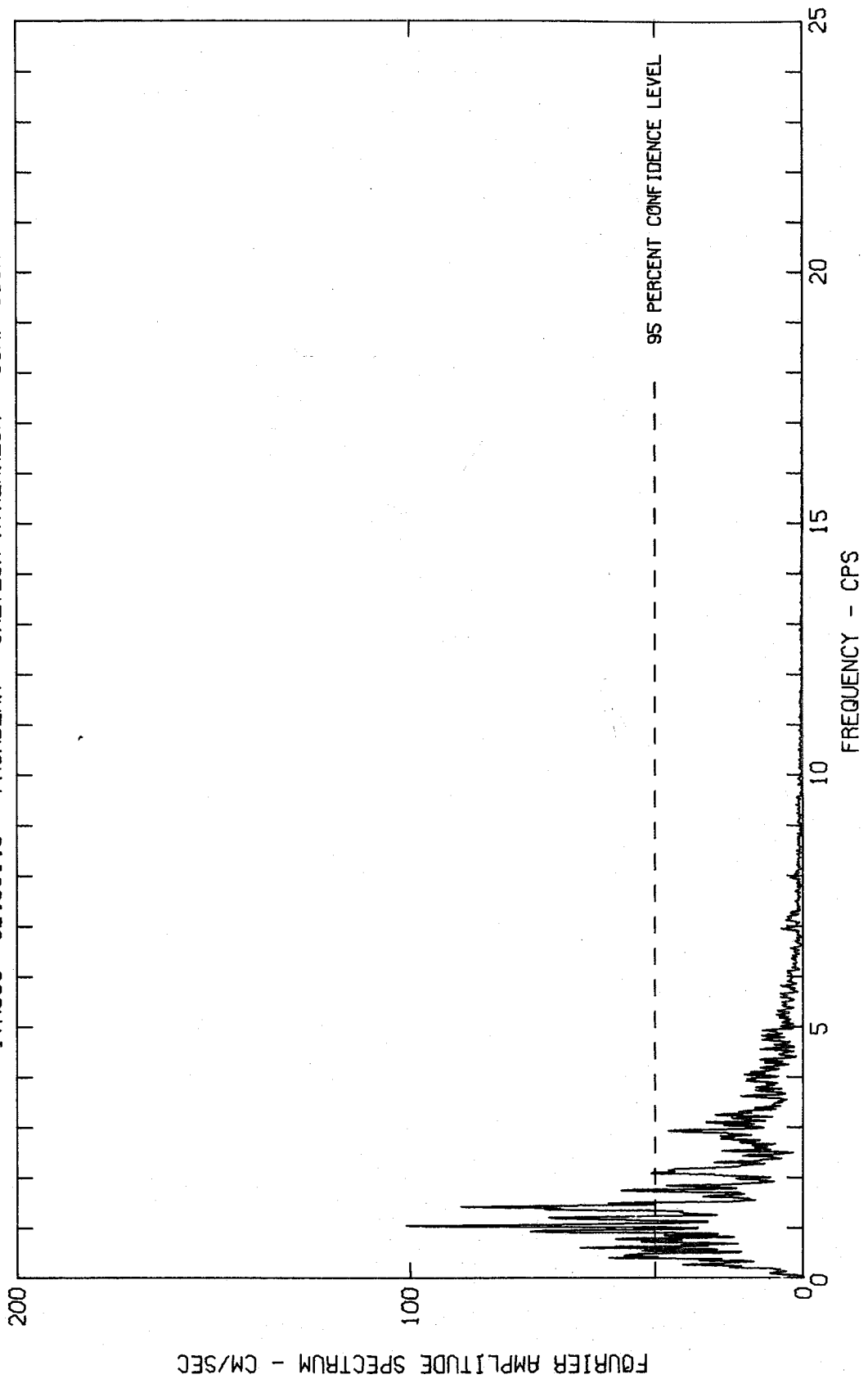
FOURIER AMPLITUDE SPECTRUM OF ACCELERATION
KERN COUNTY, CALIFORNIA EARTHQUAKE JULY 21, 1952 - 0453 PDT
IWA003 52.001.0 PASADENA - CALTECH ATHENAEUM COMP 500E



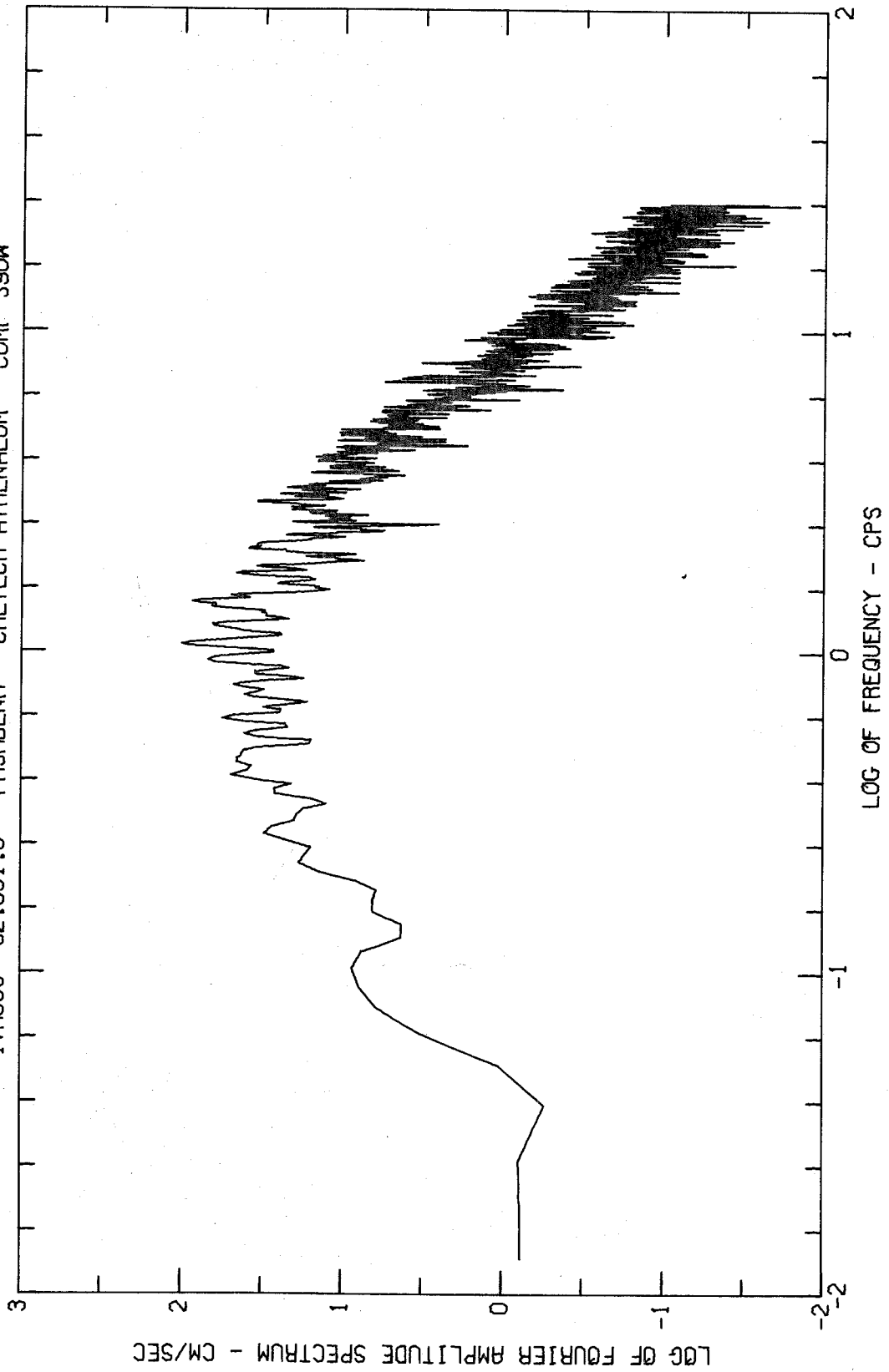
FOURIER AMPLITUDE SPECTRUM OF ACCELERATION
KERN COUNTY, CALIFORNIA EARTHQUAKE JULY 21, 1952 - 0453 PDT
IV0003 52.001.0 PASADENA - CALTECH ATHENAEUM COMP 500E



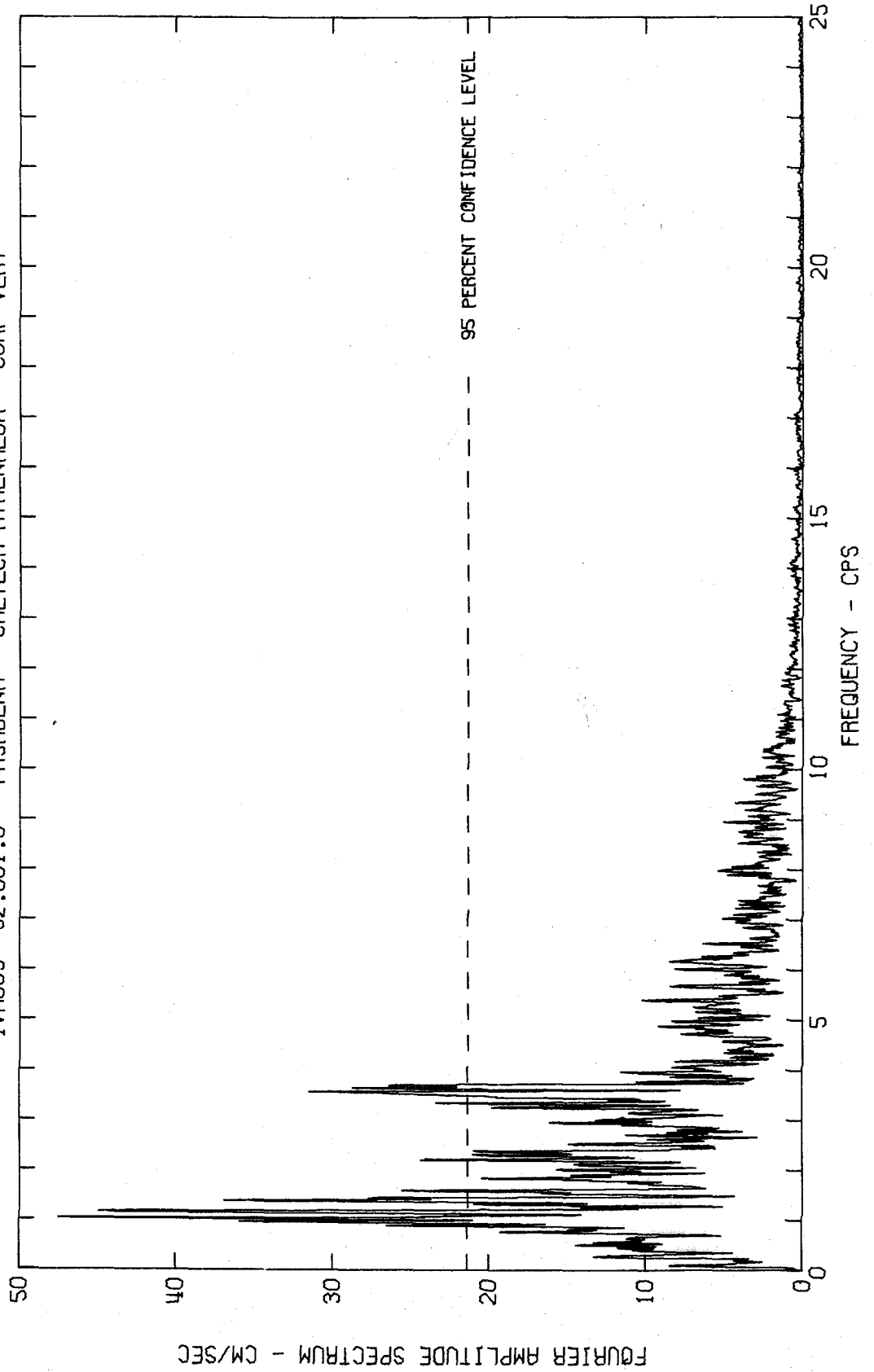
FOURIER AMPLITUDE SPECTRUM OF ACCELERATION
KERN COUNTY, CALIFORNIA EARTHQUAKE JULY 21, 1952 - 0453 PDT
IWA003 52.001.0 PASADENA - CALTECH ATHENAEUM COMP S90W



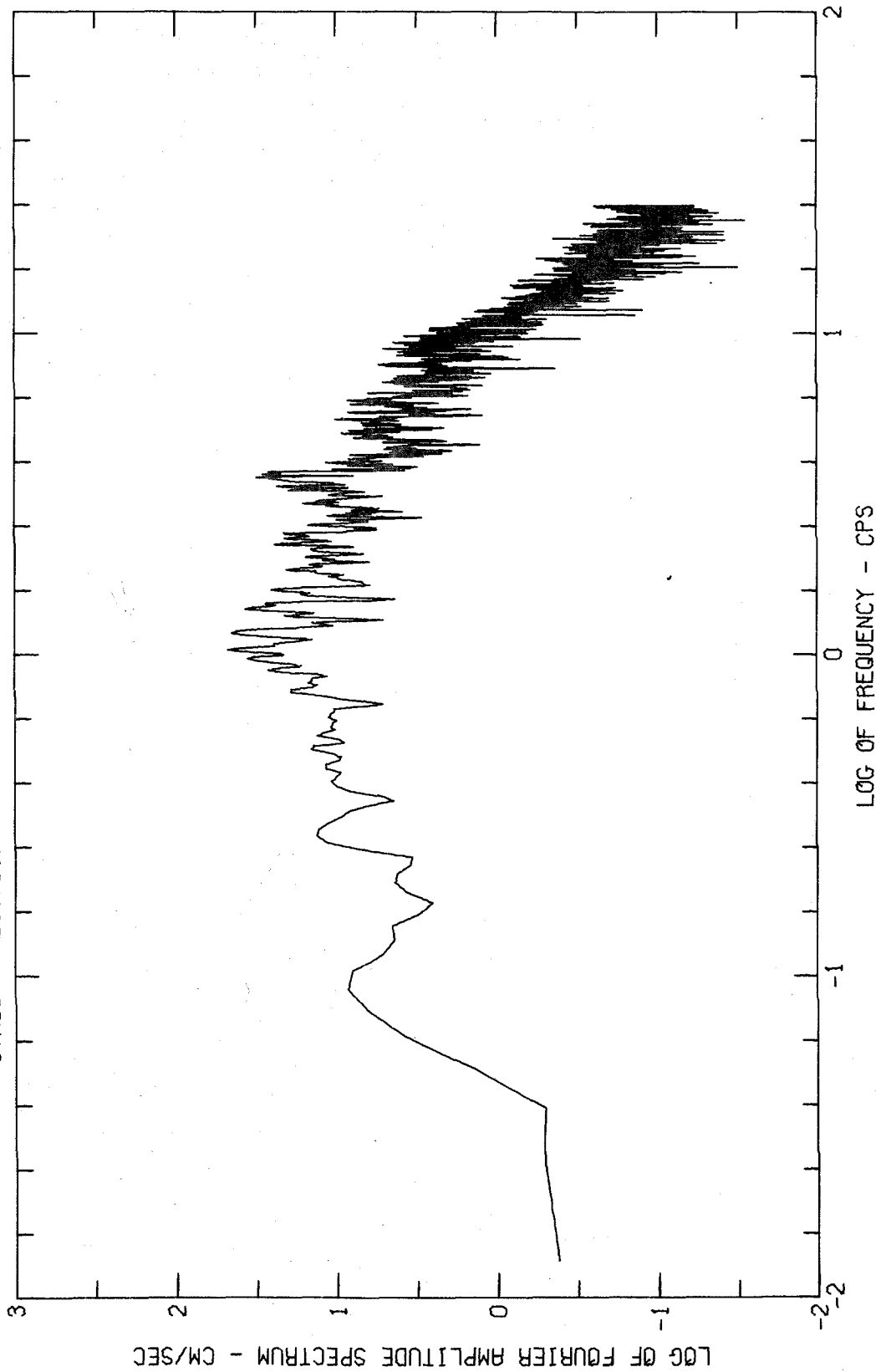
FOURIER AMPLITUDE SPECTRUM OF ACCELERATION
KERN COUNTY, CALIFORNIA EARTHQUAKE JULY 21, 1952 - 0453 PDT
IVA003 52.001.0 PASADENA - CALTECH ATHENAEUM COMP S90W



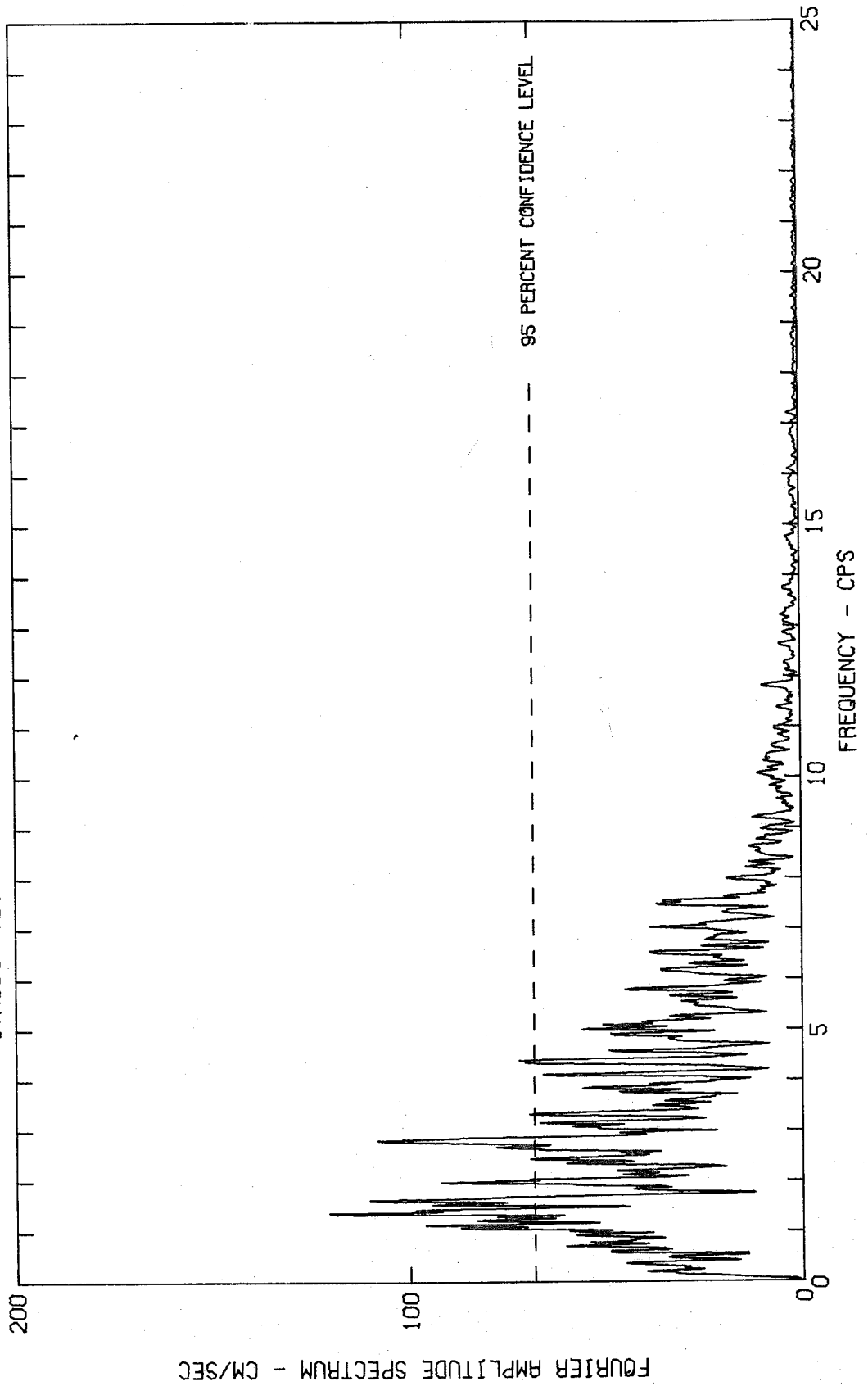
FOURIER AMPLITUDE SPECTRUM OF ACCELERATION
KERN COUNTY, CALIFORNIA EARTHQUAKE JULY 21, 1952 - 0453 PDT
IWA003 52.001.0 PASADENA - CALTECH ATHENAEUM COMP VERT



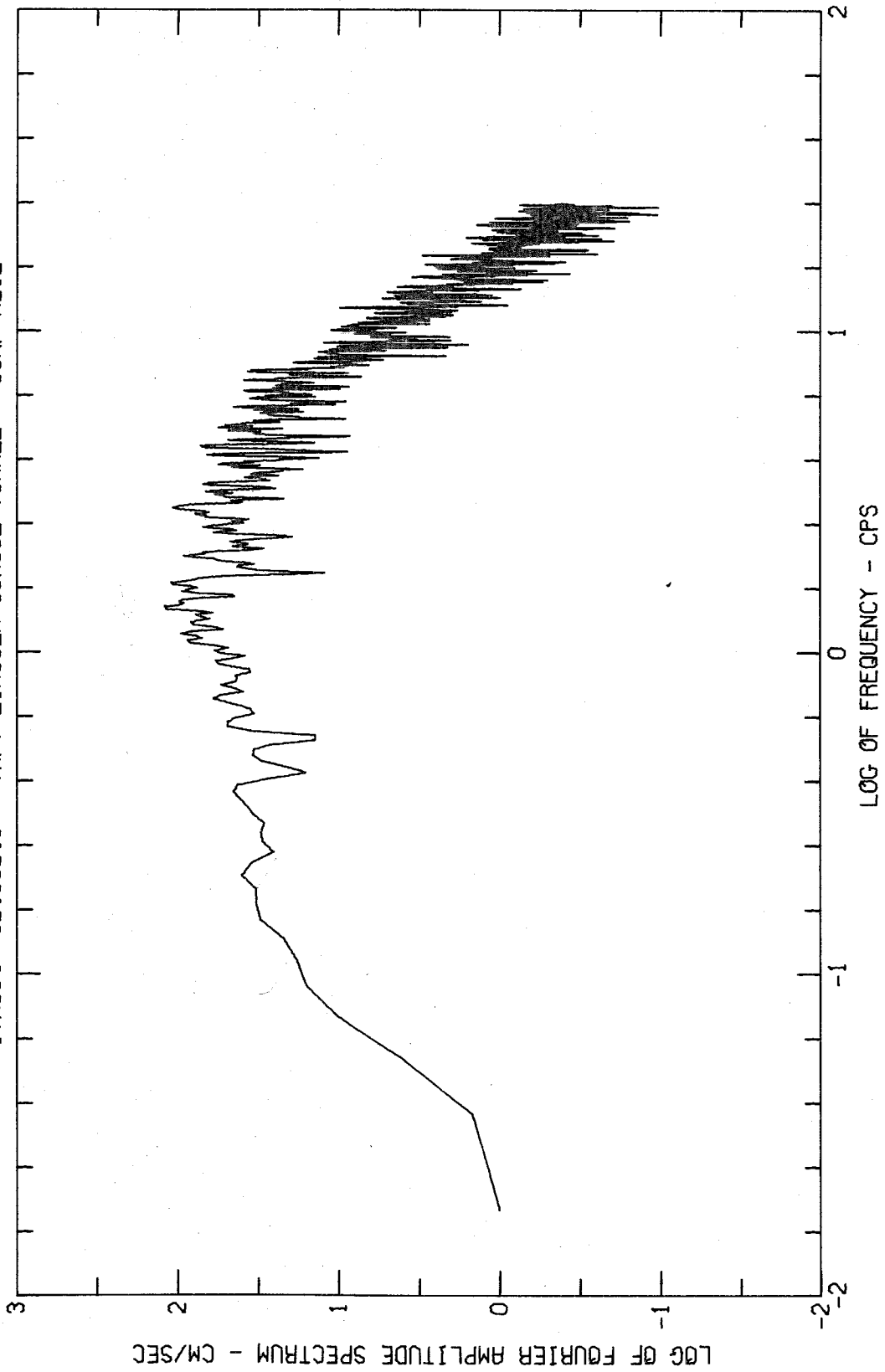
FOURIER AMPLITUDE SPECTRUM OF ACCELERATION
KERN COUNTY, CALIFORNIA EARTHQUAKE JULY 21, 1952 - 0453 PDT
IVA003 52.001.0 PASADENA - CALTECH ATHENAEUM COMP VERT



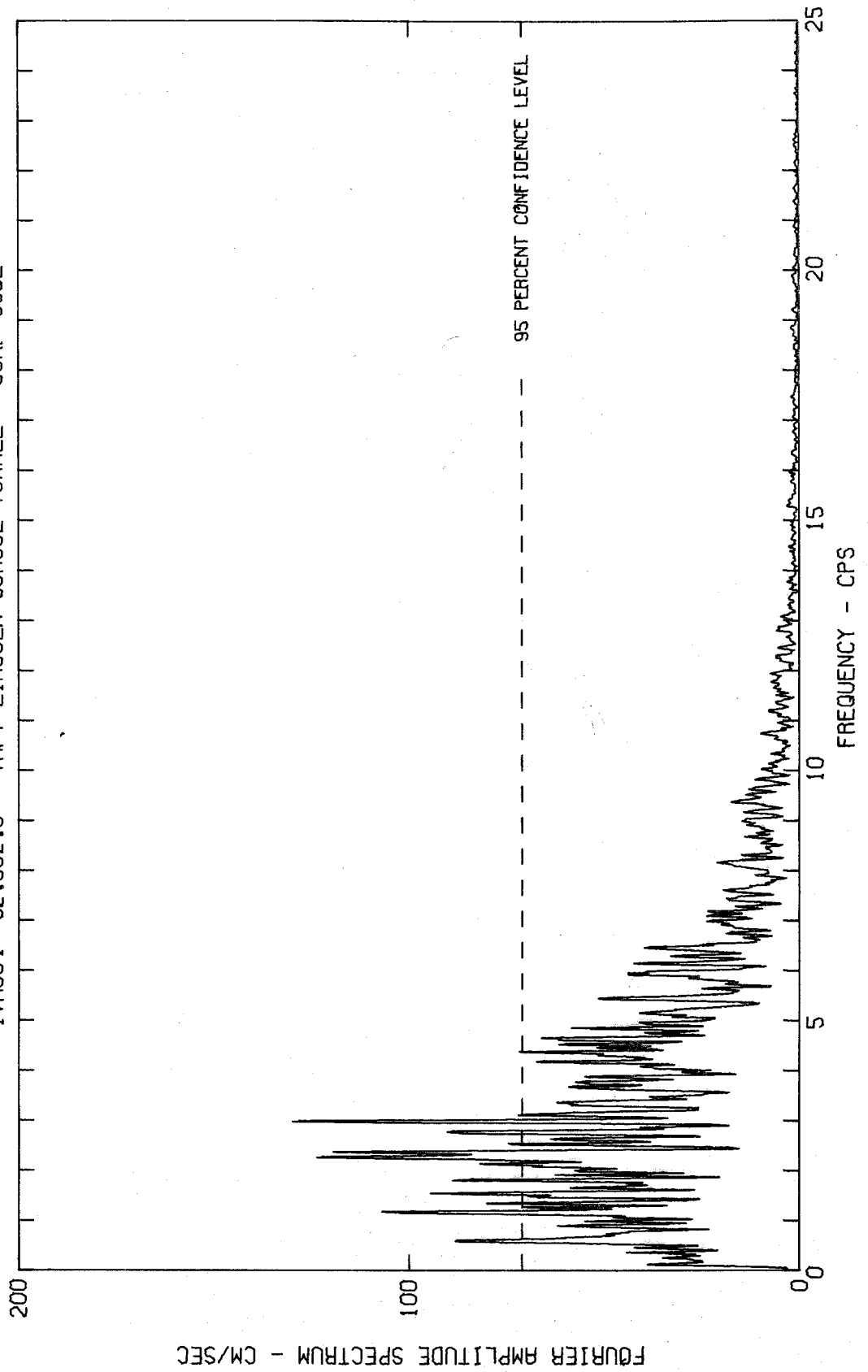
FOURIER AMPLITUDE SPECTRUM OF ACCELERATION
KERN COUNTY, CALIFORNIA EARTHQUAKE JULY 21, 1952 - 0453 PDT
IV0004 52.002.0 TAFT LINCOLN SCHOOL TUNNEL COMP N21E



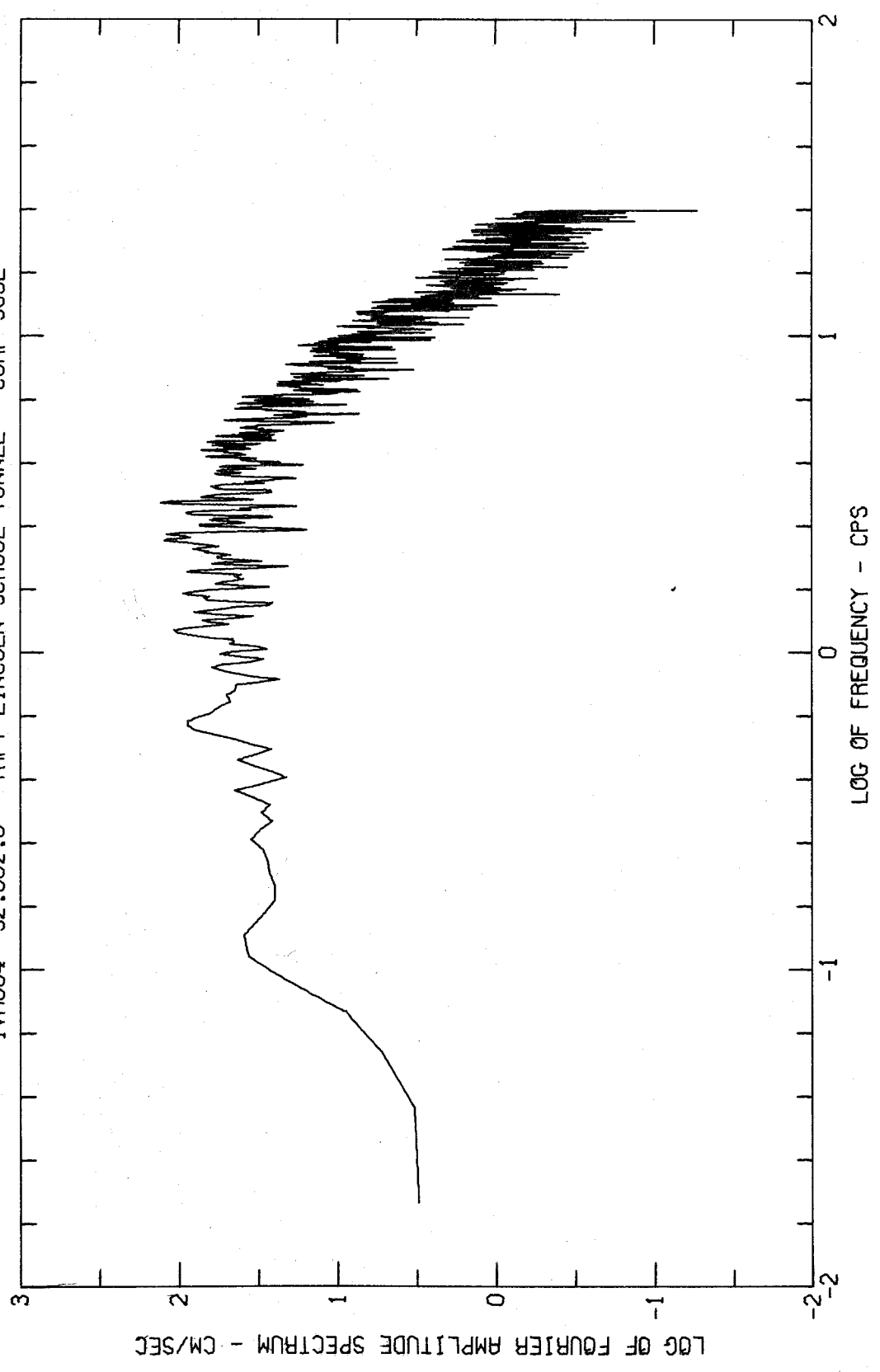
FOURIER AMPLITUDE SPECTRUM OF ACCELERATION
KERN COUNTY, CALIFORNIA EARTHQUAKE JULY 21, 1952 - 0453 PDT
IV0004 52.002.0 TAFT LINCOLN SCHOOL TUNNEL COMP N21E



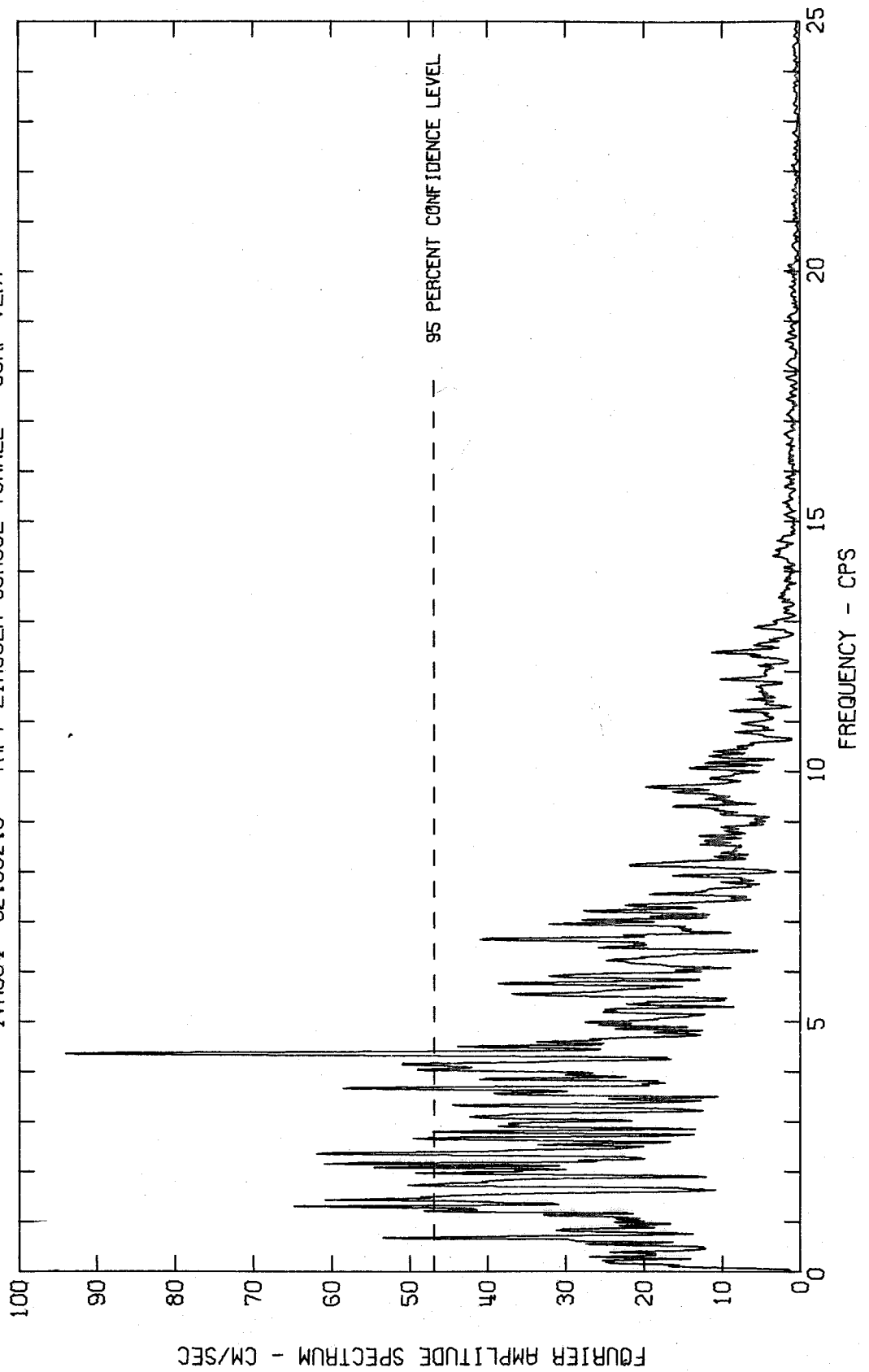
FOURIER AMPLITUDE SPECTRUM OF ACCELERATION
KERN COUNTY, CALIFORNIA EARTHQUAKE JULY 21, 1952 - 0453 PDT
IVA004 52.002.0 TAFT LINCOLN SCHOOL TUNNEL COMP S69E



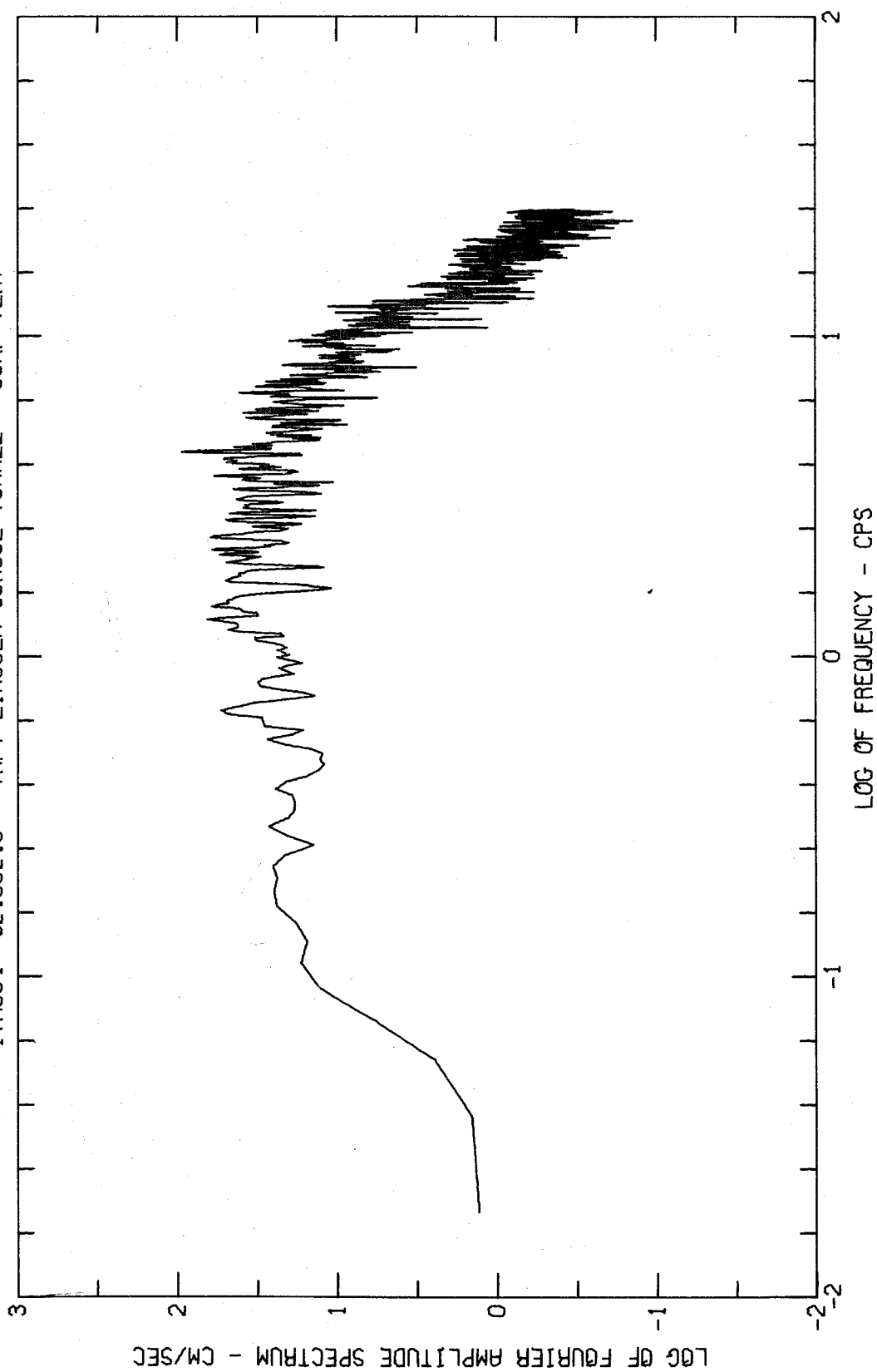
FOURIER AMPLITUDE SPECTRUM OF ACCELERATION
KERN COUNTY, CALIFORNIA EARTHQUAKE JULY 21, 1952 - 0453 PDT
IVAC004 52.002.0 TAFT LINCOLN SCHOOL TUNNEL COMP S69E



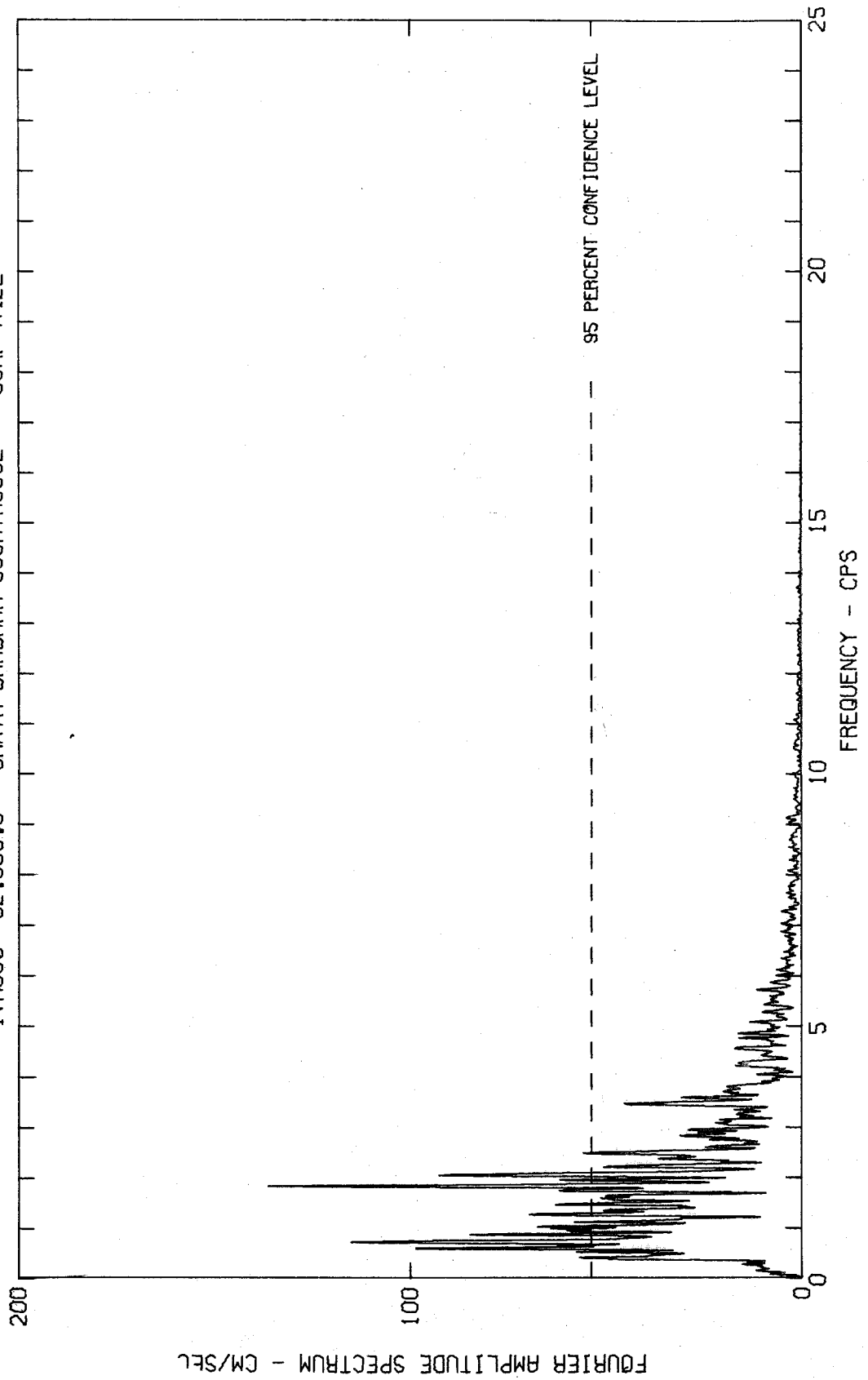
FOURIER AMPLITUDE SPECTRUM OF ACCELERATION
KERN COUNTY, CALIFORNIA EARTHQUAKE JULY 21, 1952 - 0453 PDT
IV0004 52.002.0 TAFT LINCOLN SCHOOL TUNNEL COMP VERT



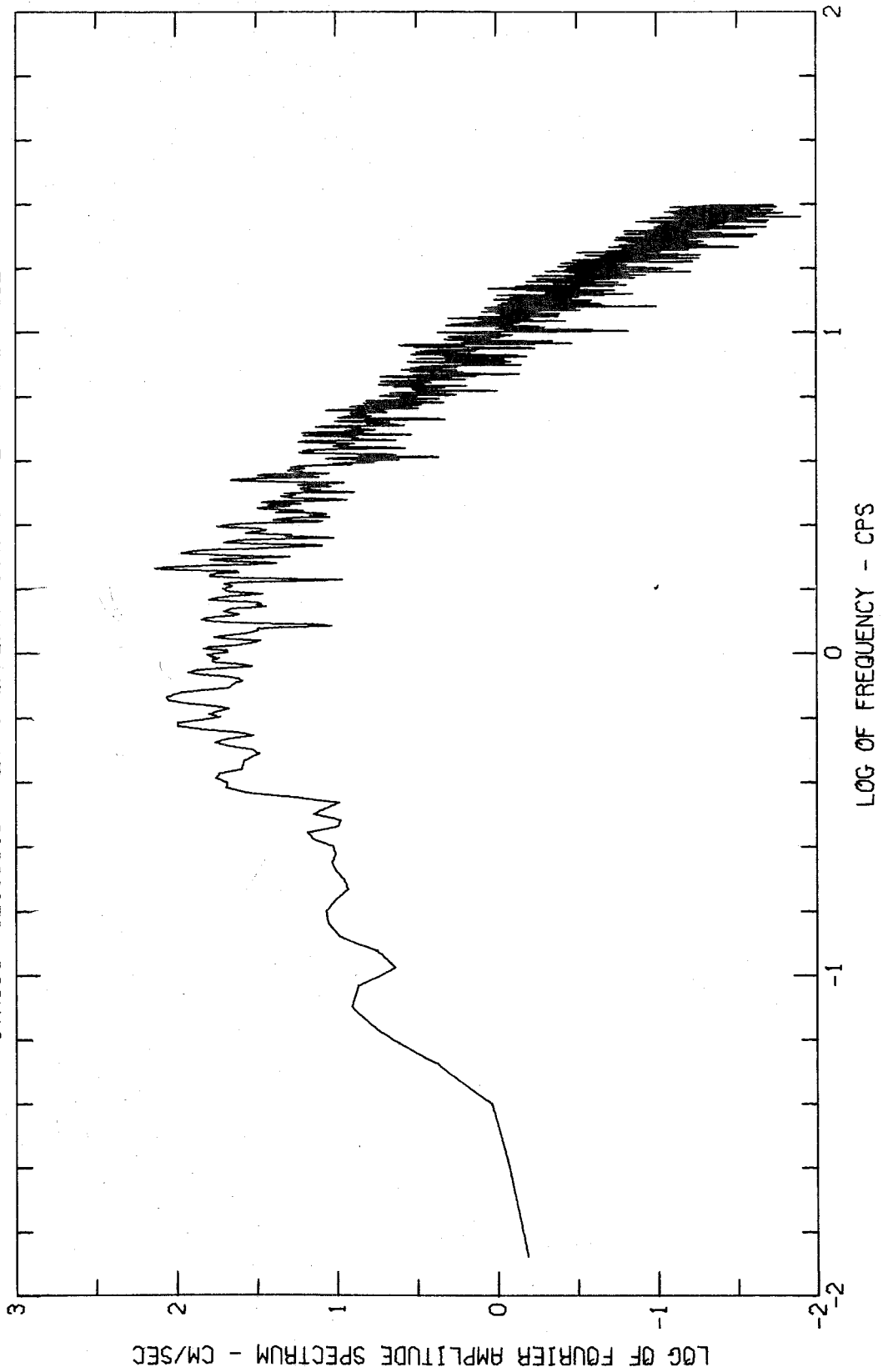
FOURIER AMPLITUDE SPECTRUM OF ACCELERATION
KERN COUNTY, CALIFORNIA EARTHQUAKE JULY 21, 1952 - 0453 PDT
IV0004 52.002.0 TAFT LINCOLN SCHOOL TUNNEL COMP VERT



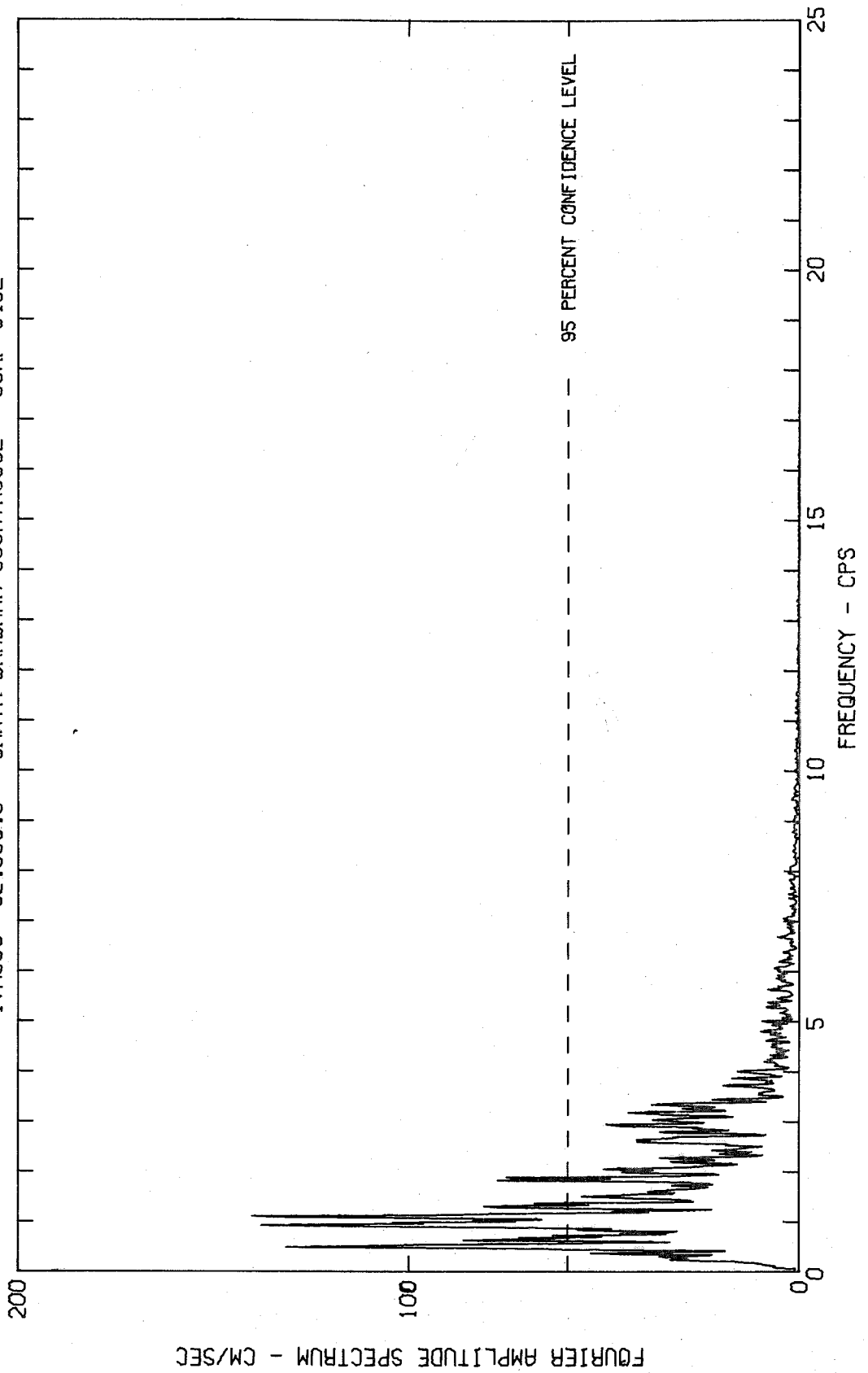
FOURIER AMPLITUDE SPECTRUM OF ACCELERATION
KERN COUNTY, CALIFORNIA EARTHQUAKE JULY 21, 1952 - 0453 PDT
IV0005 52.003.0 SANTA BARBARA COURTHOUSE COMP N42E



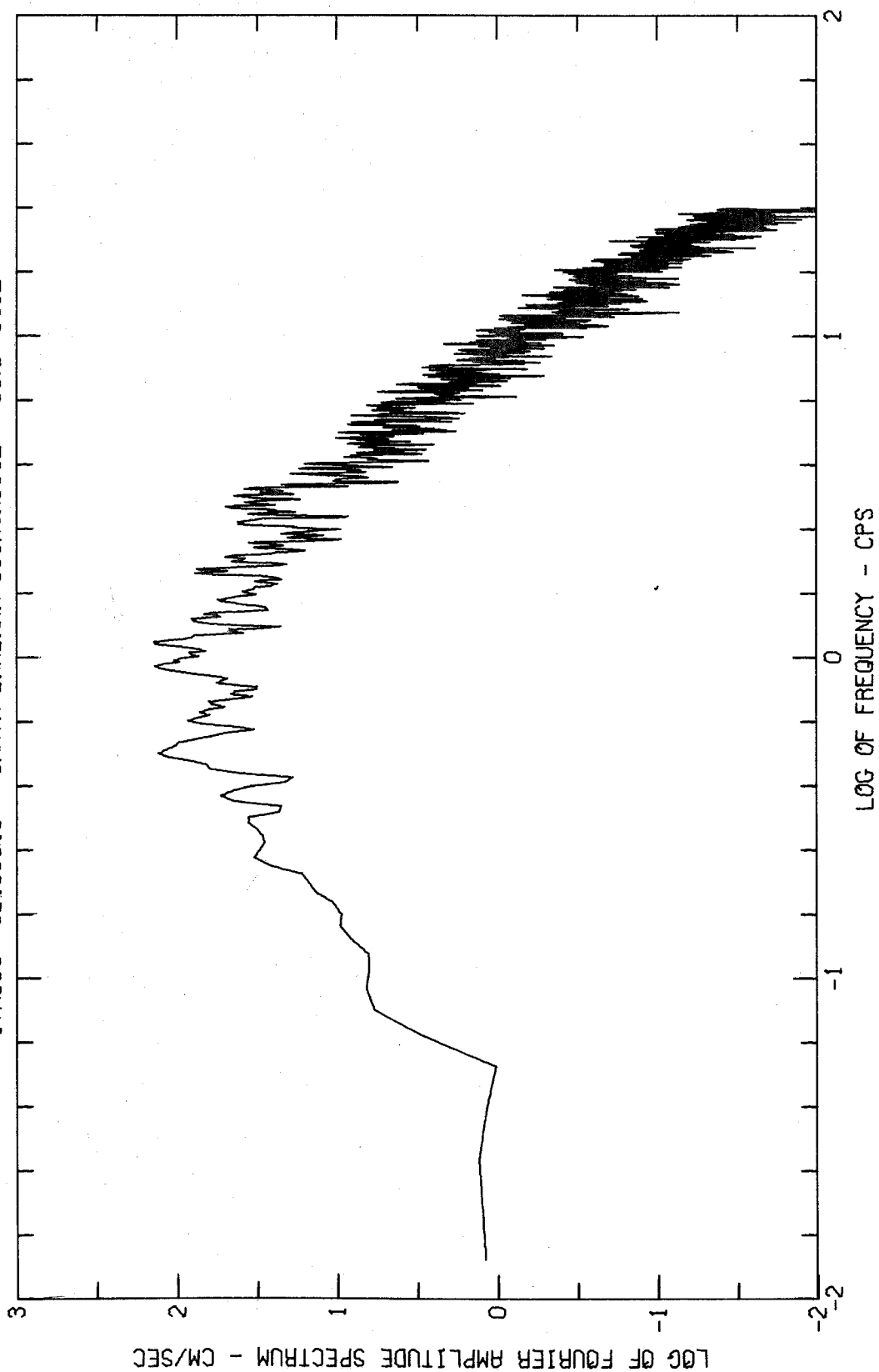
FOURIER AMPLITUDE SPECTRUM OF ACCELERATION
KERN COUNTY, CALIFORNIA EARTHQUAKE JULY 21, 1952 - 0453 PDT
IV0005 52.003.0 SANTA BARBARA COURTHOUSE COMP N42E



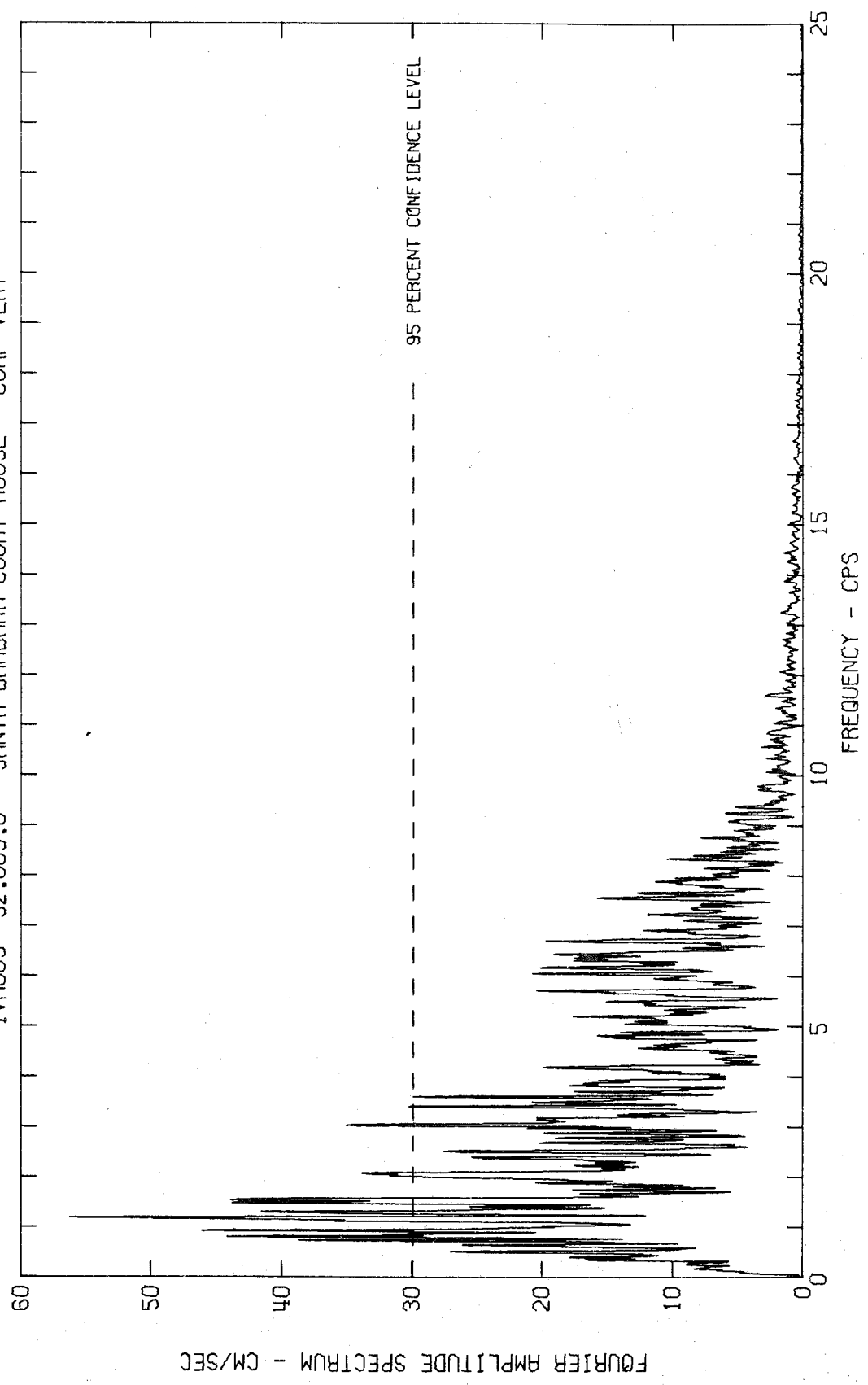
FOURIER AMPLITUDE SPECTRUM OF ACCELERATION
KERN COUNTY, CALIFORNIA EARTHQUAKE JULY 21, 1952 - 0453 PDT
IV0005 52.003.0 SANTA BARBARA COURTHOUSE COMP S48E



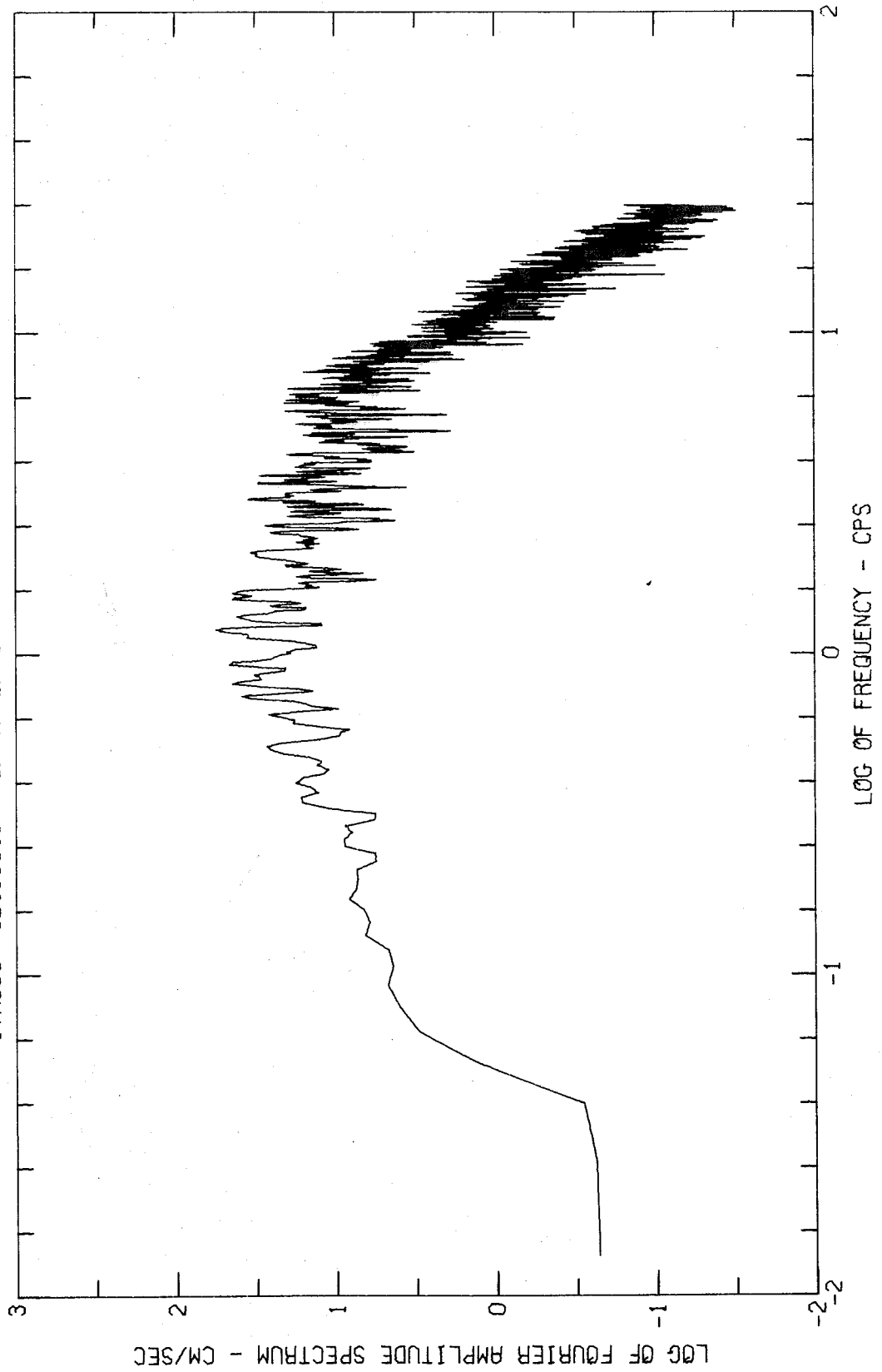
FOURIER AMPLITUDE SPECTRUM OF ACCELERATION
KERN COUNTY, CALIFORNIA EARTHQUAKE JULY 21, 1952 - 0453 PDT
1VA005 52.003.0 SANTA BARBARA COURTHOUSE COMP S48E



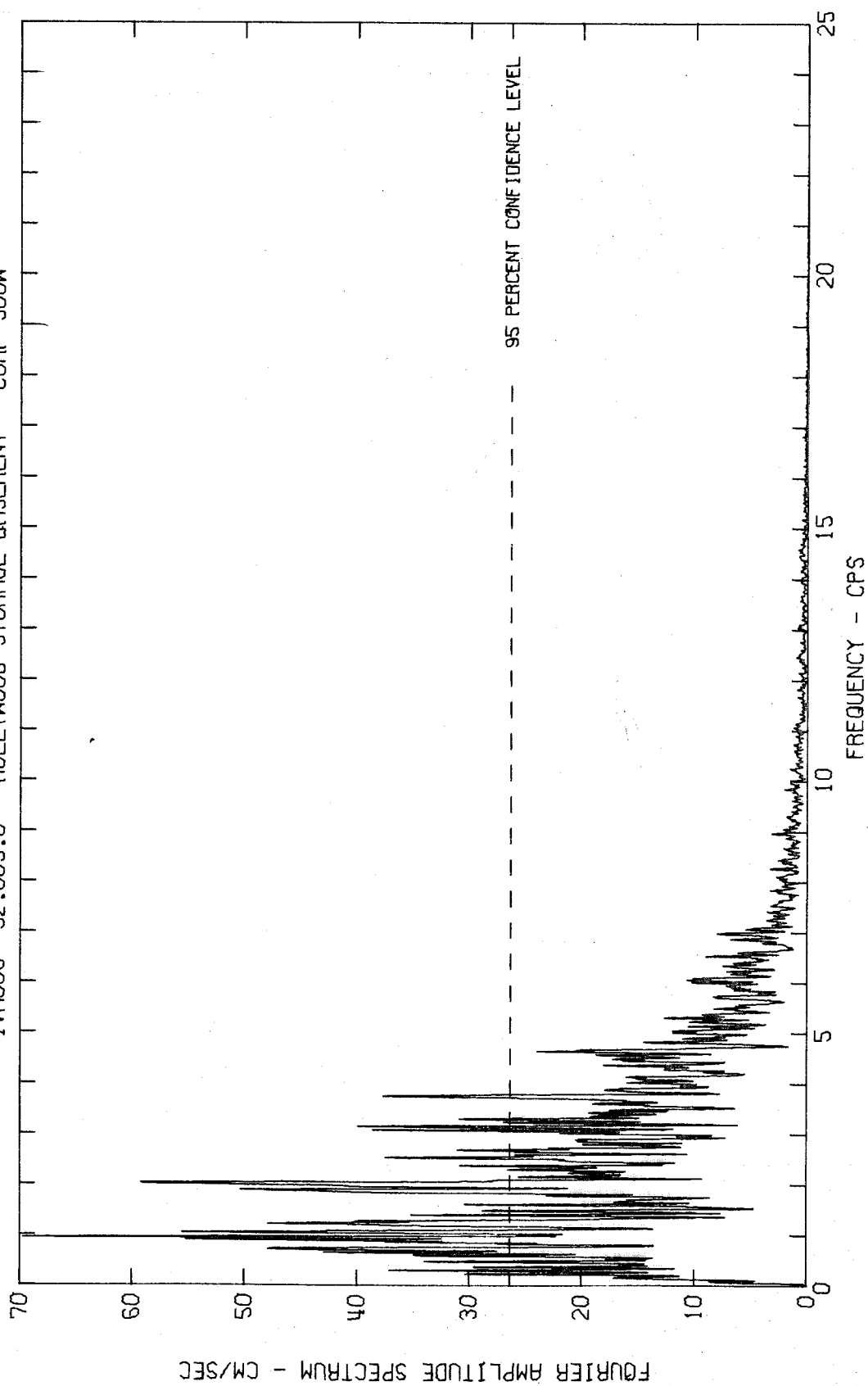
FOURIER AMPLITUDE SPECTRUM OF ACCELERATION
KERN COUNTY, CALIFORNIA EARTHQUAKE JULY 21, 1952 - 0453 PDT
IWA005 52.003.0 SANTA BARBARA COURT HOUSE COMP VERT



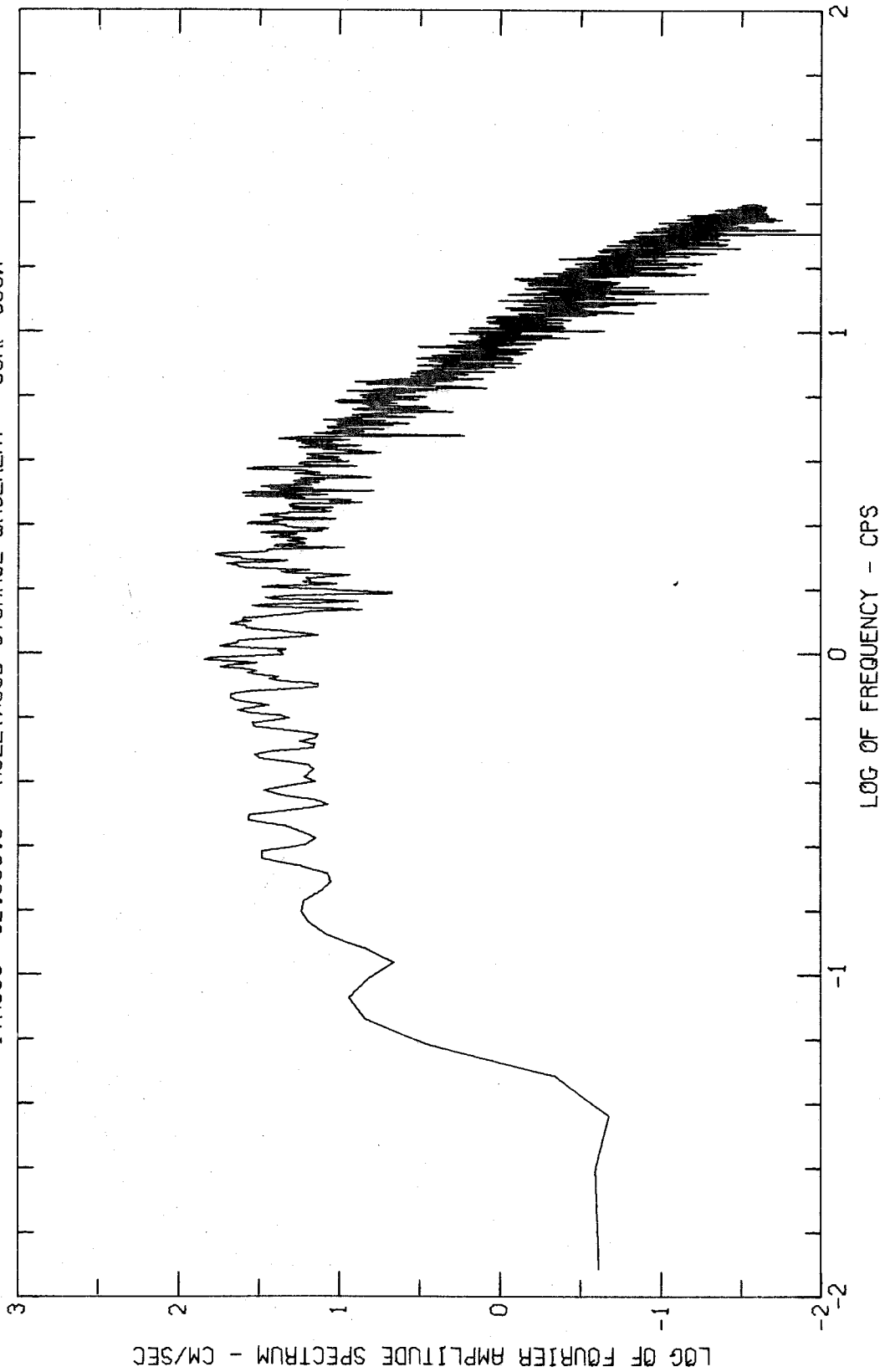
FOURIER AMPLITUDE SPECTRUM OF ACCELERATION
KERN COUNTY, CALIFORNIA EARTHQUAKE JULY 21, 1952 - 04:53 PDT
IVA005 52.003.0 SANTA BARBARA COURT HOUSE COMP VERT



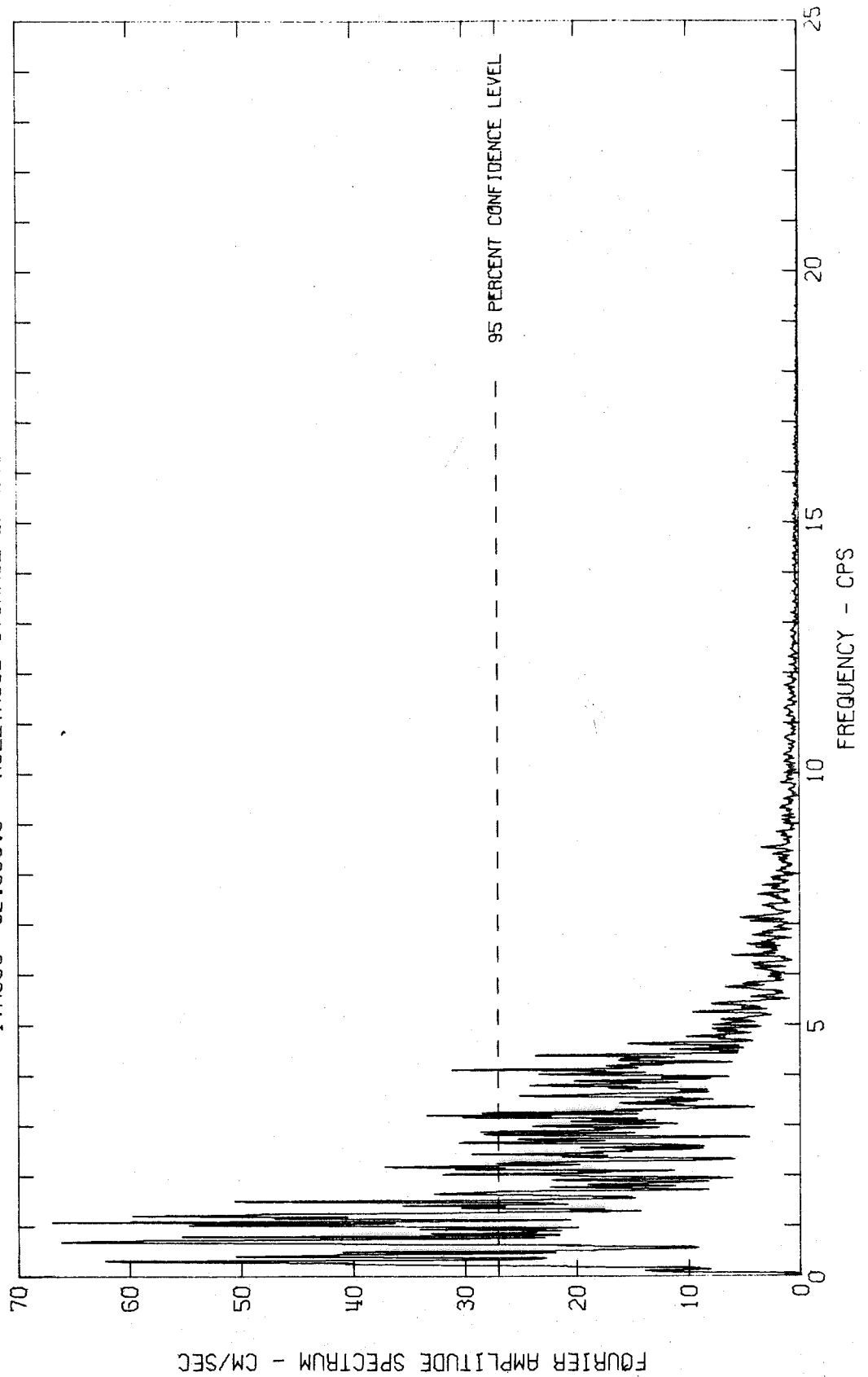
FOURIER AMPLITUDE SPECTRUM OF ACCELERATION
KERN COUNTY, CALIFORNIA EARTHQUAKE JULY 21, 1952 - 0453 PDT
IWA006 52.005.0 HOLLYWOOD STORAGE BASEMENT COMP S00W



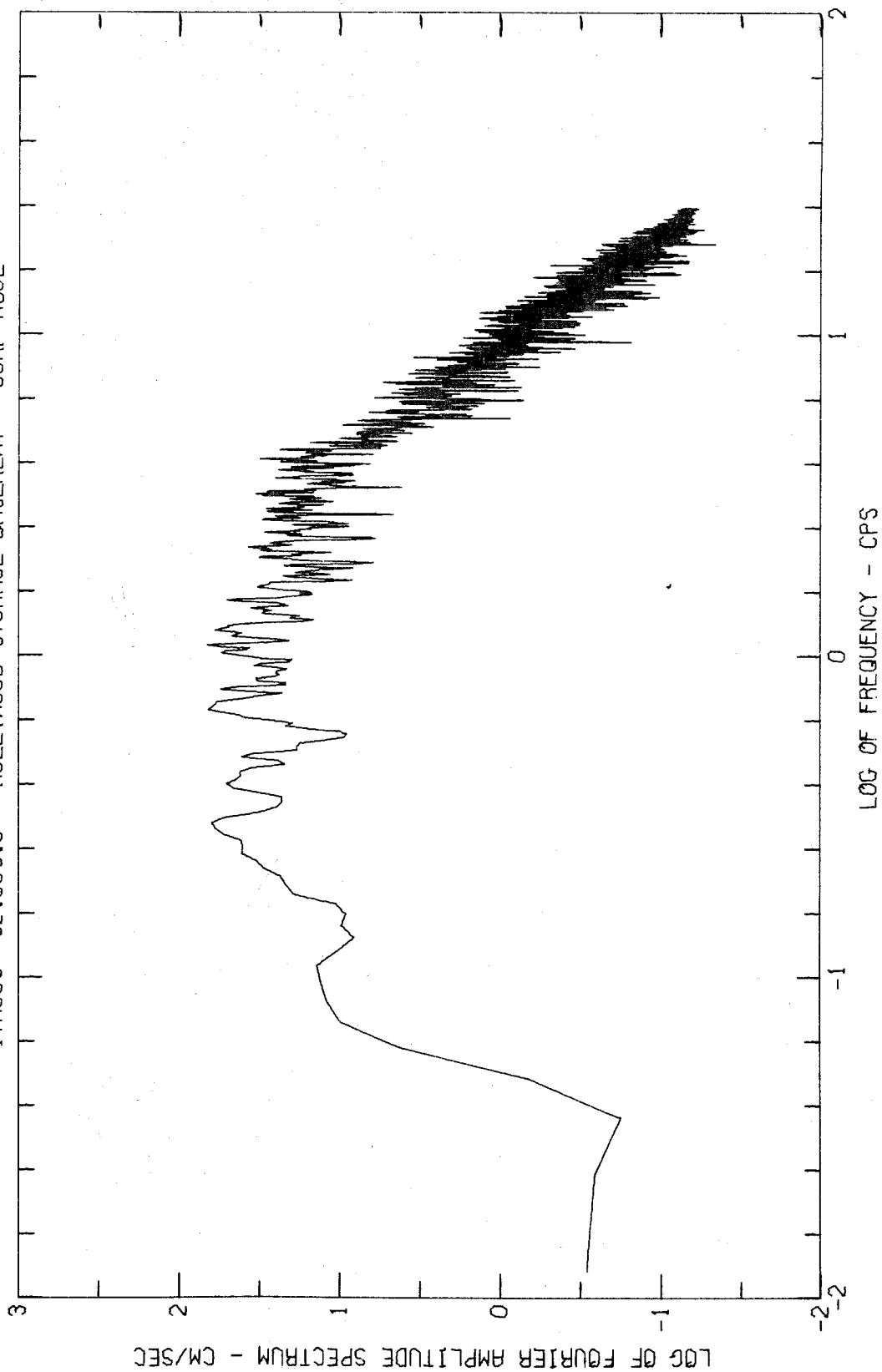
FOURIER AMPLITUDE SPECTRUM OF ACCELERATION
KERN COUNTY, CALIFORNIA EARTHQUAKE JULY 21, 1952 - 0453 PDT
IVA006 52.005.0 HOLLYWOOD STORAGE BASEMENT COMP 500W



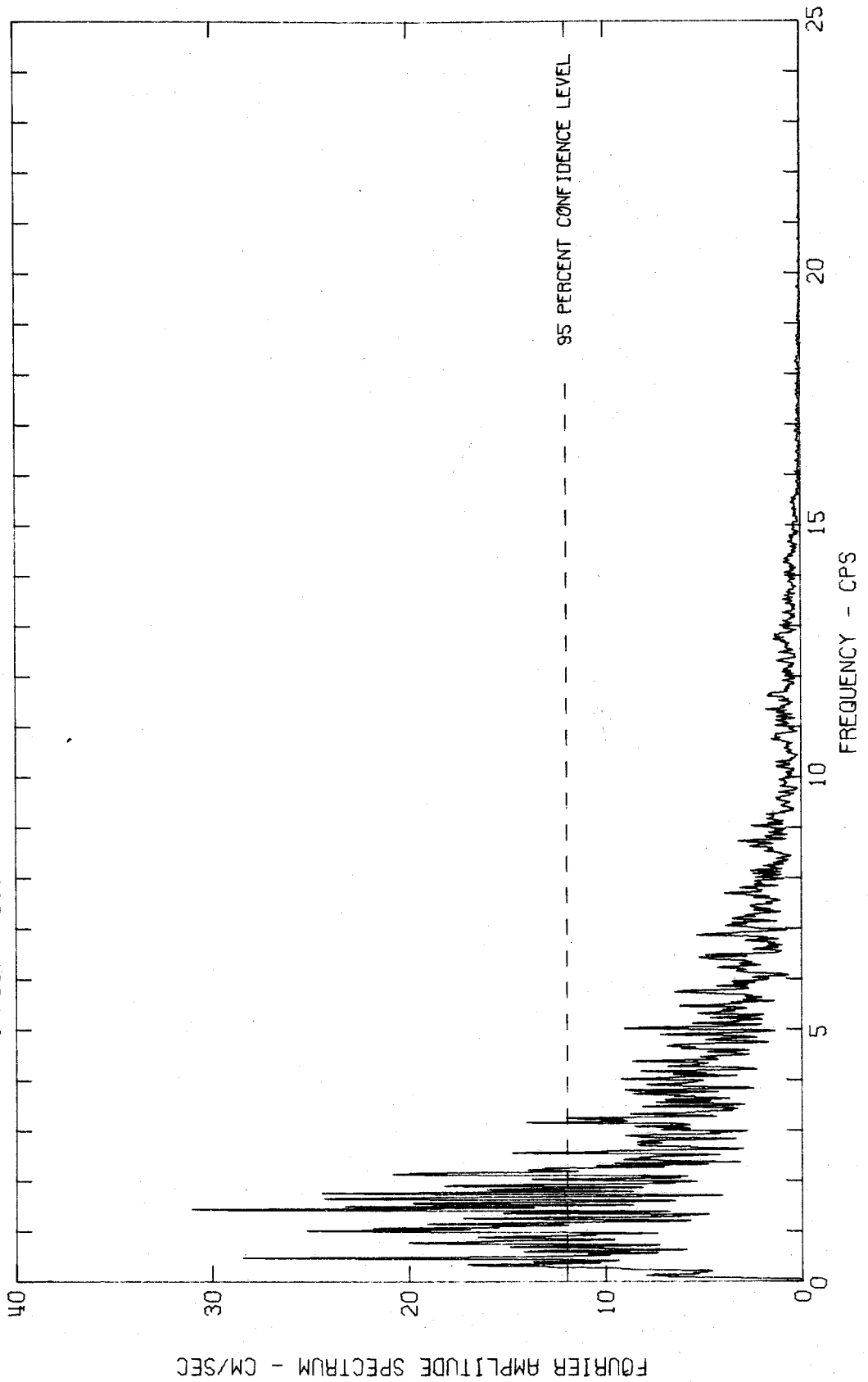
FOURIER AMPLITUDE SPECTRUM OF ACCELERATION
KERN COUNTY, CALIFORNIA EARTHQUAKE JULY 21, 1952 - 0453 PDT
IWA006 52.005.0 HOLLYWOOD STORAGE BASEMENT COMP N90E



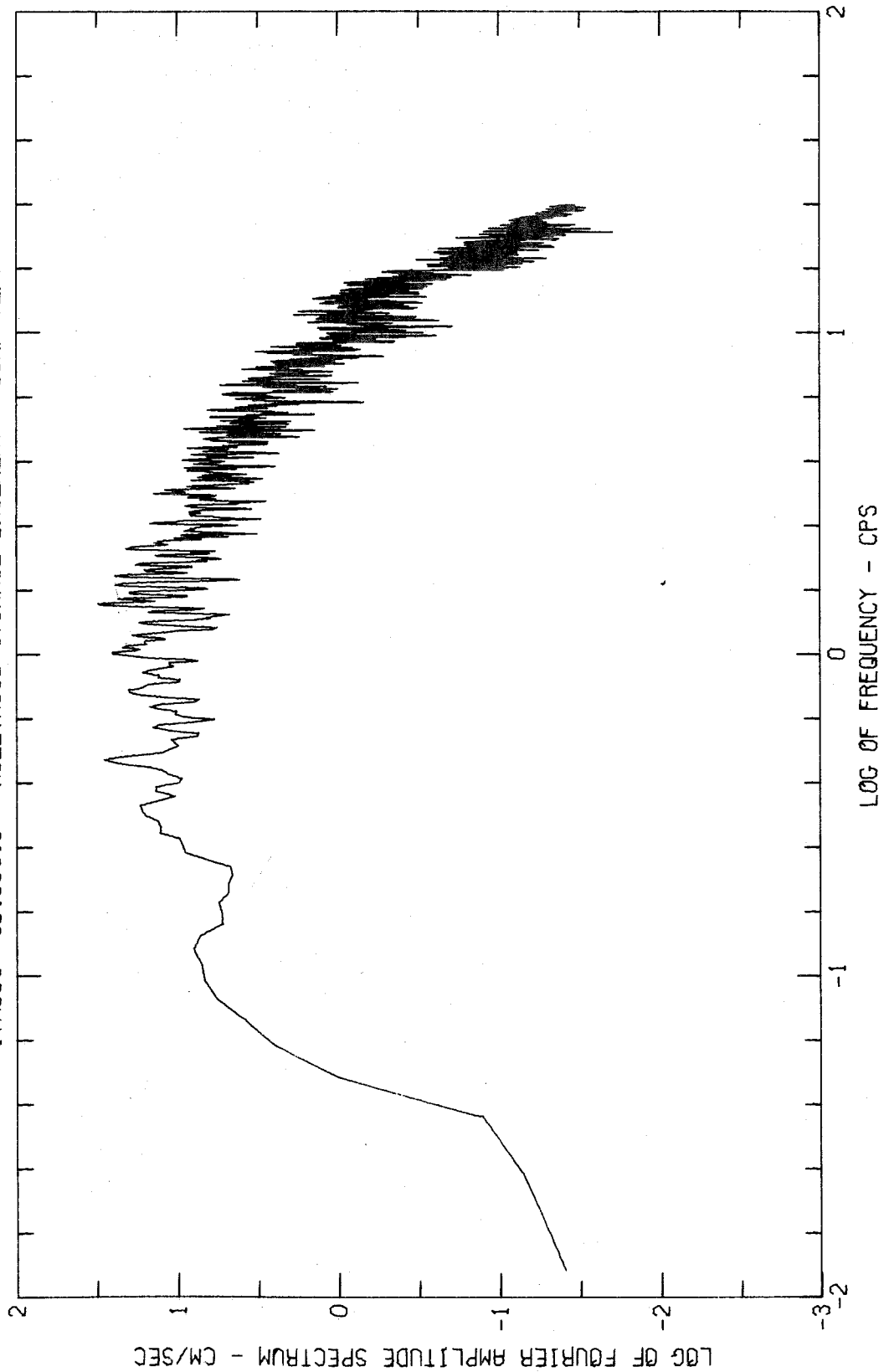
FOURIER AMPLITUDE SPECTRUM OF ACCELERATION
KERN COUNTY, CALIFORNIA EARTHQUAKE JULY 21, 1952 - 0453 PDT
IVA006 52.005.0 HOLLYWOOD STORAGE BASEMENT COMP NSOE



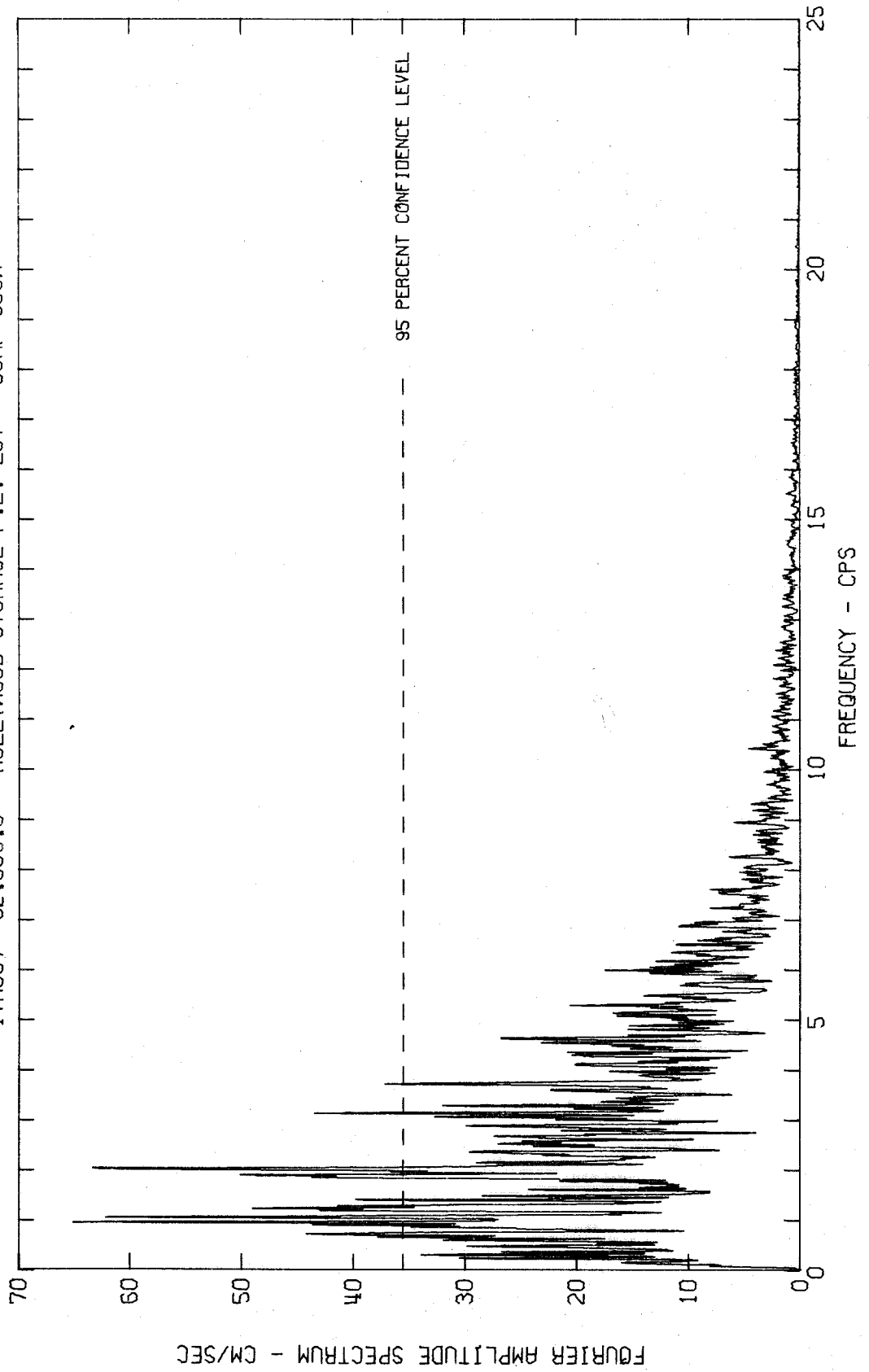
FOURIER AMPLITUDE SPECTRUM OF ACCELERATION
KERN COUNTY, CALIFORNIA EARTHQUAKE JULY 21, 1952 - 0453 PDT
IV0006 52.005.0 HOLLYWOOD STORAGE BASEMENT COMP VERT



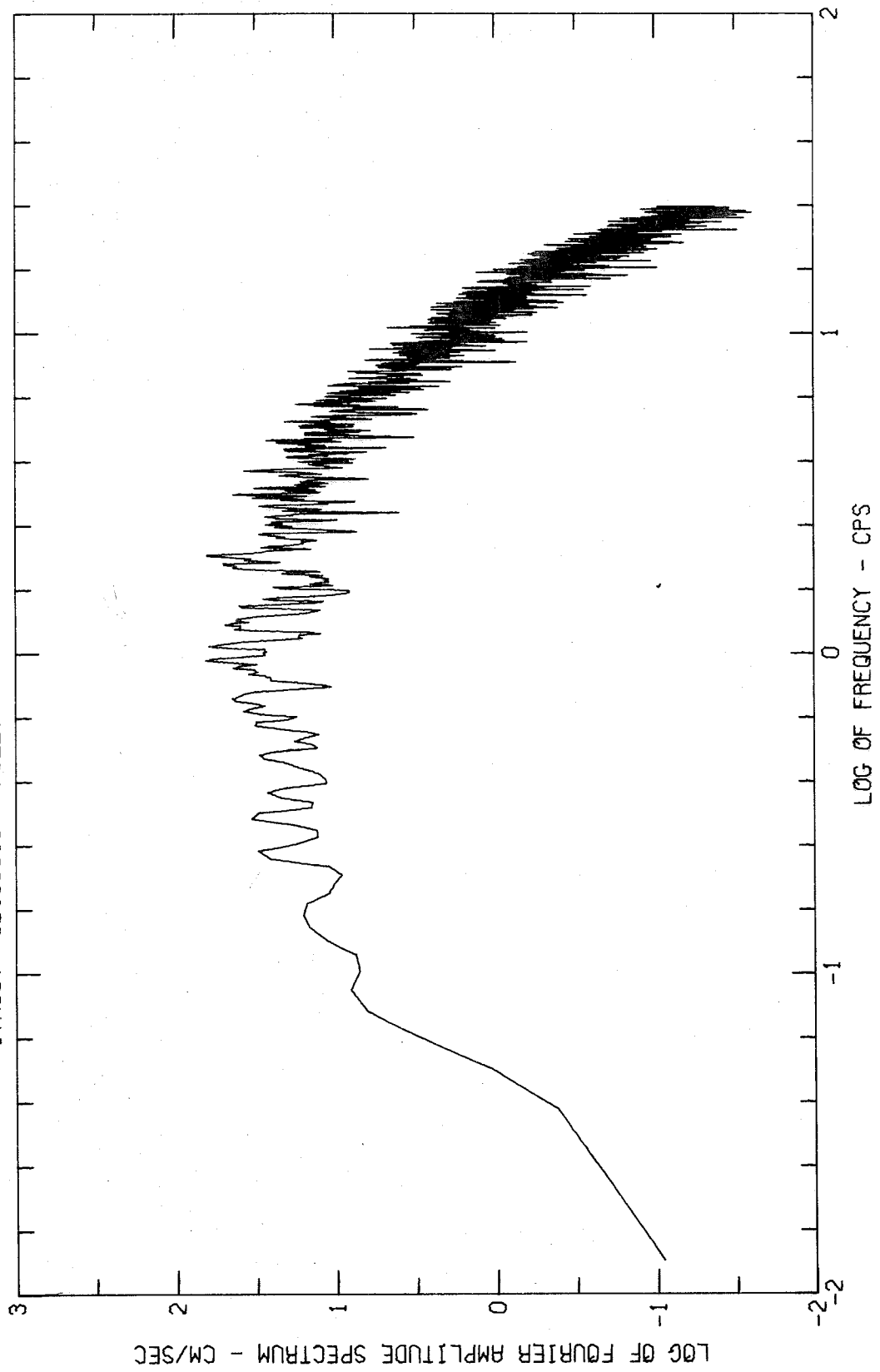
FOURIER AMPLITUDE SPECTRUM OF ACCELERATION
KERN COUNTY, CALIFORNIA EARTHQUAKE JULY 21, 1952 - 0453 PDT
IVAC05 52.005.0 HOLLYWOOD STORAGE BASEMENT COMP VERT



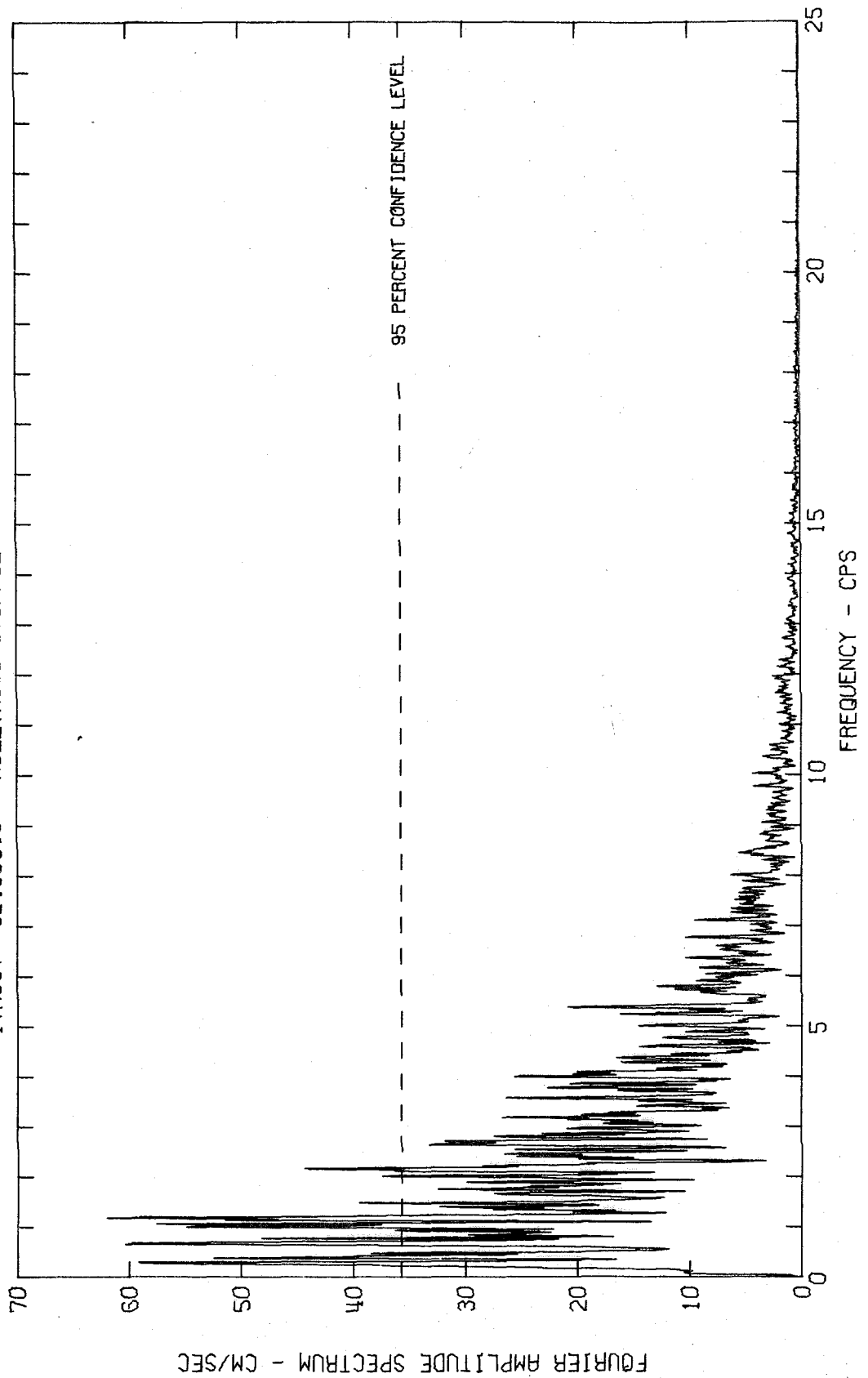
FOURIER AMPLITUDE SPECTRUM OF ACCELERATION
KERN COUNTY, CALIFORNIA EARTHQUAKE JULY 21, 1952 - 0453 PDT
IVR007 52.006.0 HOLLYWOOD STORAGE P.E. LOT COMP S00W



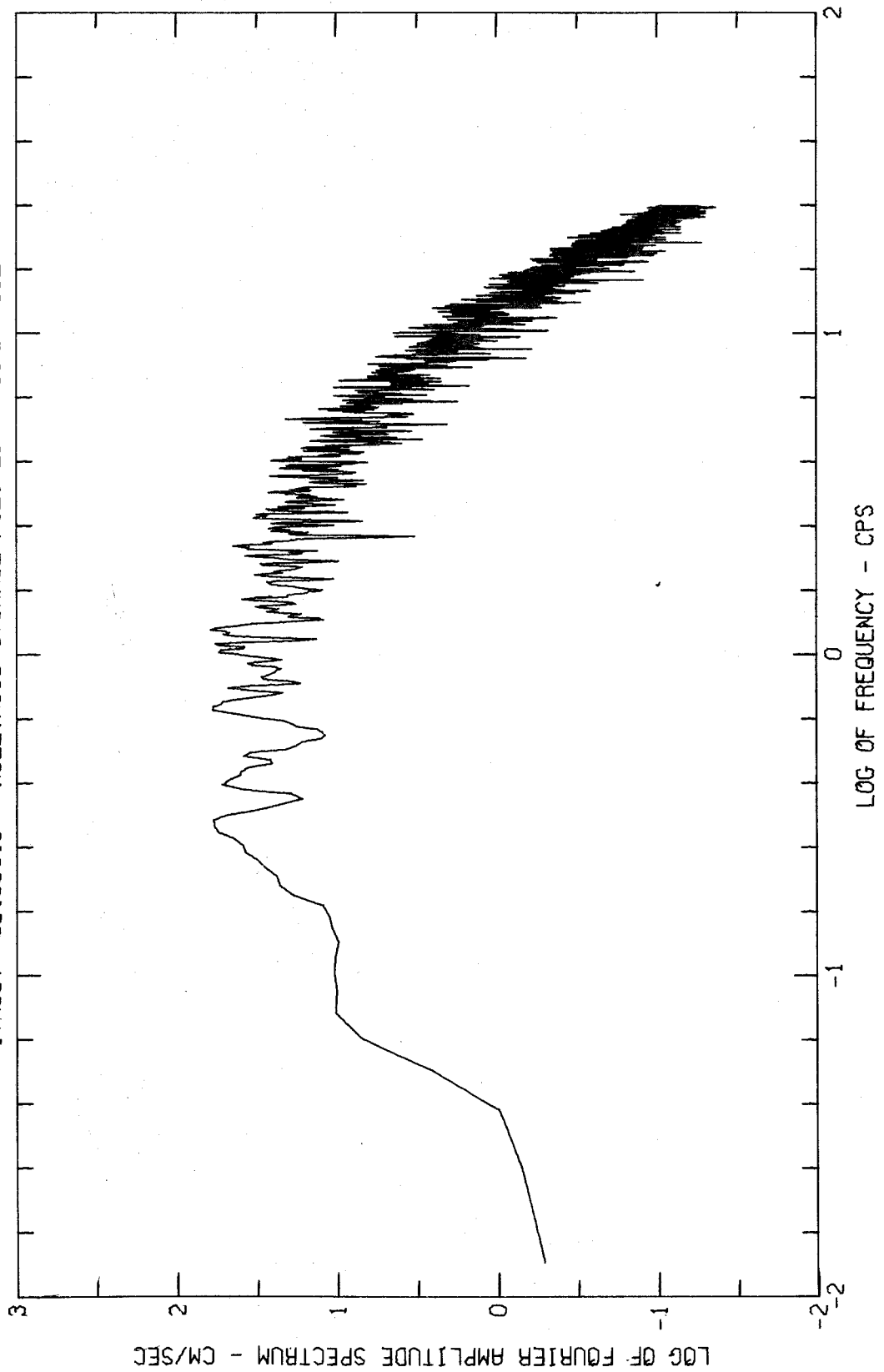
FOURIER AMPLITUDE SPECTRUM OF ACCELERATION
KERN COUNTY, CALIFORNIA EARTHQUAKE JULY 21, 1952 - 0453 PDT
IVAC07 52.006.0 HOLLYWOOD STORAGE P.E. LOT COMP 500W



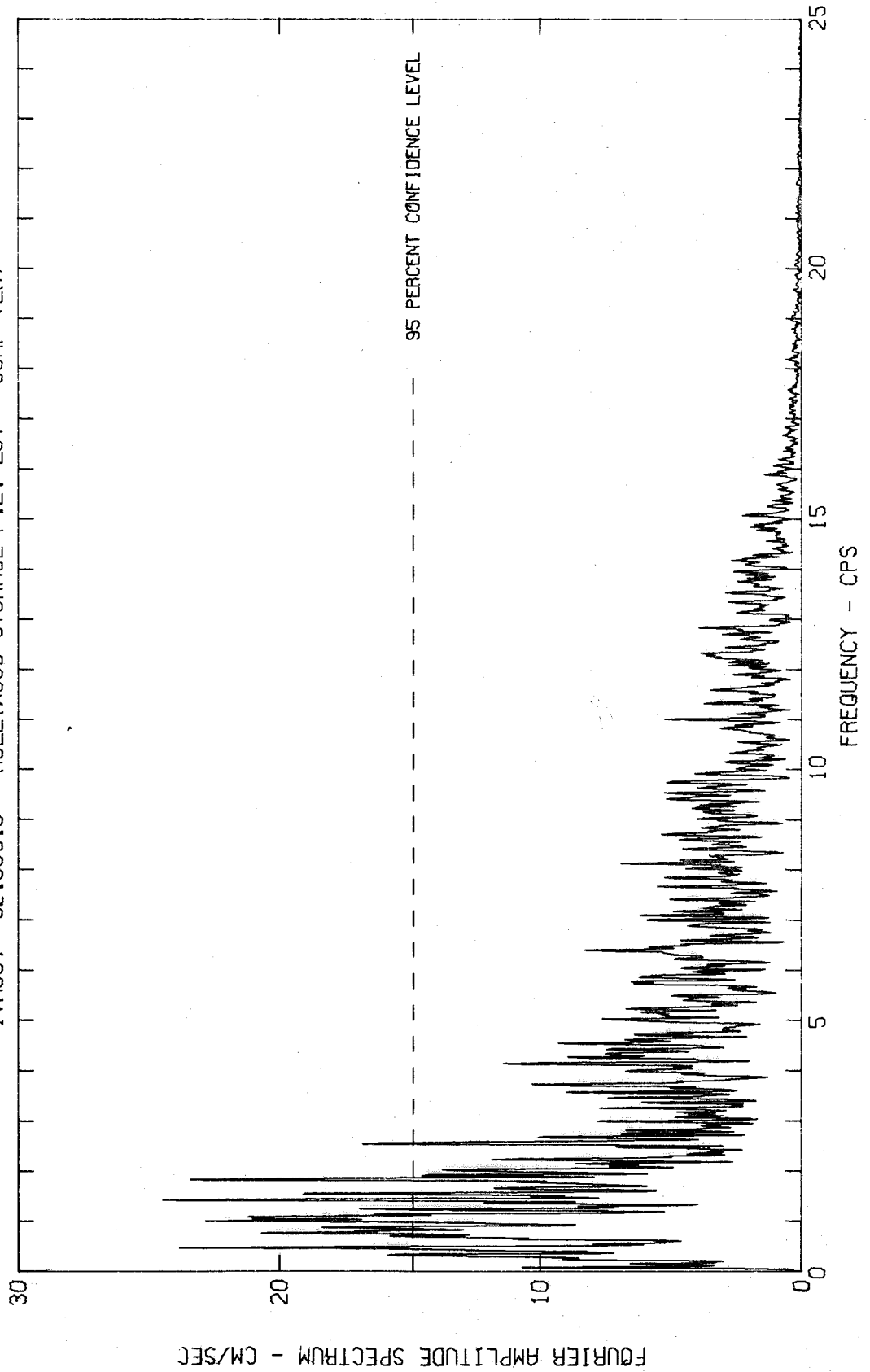
FOURIER AMPLITUDE SPECTRUM OF ACCELERATION
KERN COUNTY, CALIFORNIA EARTHQUAKE JULY 21, 1952 - 0453 PDT
IVA007 52.006.0 HOLLYWOOD STORAGE P.E. LOT COMP N90E



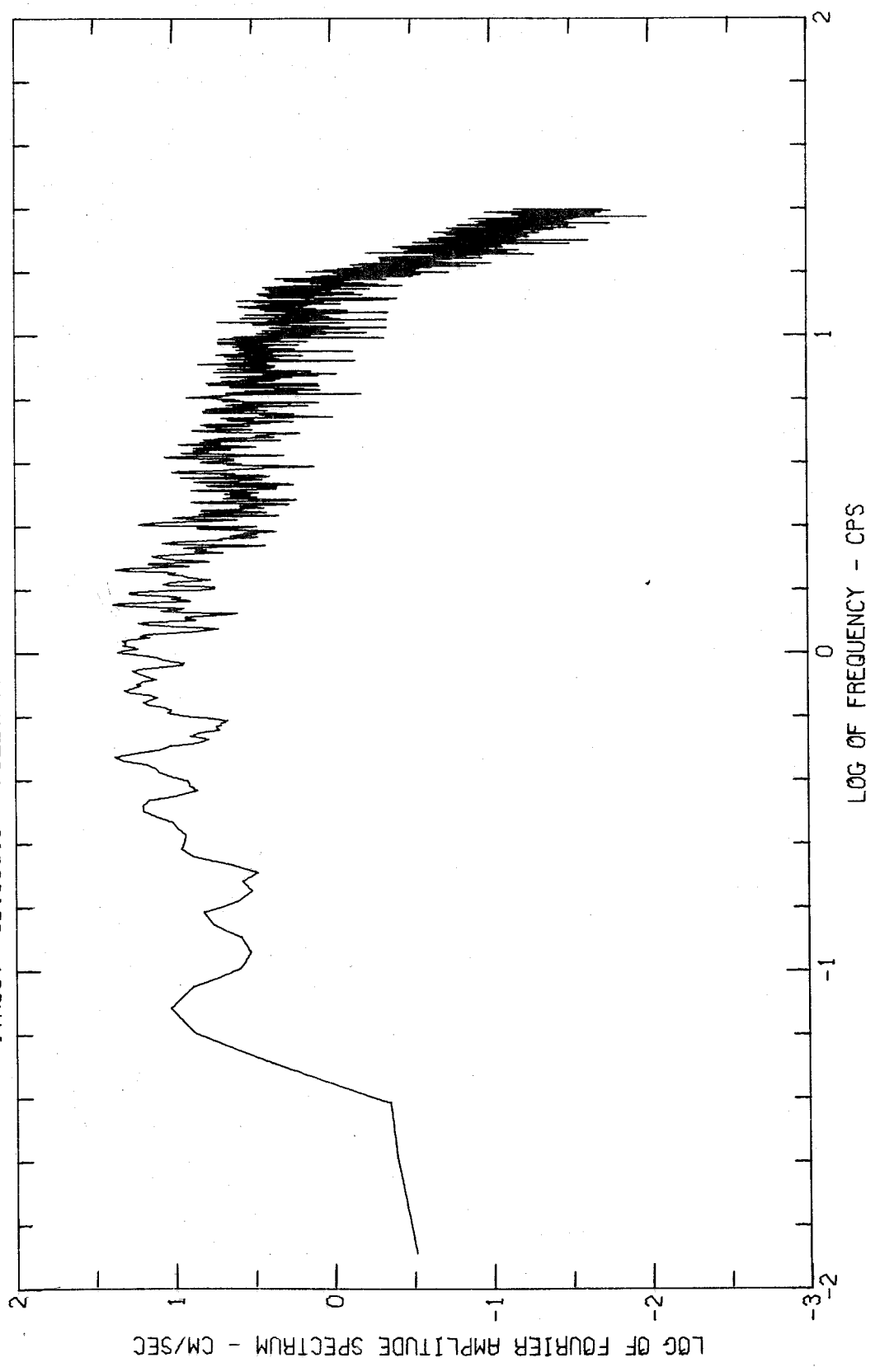
FOURIER AMPLITUDE SPECTRUM OF ACCELERATION
KERN COUNTY, CALIFORNIA EARTHQUAKE JULY 21, 1952 - 0453 POT
IVA007 52.006.0 HOLLYWOOD STORAGE P.E. LOT COMP N90E



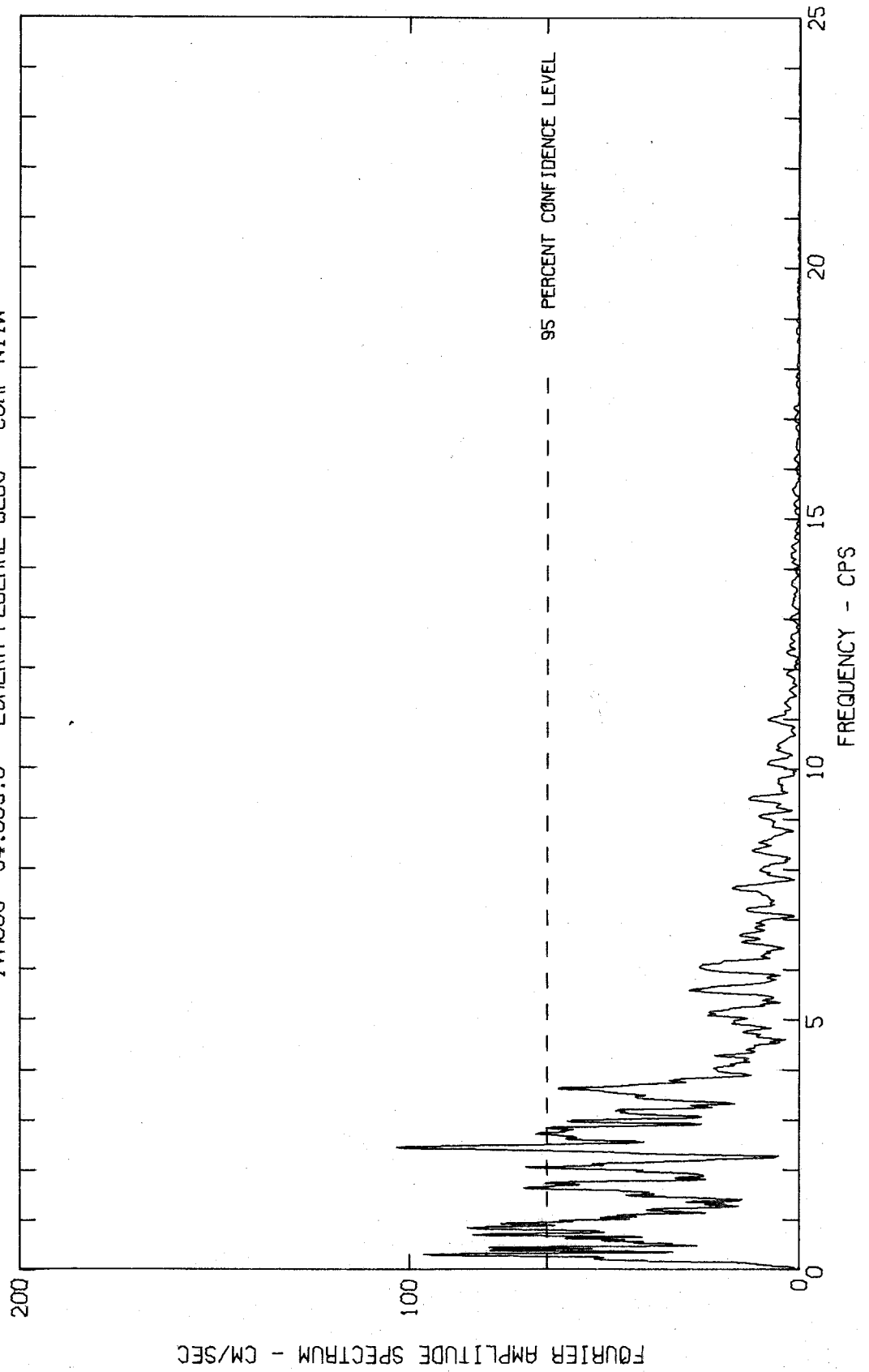
FOURIER AMPLITUDE SPECTRUM OF ACCELERATION
KERN COUNTY, CALIFORNIA EARTHQUAKE JULY 21, 1952 - 0453 PDT
IVAD07 52.006.0 HOLLYWOOD STORAGE P.E. LOT COMP VERT



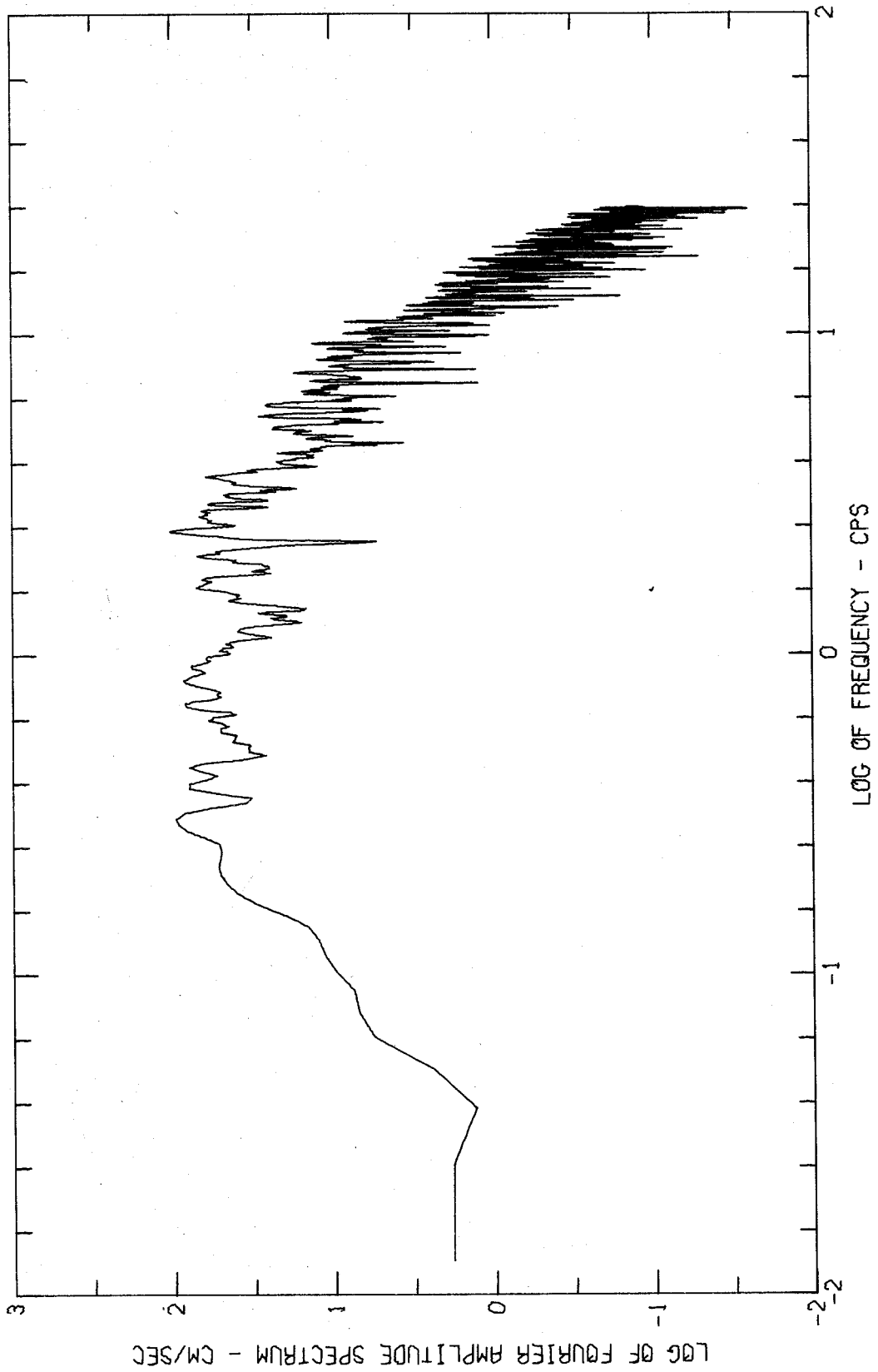
FOURIER AMPLITUDE SPECTRUM OF ACCELERATION
KERN COUNTY, CALIFORNIA EARTHQUAKE JULY 21, 1952 - 0453 PDT
JVA007 52.006.0 HOLLYWOOD STORAGE P.E. LOT COMP VERT



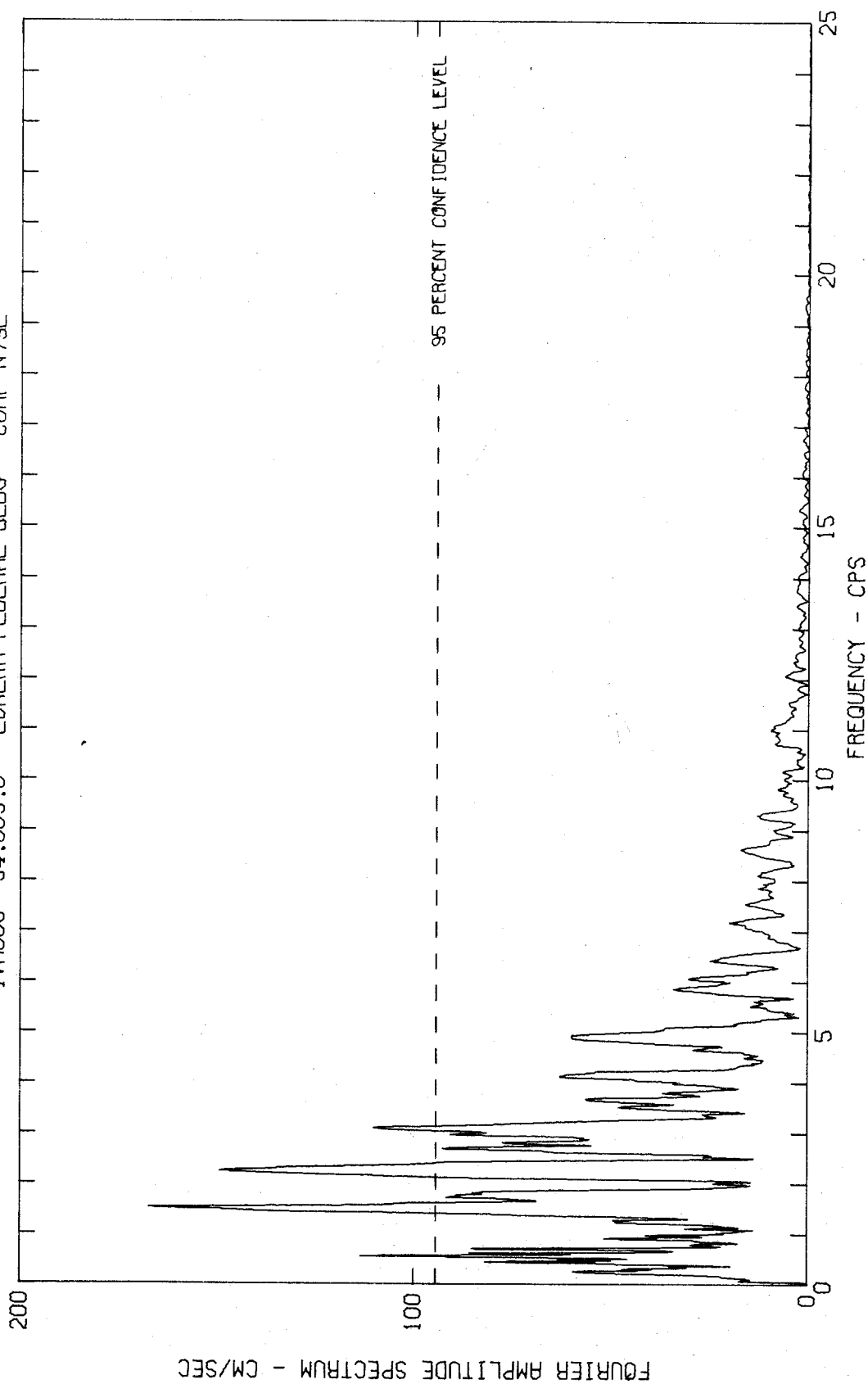
FOURIER AMPLITUDE SPECTRUM OF ACCELERATION
EUREKA EARTHQUAKE DEC 21, 1954 - 1156 PST
IVR008 54.003.0 EUREKA FEDERAL BLDG COMP N11W



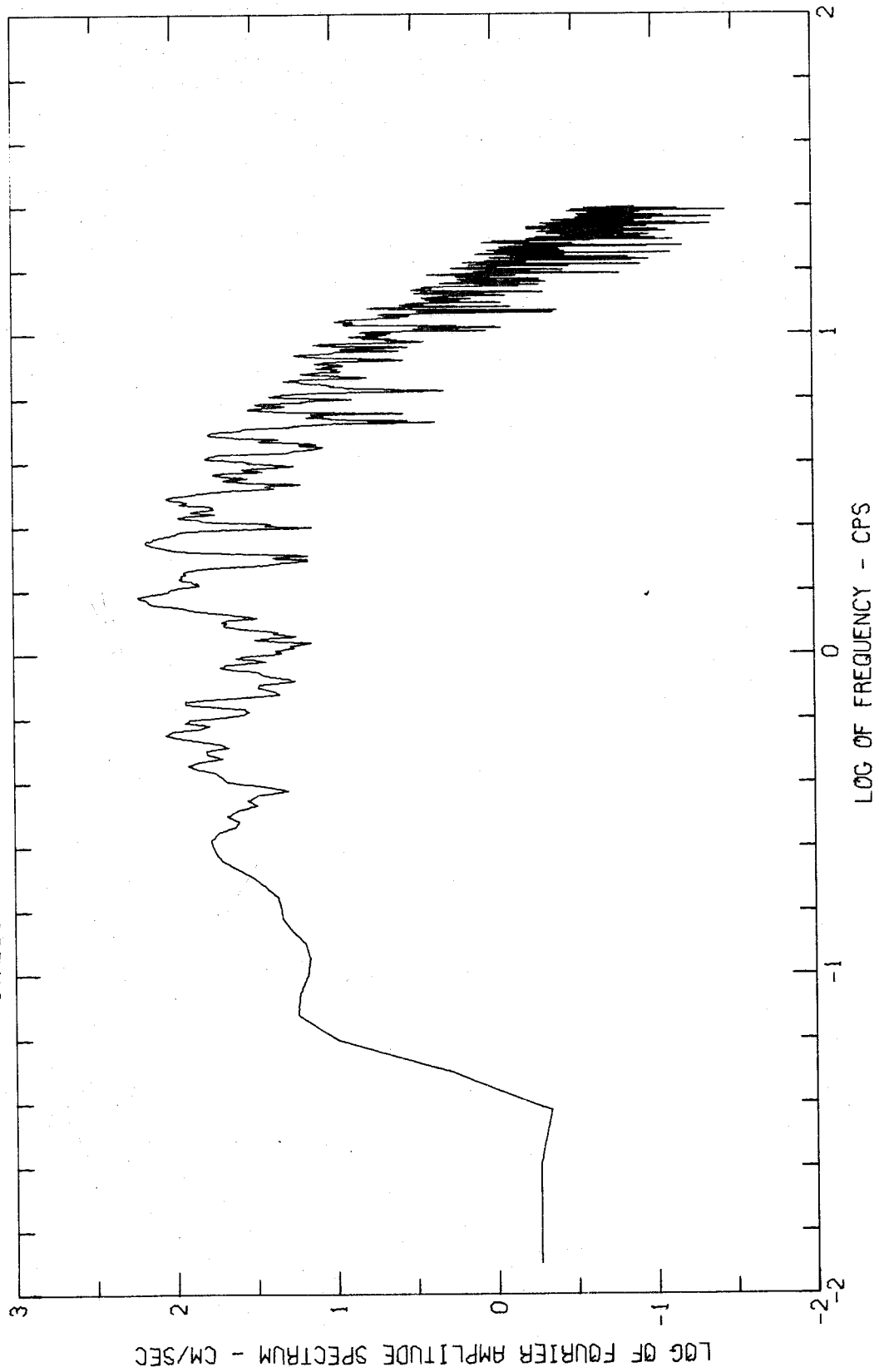
FOURIER AMPLITUDE SPECTRUM OF ACCELERATION
EUREKA EARTHQUAKE DEC 21, 1954 - 1156 PST
IVR008 54.003.0 EUREKA FEDERAL BLDG COMP N11W



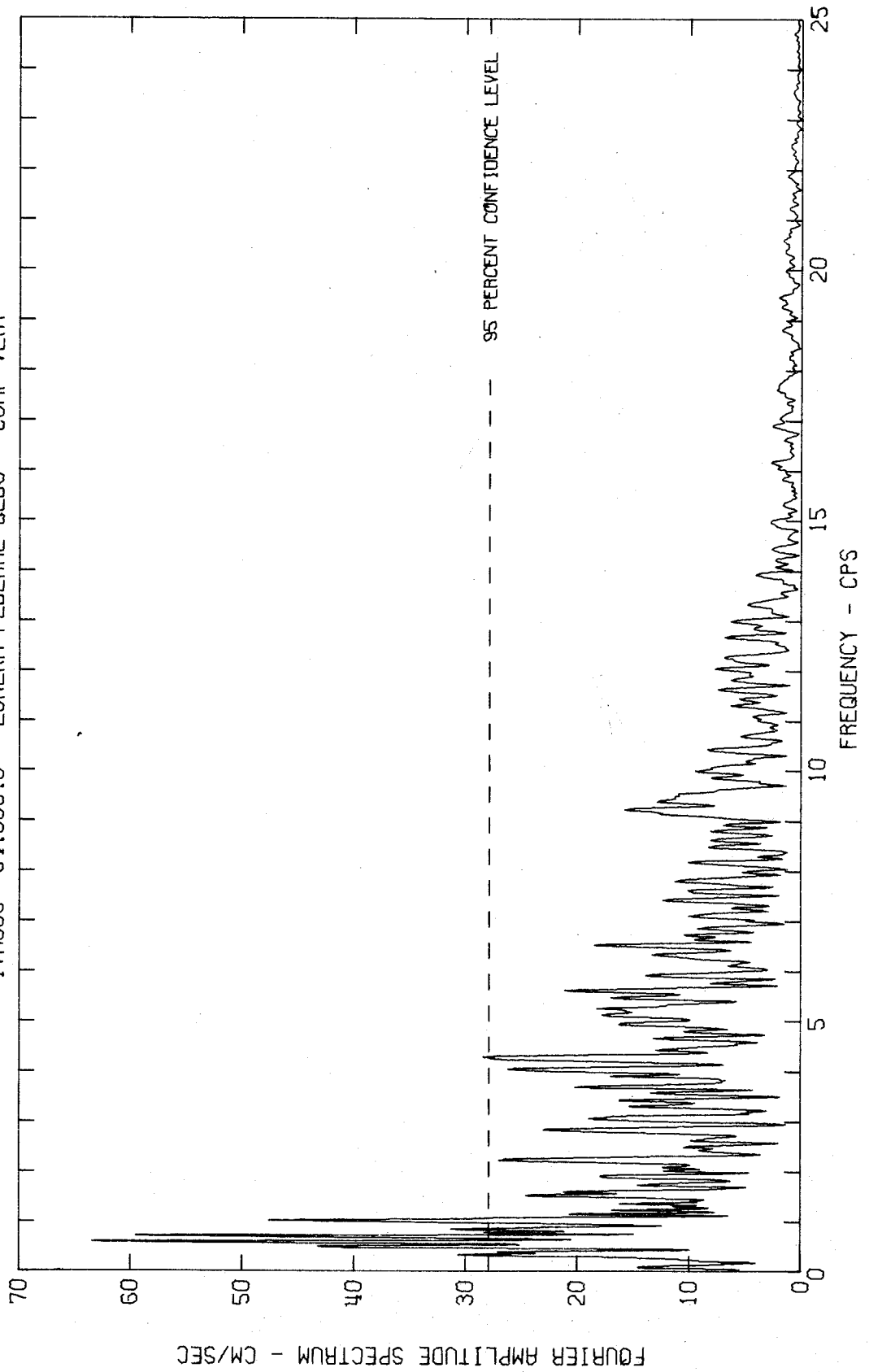
FOURIER AMPLITUDE SPECTRUM OF ACCELERATION
EUREKA EARTHQUAKE DEC 21, 1954 - 1156 PST
IWA008 54.003.0 EUREKA FEDERAL BLDG COMP N79E



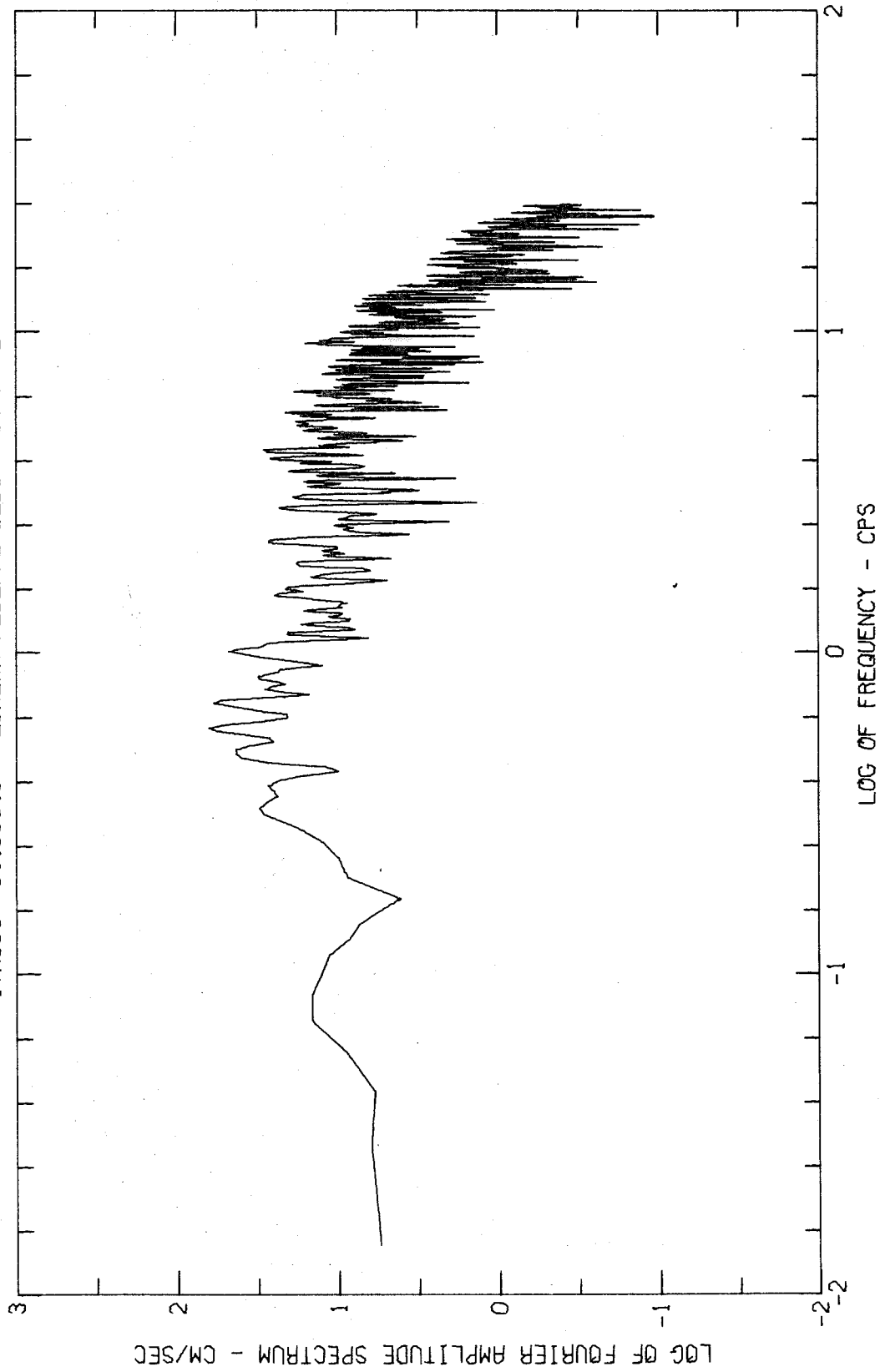
FOURIER AMPLITUDE SPECTRUM OF ACCELERATION
EUREKA EARTHQUAKE DEC 21, 1954 - 1156 PST
11V0008 54.003.0 EUREKA FEDERAL BLDG COMP N79E



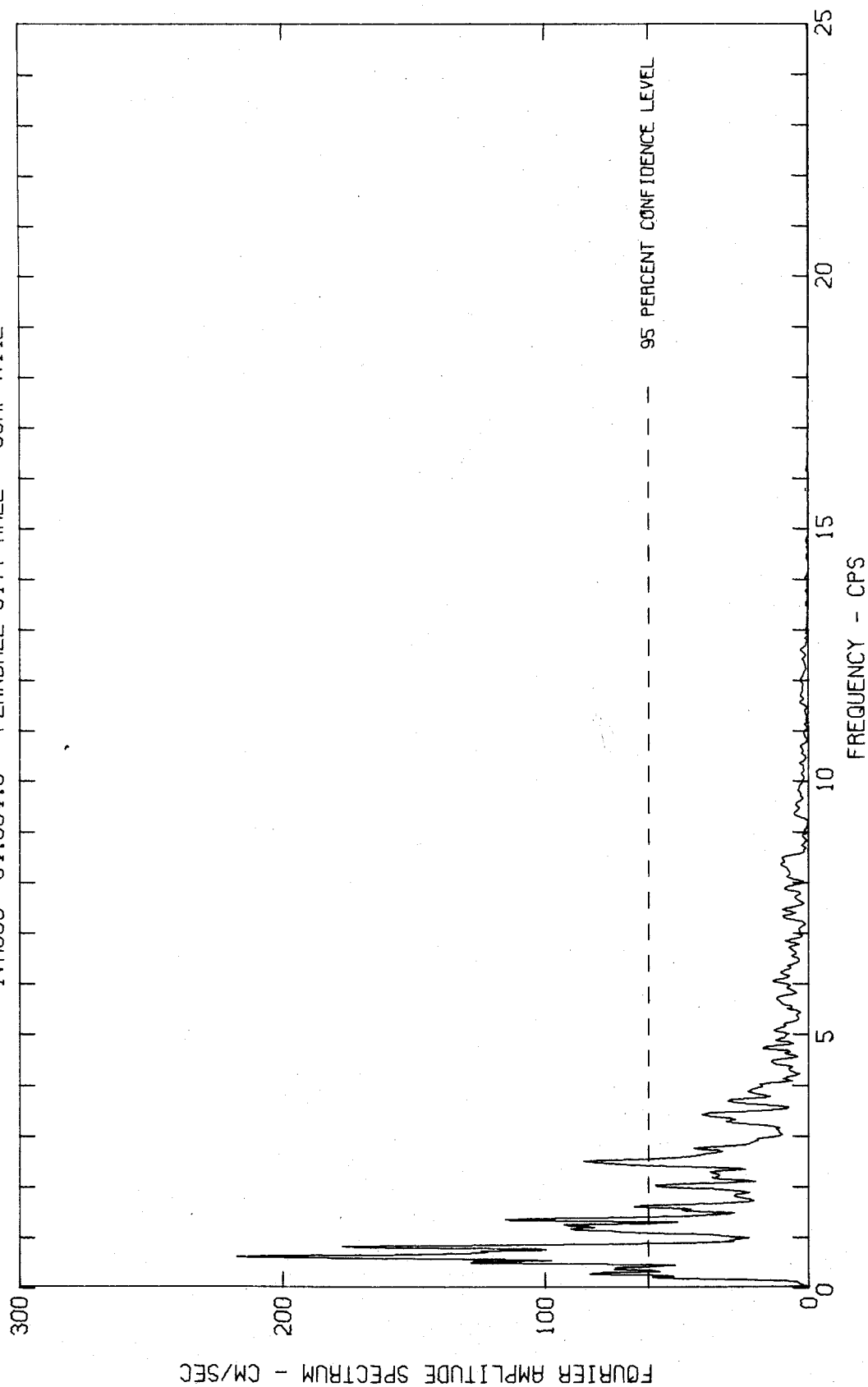
FOURIER AMPLITUDE SPECTRUM OF ACCELERATION
EUREKA EARTHQUAKE DEC 21, 1954 - 1156 PST
IWA008 54.003.0 EUREKA FEDERAL BLDG COMP VERT



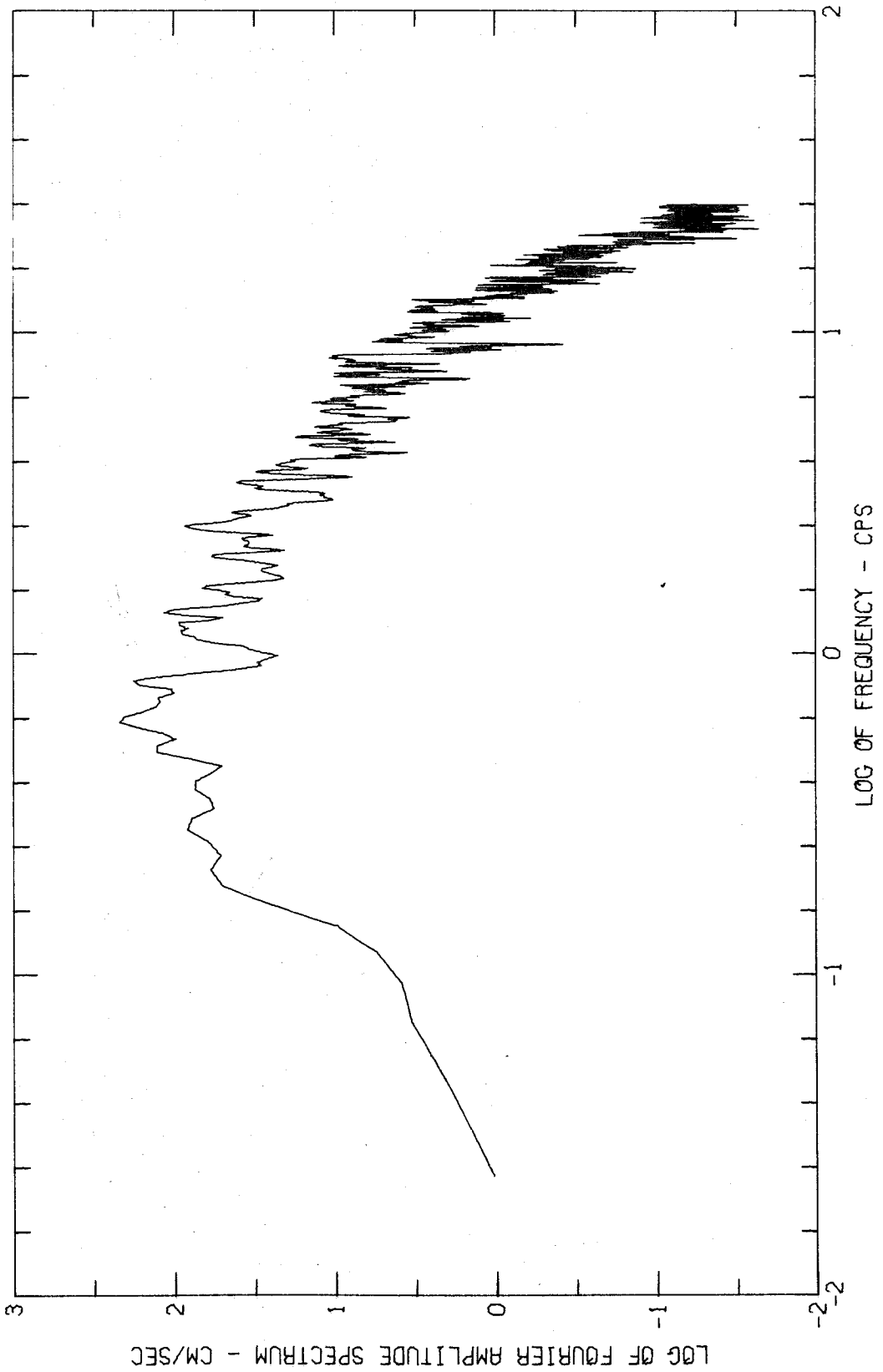
FOURIER AMPLITUDE SPECTRUM OF ACCELERATION
EUREKA EARTHQUAKE DEC 21, 1954 - 1156 PST
IVA008 54.003.0 EUREKA FEDERAL BLDG COMP VERT



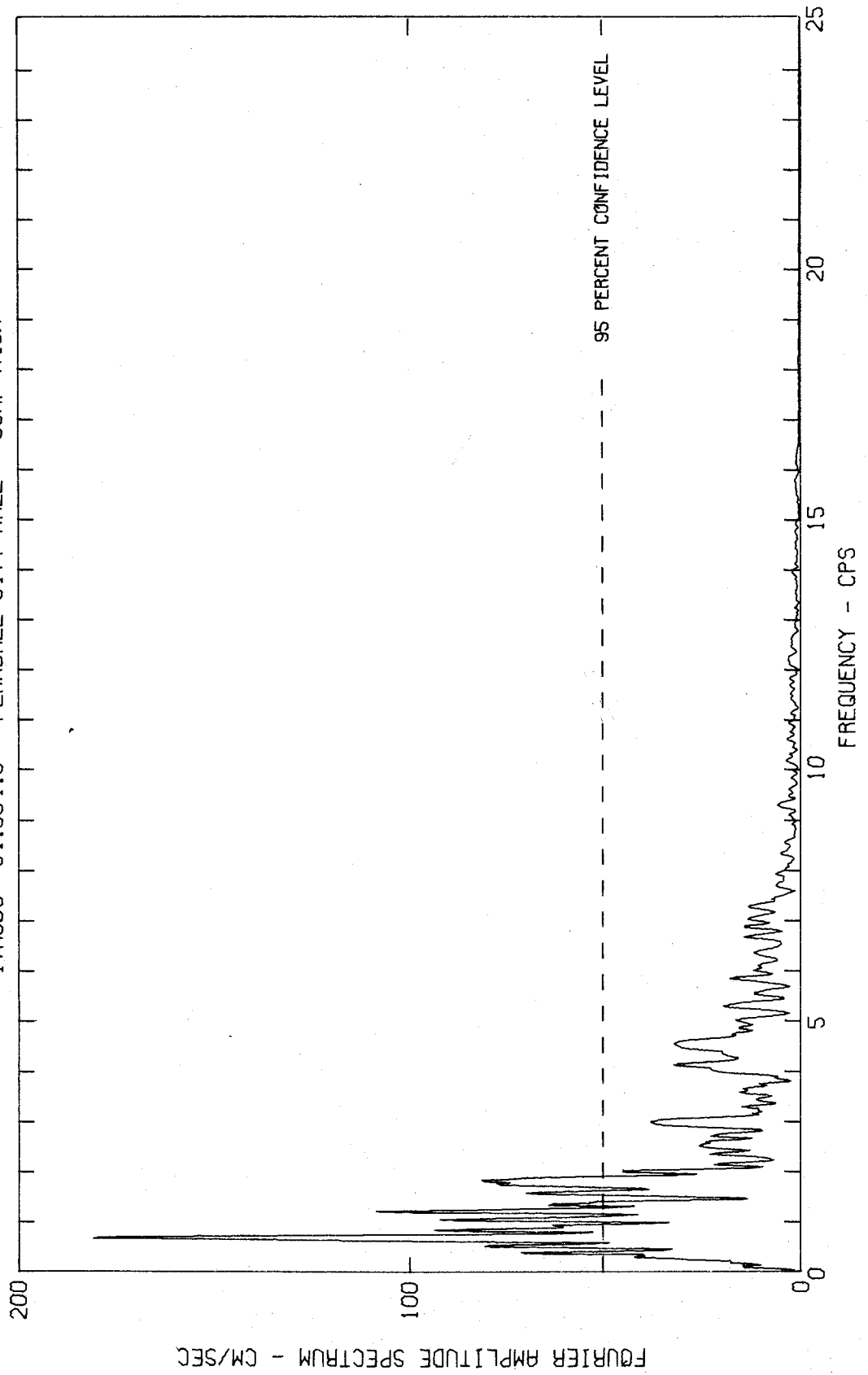
FOURIER AMPLITUDE SPECTRUM OF ACCELERATION
EUREKA EARTHQUAKE DEC 21, 1954 - 1156 PST
IWA009 54.004.0 FERNDAL CITY HALL COMP N44E



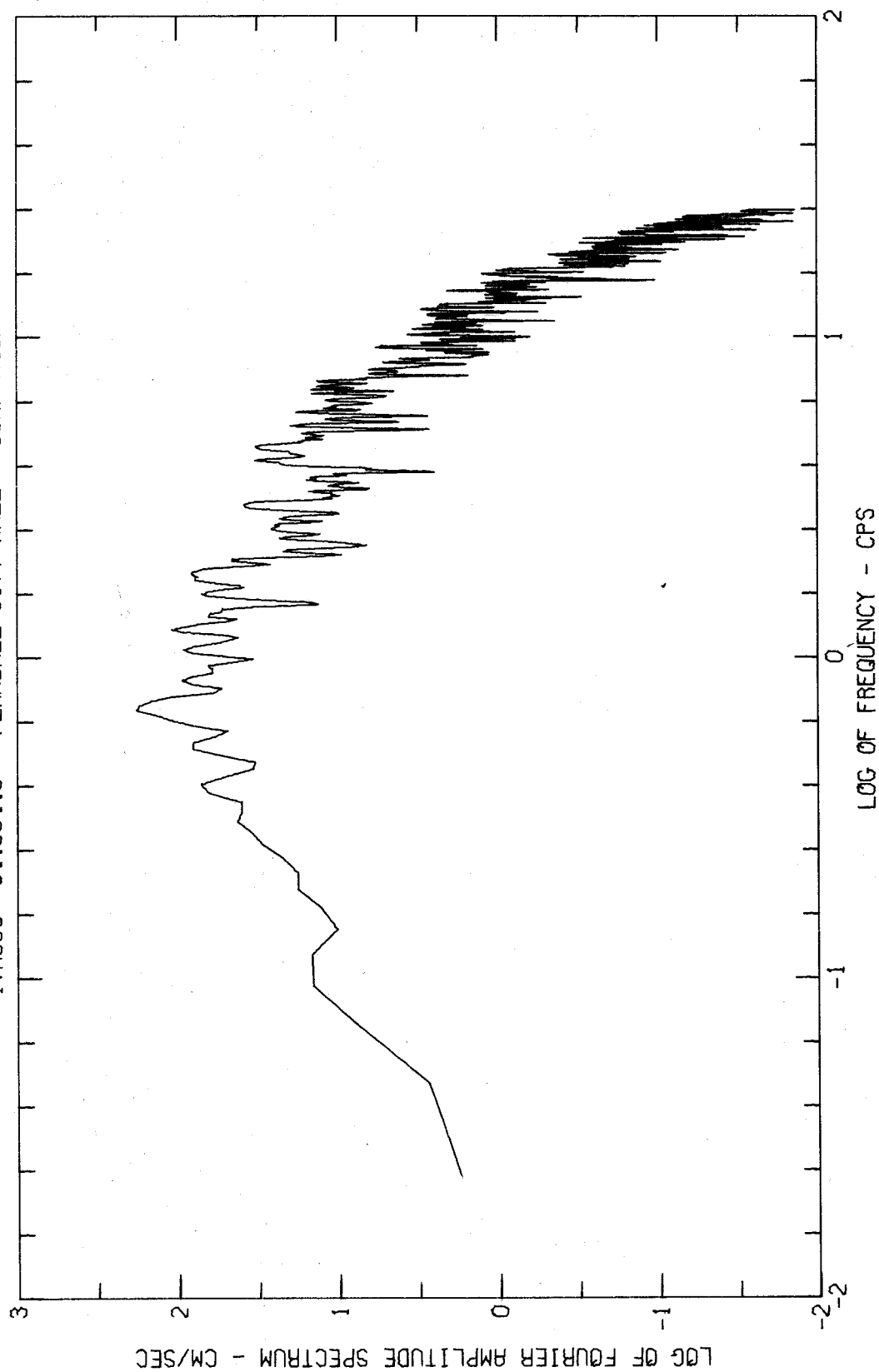
FOURIER AMPLITUDE SPECTRUM OF ACCELERATION
EUREKA EARTHQUAKE DEC 21, 1954 - 1156 PST
IV0009 54.004.0 FERNDALE CITY HALL COMP N44E



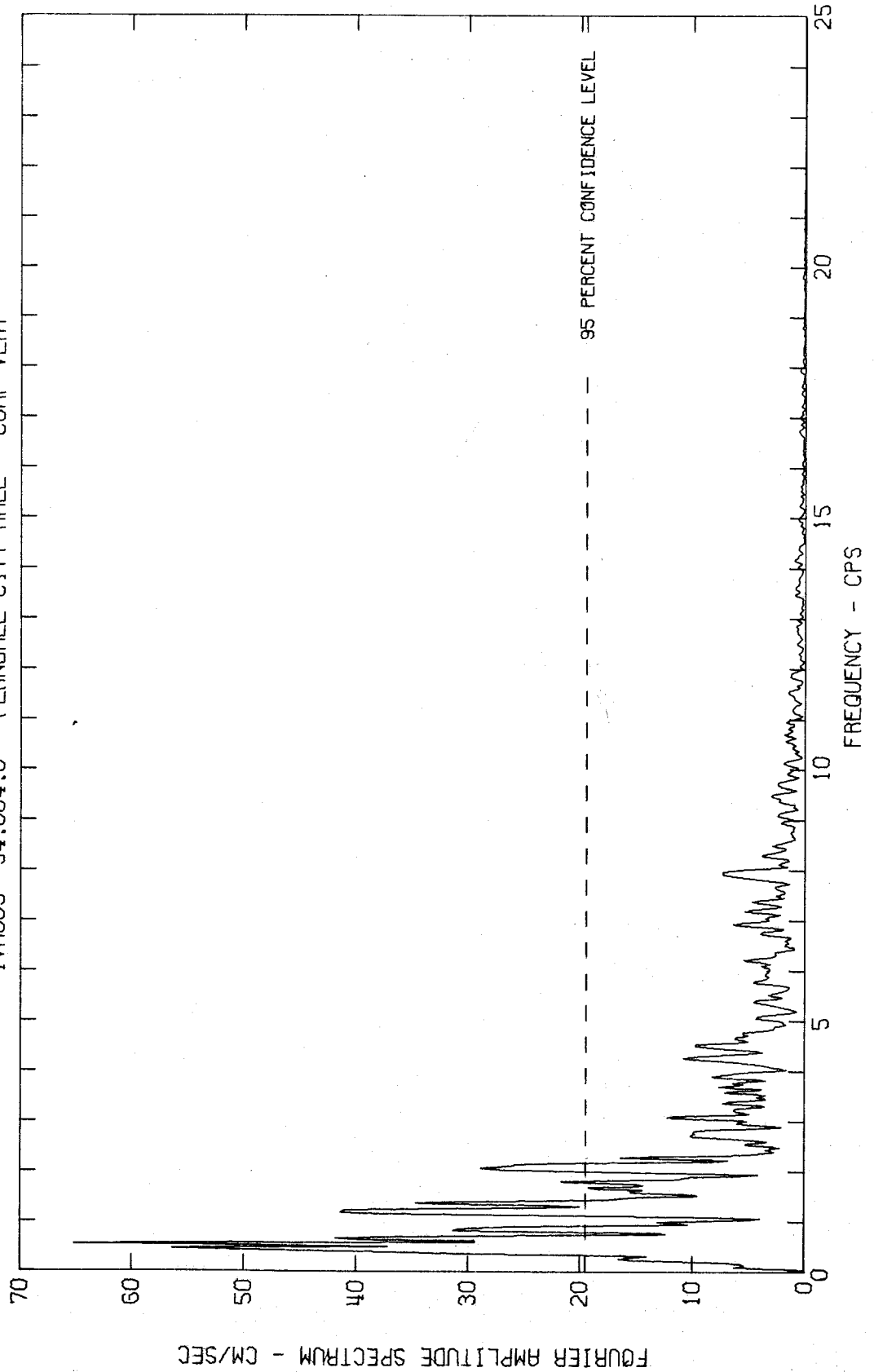
FOURIER AMPLITUDE SPECTRUM OF ACCELERATION
EUREKA EARTHQUAKE DEC 21, 1954 - 1156 PST
IVR009 54.004.0 FERNDAL CITY HALL COMP N46W



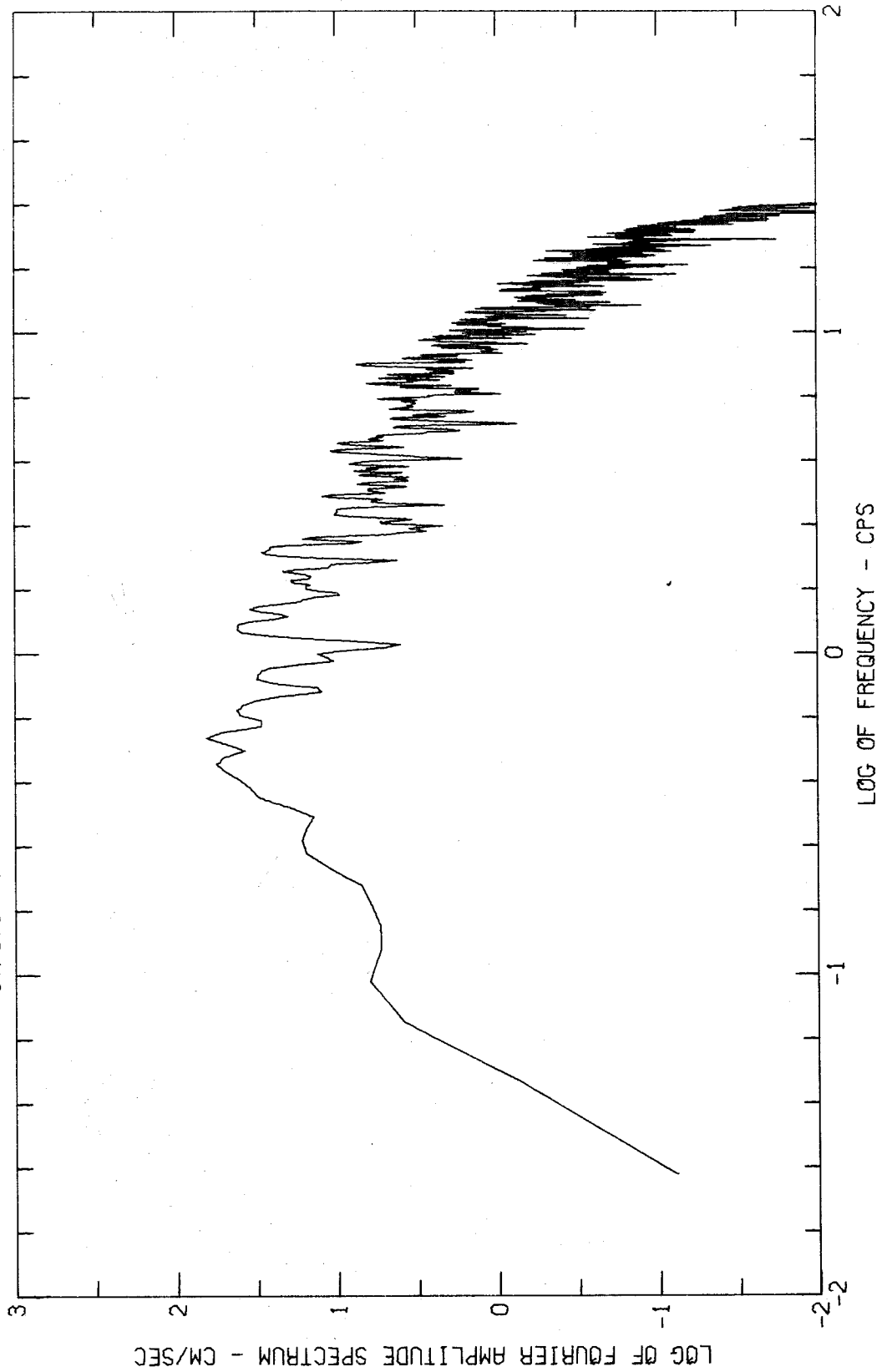
FOURIER AMPLITUDE SPECTRUM OF ACCELERATION
EUREKA EARTHQUAKE DEC 21, 1954 - 1156 PST
1V0009 54.004.0 FERNDALE CITY HALL COMP N46W



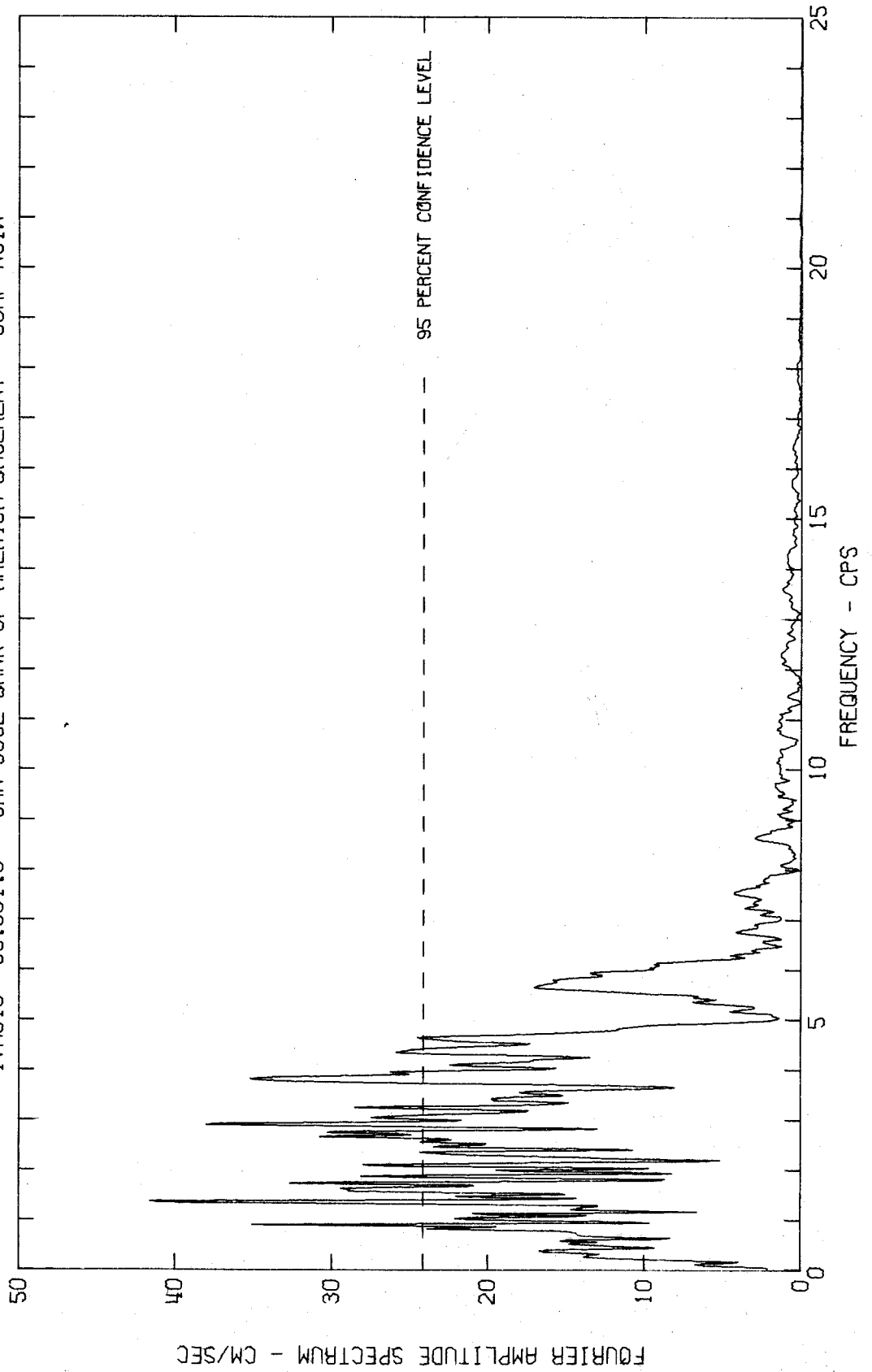
FOURIER AMPLITUDE SPECTRUM OF ACCELERATION
EUREKA EARTHQUAKE DEC 21, 1954 - 1156 PST
IVA009 54.004.0 FERDALE CITY HALL COMP VERT



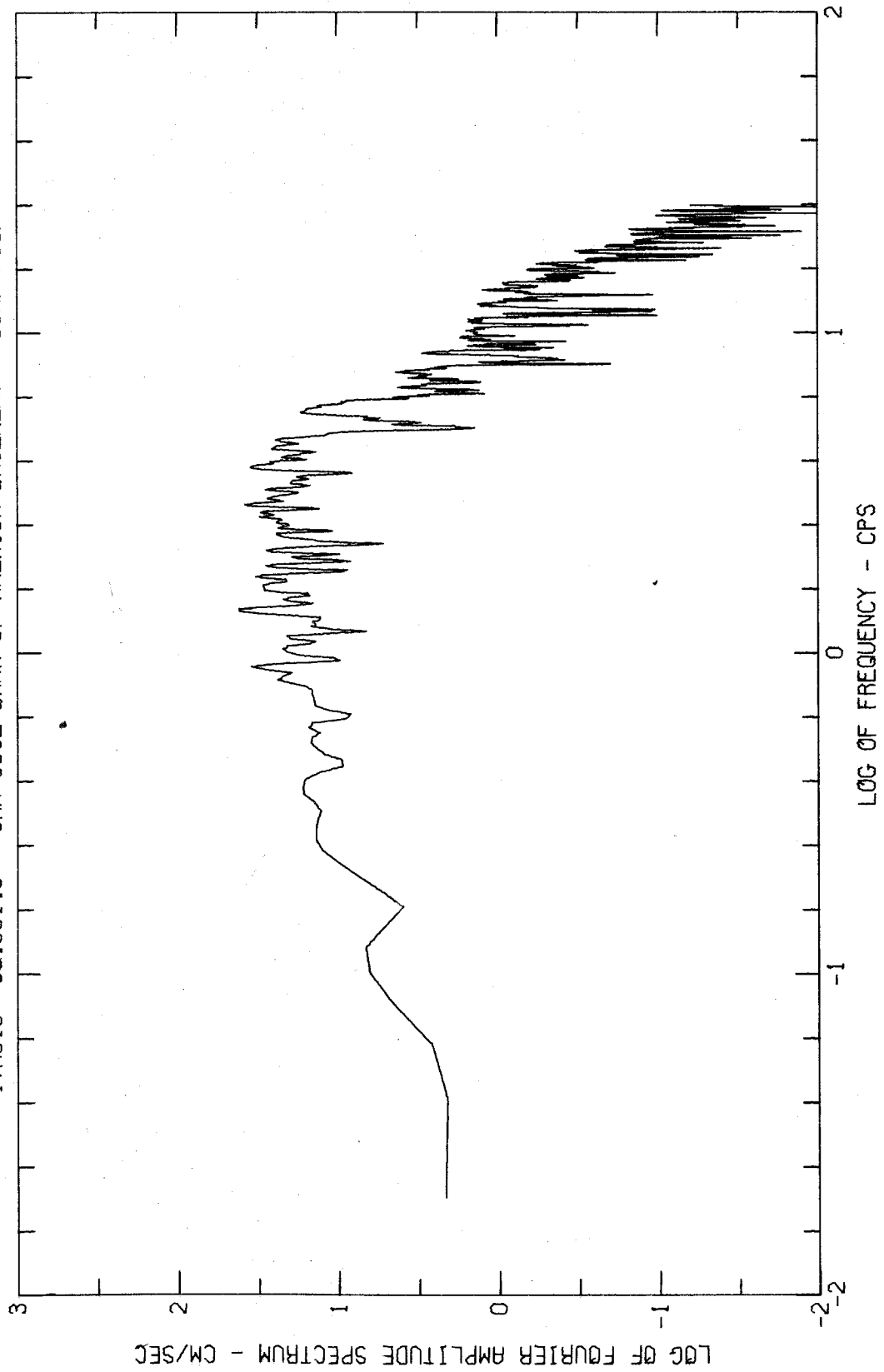
FOURIER AMPLITUDE SPECTRUM OF ACCELERATION
EUREKA EARTHQUAKE DEC 21, 1954 - 1156 PST
IV0009 54.004.0 FERNDAL CITY HALL COMP VERT

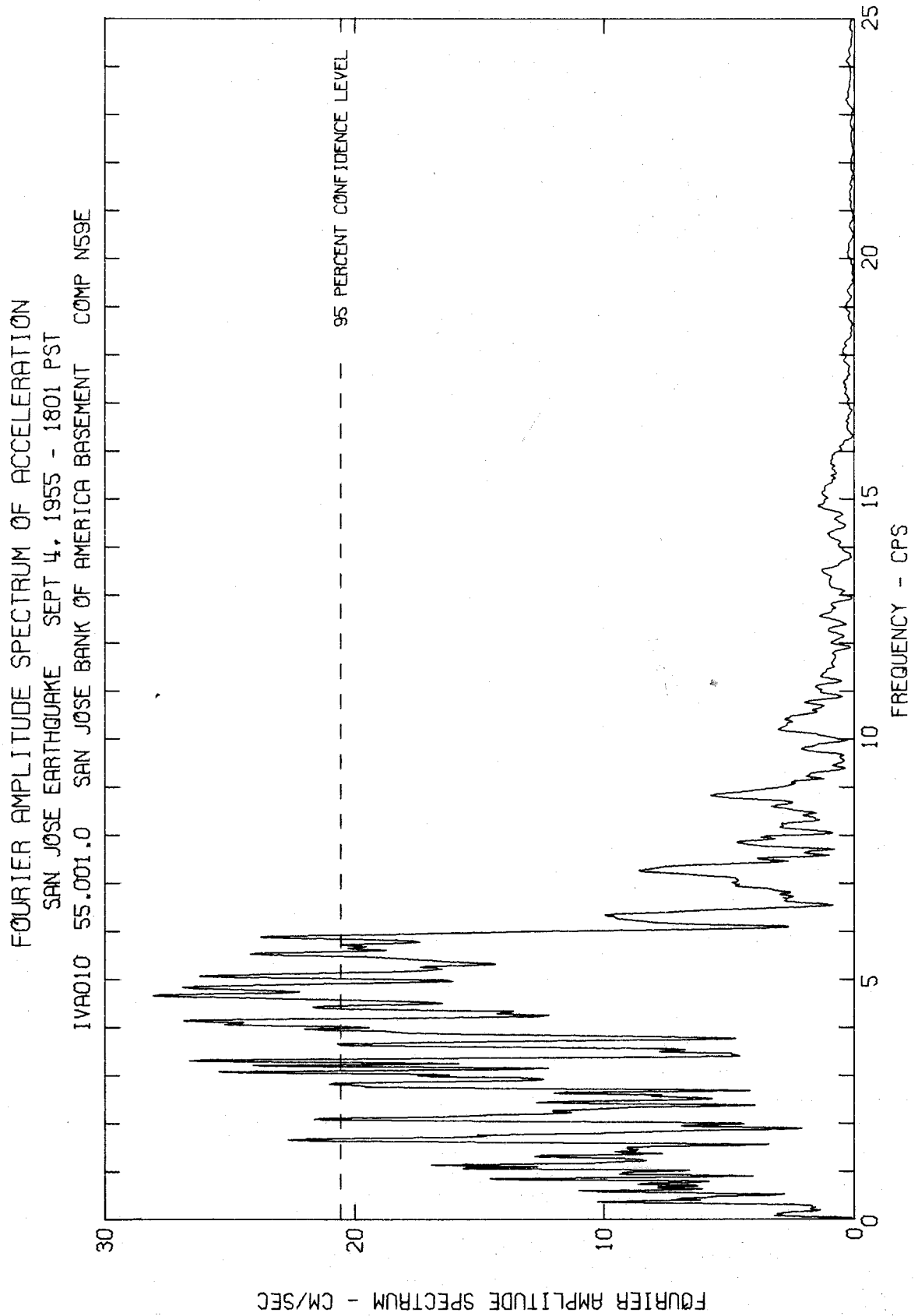


FOURIER AMPLITUDE SPECTRUM OF ACCELERATION
SAN JOSE EARTHQUAKE SEPT 4, 1955 - 1801 PST
IVAO10 55.001.0 SAN JOSE BANK OF AMERICA BASEMENT COMP N31W



FOURIER AMPLITUDE SPECTRUM OF ACCELERATION
SAN JOSE EARTHQUAKE SEPT 4, 1955 - 1801 PST
IWA010 55.001.0 SAN JOSE BANK OF AMERICA BASEMENT COMP N31W

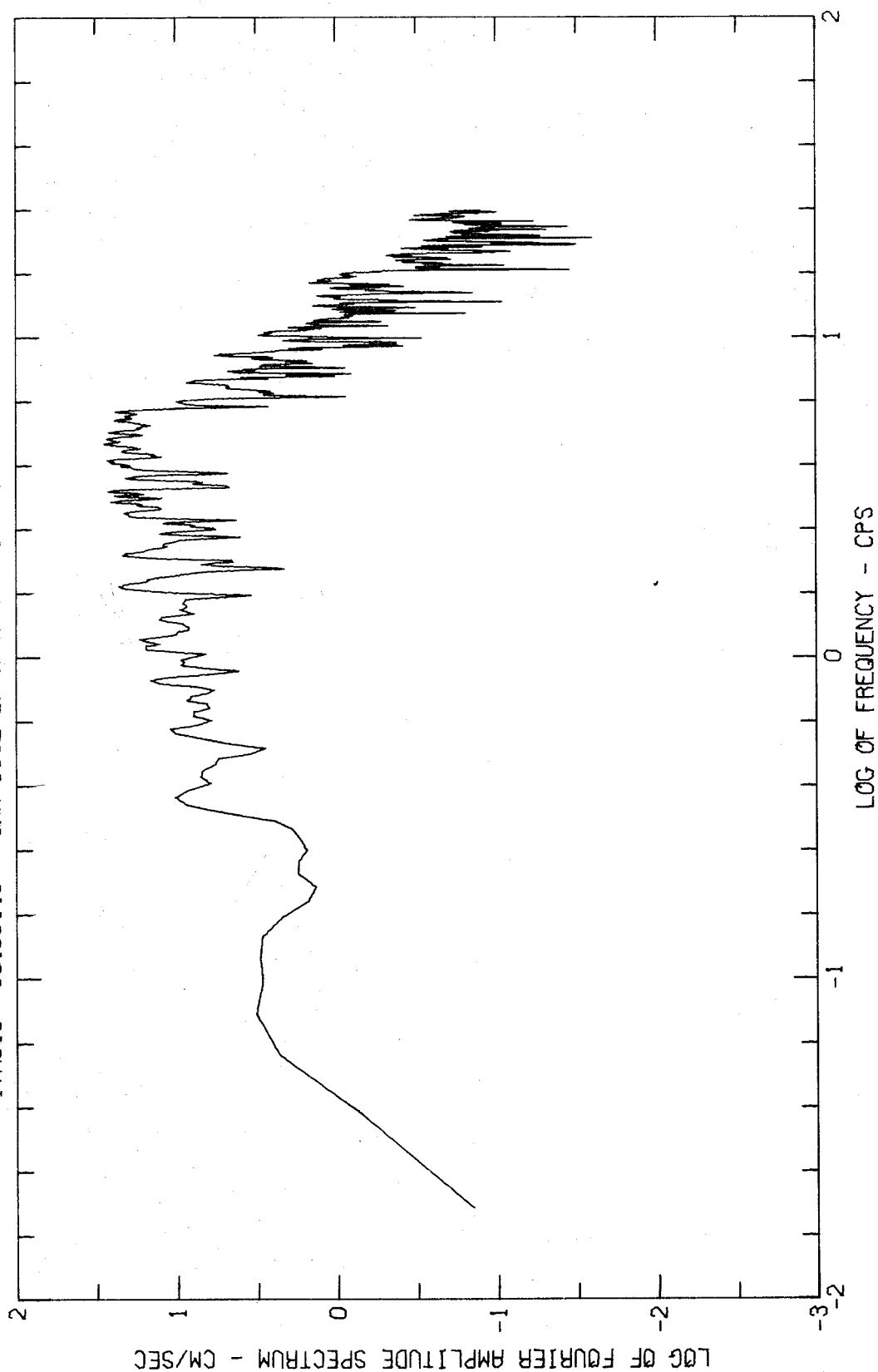




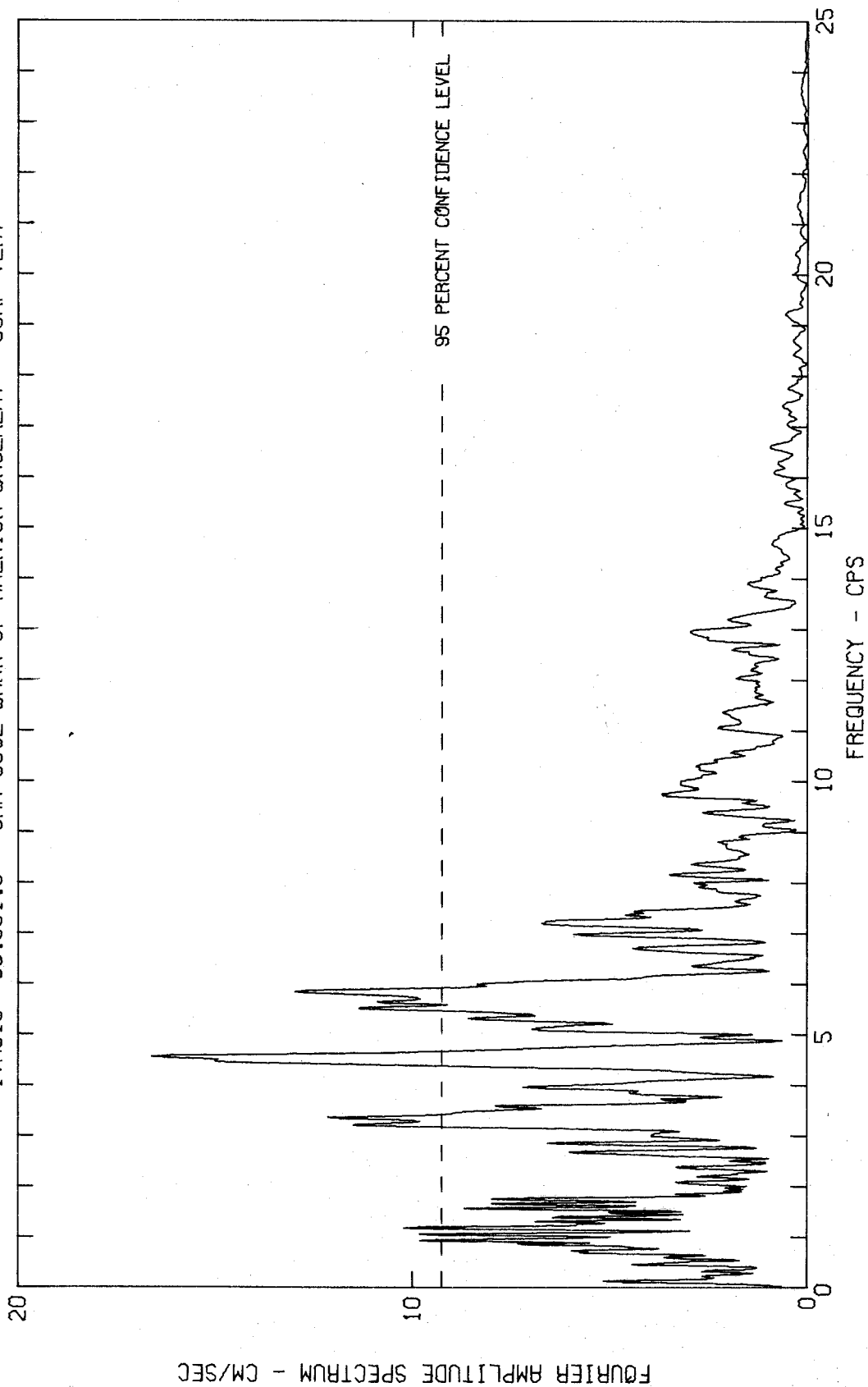
FOURIER AMPLITUDE SPECTRUM OF ACCELERATION

SAN JOSE EARTHQUAKE SEPT 4, 1955 - 1801 PST

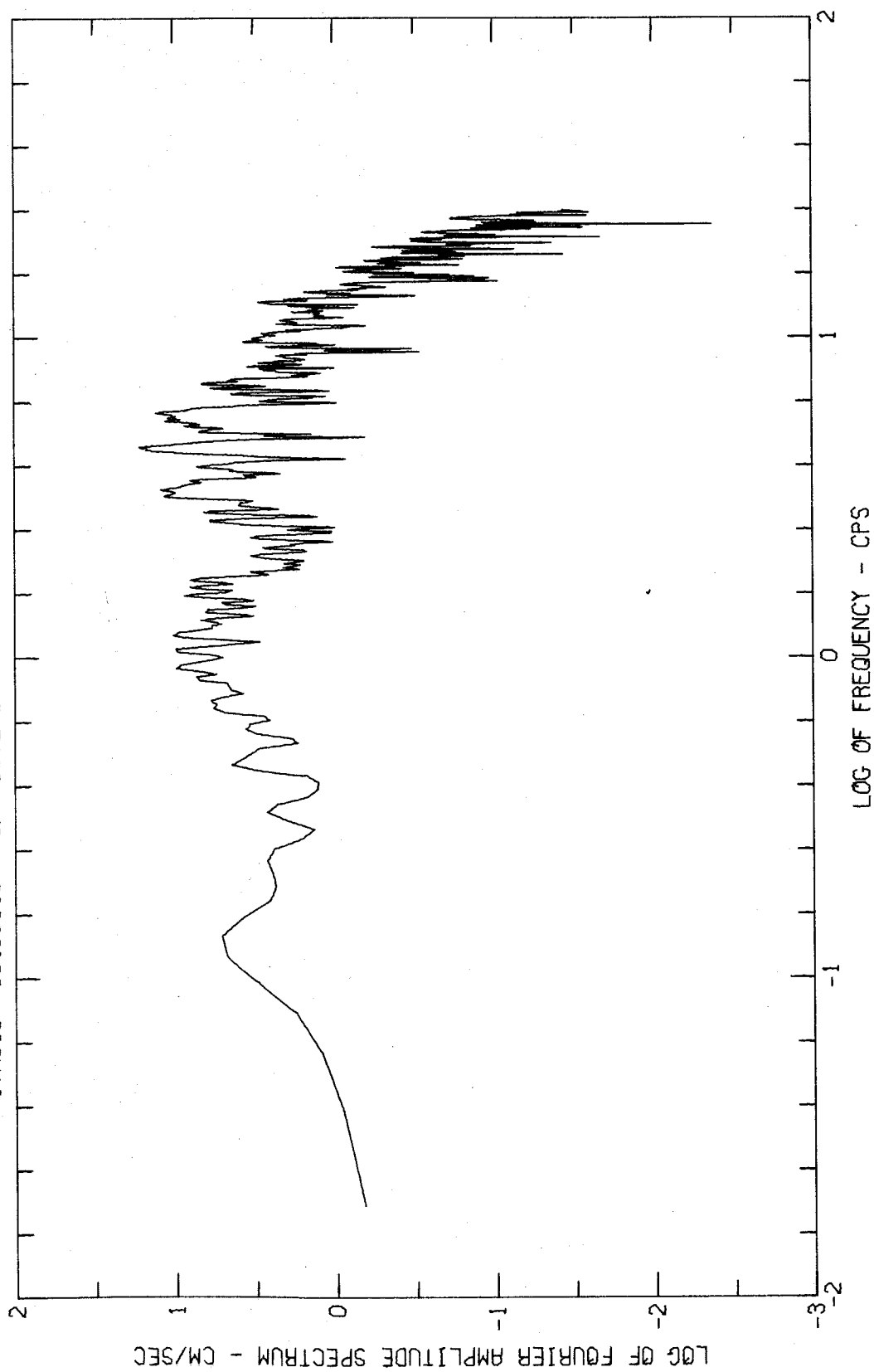
IWA010 55.001.0 SAN JOSE BANK OF AMERICA BASEMENT COMP N59E

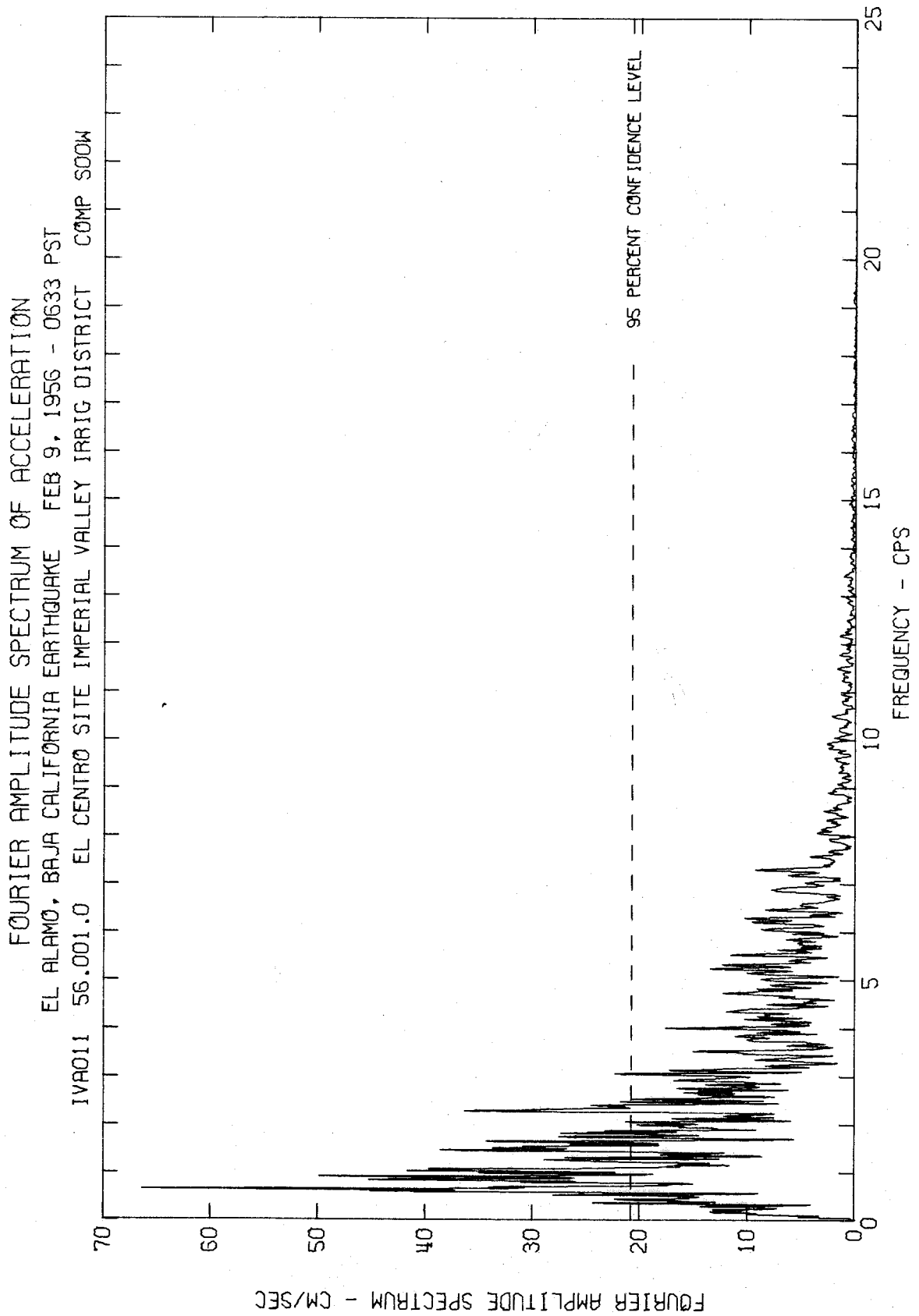


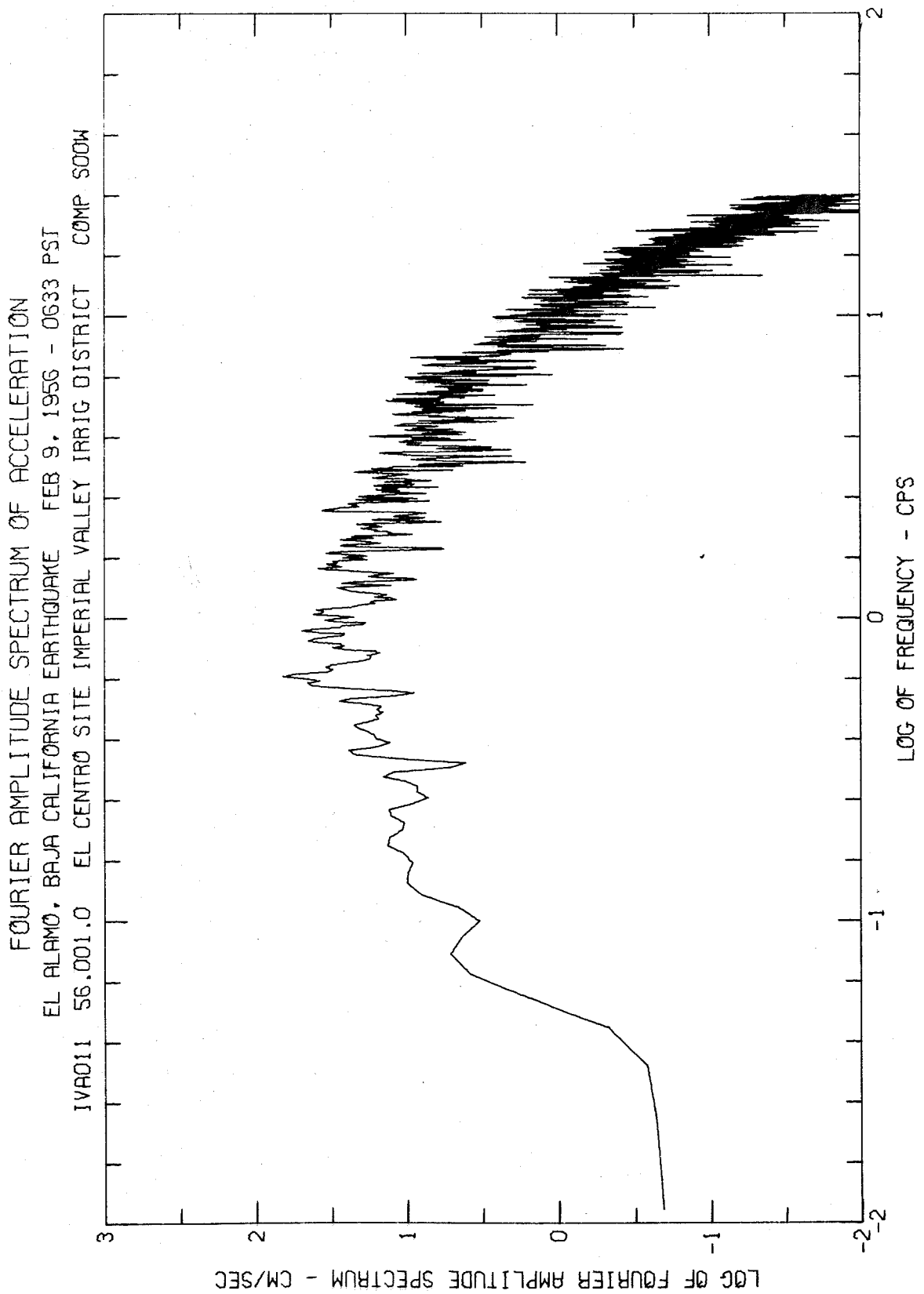
FOURIER AMPLITUDE SPECTRUM OF ACCELERATION
SAN JOSE EARTHQUAKE SEPT 4, 1955 - 1801 PST
IWA010 55.001.0 SAN JOSE BANK OF AMERICA BASEMENT COMP VERT

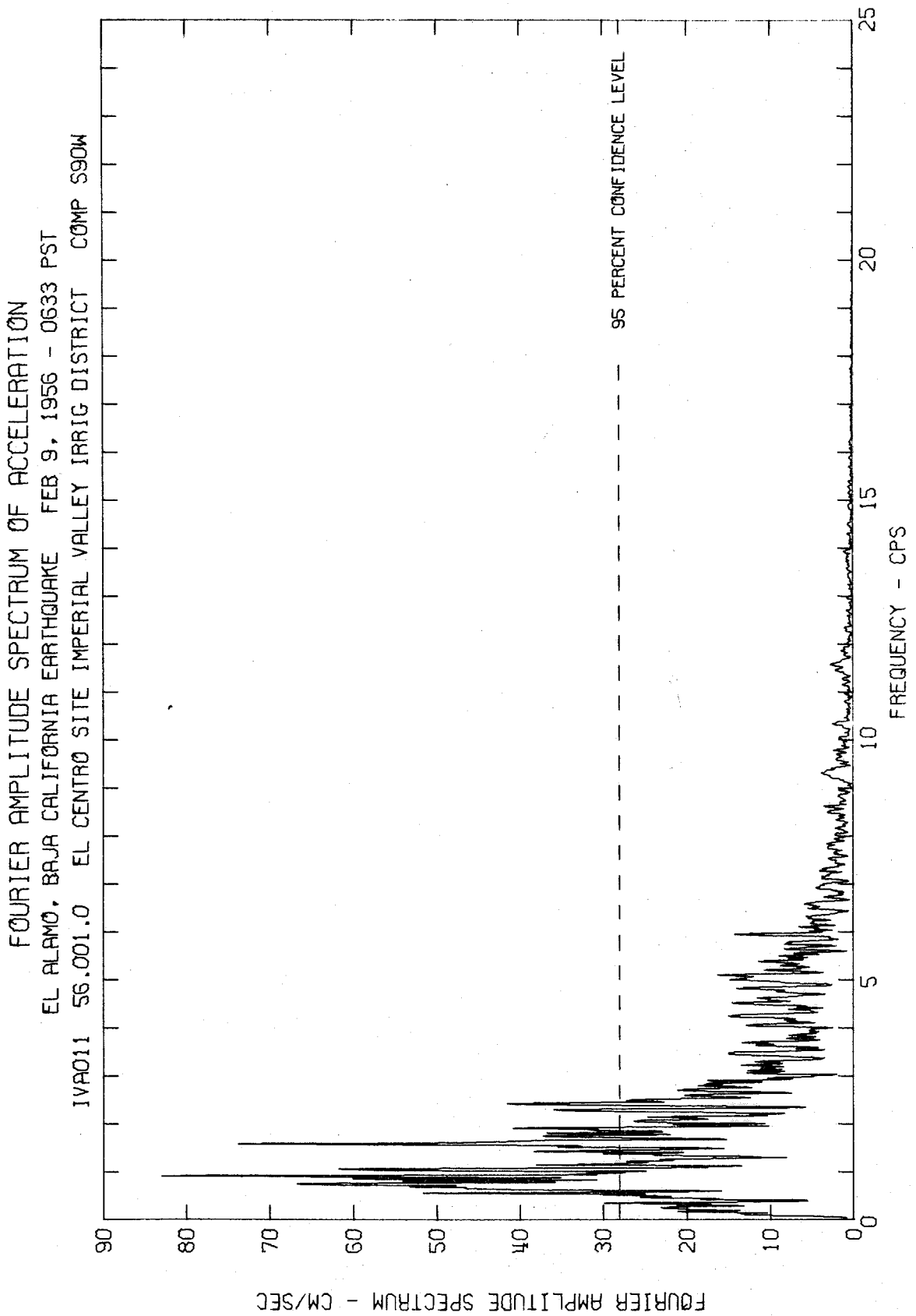


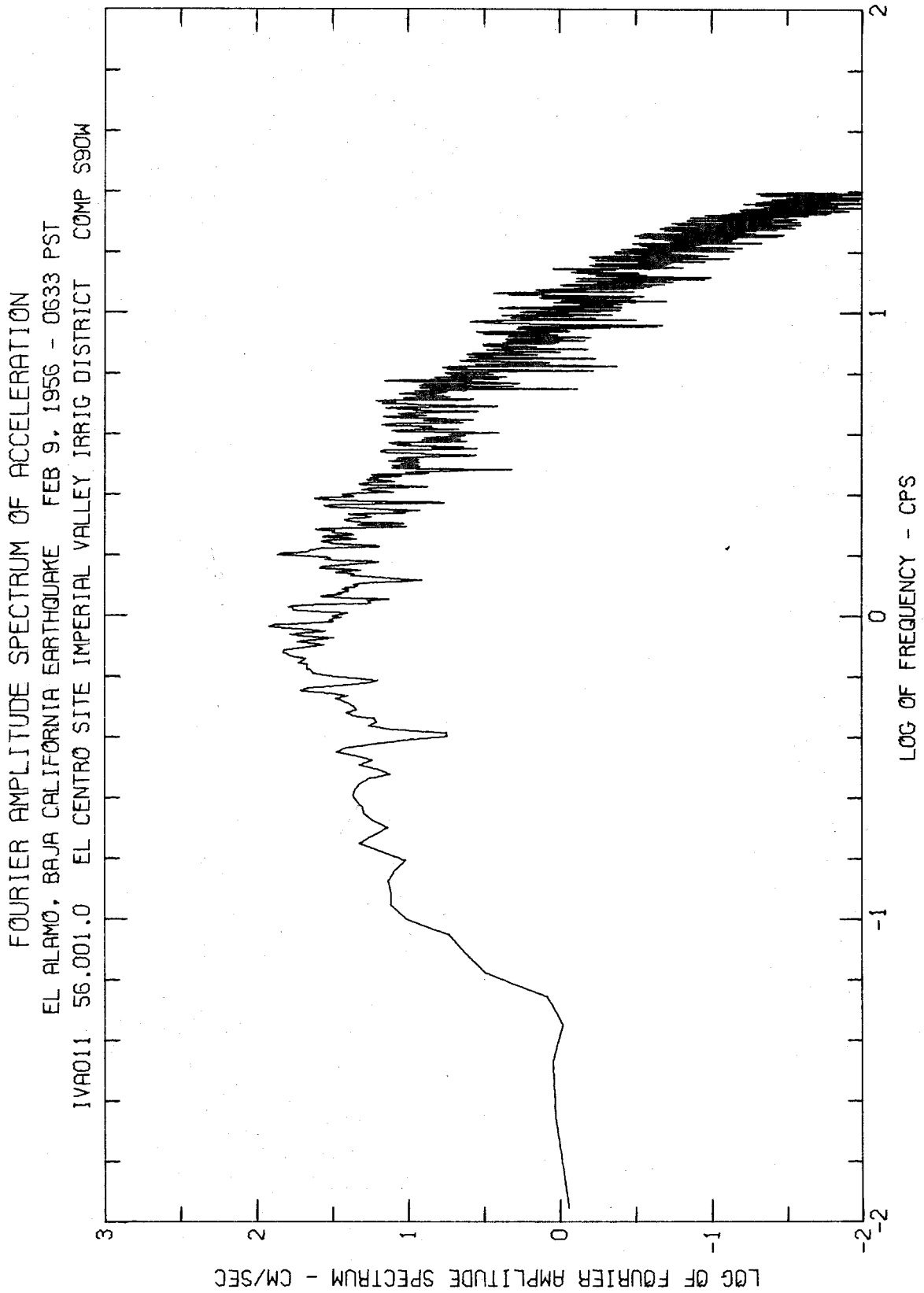
FOURIER AMPLITUDE SPECTRUM OF ACCELERATION
SAN JOSE EARTHQUAKE SEPT 4, 1955 - 1801 PST
IWA010 55.001.0 SAN JOSE BANK OF AMERICA BASEMENT COMP VERT



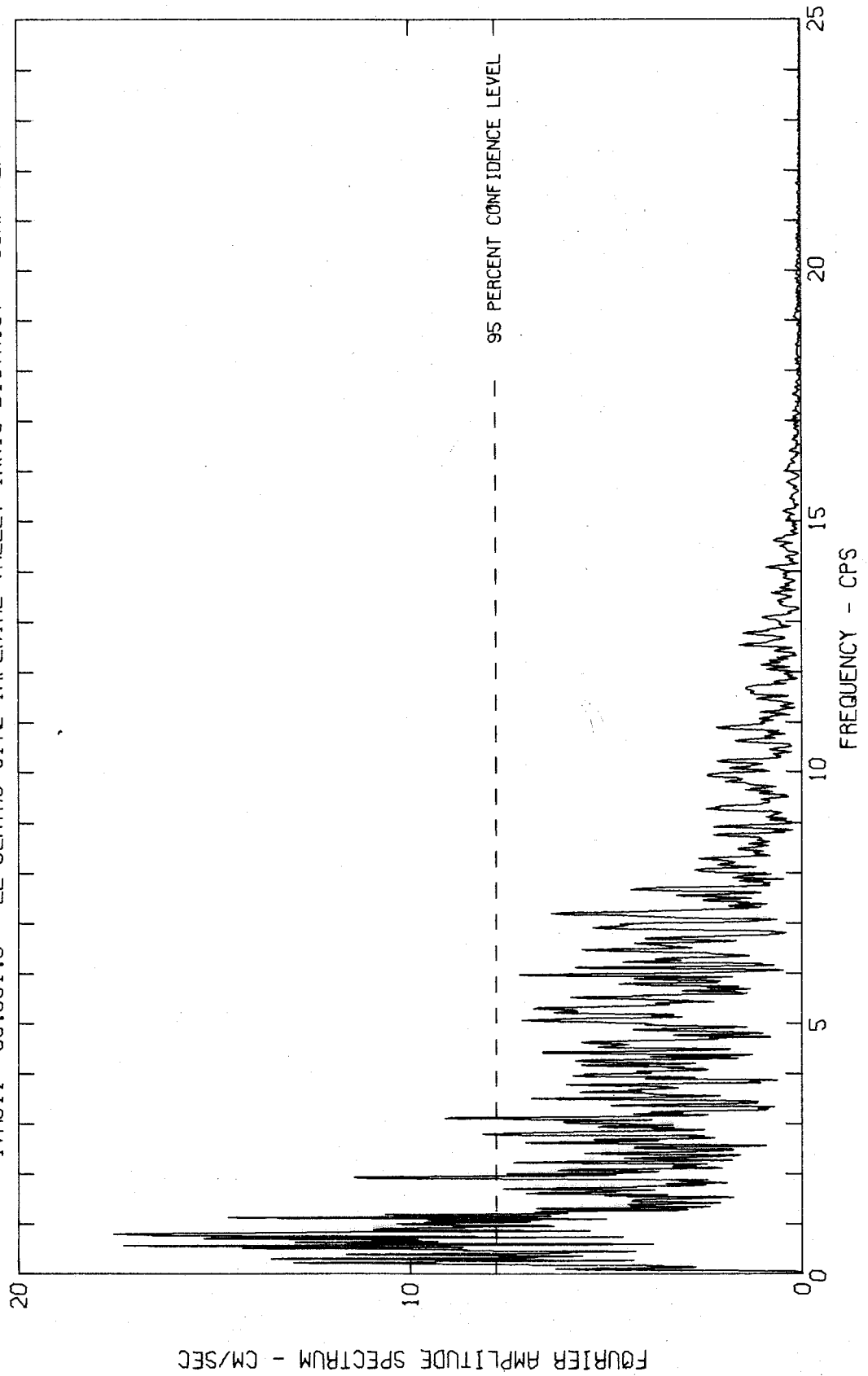




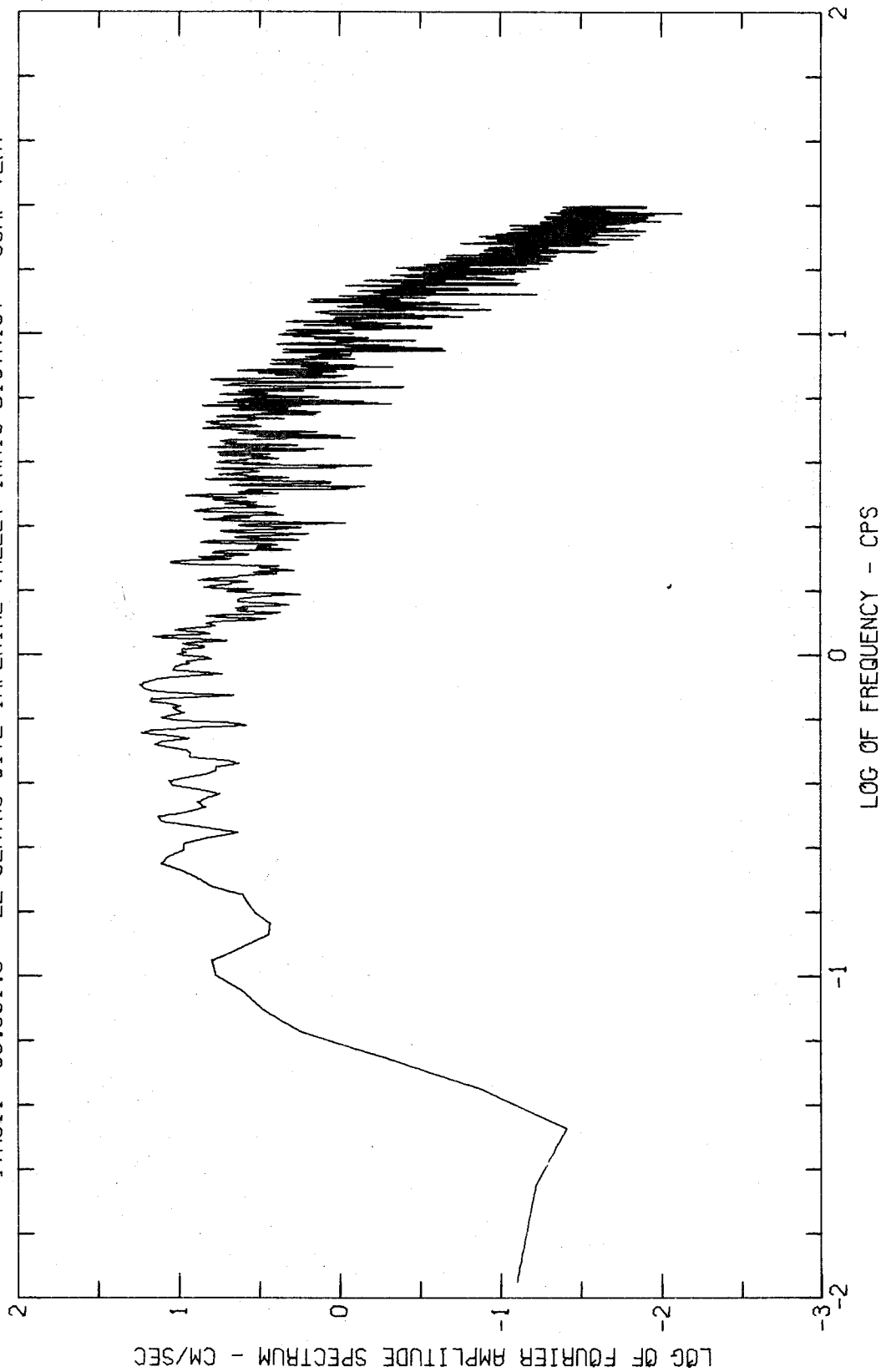


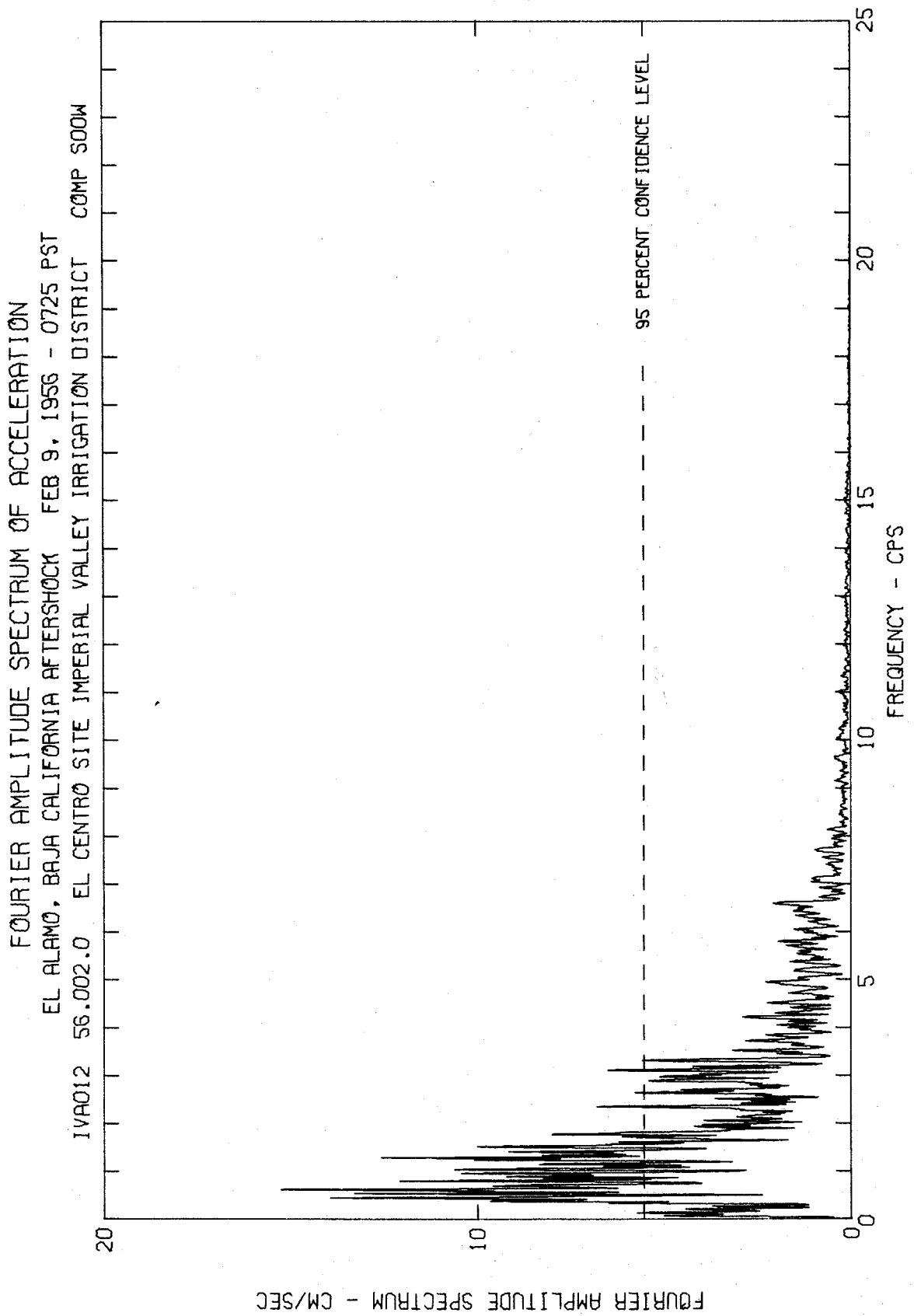


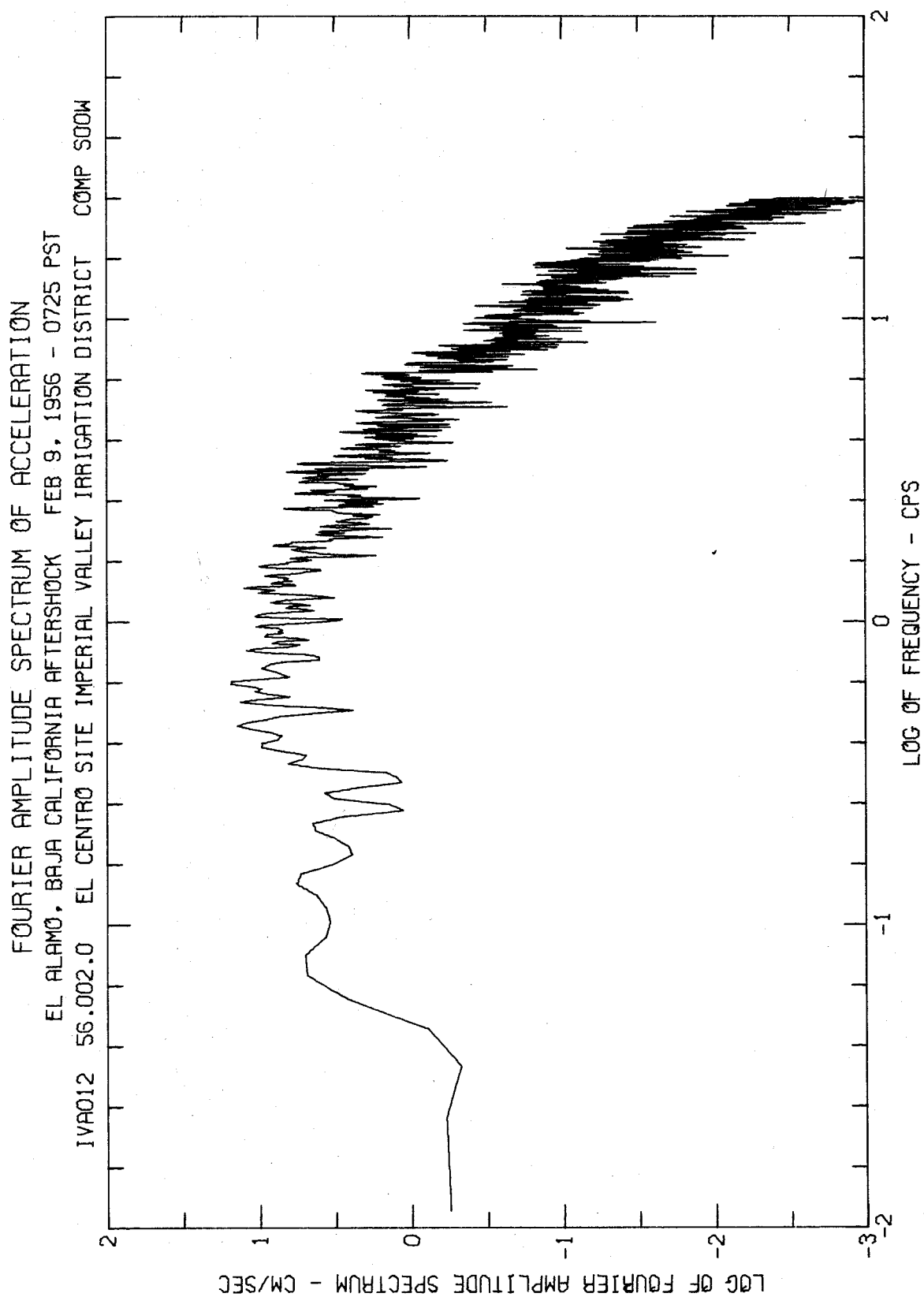
FOURIER AMPLITUDE SPECTRUM OF ACCELERATION
EL ALAMO, BAJA CALIFORNIA EARTHQUAKE FEB 9, 1956 - 0633 PST
IWA011 56.001.0 EL CENTRO SITE IMPERIAL VALLEY IRRIG DISTRICT COMP VERT

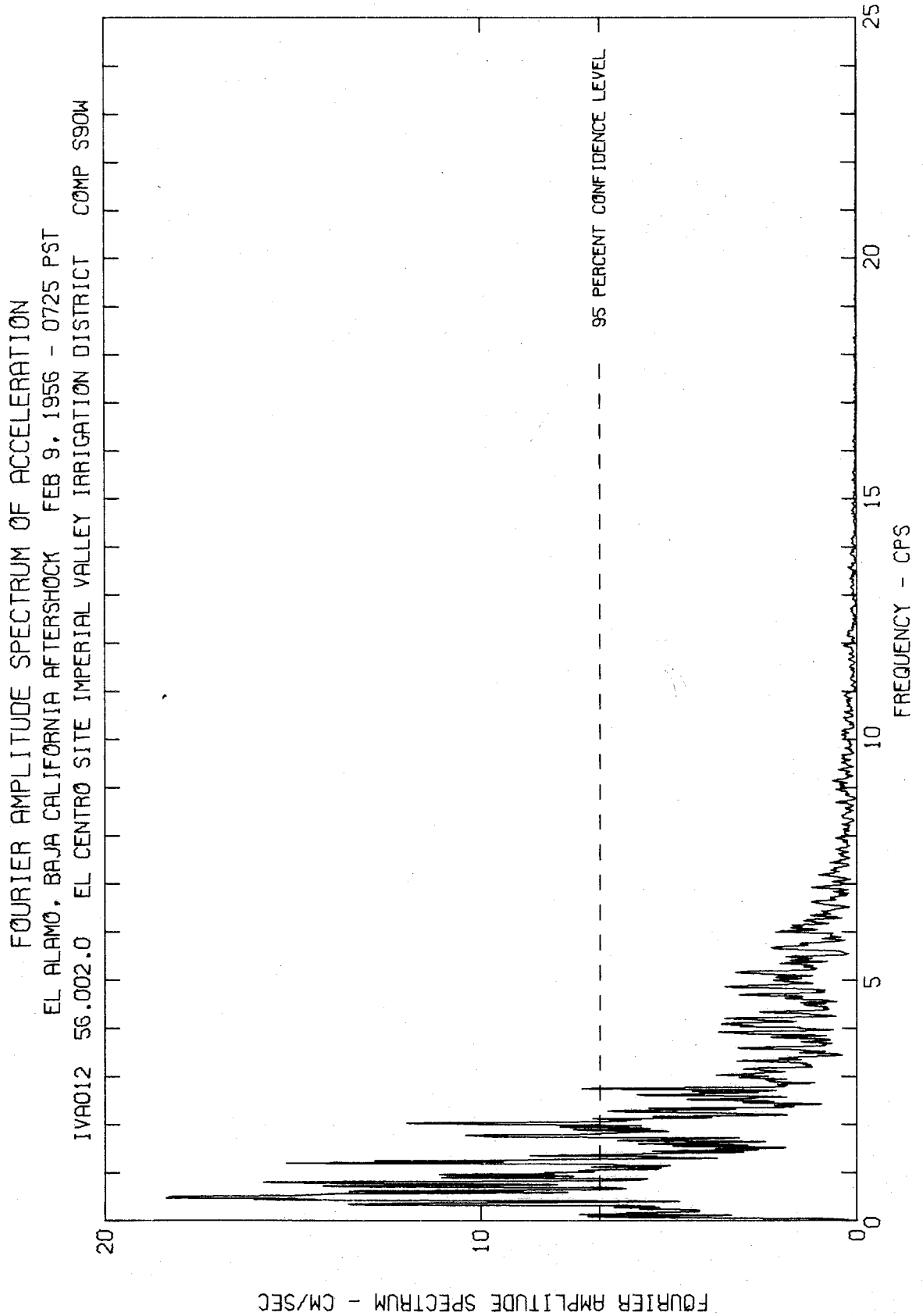


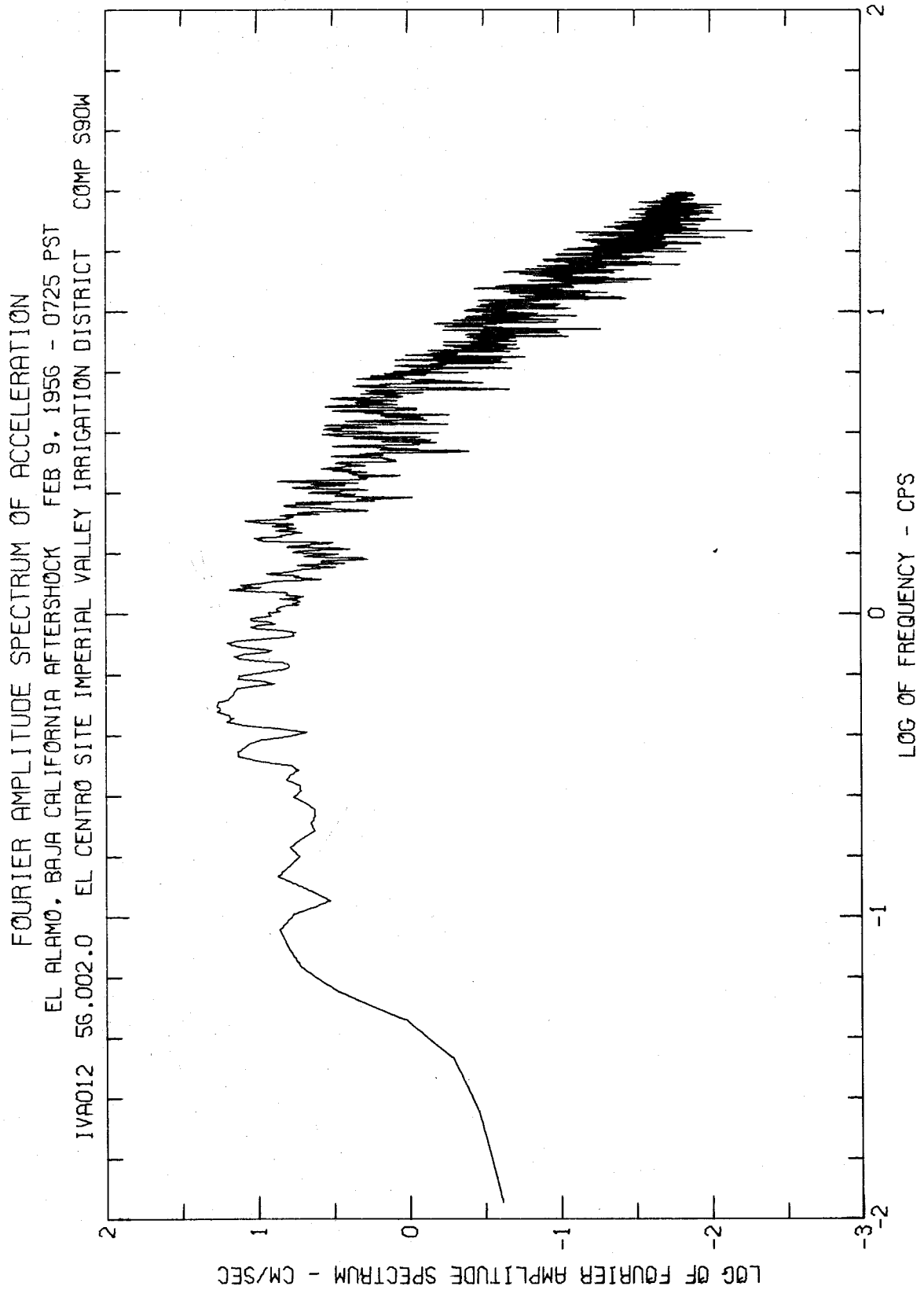
FOURIER AMPLITUDE SPECTRUM OF ACCELERATION
EL ALAMO, BAJA CALIFORNIA EARTHQUAKE FEB 9, 1956 - 0633 PST
IWA011 56.001.0 EL CENTRO SITE IMPERIAL VALLEY IRRIG DISTRICT COMP VERT

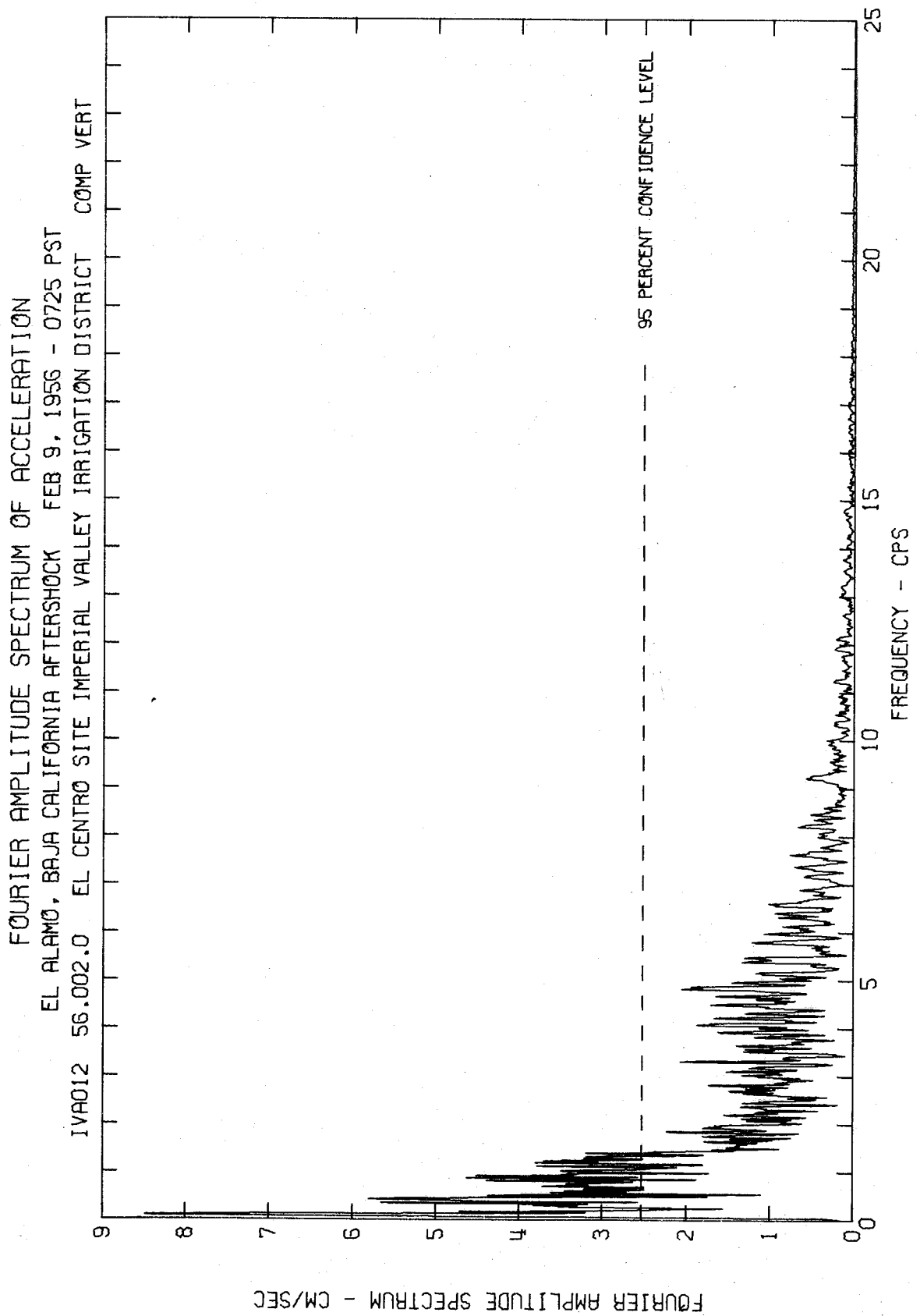


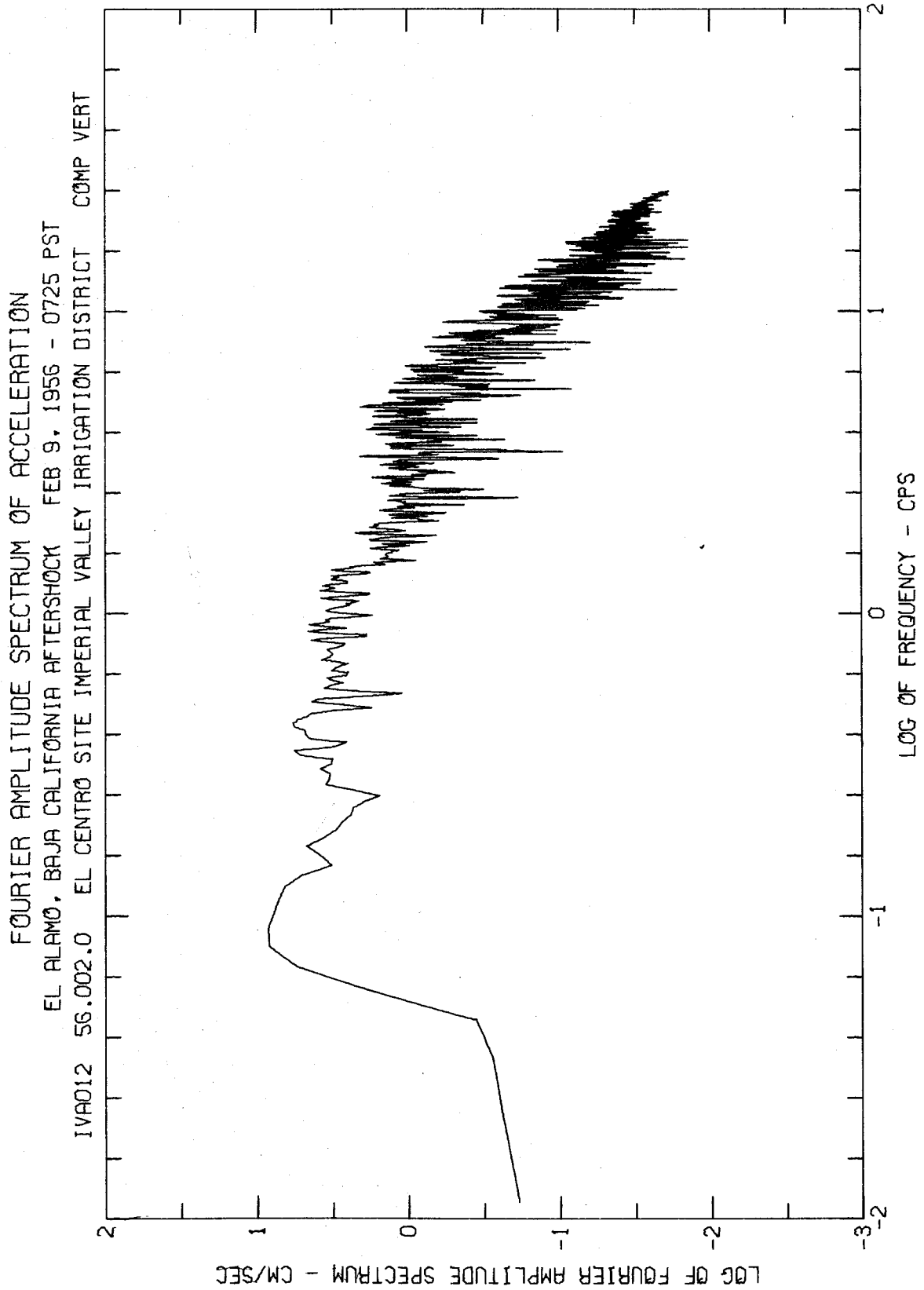


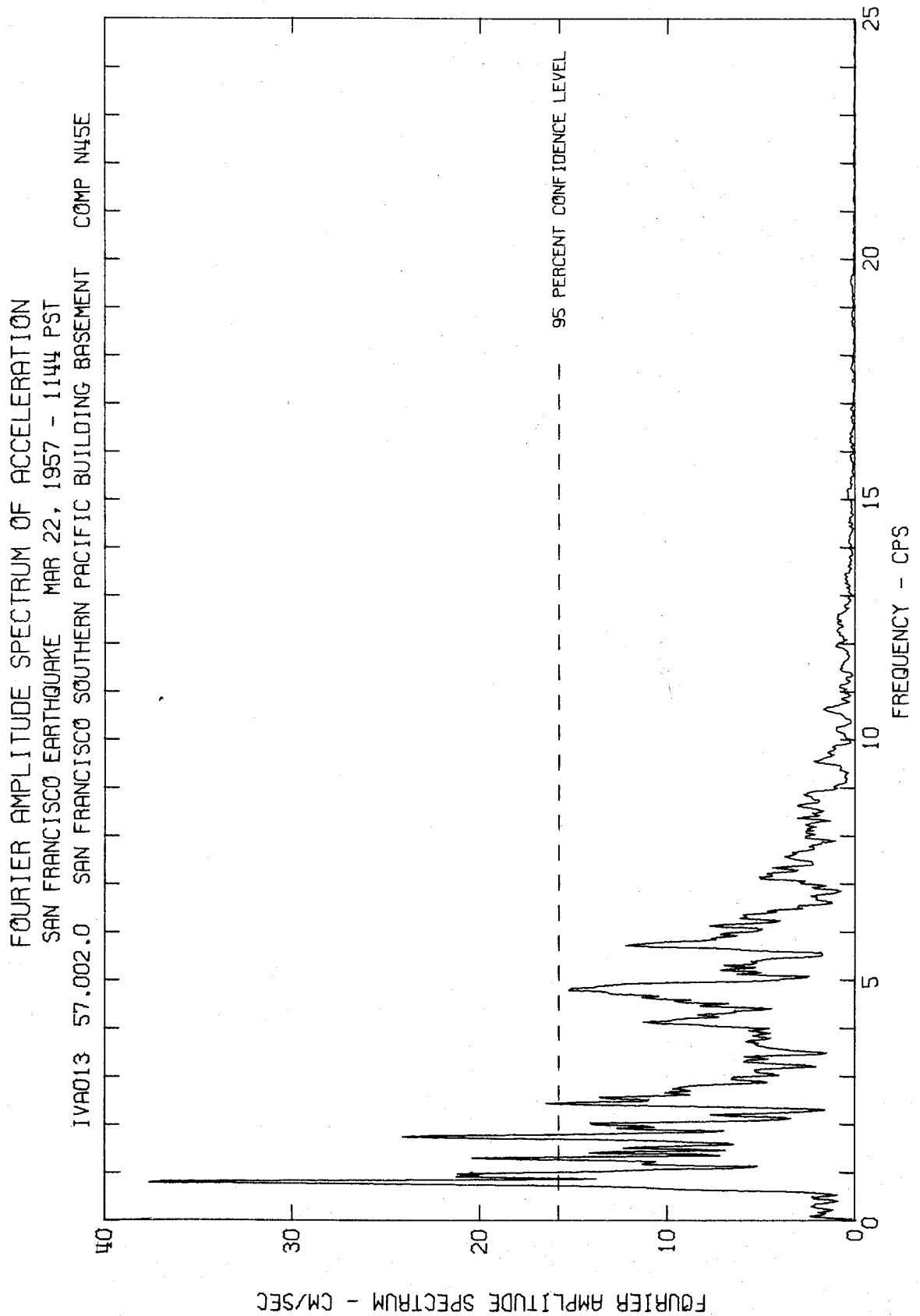


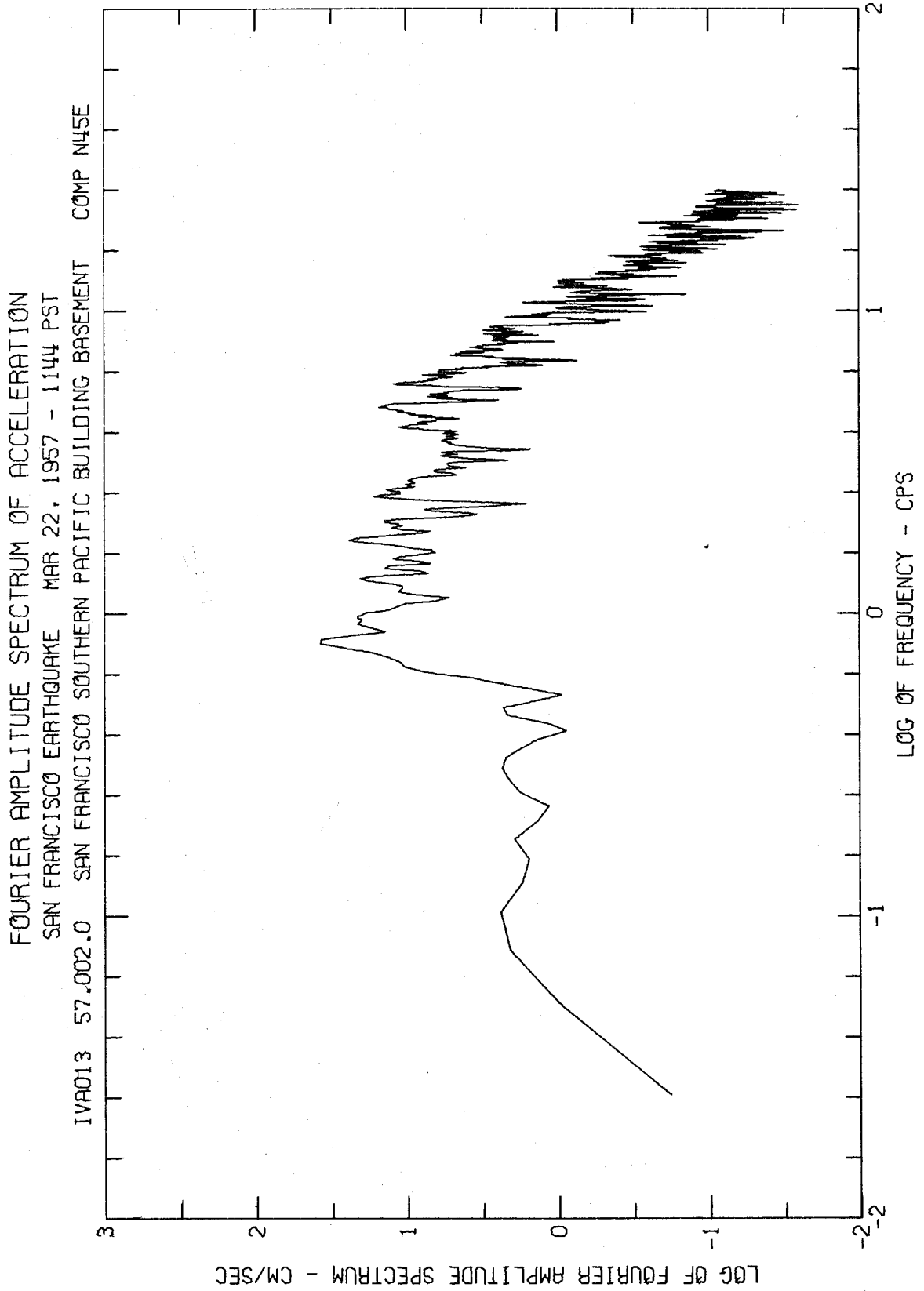


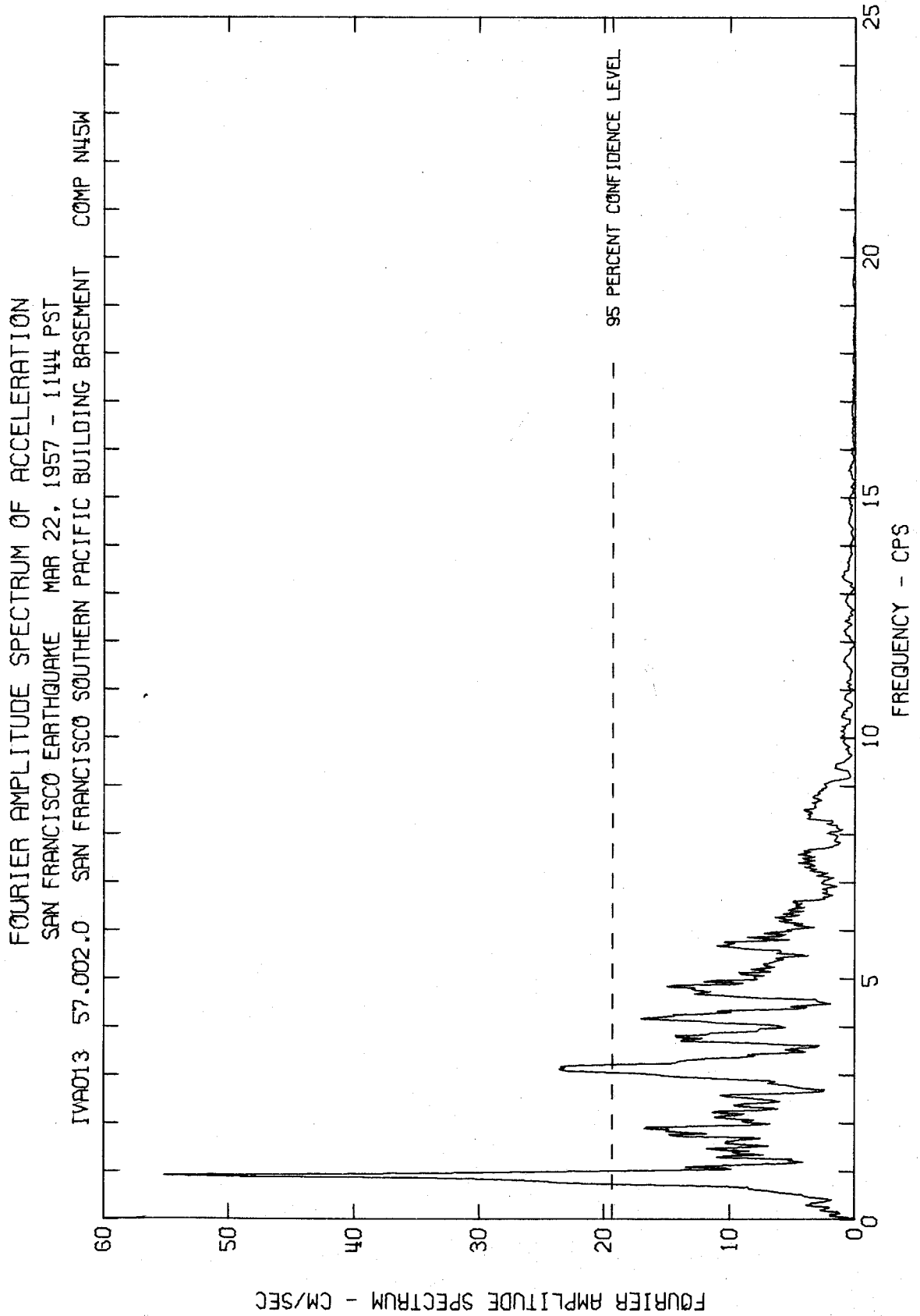


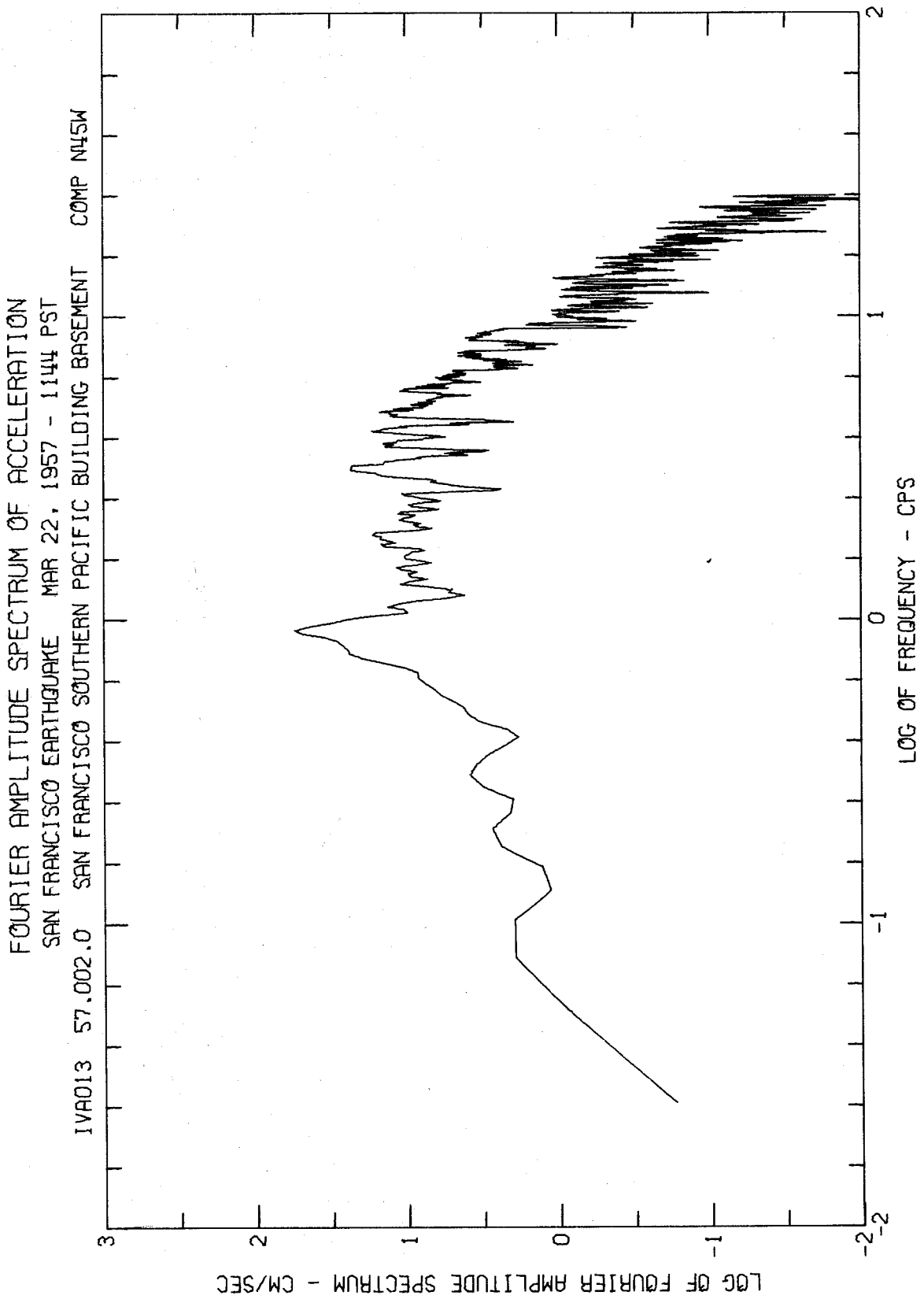


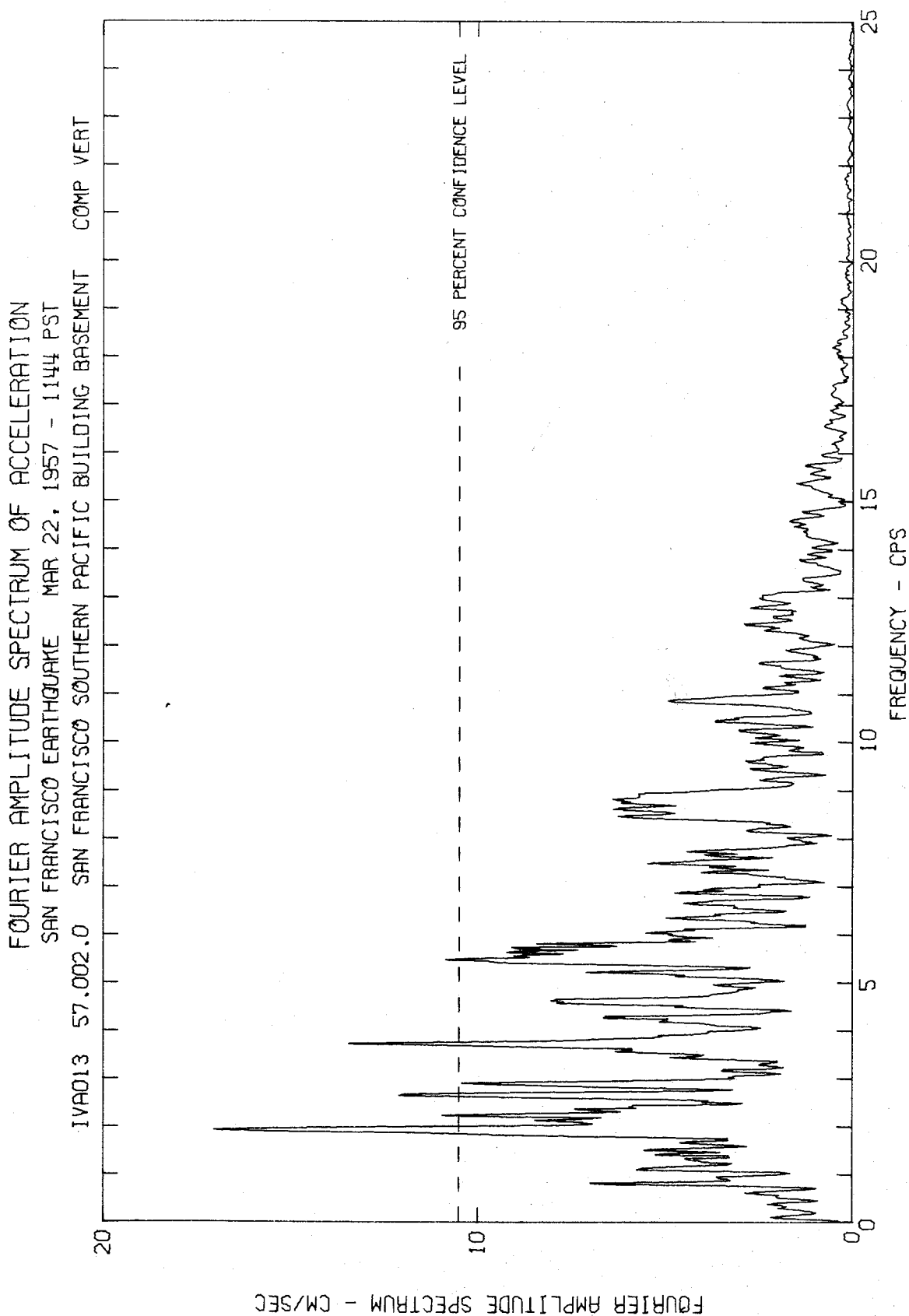


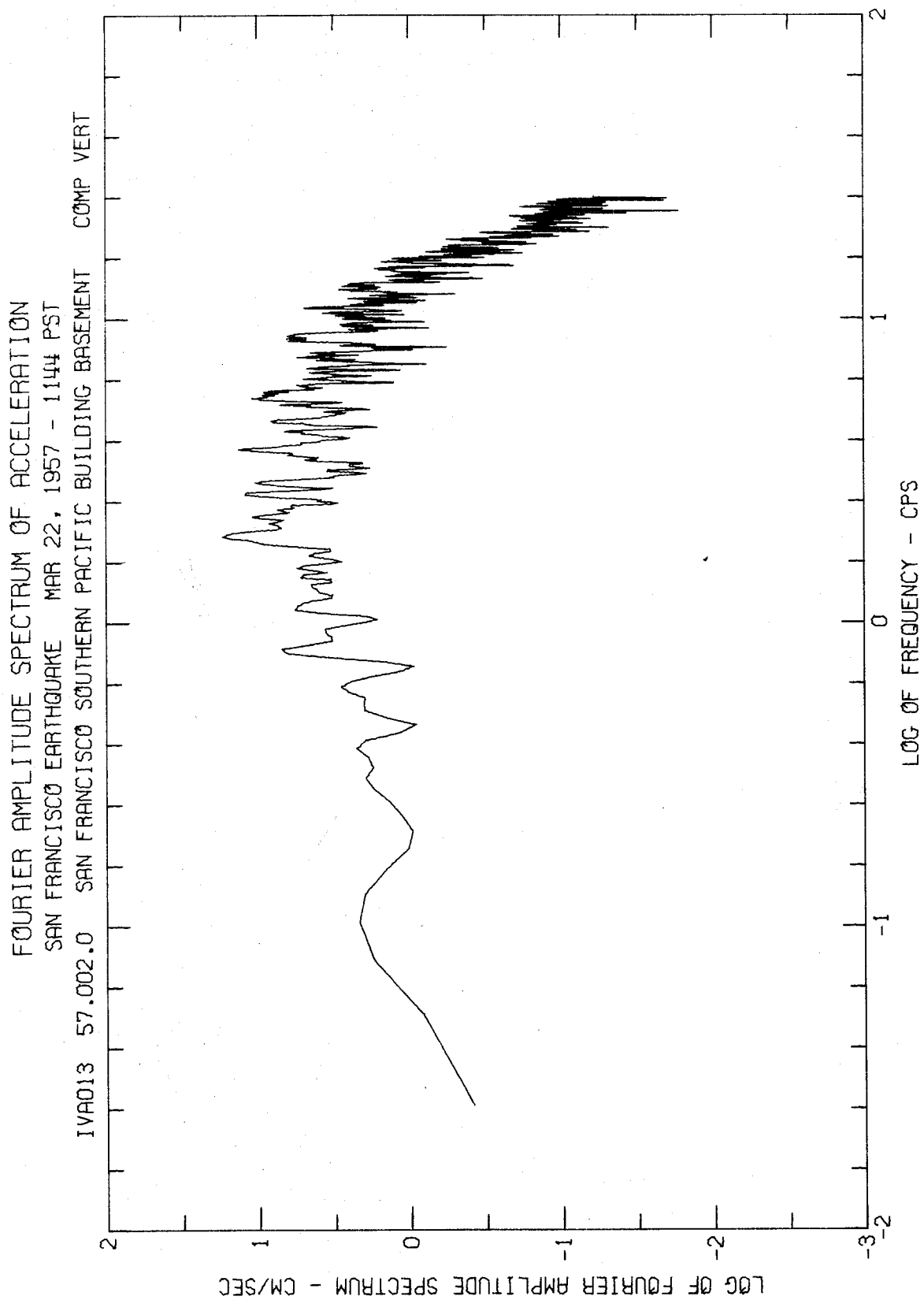




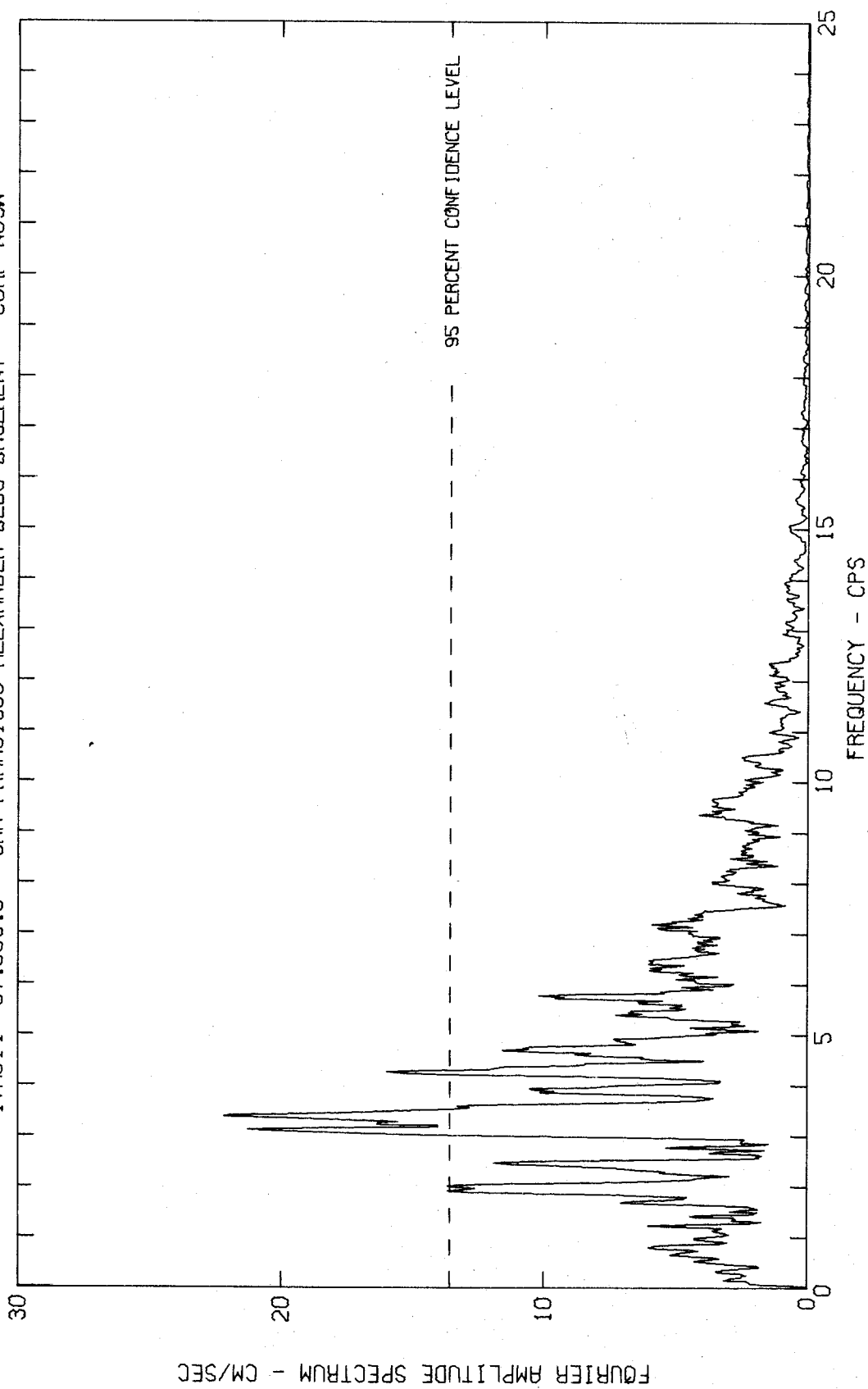




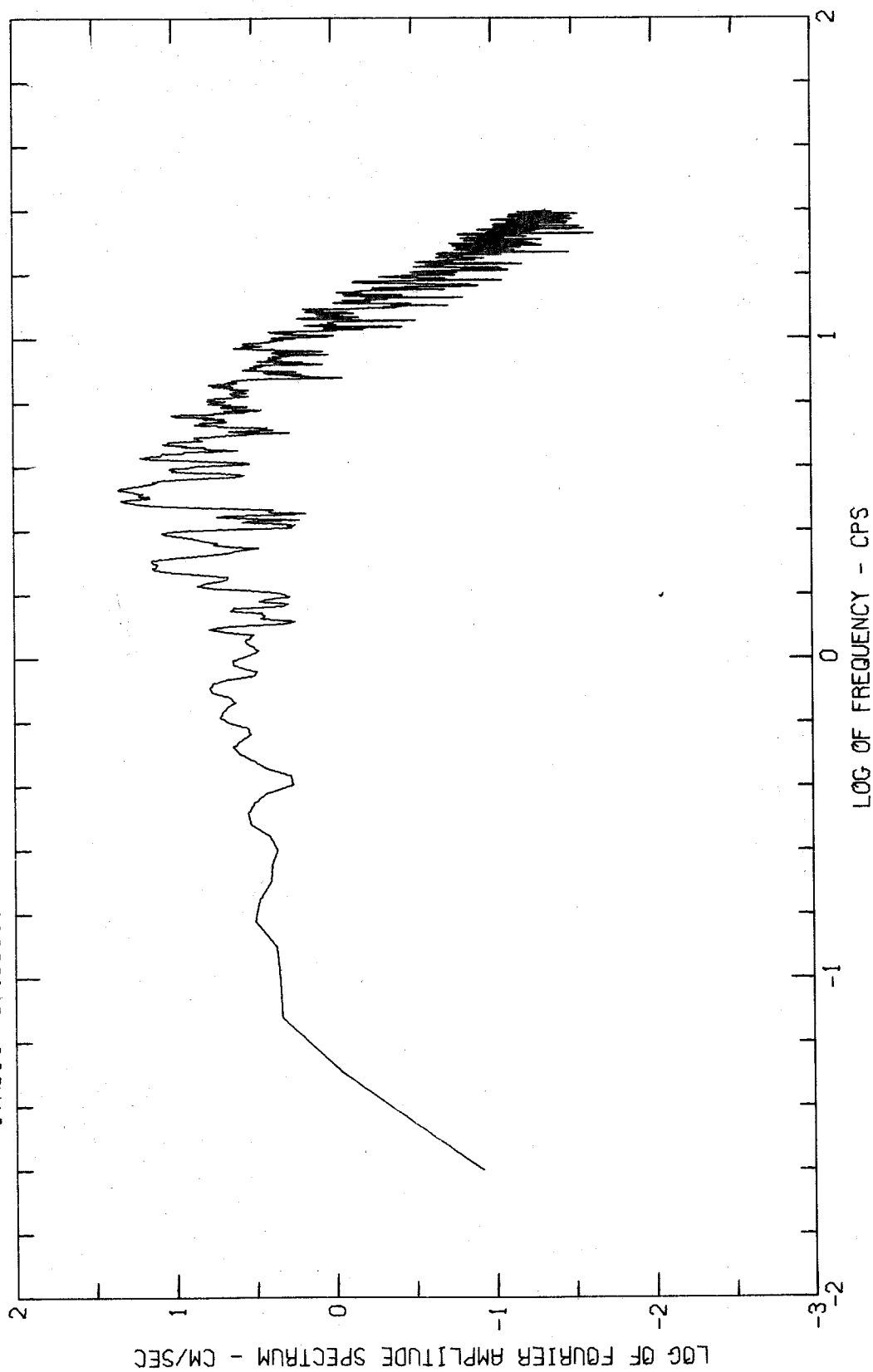




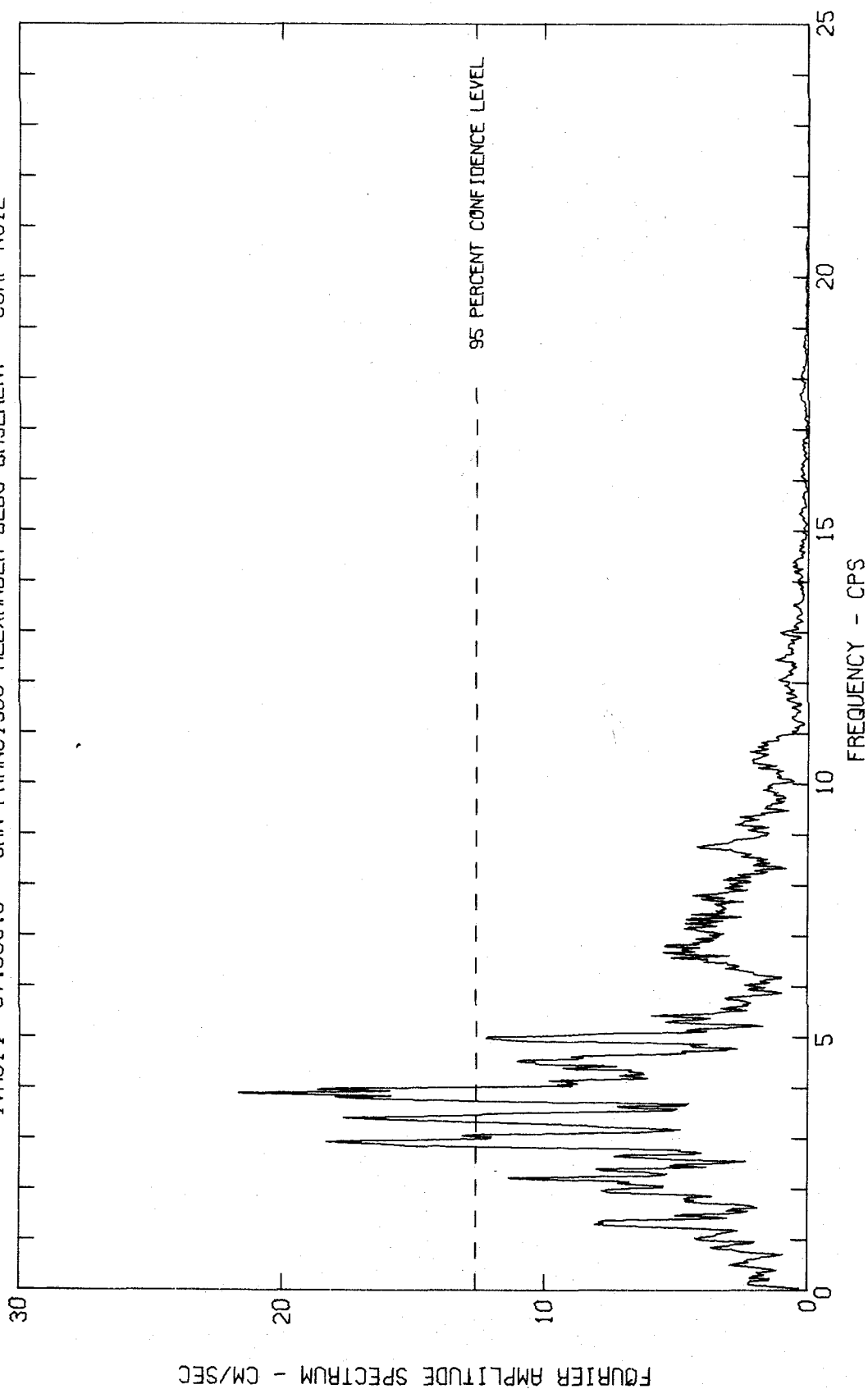
FOURIER AMPLITUDE SPECTRUM OF ACCELERATION
SAN FRANCISCO EARTHQUAKE MAR 22, 1957 - 1144 PST
IWA014 57.003.0 SAN FRANCISCO ALEXANDER BLDG BASEMENT COMP NOSW



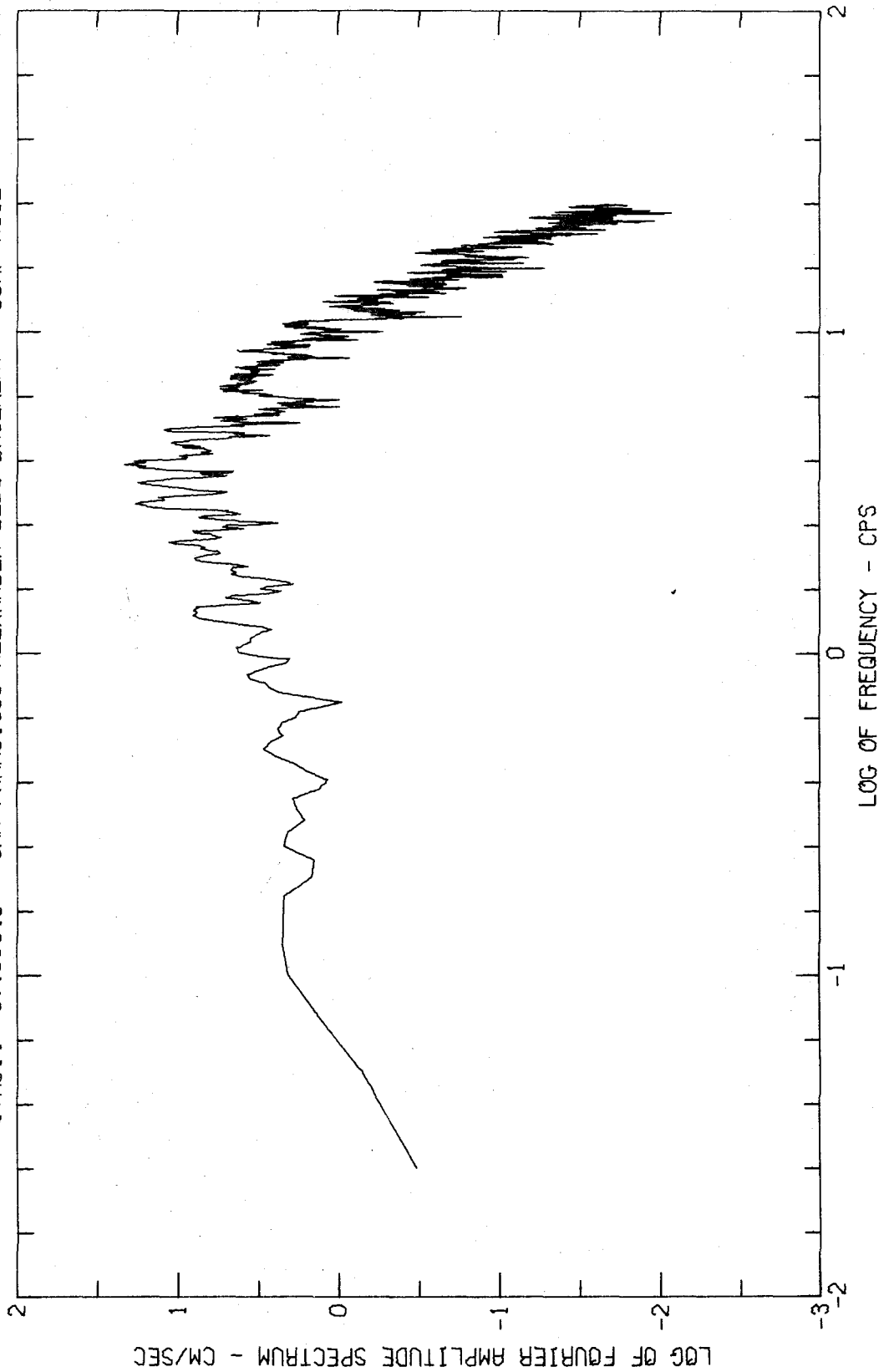
FOURIER AMPLITUDE SPECTRUM OF ACCELERATION
 SAN FRANCISCO EARTHQUAKE MAR 22, 1957 - 1144 PST
 IVA014 57.003.0 SAN FRANCISCO ALEXANDER BLDG BASEMENT COMP N08W



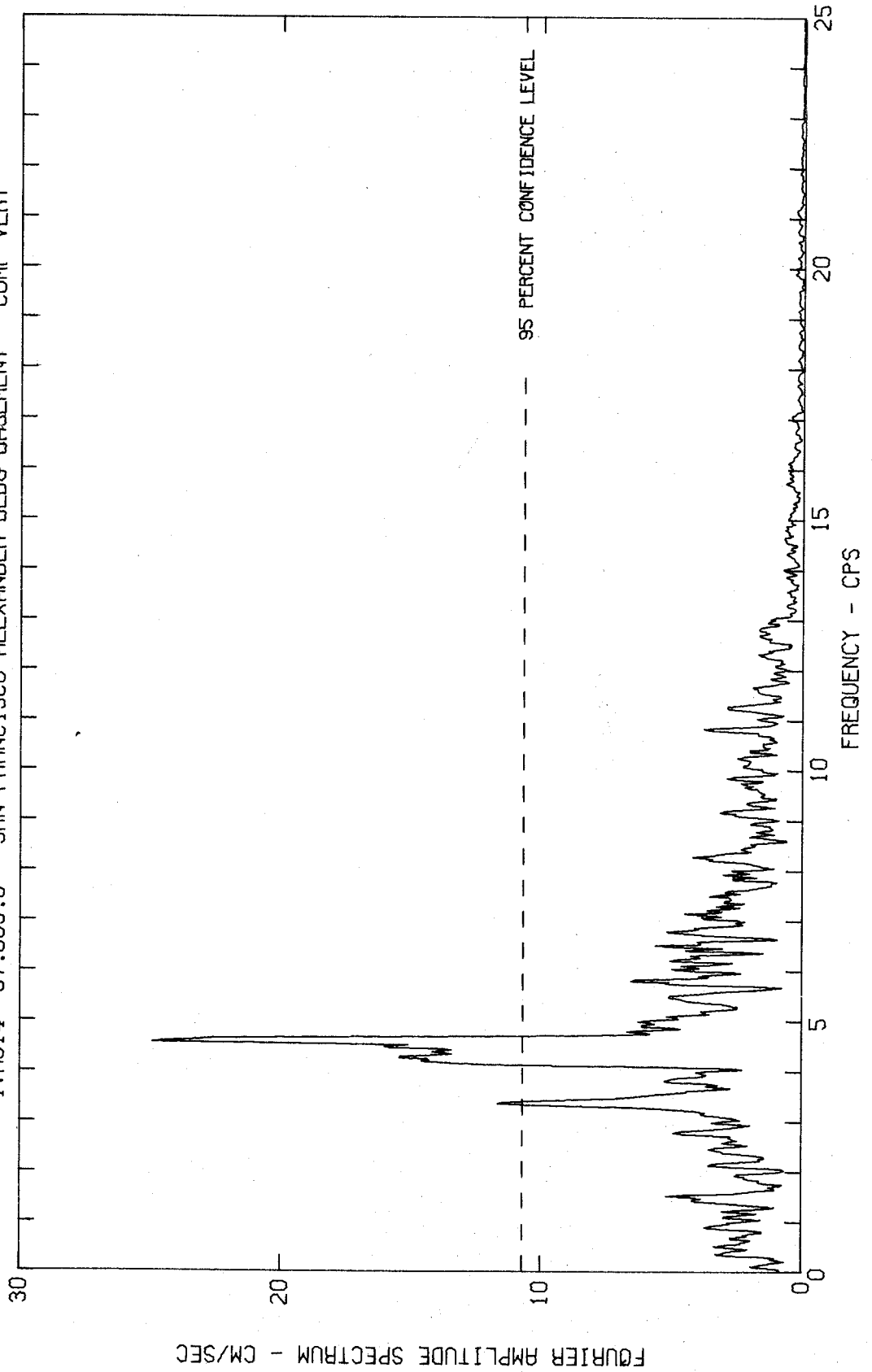
FOURIER AMPLITUDE SPECTRUM OF ACCELERATION
SAN FRANCISCO EARTHQUAKE MAR 22, 1957 - 1144 PST
IWA014 57.003.0 SAN FRANCISCO ALEXANDER BLDG BASEMENT COMP N81E



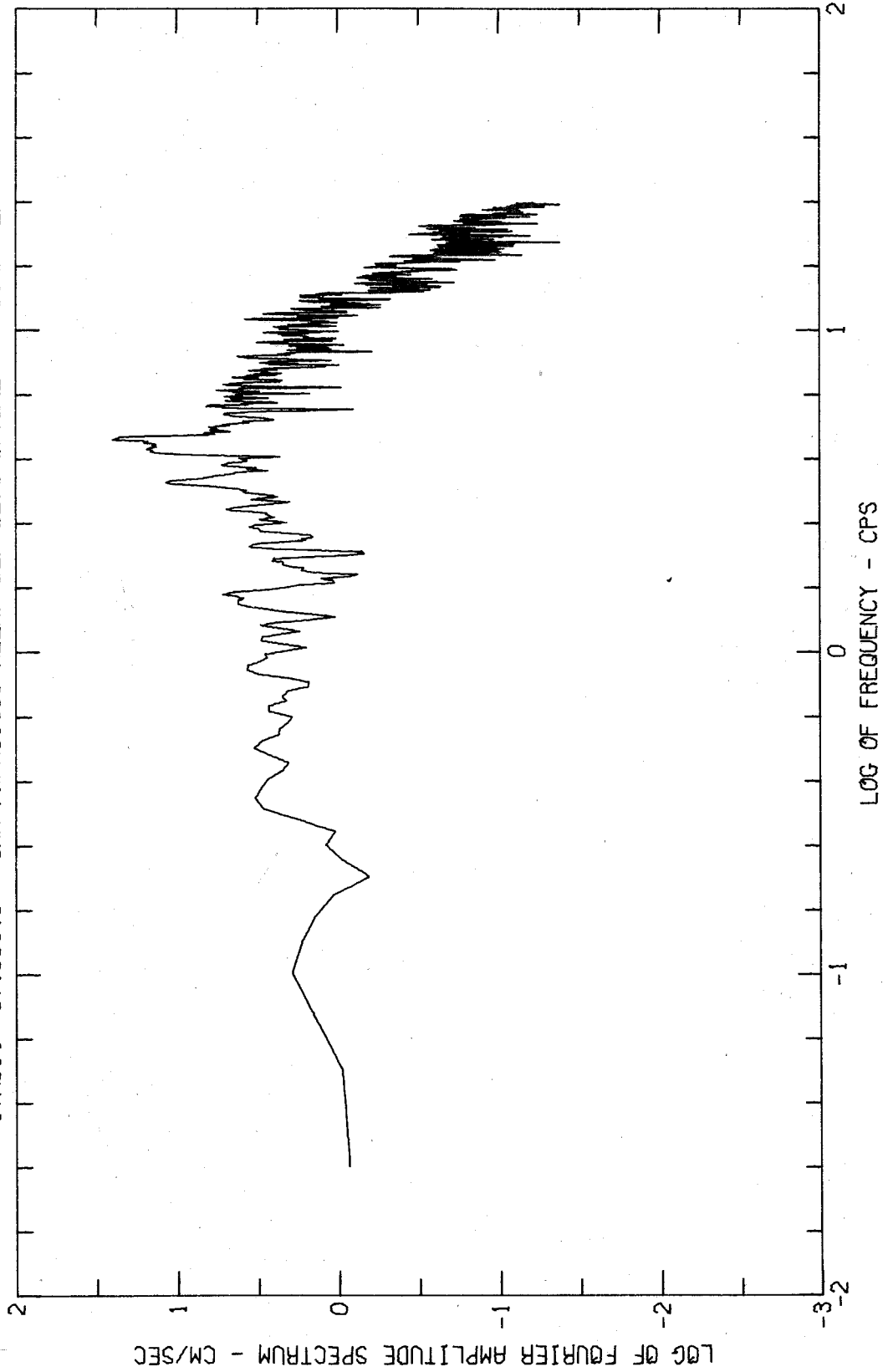
FOURIER AMPLITUDE SPECTRUM OF ACCELERATION
SAN FRANCISCO EARTHQUAKE MAR 22, 1957 - 1144 PST
IWA014 57.003.0 SAN FRANCISCO ALEXANDER BLDG BASEMENT COMP N81E



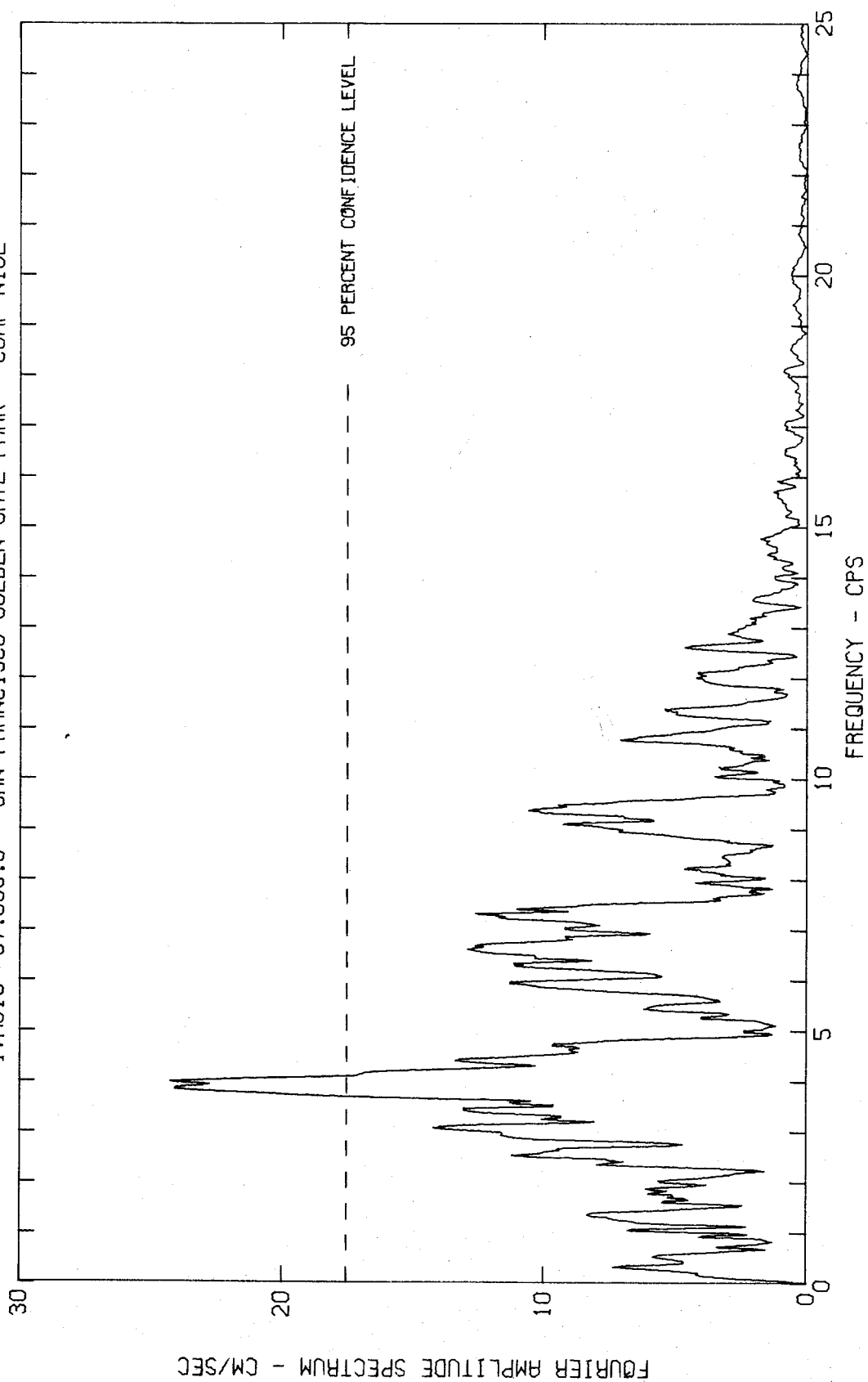
FOURIER AMPLITUDE SPECTRUM OF ACCELERATION
SAN FRANCISCO EARTHQUAKE MAR 22, 1957 - 1144 PST
IWA014 57.003.0 SAN FRANCISCO ALEXANDER BLDG BASEMENT COMP VERT



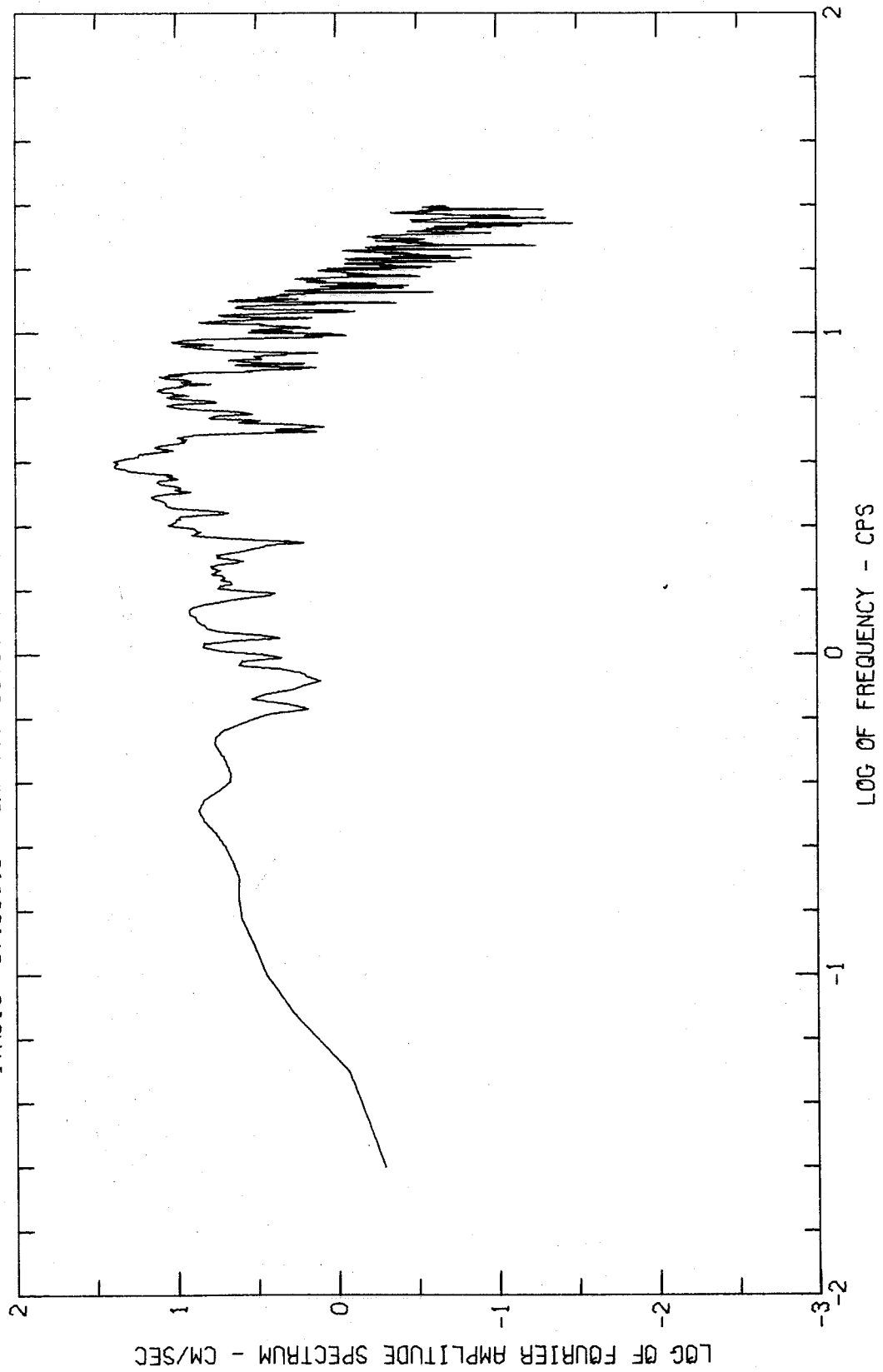
FOURIER AMPLITUDE SPECTRUM OF ACCELERATION
SAN FRANCISCO EARTHQUAKE MAR 22, 1957 - 1144 PST
IVA014 57.003.0 SAN FRANCISCO ALEXANDER BLDG BASEMENT COMP VERT



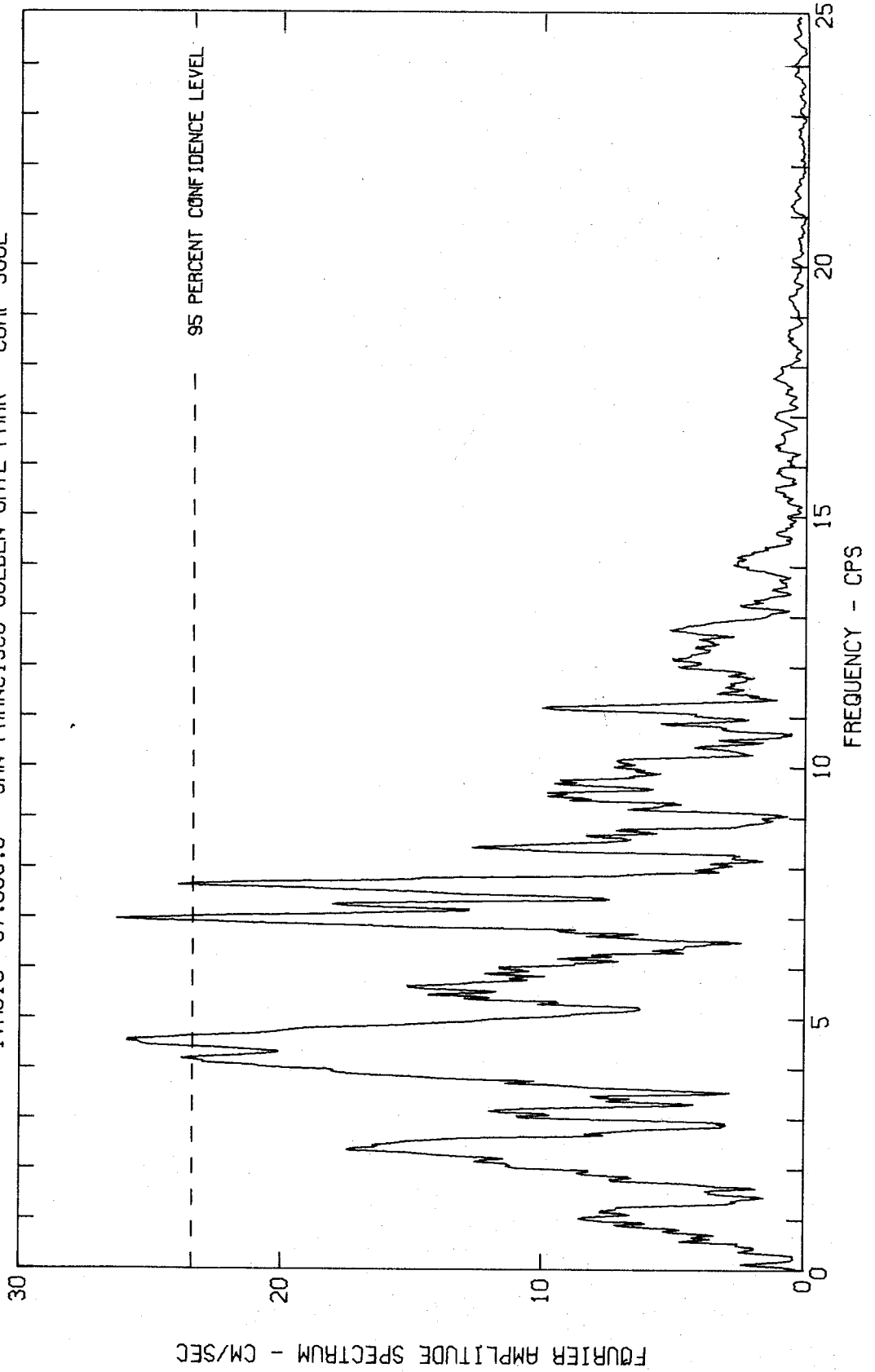
FOURIER AMPLITUDE SPECTRUM OF ACCELERATION
SAN FRANCISCO EARTHQUAKE MAR 22, 1957 - 1144 PST
IVA015 57.006.0 SAN FRANCISCO GOLDEN GATE PARK COMP N10E



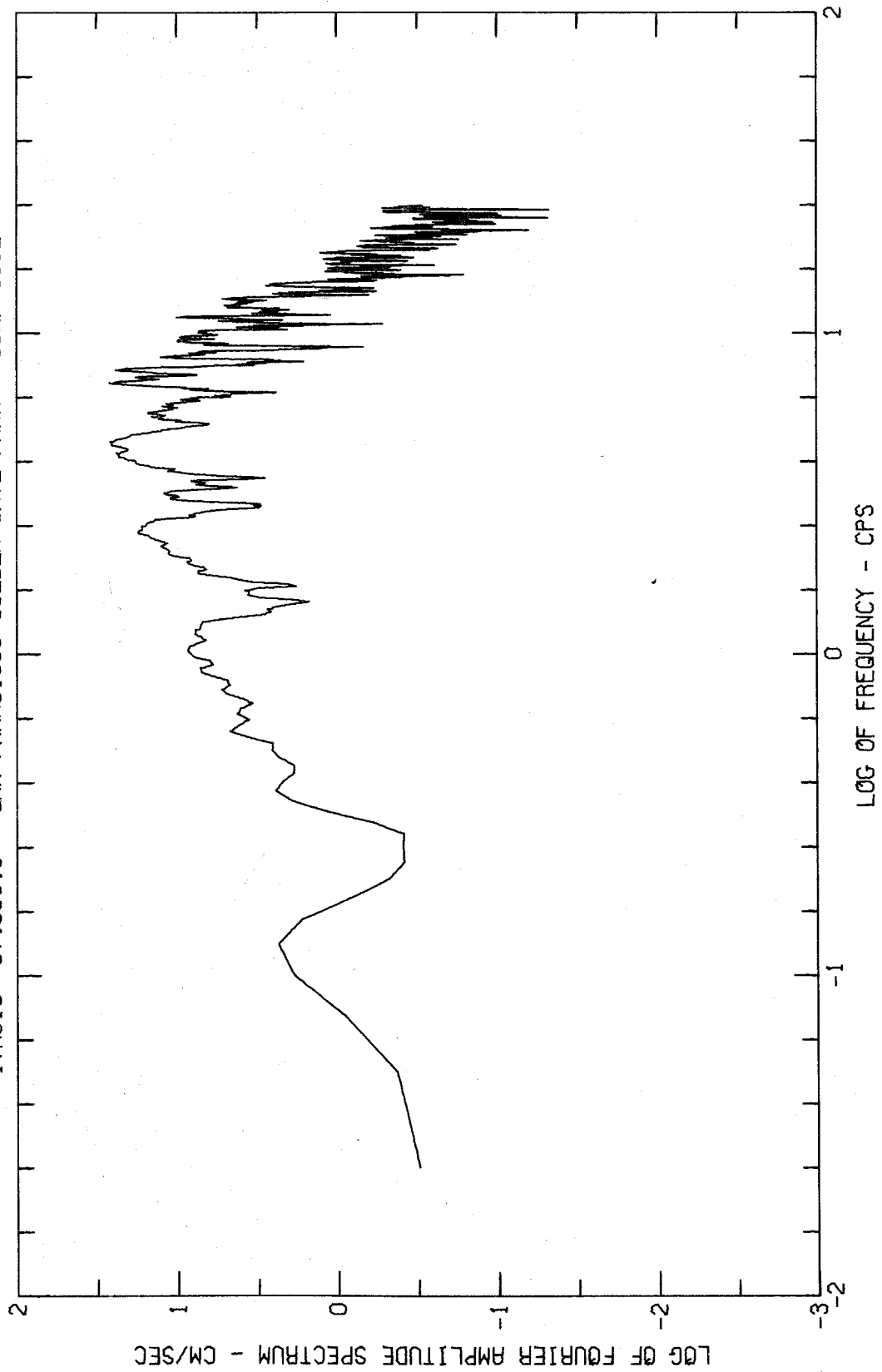
FOURIER AMPLITUDE SPECTRUM OF ACCELERATION
SAN FRANCISCO EARTHQUAKE MAR 22, 1957 - 1144 PST
IWA015 57.006.0 SAN FRANCISCO GOLDEN GATE PARK COMP N10E



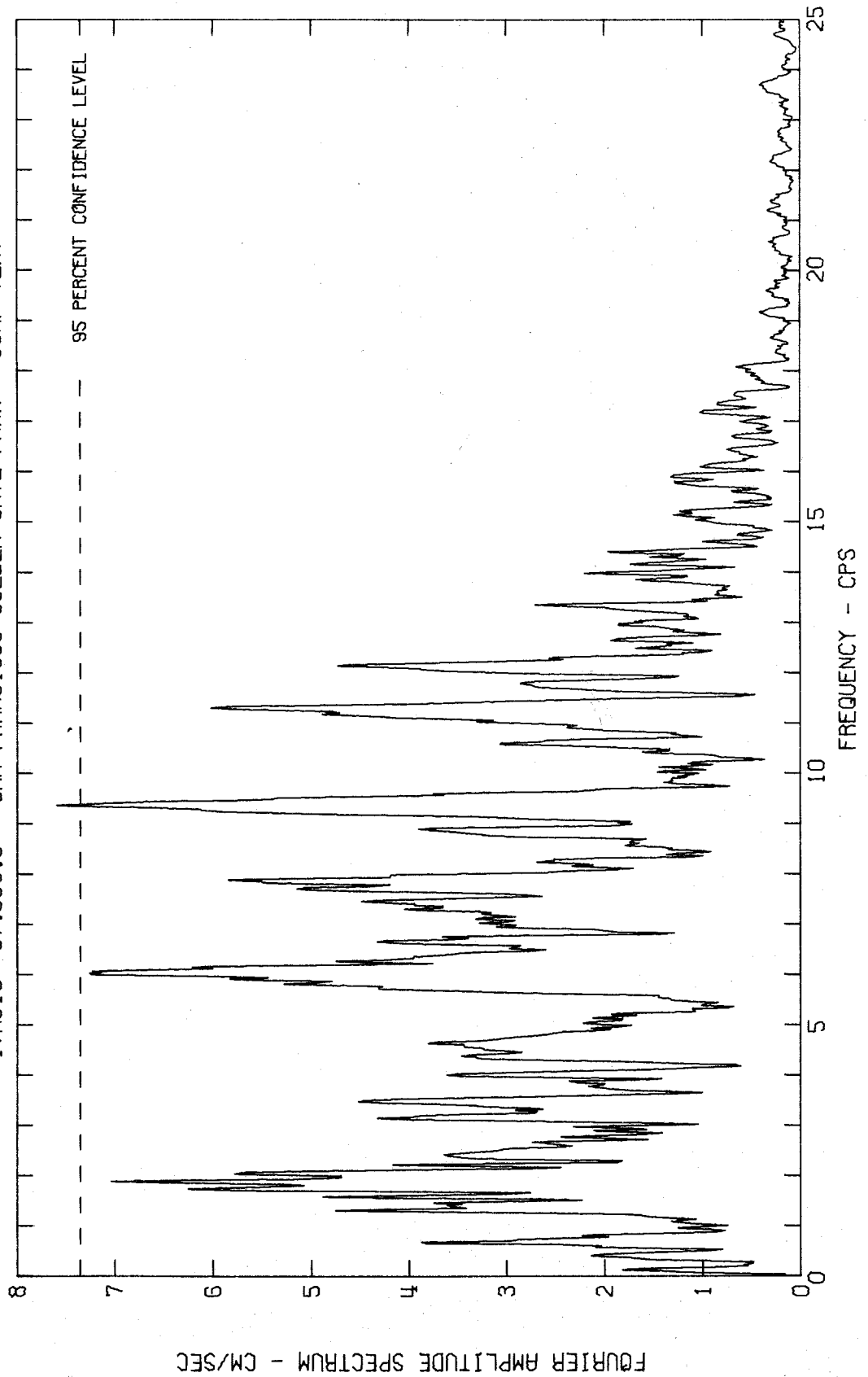
FOURIER AMPLITUDE SPECTRUM OF ACCELERATION
SAN FRANCISCO EARTHQUAKE MAR 22, 1957 - 1144 PST
IWA015 57.006.0 SAN FRANCISCO GOLDEN GATE PARK COMP S80E



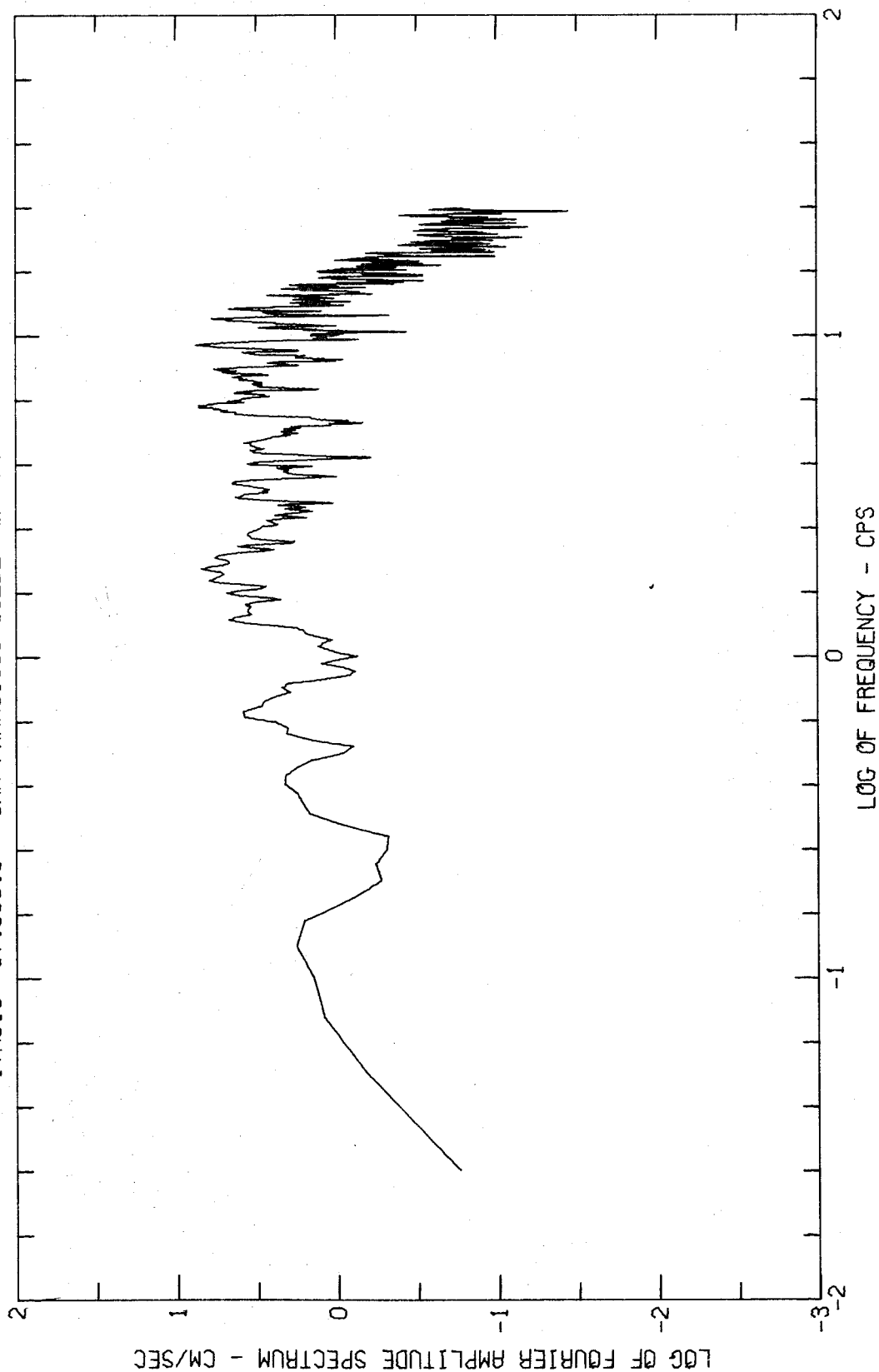
FOURIER AMPLITUDE SPECTRUM OF ACCELERATION
SAN FRANCISCO EARTHQUAKE MAR 22, 1957 - 1144 PST
IWA015 57.006.0 SAN FRANCISCO GOLDEN GATE PARK COMP S80E



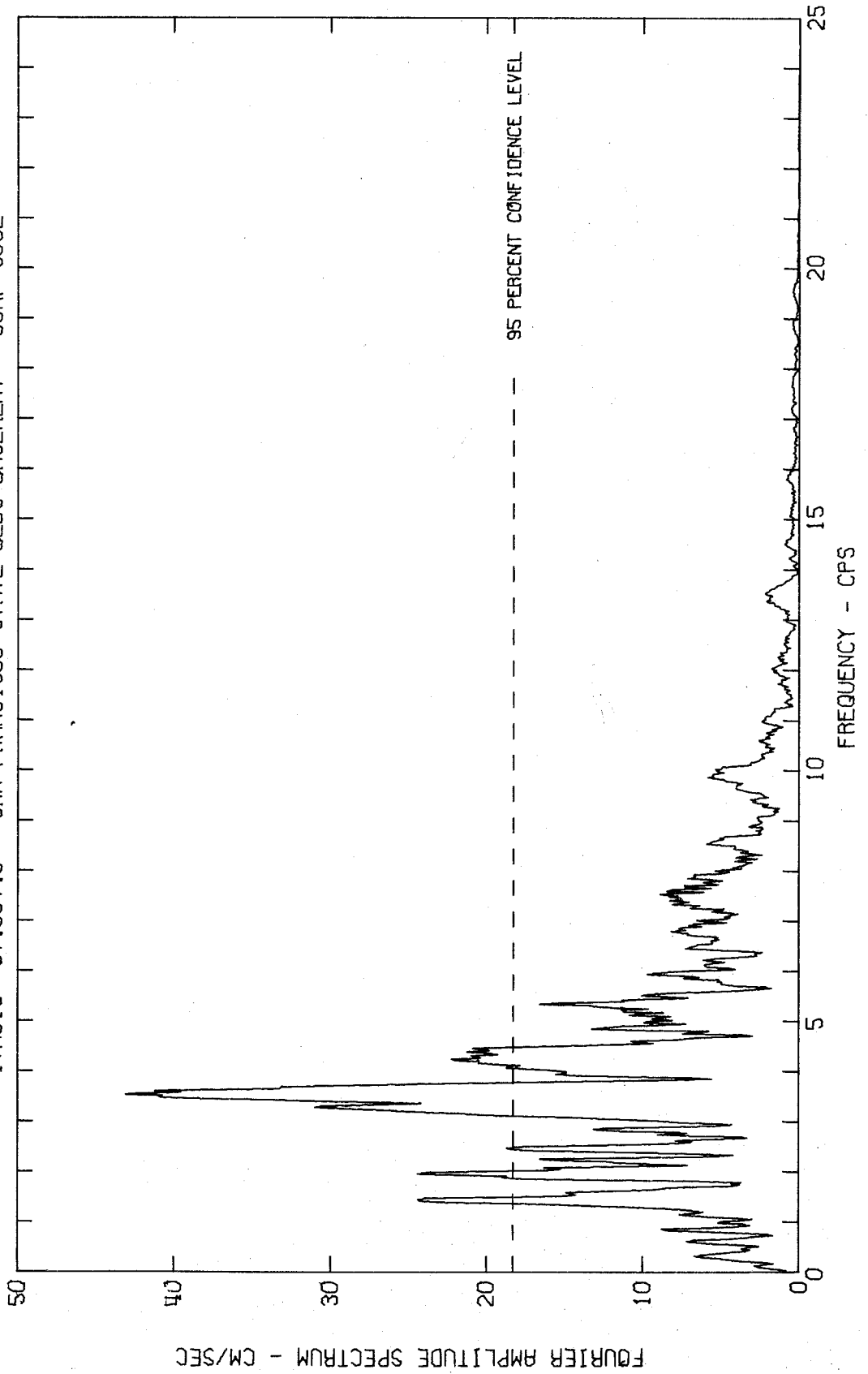
FOURIER AMPLITUDE SPECTRUM OF ACCELERATION
SAN FRANCISCO EARTHQUAKE MAR 22, 1957 - 1144 PST
IWA015 57.006.0 SAN FRANCISCO GOLDEN GATE PARK COMP VERT



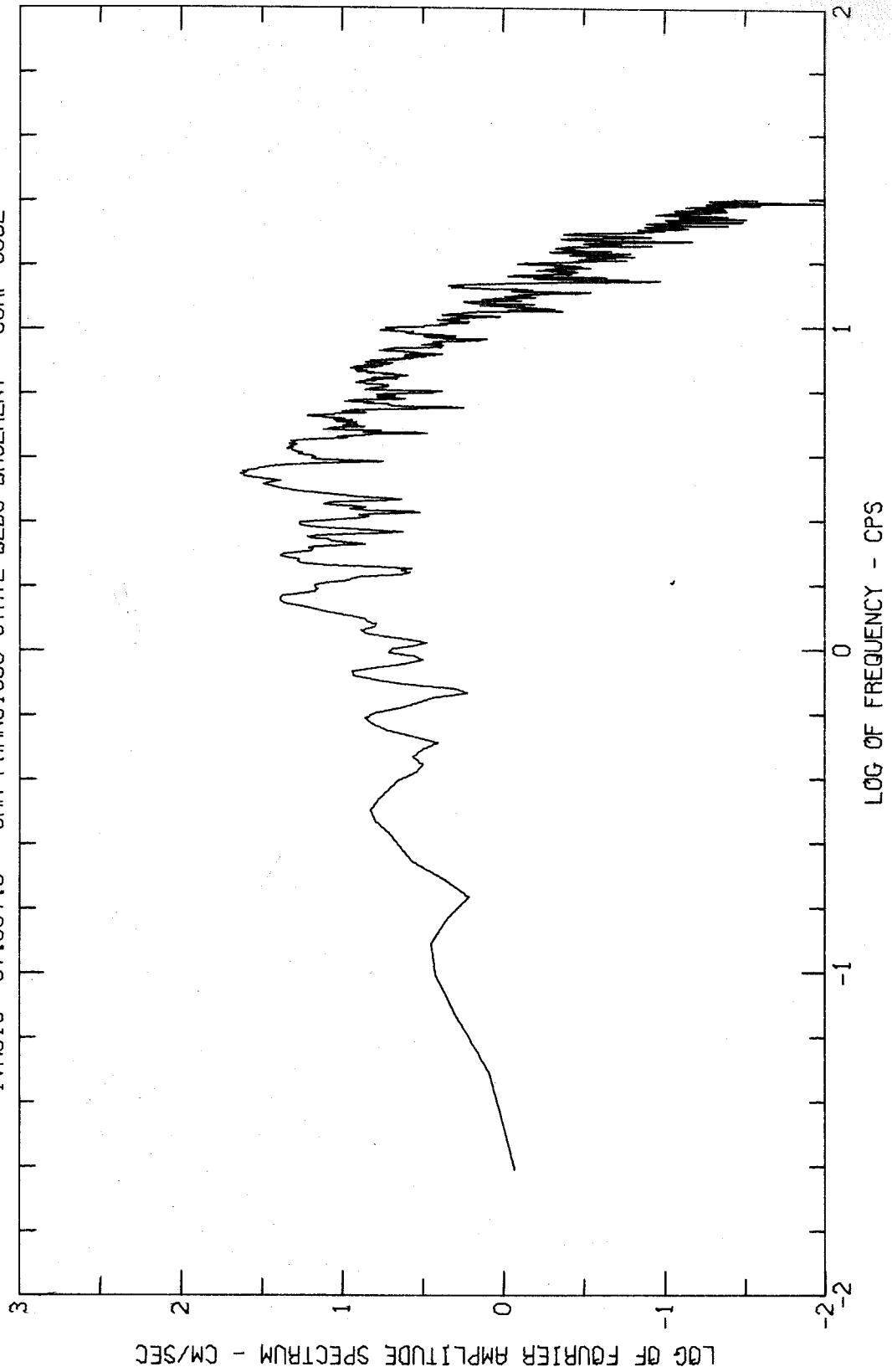
FOURIER AMPLITUDE SPECTRUM OF ACCELERATION
SAN FRANCISCO EARTHQUAKE MAR 22, 1957 - 1144 PST
IWA015 57.006.0 SAN FRANCISCO GOLDEN GATE PARK COMP VERT



FOURIER AMPLITUDE SPECTRUM OF ACCELERATION
SAN FRANCISCO EARTHQUAKE MAR 22, 1957 - 1144 PST
IWA016 57.007.0 SAN FRANCISCO STATE BLDG BASEMENT COMP S09E



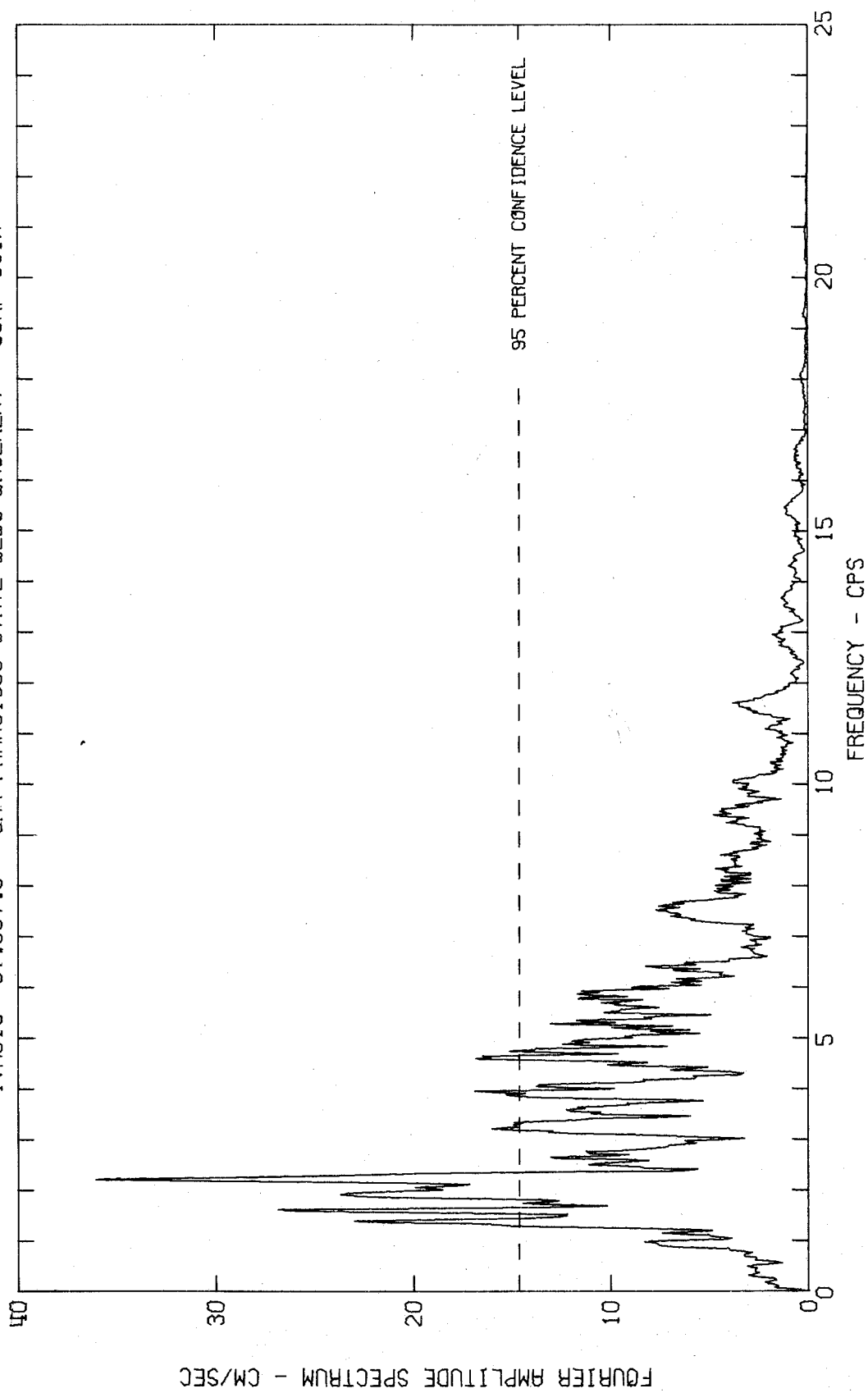
FOURIER AMPLITUDE SPECTRUM OF ACCELERATION
SAN FRANCISCO EARTHQUAKE MAR 22, 1957 - 1144 PST
IWA016 57.007.0 SAN FRANCISCO STATE BLDG BASEMENT COMP S09E



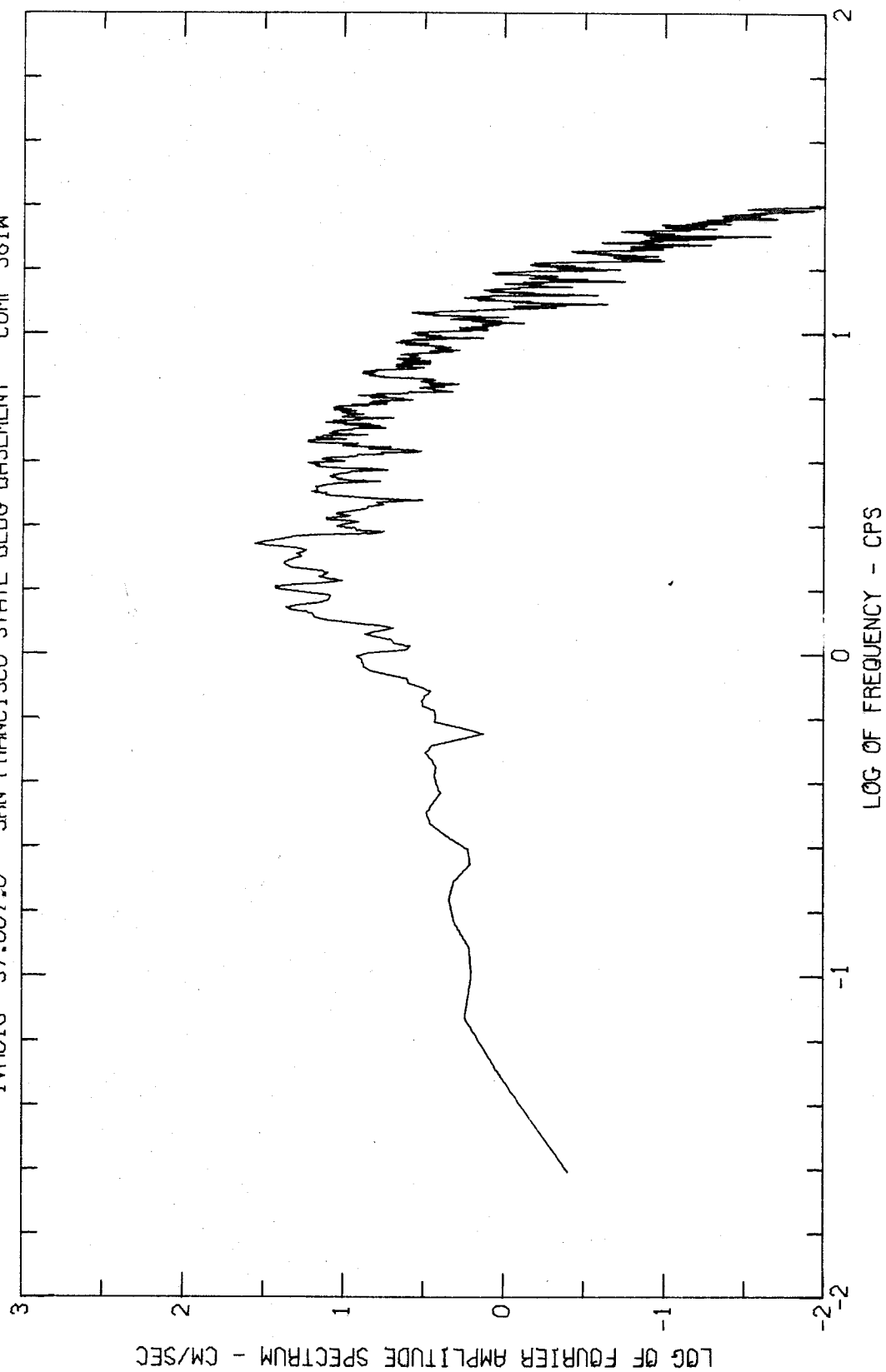
FOURIER AMPLITUDE SPECTRUM OF ACCELERATION

SAN FRANCISCO EARTHQUAKE MAR 22, 1957 - 1144 PST

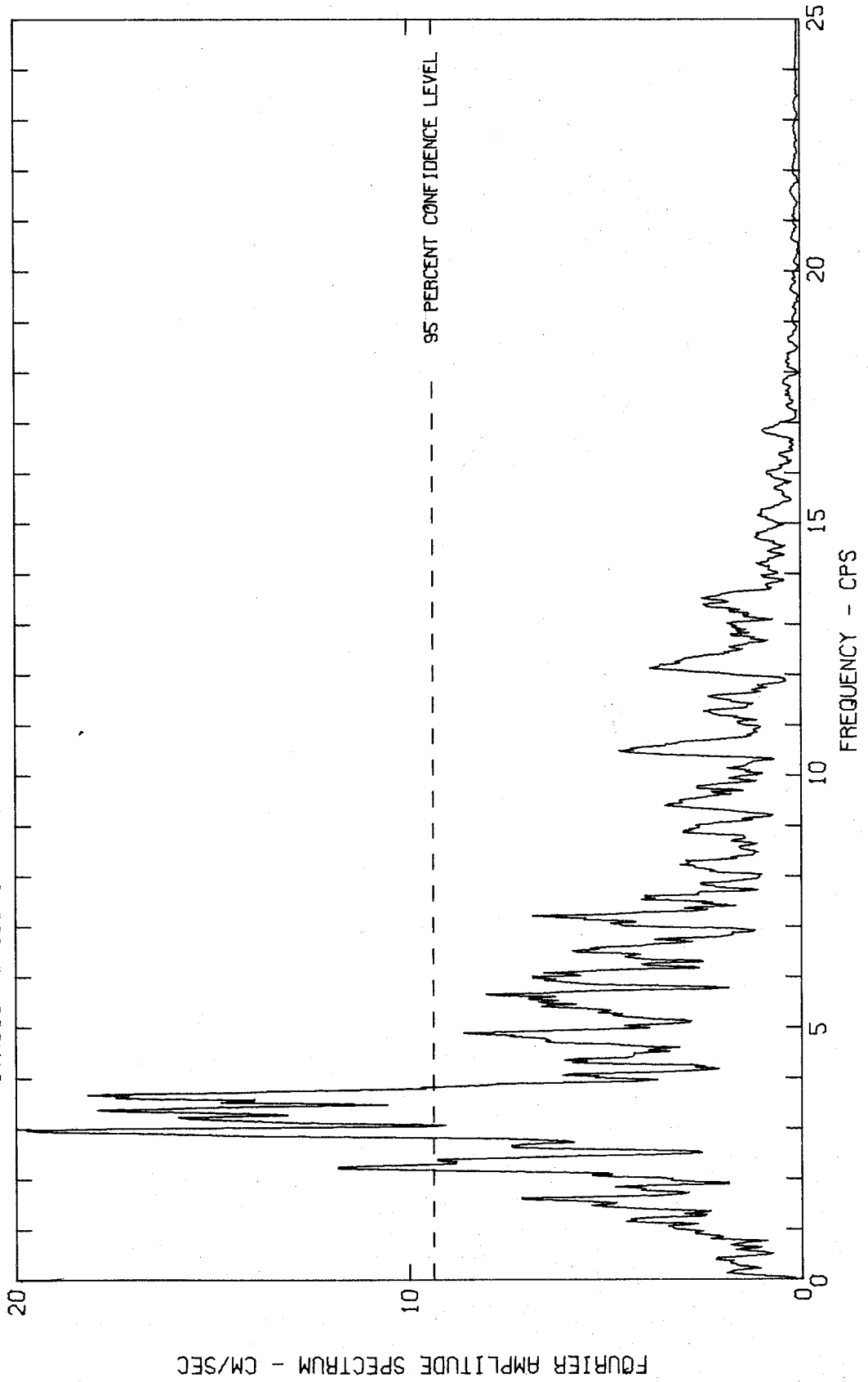
IWA016 57.007.0 SAN FRANCISCO STATE BLDG BASEMENT COMP S81W



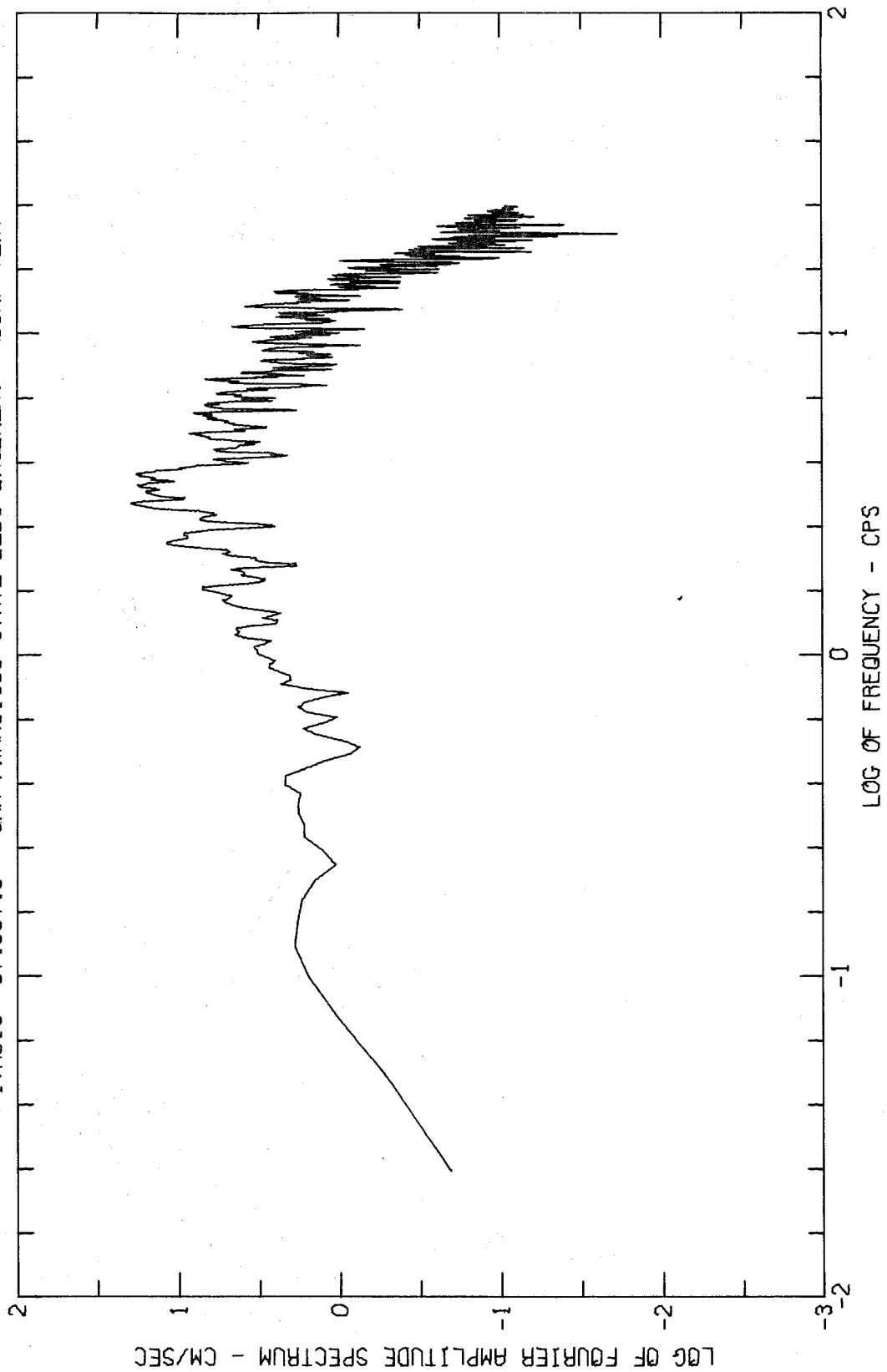
FOURIER AMPLITUDE SPECTRUM OF ACCELERATION
SAN FRANCISCO EARTHQUAKE MAR 22, 1957 - 1144 PST
IWA016 57.007.0 SAN FRANCISCO STATE BLDG BASEMENT COMP S81W



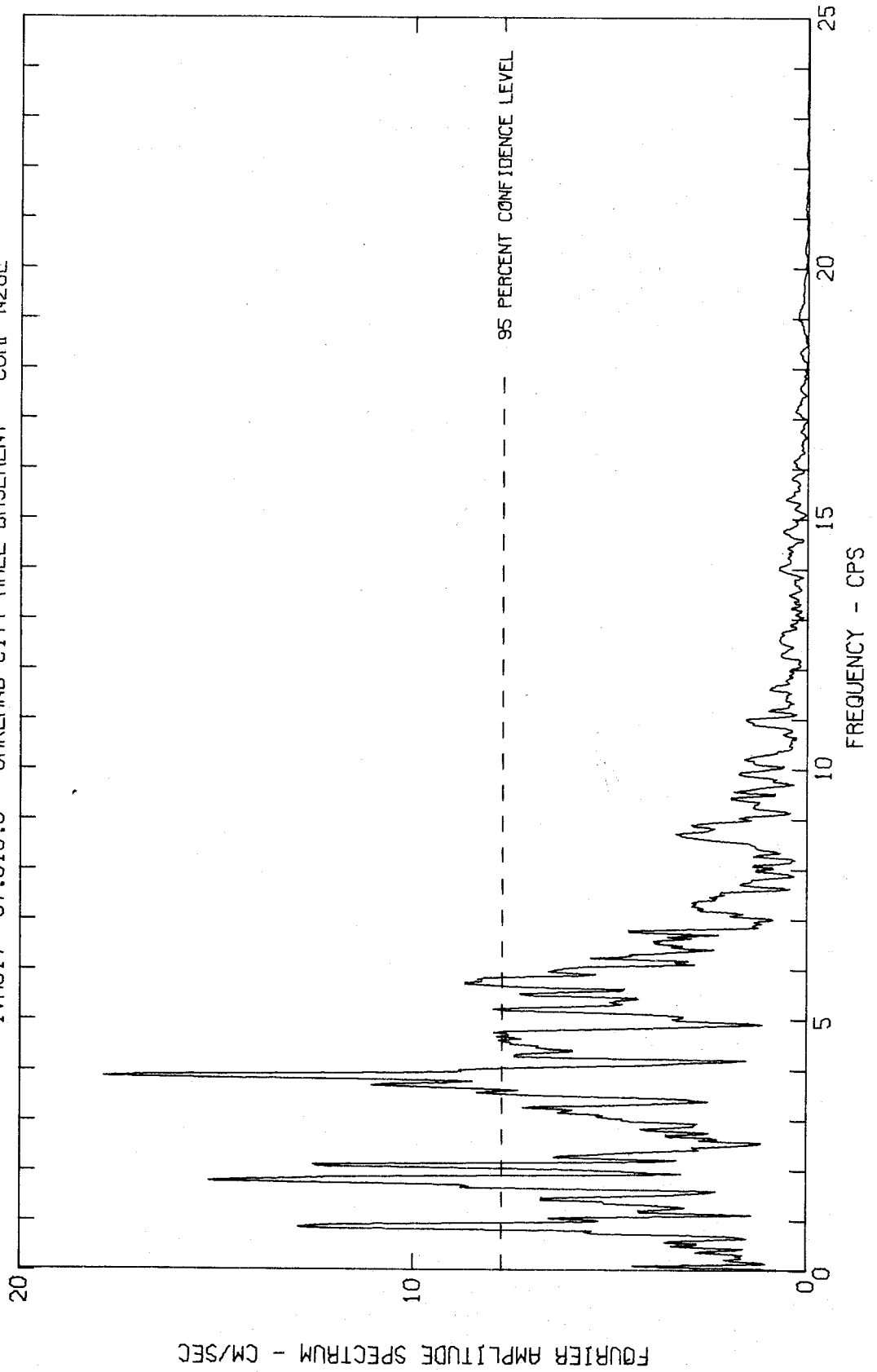
FOURIER AMPLITUDE SPECTRUM OF ACCELERATION
SAN FRANCISCO EARTHQUAKE MAR 22, 1957 - 1144 PST
IWA016 57.007.0 SAN FRANCISCO STATE BLDG BASEMENT COMP VERT



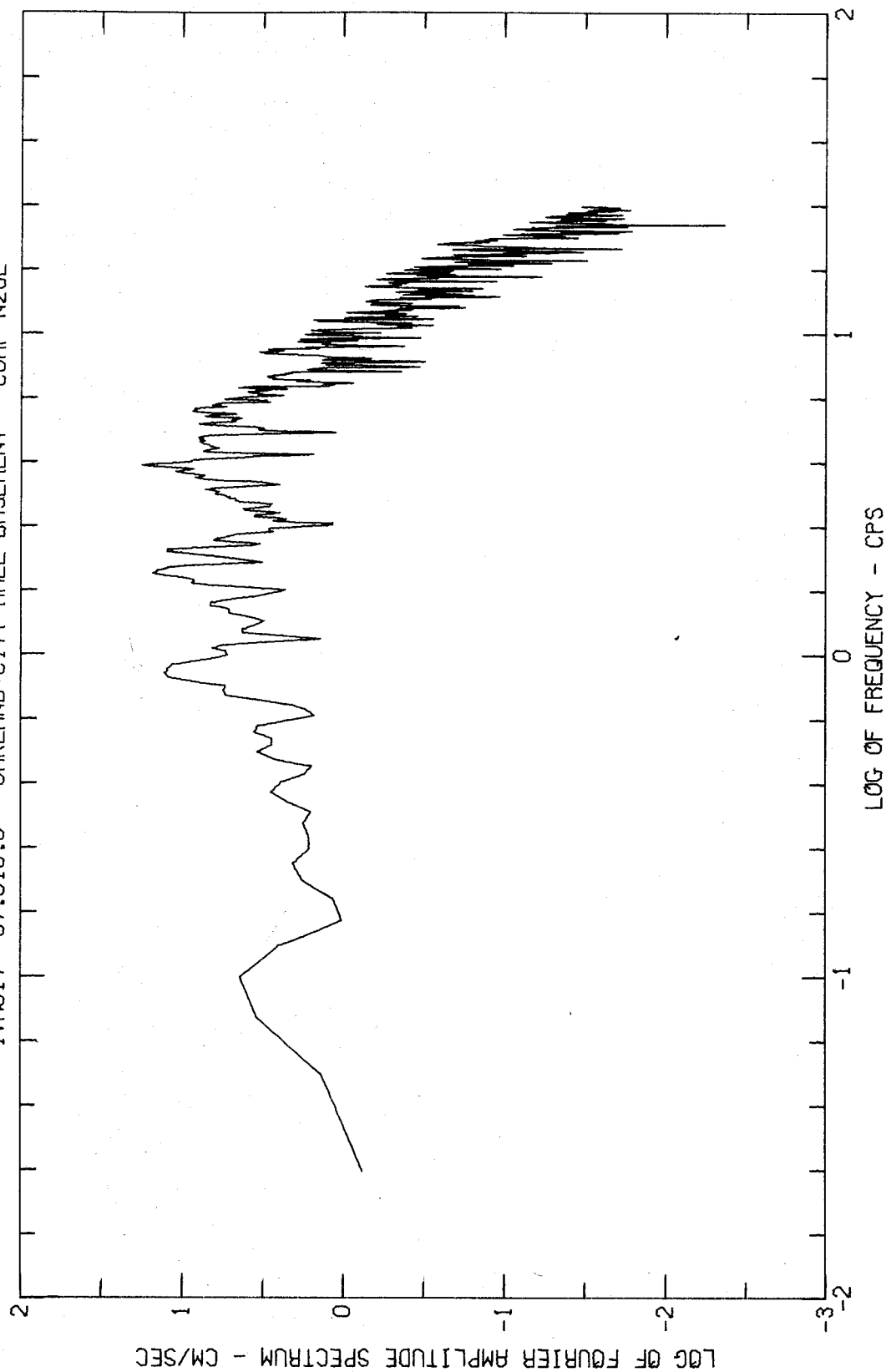
FOURIER AMPLITUDE SPECTRUM OF ACCELERATION
SAN FRANCISCO EARTHQUAKE MAR 22, 1957 - 1144 PST
IWA016 57.007.0 SAN FRANCISCO STATE BLDG BASEMENT COMP VERT



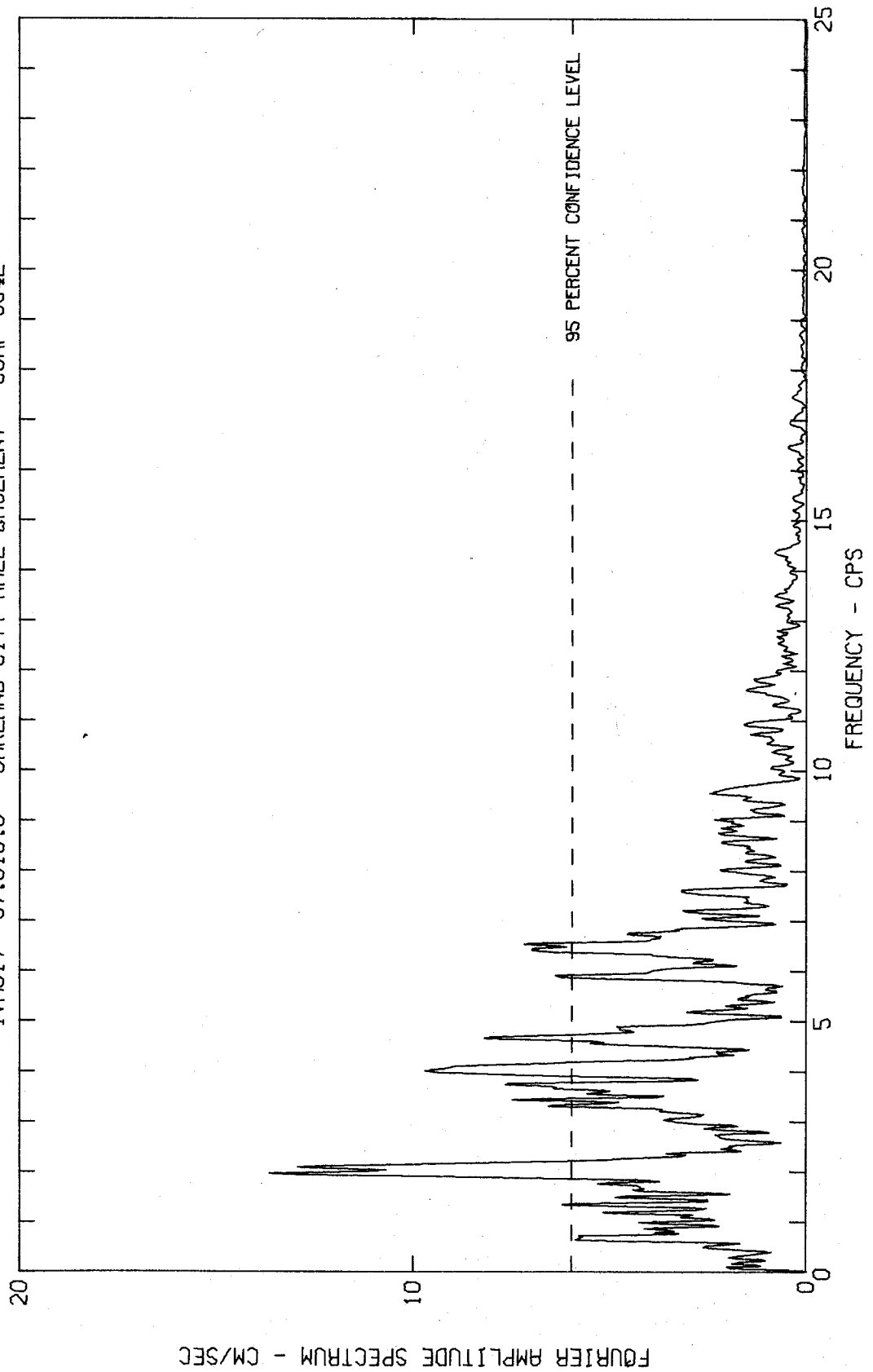
FOURIER AMPLITUDE SPECTRUM OF ACCELERATION
SAN FRANCISCO EARTHQUAKE MAR 22, 1957 - 1144 PST
IWA017 57.010.0 OAKLAND CITY HALL BASEMENT COMP N26E



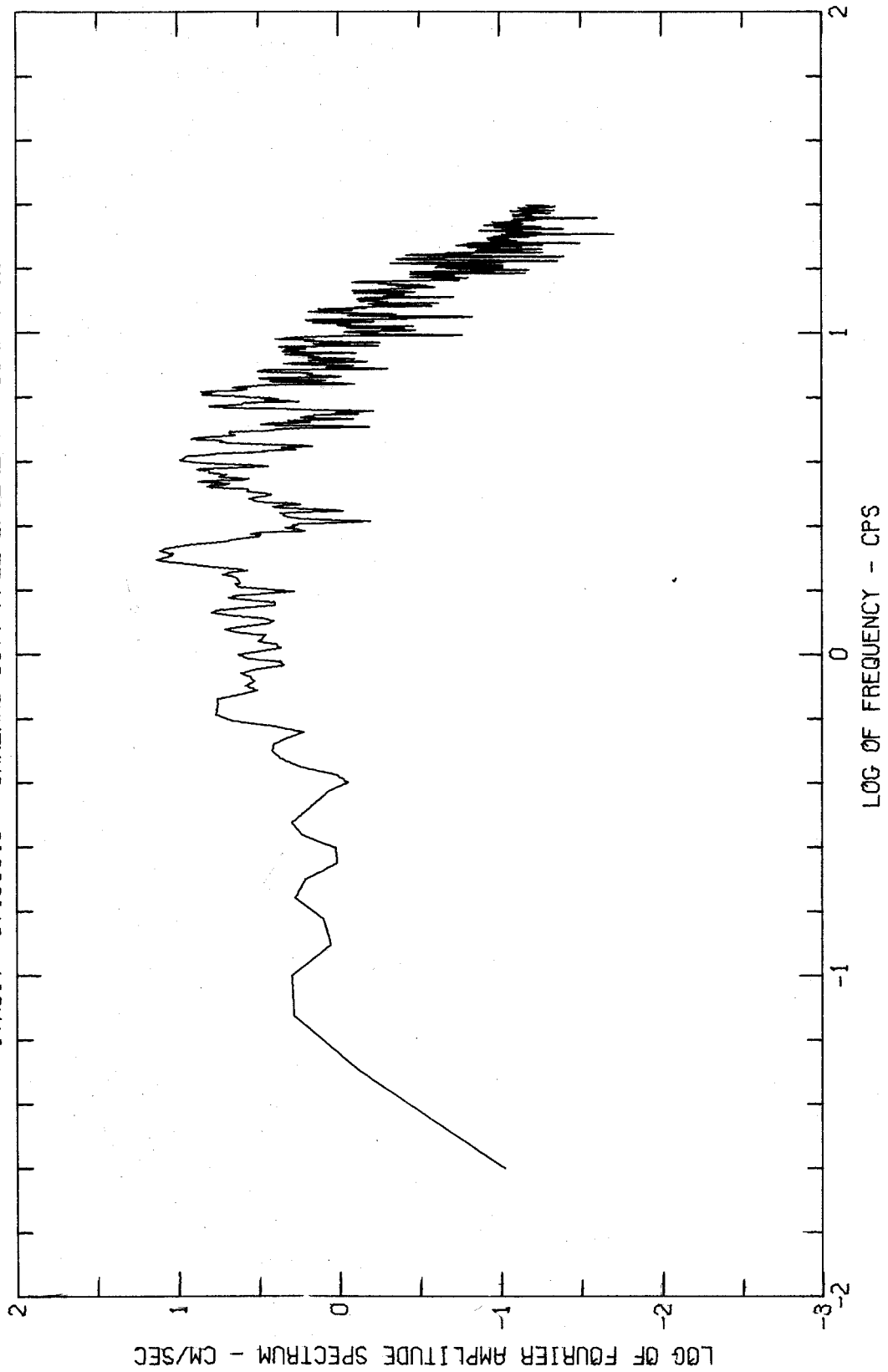
FOURIER AMPLITUDE SPECTRUM OF ACCELERATION
SAN FRANCISCO EARTHQUAKE MAR 22, 1957 - 1144 PST
IWA017 57.010.0 OAKLAND CITY HALL BASEMENT COMP N26E



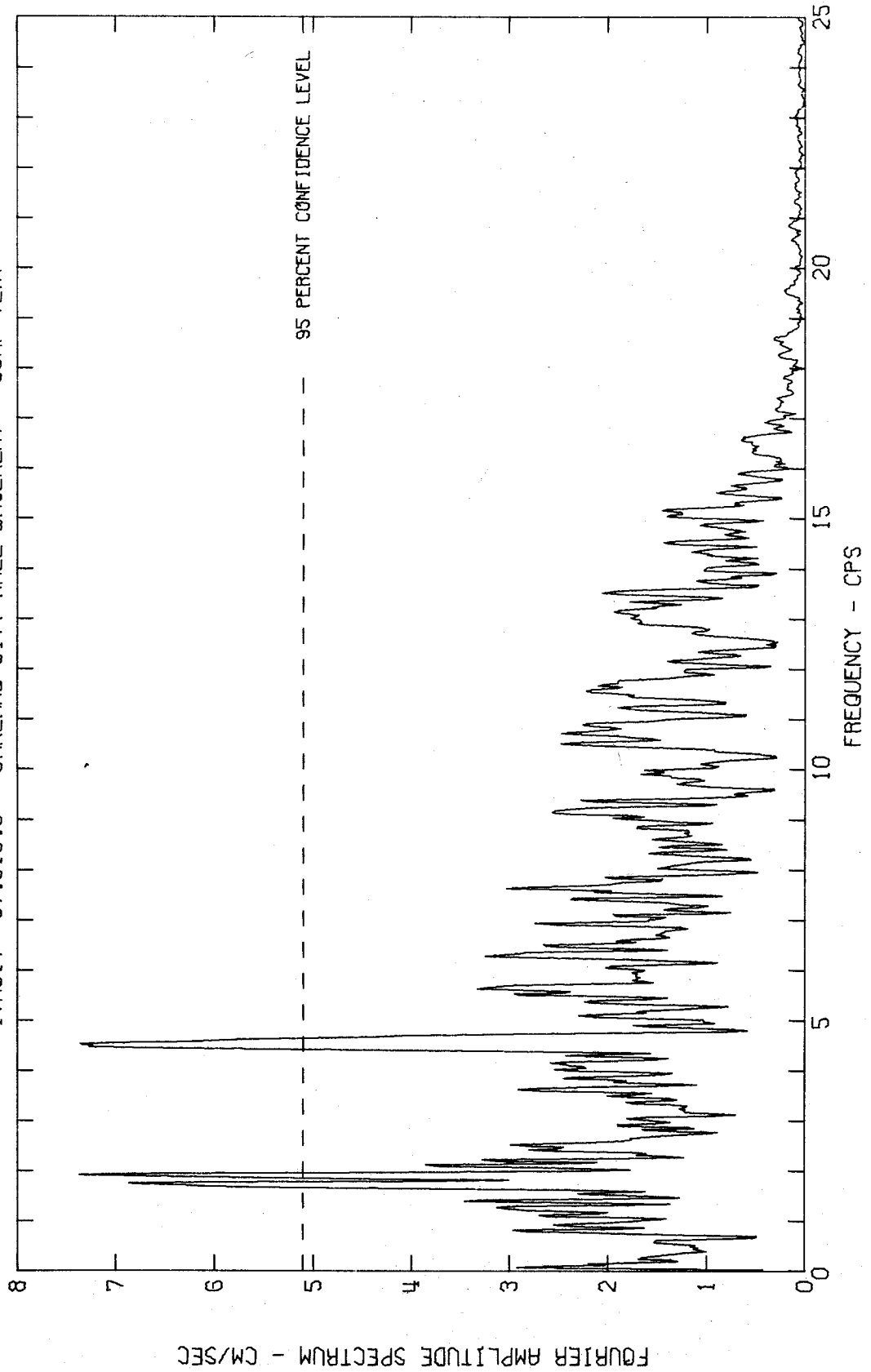
FOURIER AMPLITUDE SPECTRUM OF ACCELERATION
SAN FRANCISCO EARTHQUAKE MAR 22, 1957 - 1144 PST
IWA017 57.010.0 OAKLAND CITY HALL BASEMENT COMP S64E



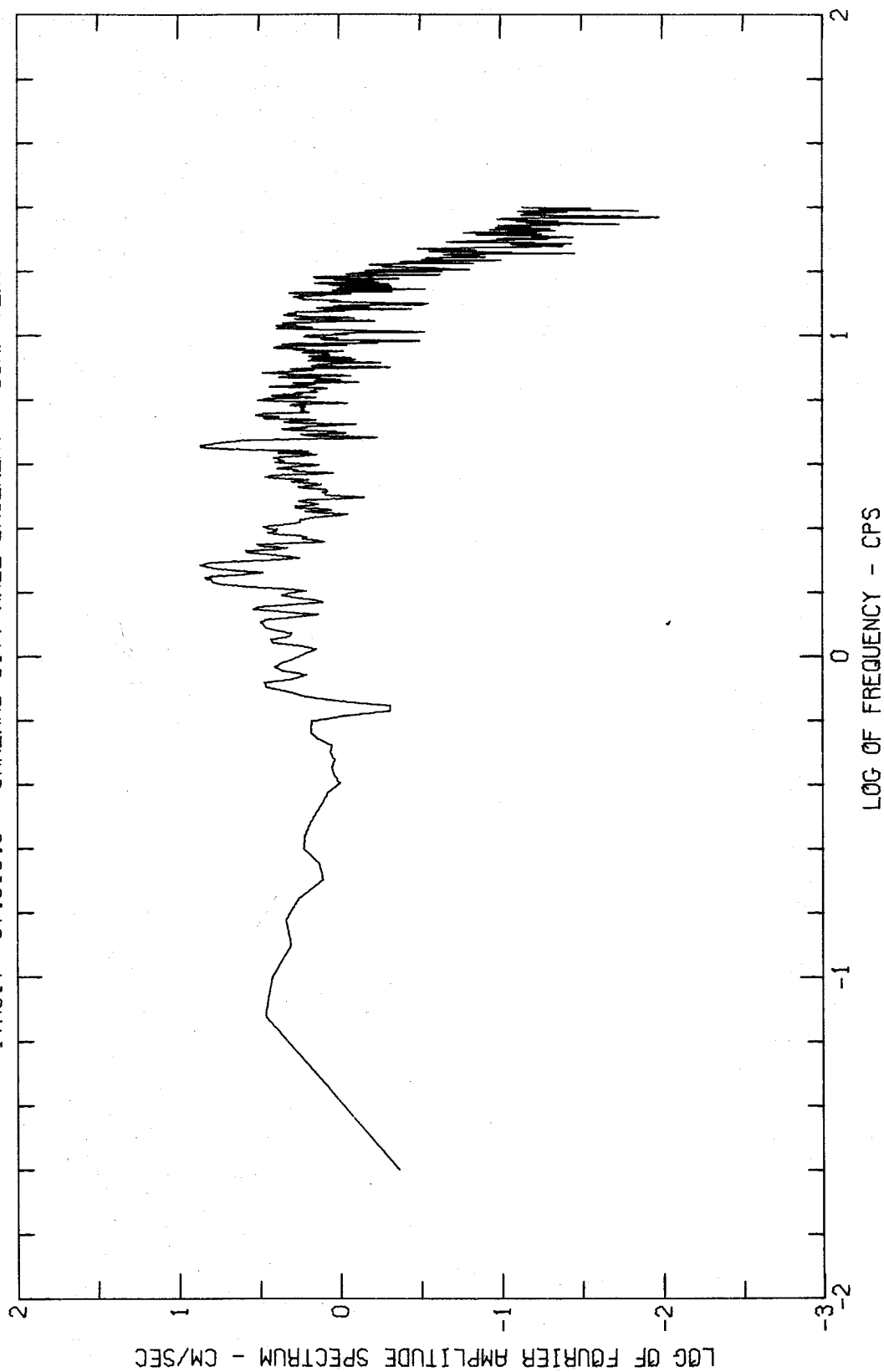
FOURIER AMPLITUDE SPECTRUM OF ACCELERATION
SAN FRANCISCO EARTHQUAKE MAR 22, 1957 - 1144 PST
IVA017 57.010.0 OAKLAND CITY HALL BASEMENT COMP SG4E



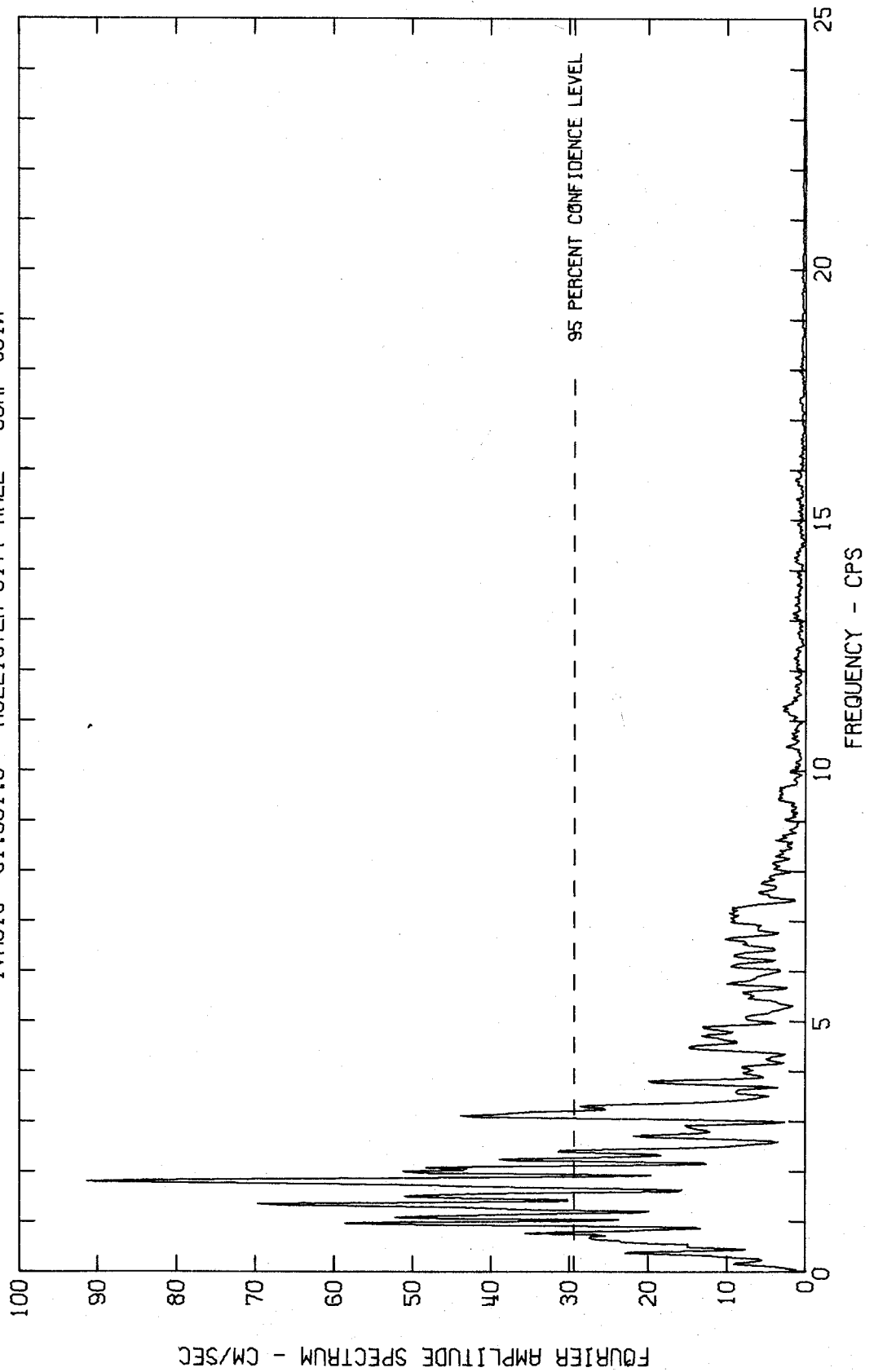
FOURIER AMPLITUDE SPECTRUM OF ACCELERATION
SAN FRANCISCO EARTHQUAKE MAR 22, 1957 - 1144 PST
IWA017 57.010.0 OAKLAND CITY HALL BASEMENT COMP VERT



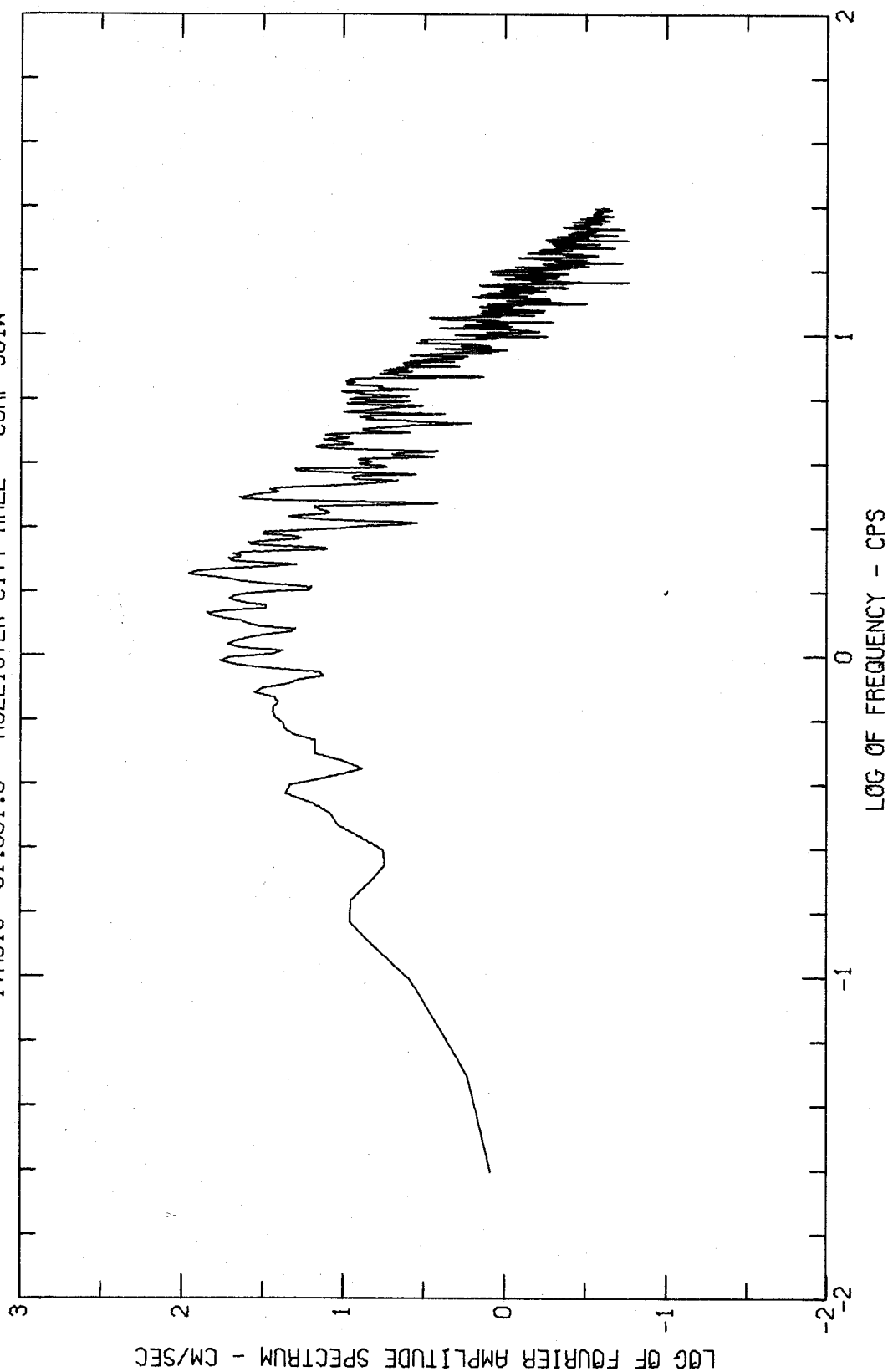
FOURIER AMPLITUDE SPECTRUM OF ACCELERATION
SAN FRANCISCO EARTHQUAKE MAR 22, 1957 - 1144 PST
IWA017 57.010.0 OAKLAND CITY HALL BASEMENT COMP VERT



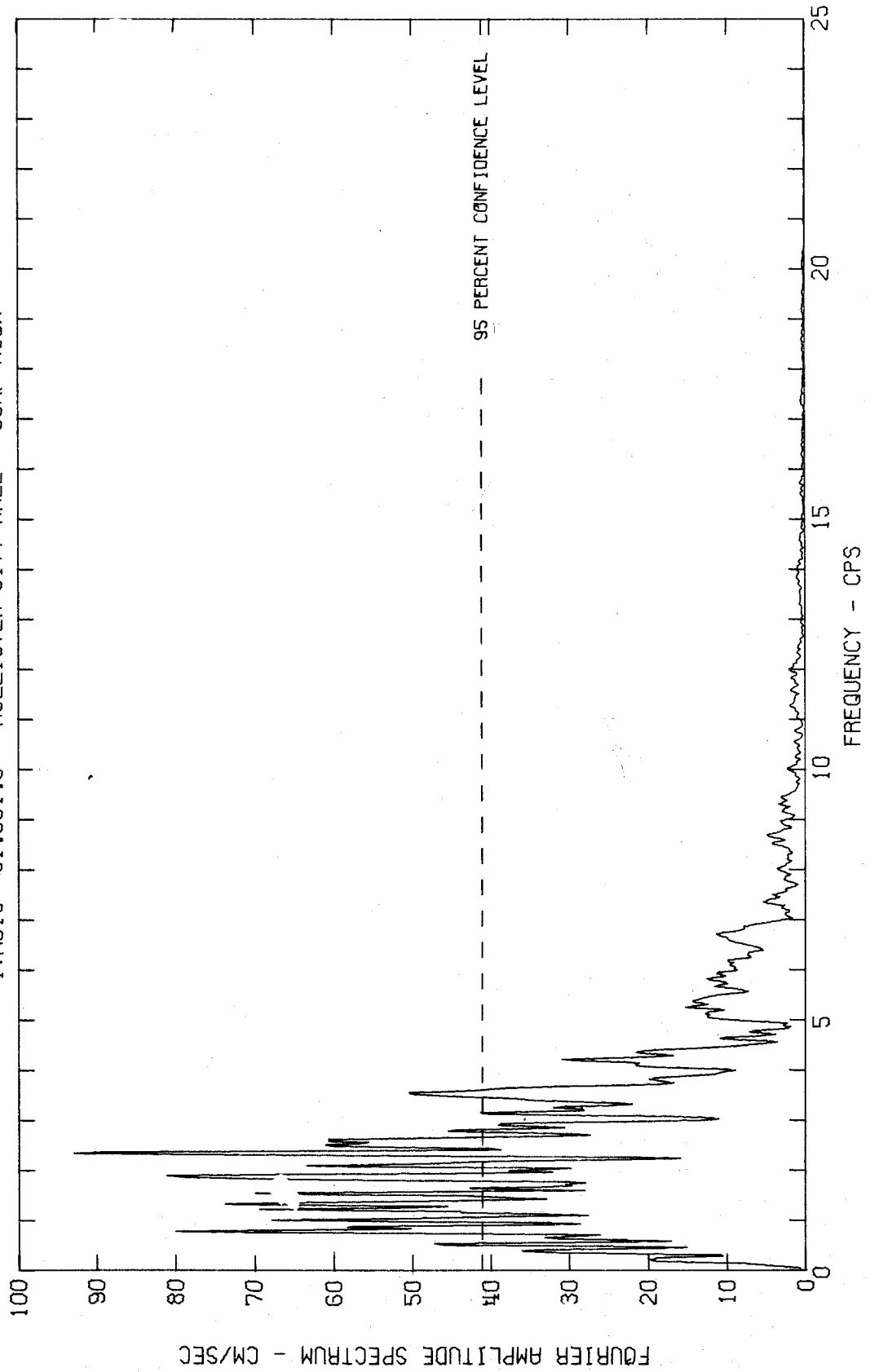
FOURIER AMPLITUDE SPECTRUM OF ACCELERATION
HOLLISTER EARTHQUAKE APR 8, 1961 - 2323 PST
IVAO18 61.001.0 HOLLISTER CITY HALL COMP S01W



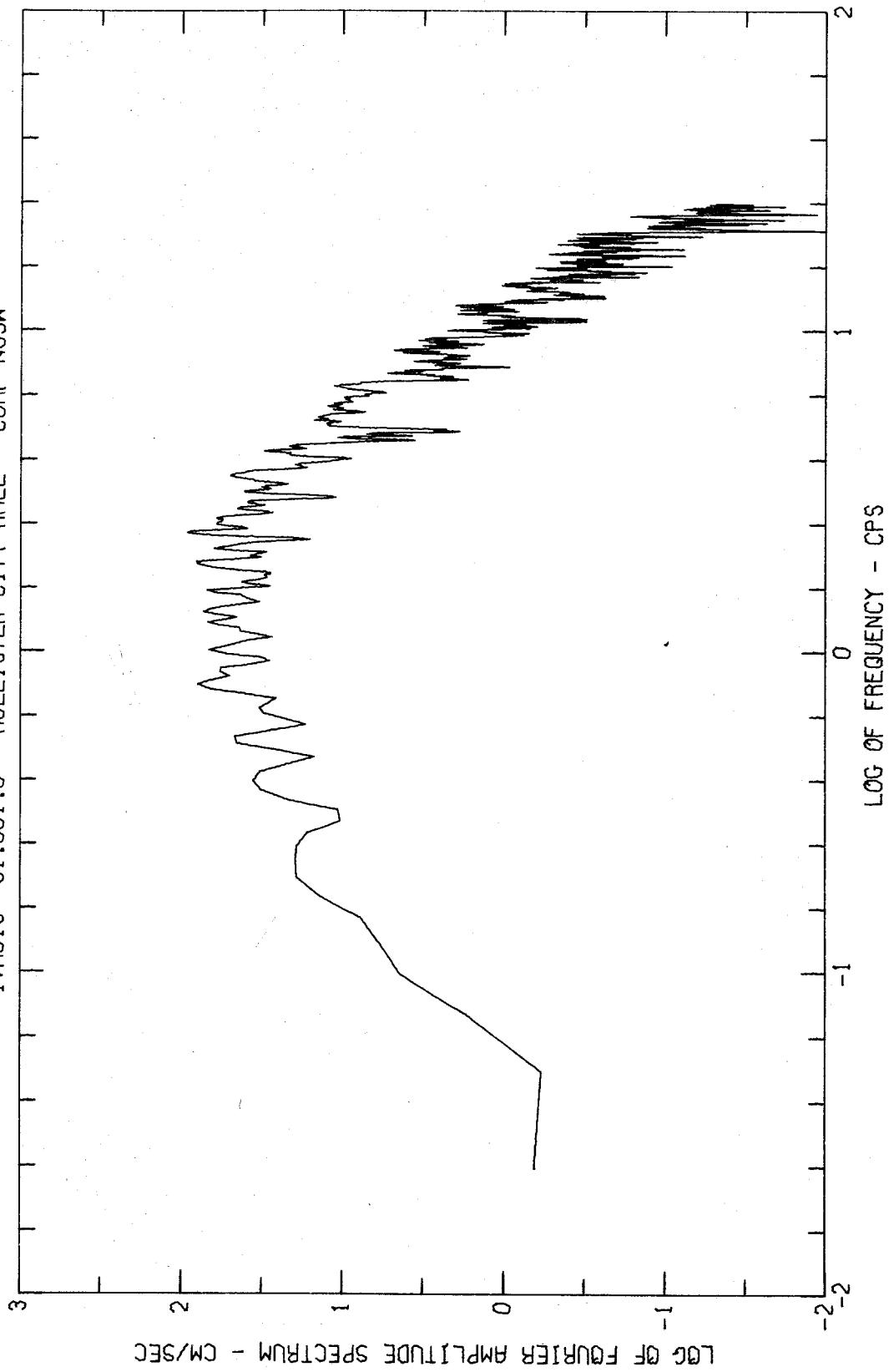
FOURIER AMPLITUDE SPECTRUM OF ACCELERATION
HOLLISTER EARTHQUAKE APR 8, 1961 - 2323 PST
IVAD18 61.001.0 HOLLISTER CITY HALL COMP S01W



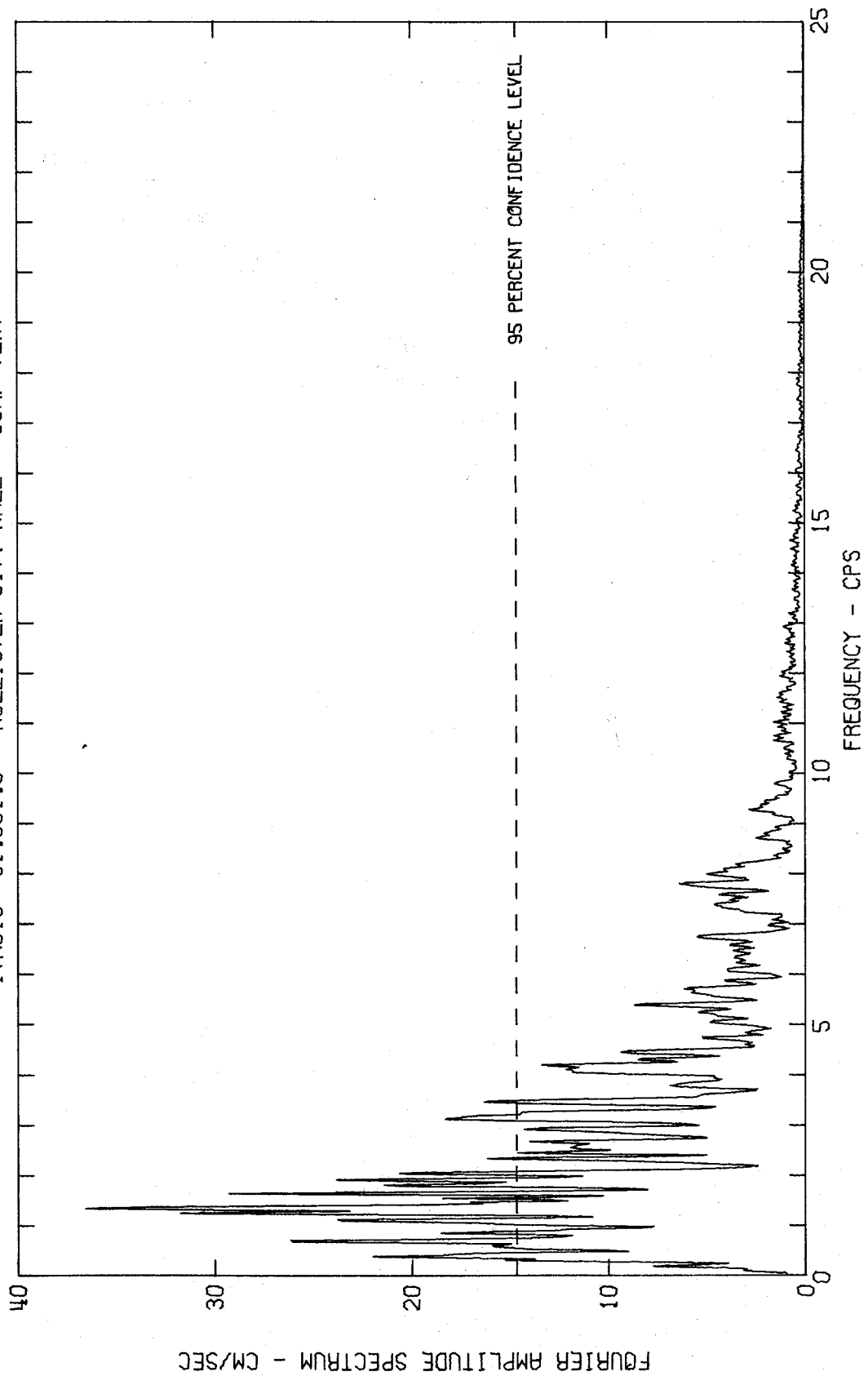
FOURIER AMPLITUDE SPECTRUM OF ACCELERATION
HOLLISTER EARTHQUAKE APR 8, 1961 - 2323 PST
IWA018 61.001.0 HOLLISTER CITY HALL COMP N89W



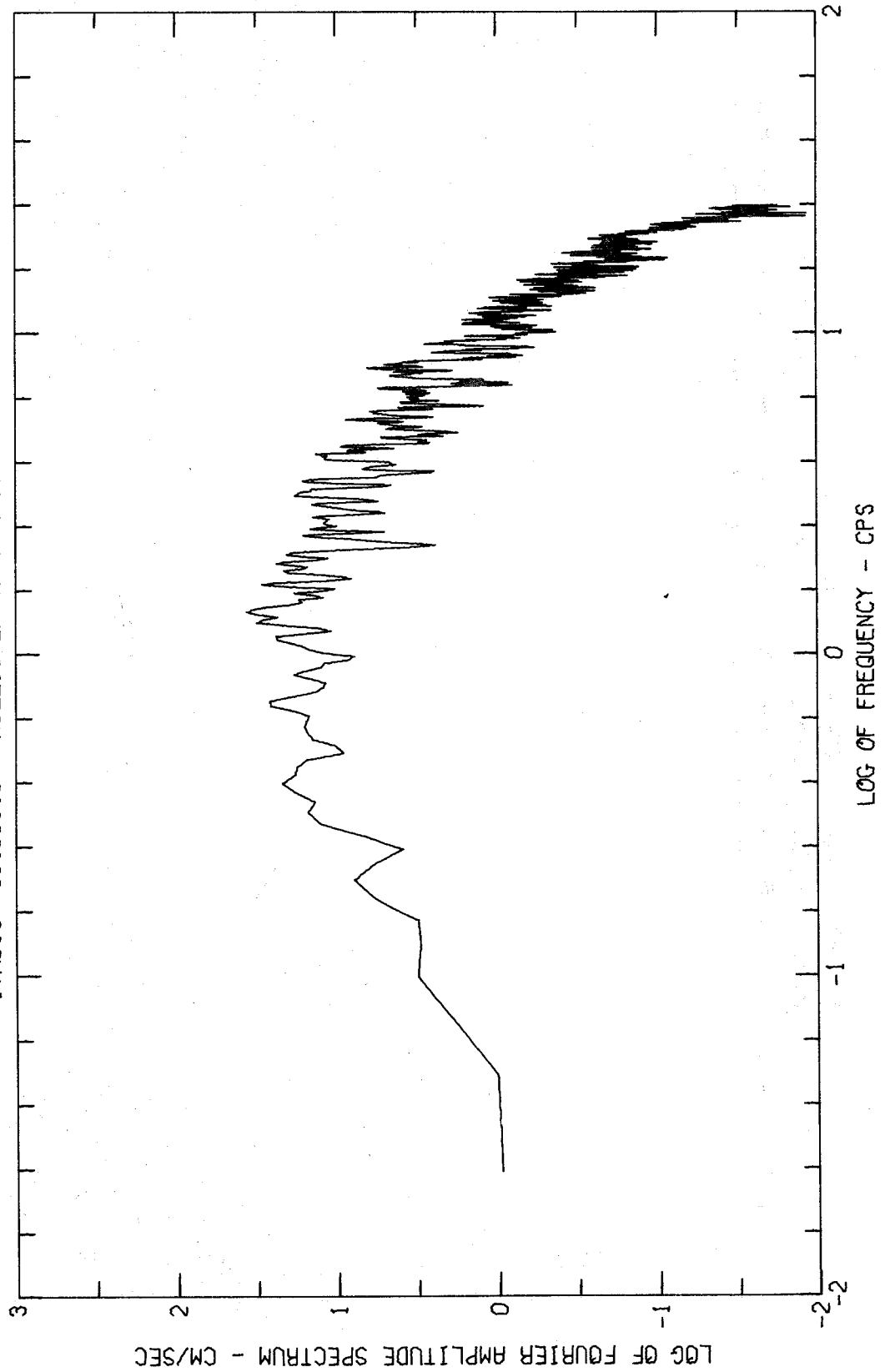
FOURIER AMPLITUDE SPECTRUM OF ACCELERATION
HOLLISTER EARTHQUAKE APR 8, 1961 - 2323 PST
IVA018 61.001.0 HOLLISTER CITY HALL COMP N89W

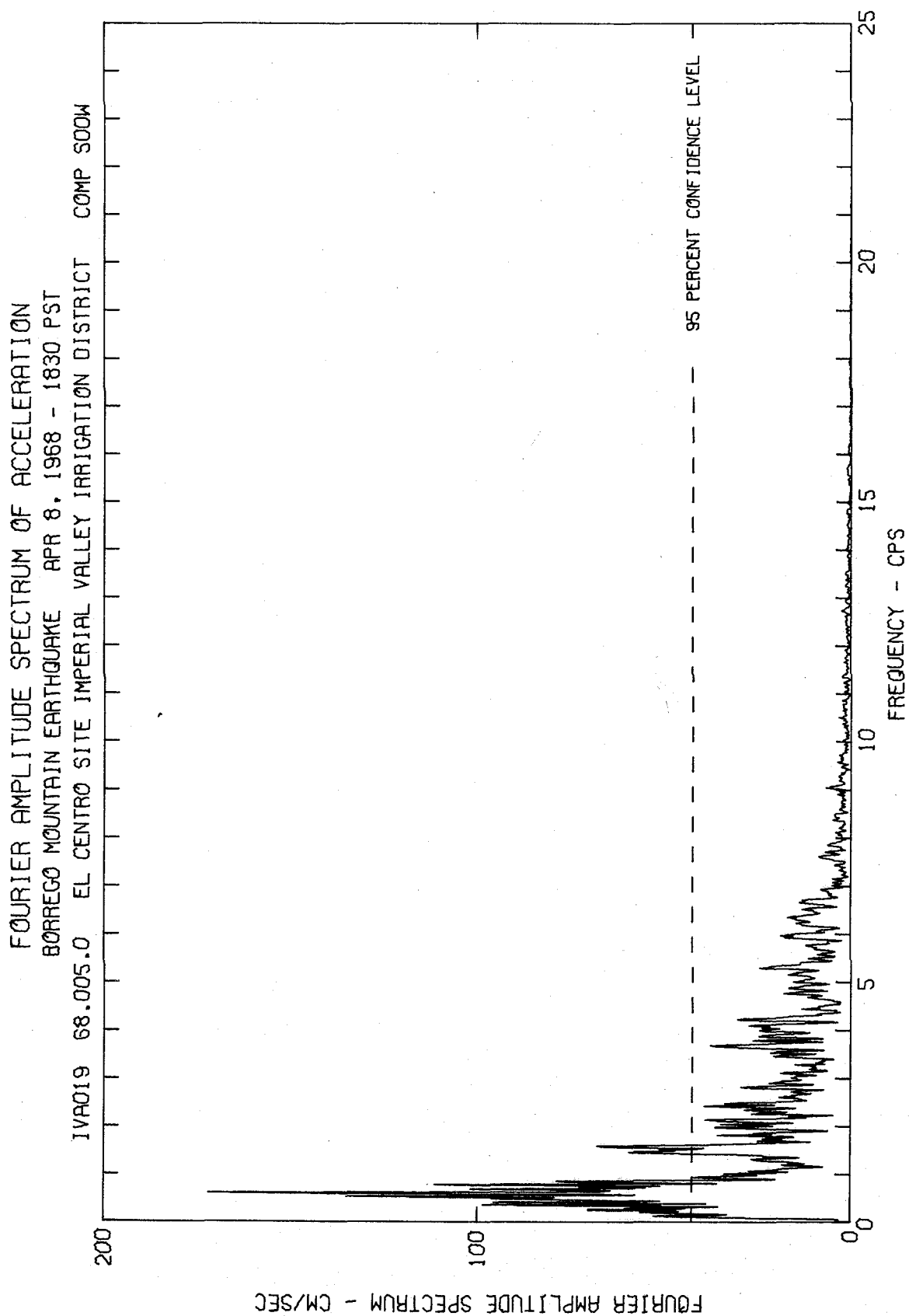


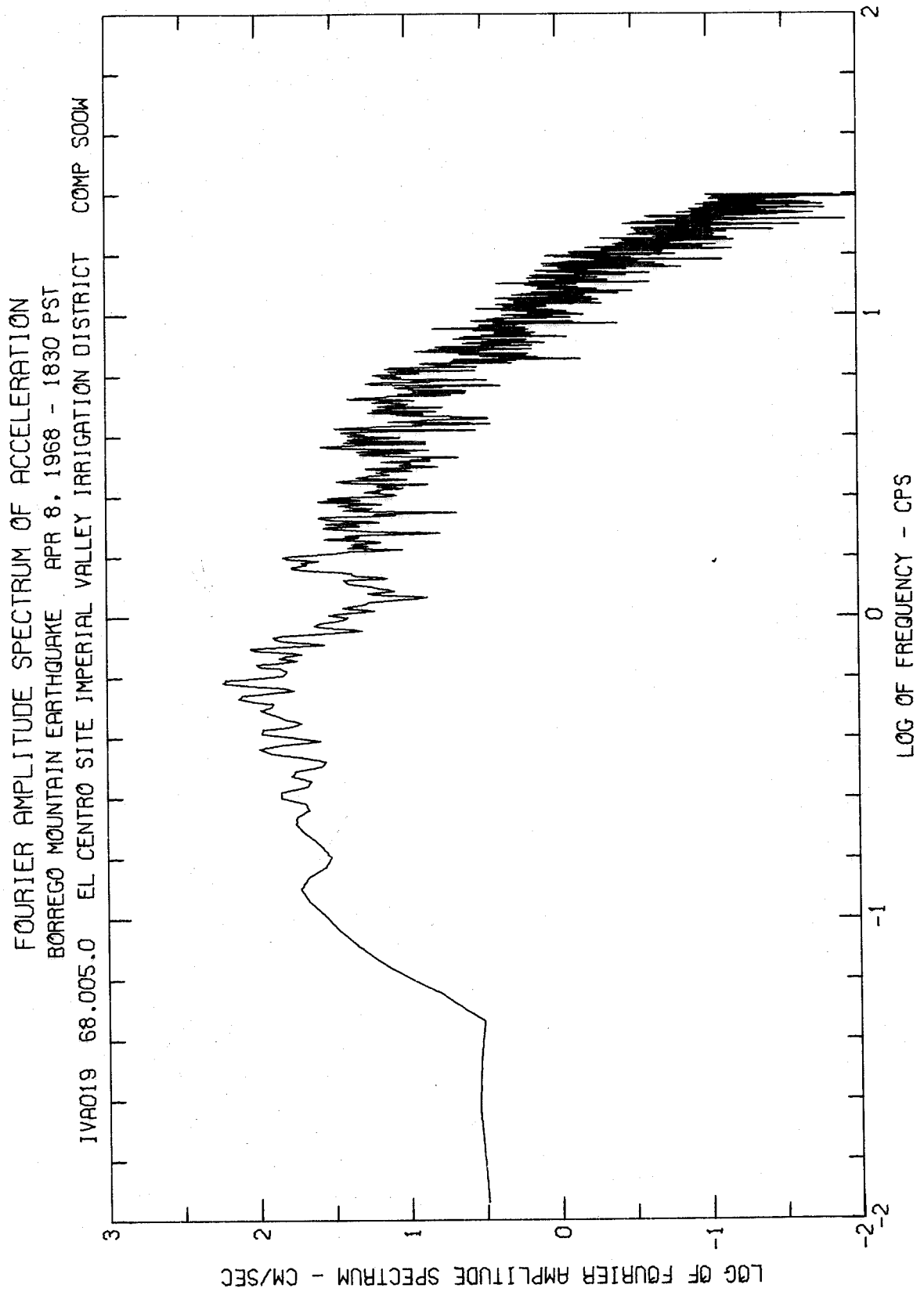
FOURIER AMPLITUDE SPECTRUM OF ACCELERATION
HOLLISTER EARTHQUAKE APR 8, 1961 - 2323 PST
IWA018 61.001.0 HOLLISTER CITY HALL COMP VERT

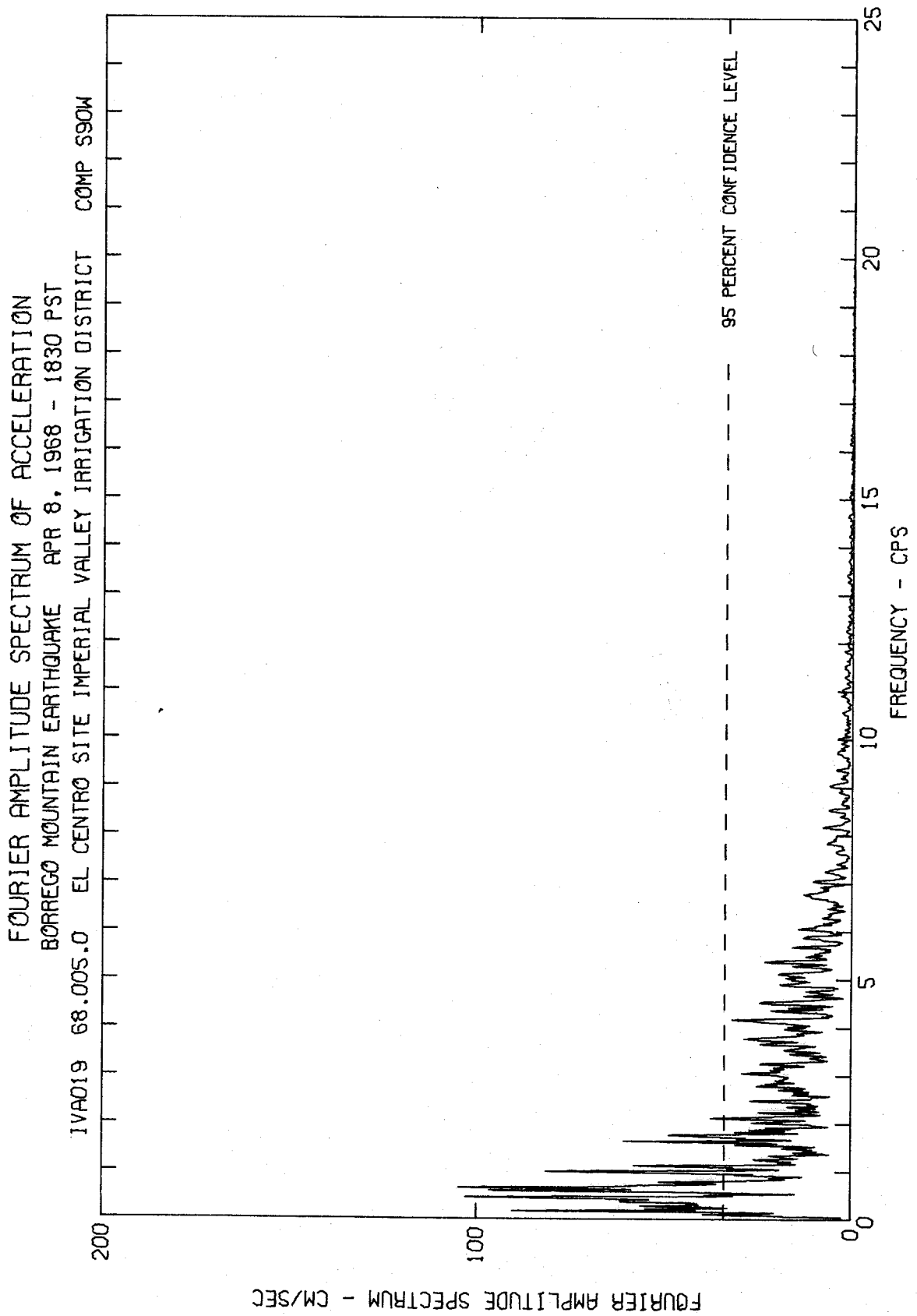


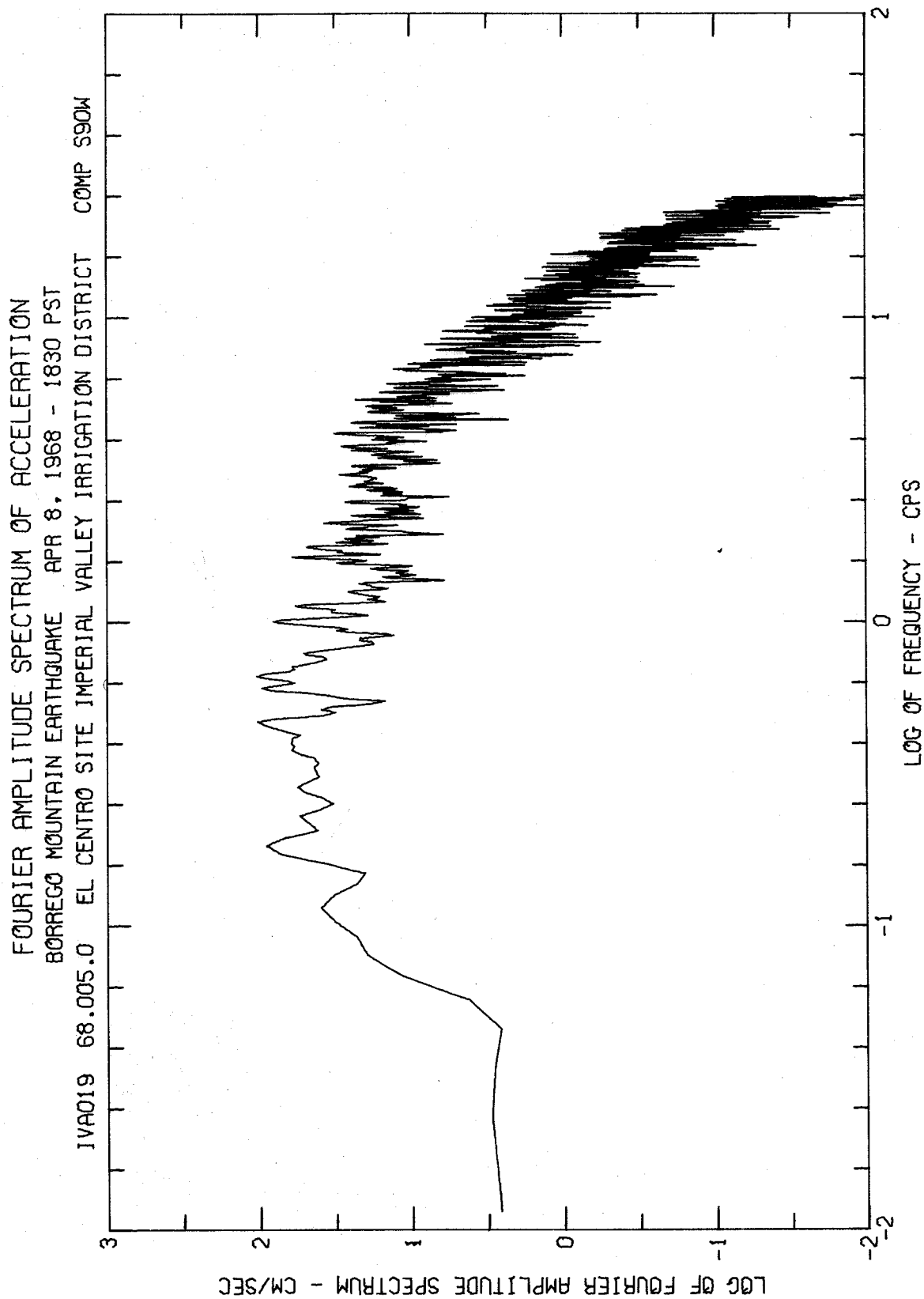
FOURIER AMPLITUDE SPECTRUM OF ACCELERATION
HOLLISTER EARTHQUAKE APR 8, 1961 - 2323 PST
IVAO18 61.001.0 HOLLISTER CITY HALL COMP VERT

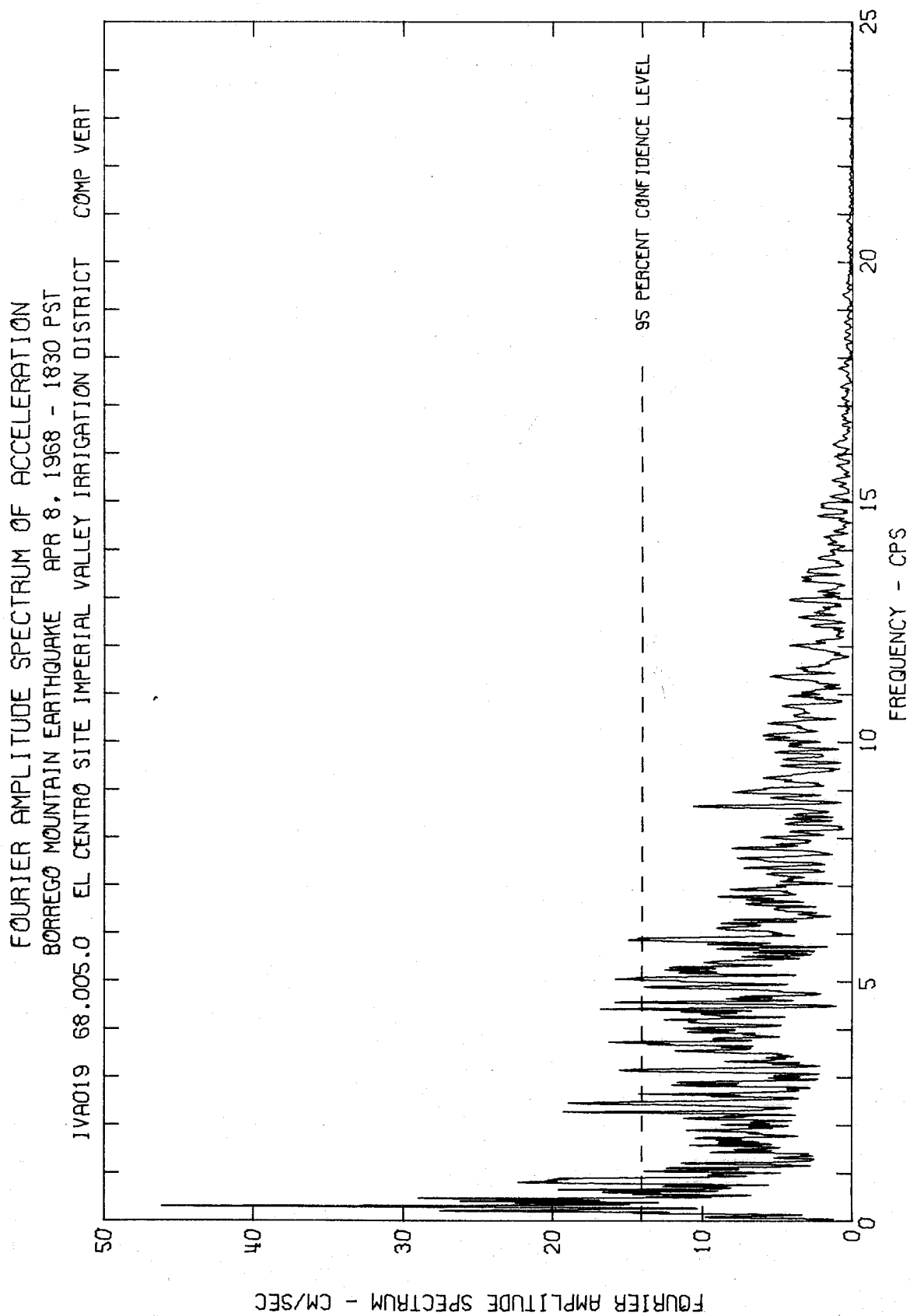


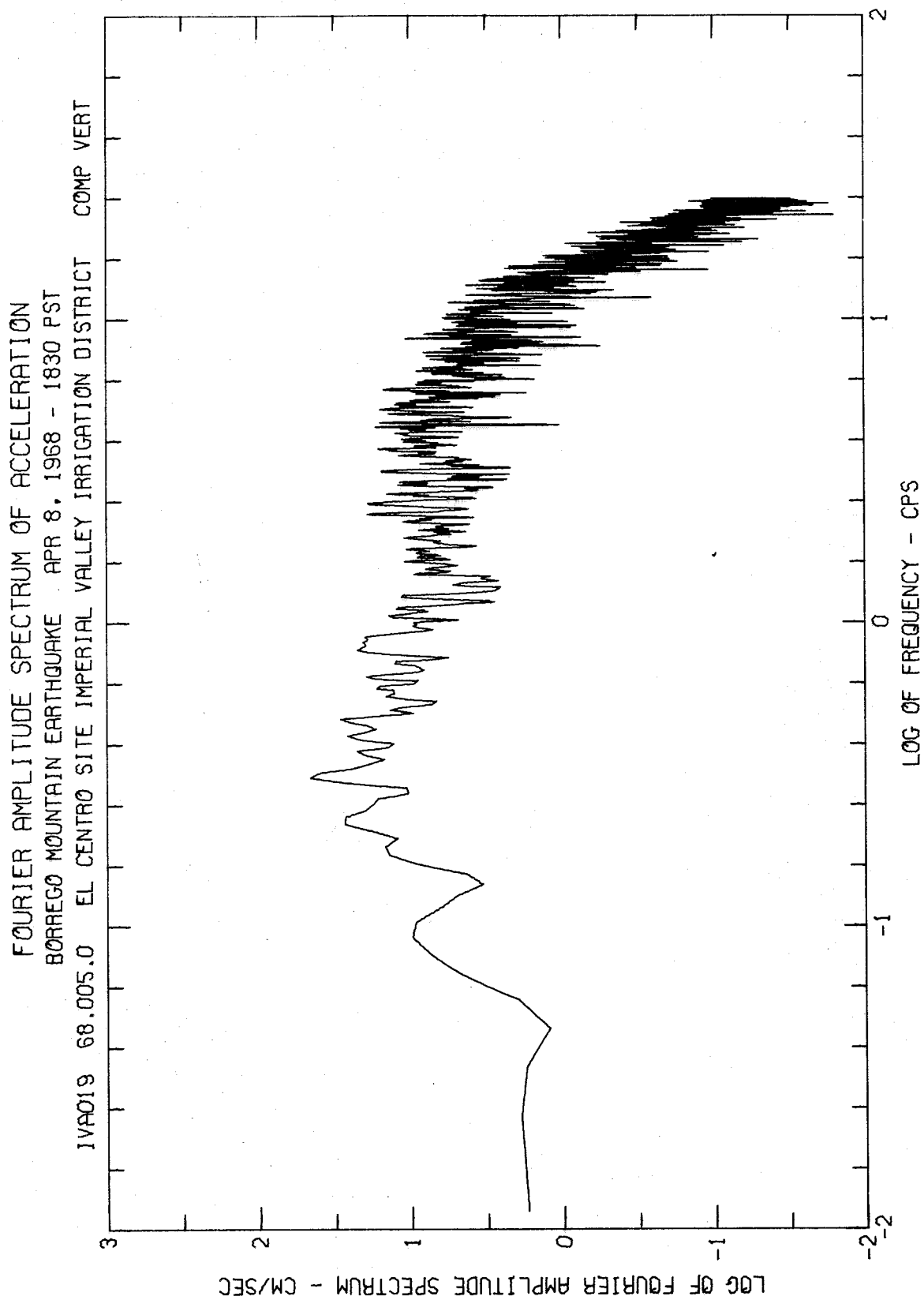




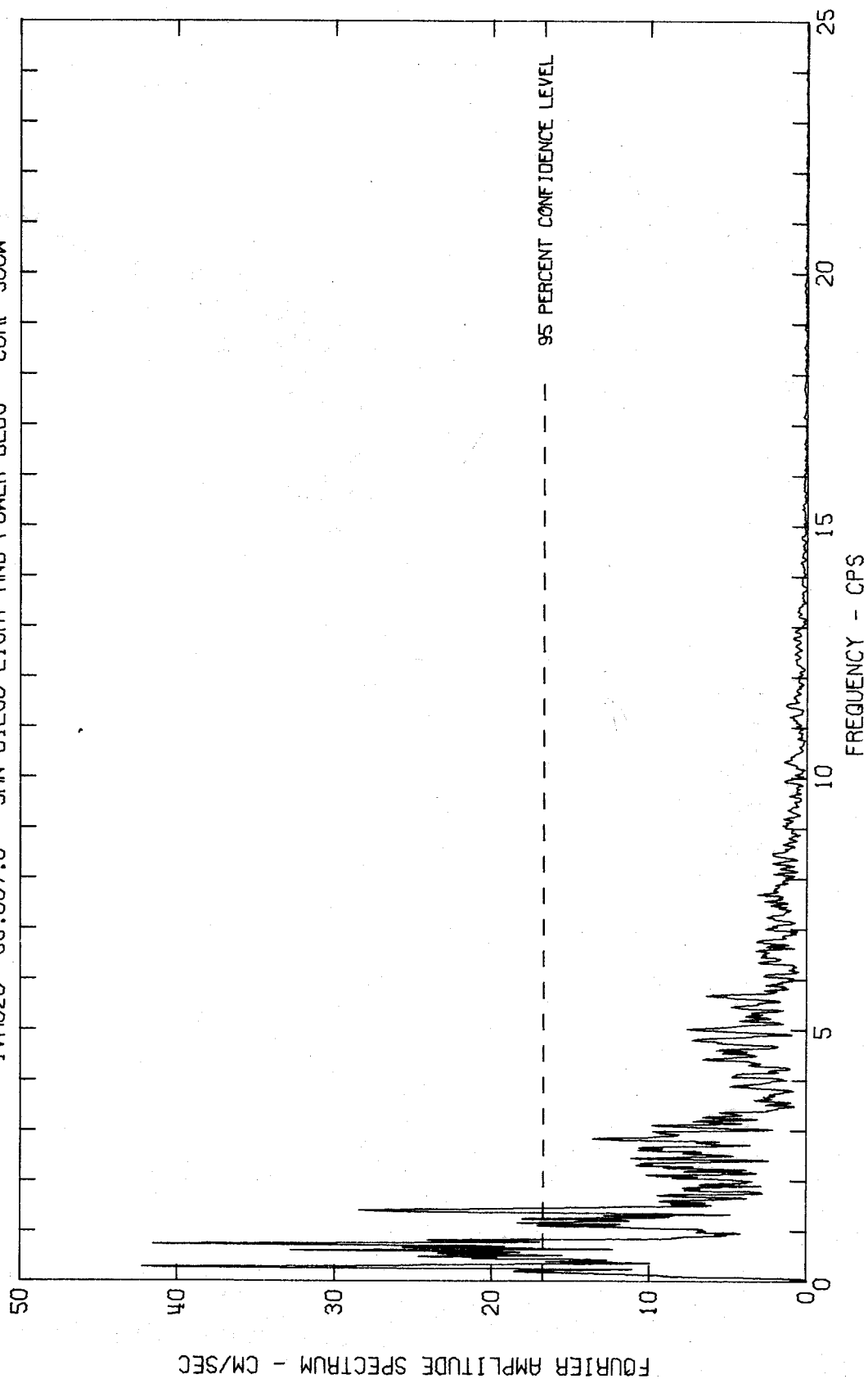




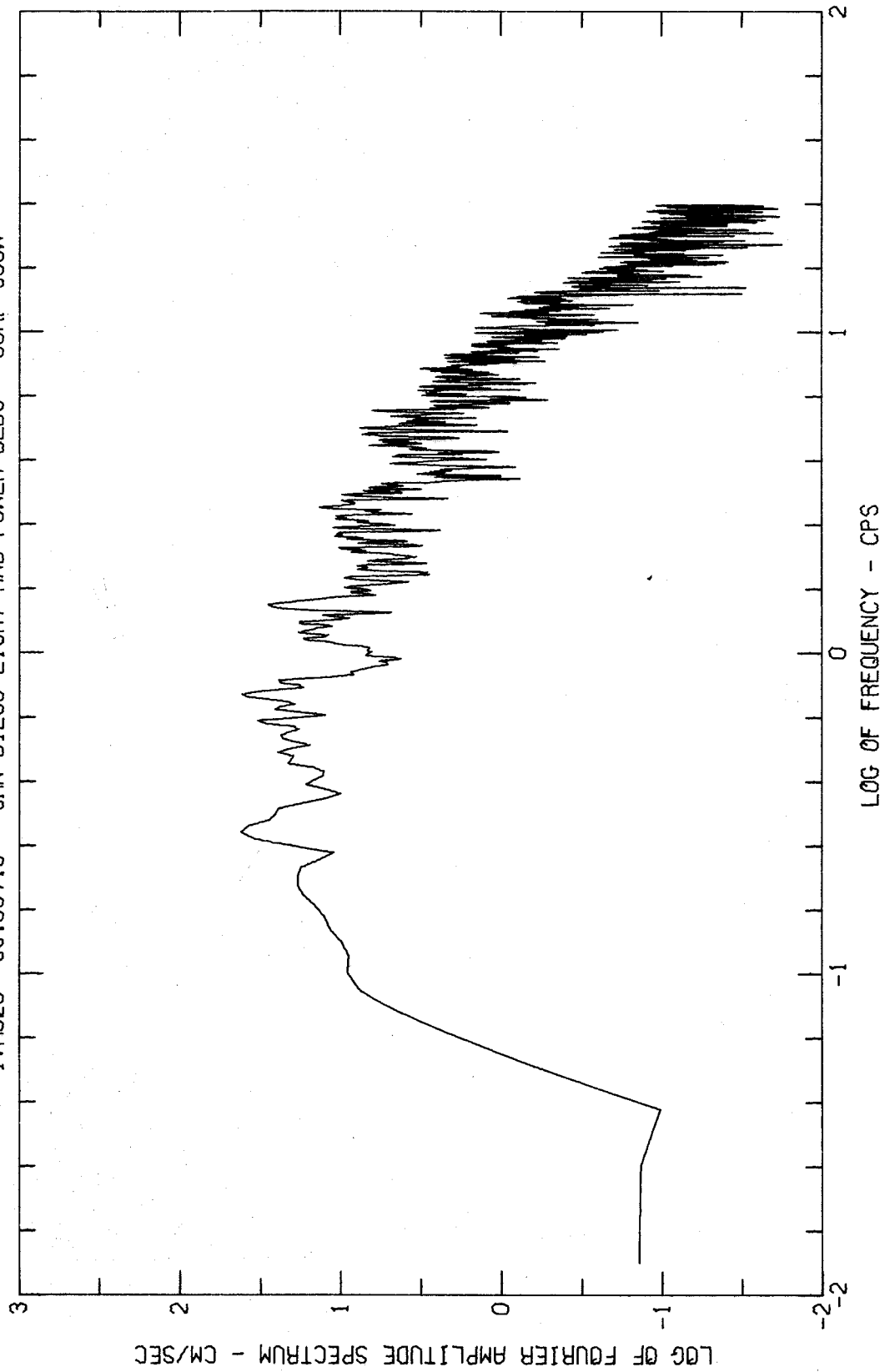




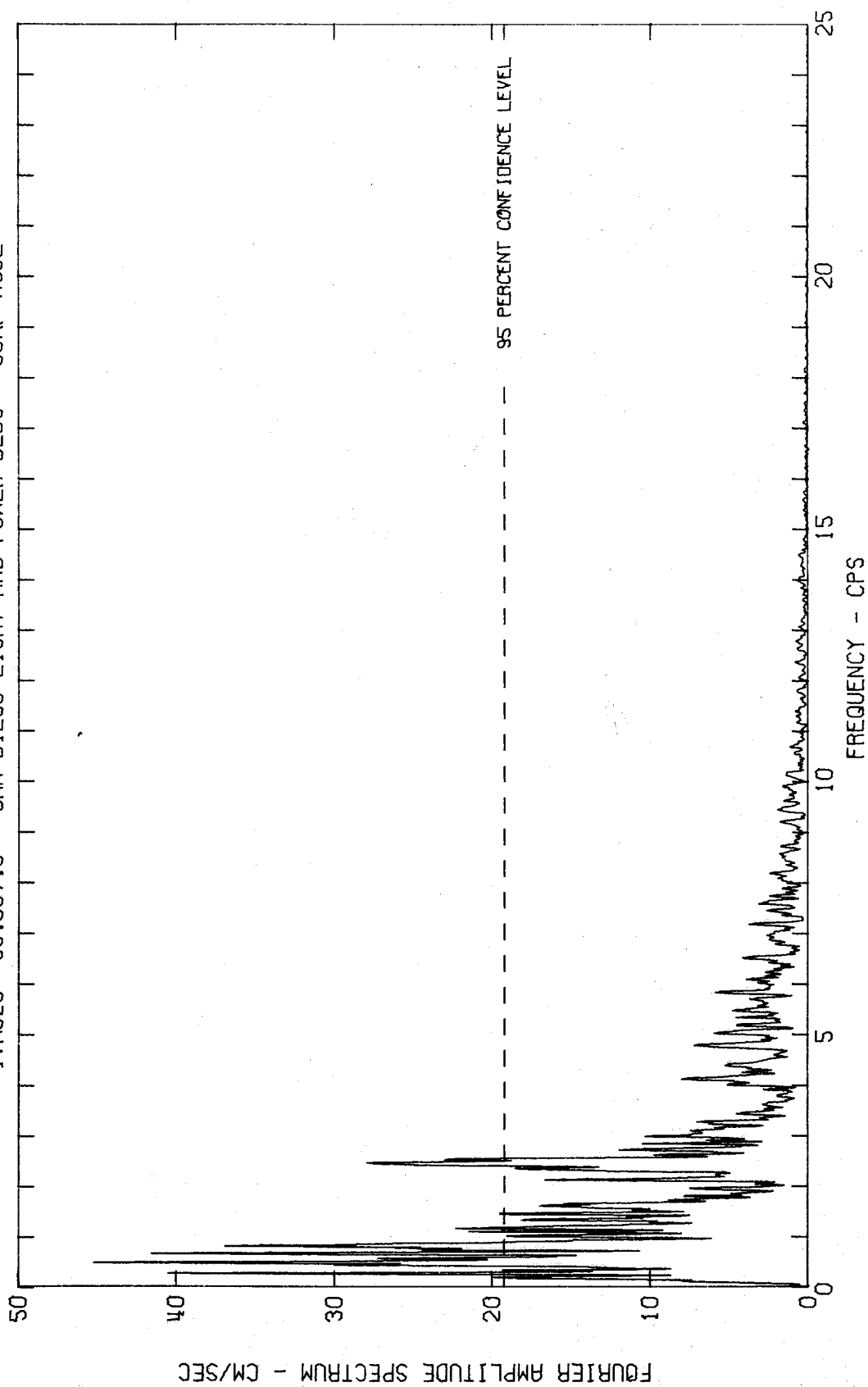
FOURIER AMPLITUDE SPECTRUM OF ACCELERATION
BORREGO MOUNTAIN EARTHQUAKE APR 8, 1968 - 1830 PST
1VA020 68.007.0 SAN DIEGO LIGHT AND POWER BLDG COMP 500W



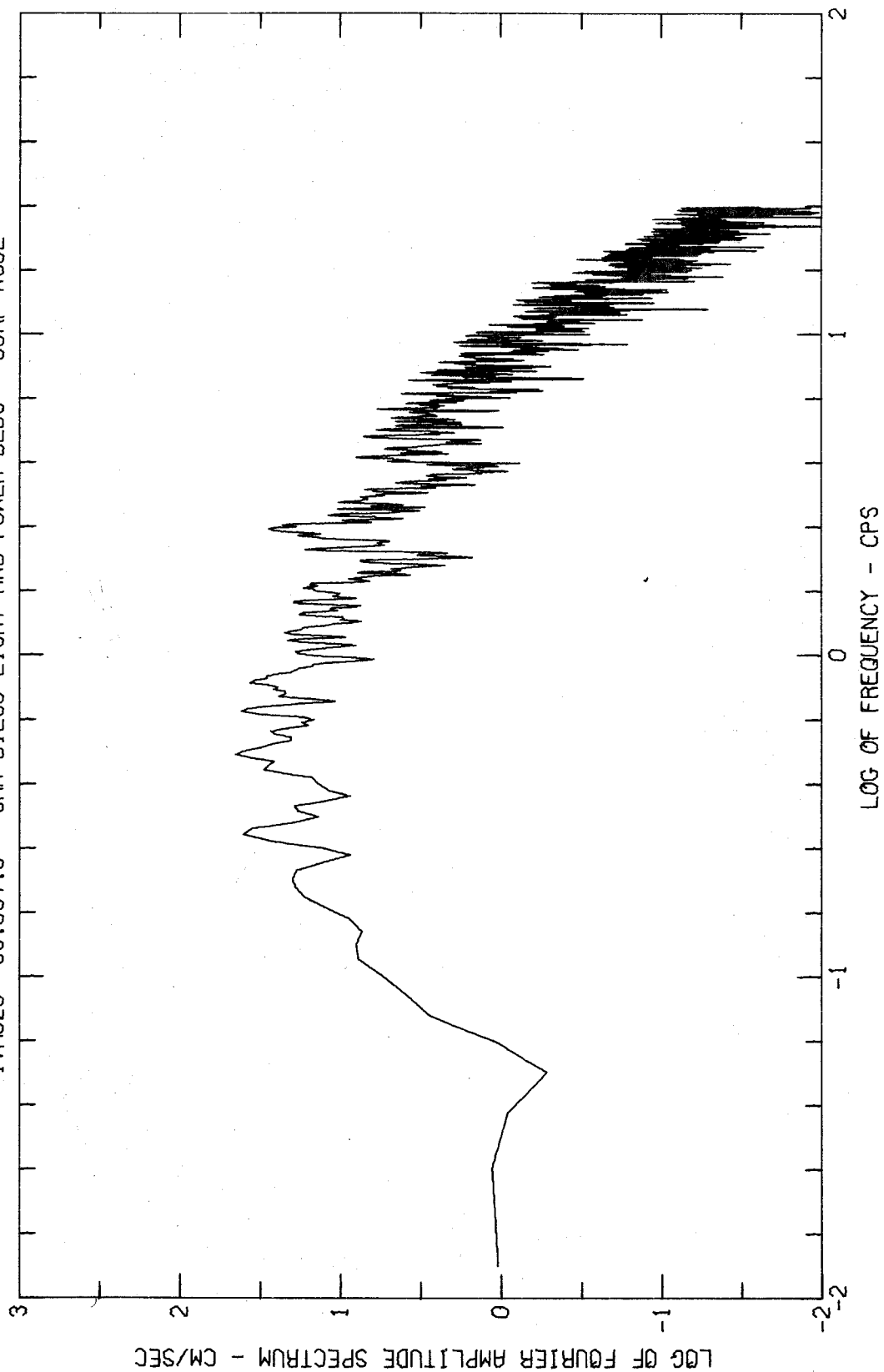
FOURIER AMPLITUDE SPECTRUM OF ACCELERATION
BORREGO MOUNTAIN EARTHQUAKE APR 8, 1968 - 1830 PST
1VA020 68.007.0 SAN DIEGO LIGHT AND POWER BLDG COMP S00W



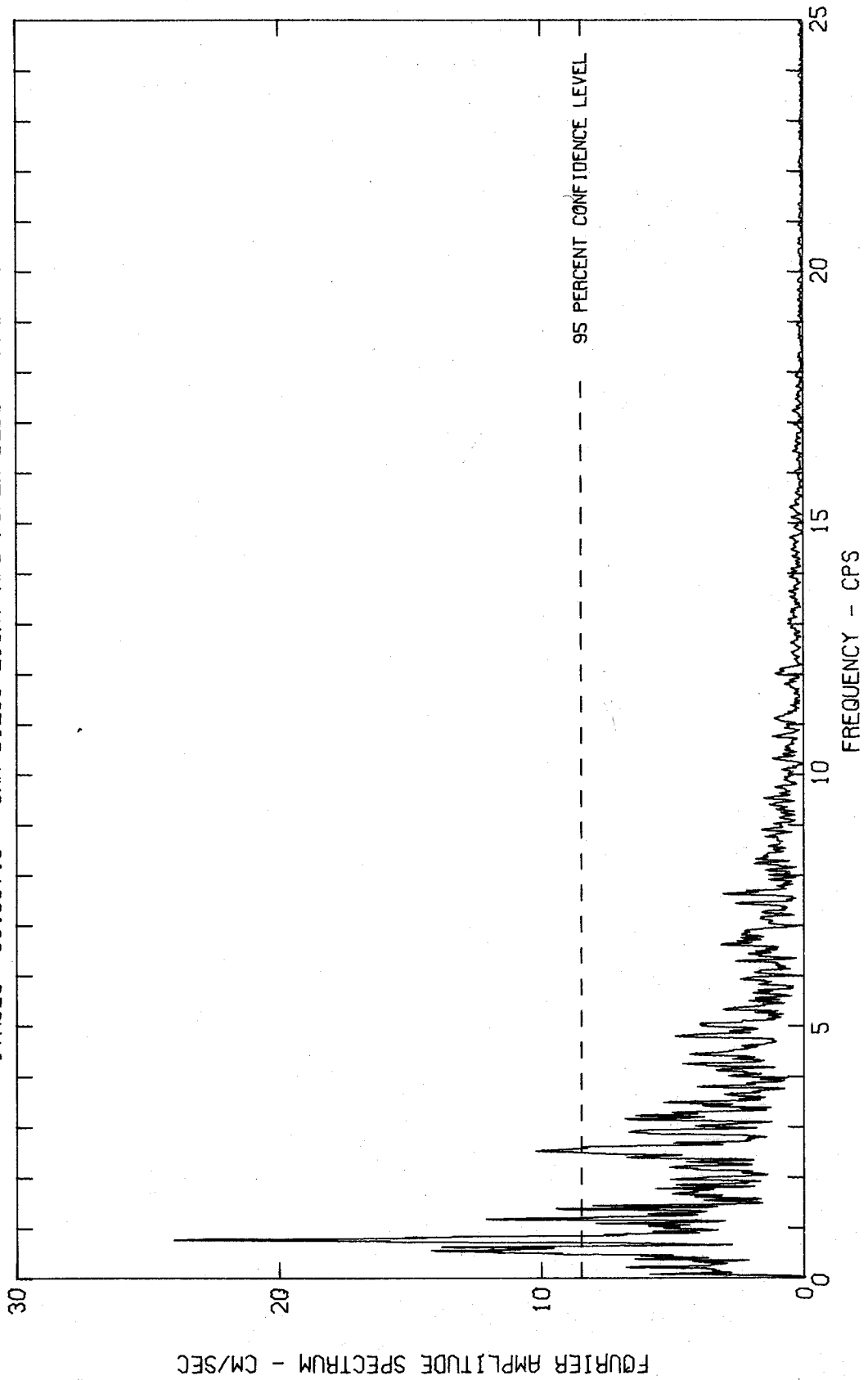
FOURIER AMPLITUDE SPECTRUM OF ACCELERATION
BORREGO MOUNTAIN EARTHQUAKE APR 8, 1968 - 1830 PST
JVA020 68.007.0 SAN DIEGO LIGHT AND POWER BLDG COMP N90E



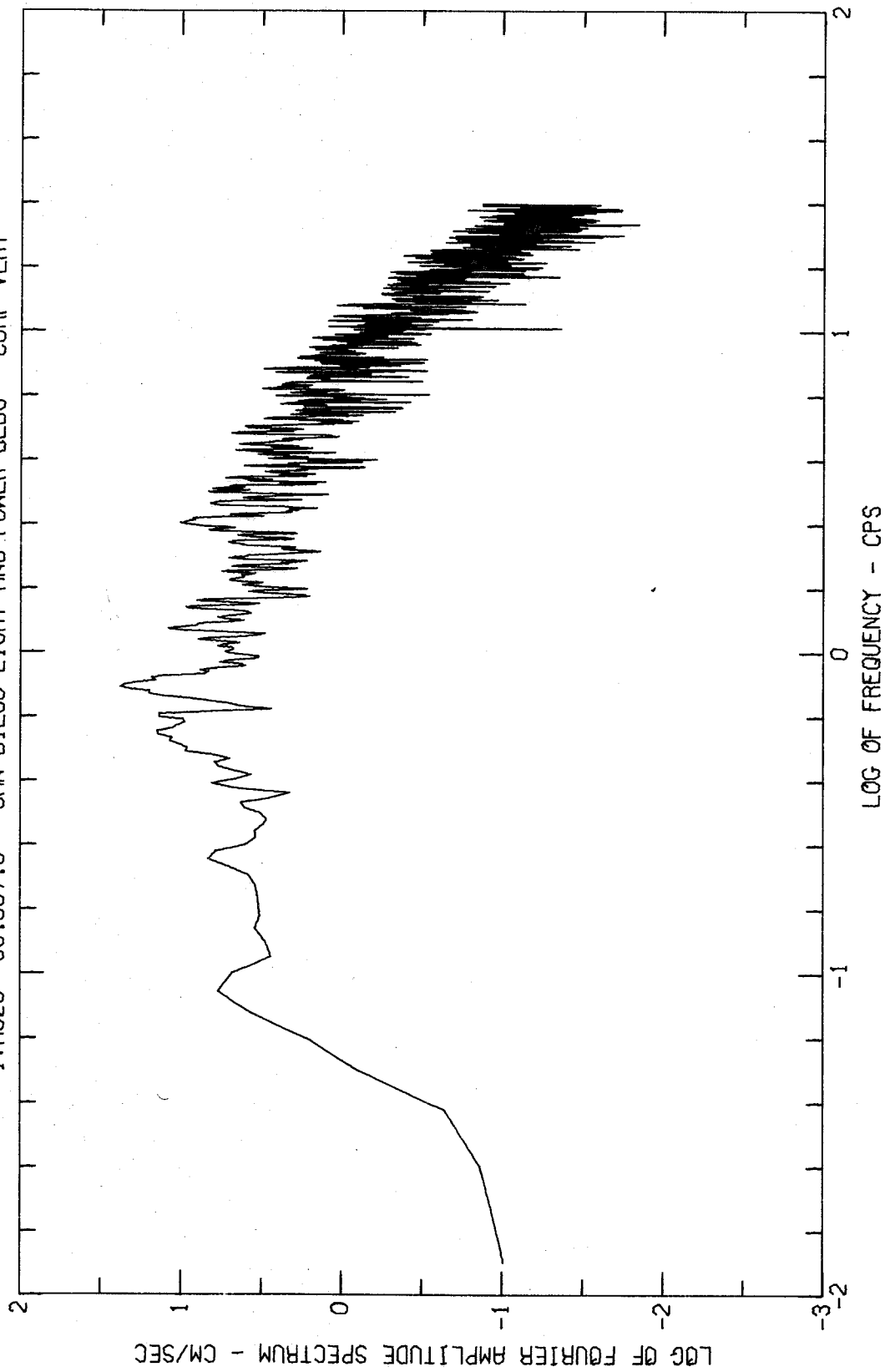
FOURIER AMPLITUDE SPECTRUM OF ACCELERATION
BORREGO MOUNTAIN EARTHQUAKE APR 8, 1968 - 1830 PST
IWA020 68.007.0 SAN DIEGO LIGHT AND POWER BLDG COMP N90E



FOURIER AMPLITUDE SPECTRUM OF ACCELERATION
BORREGO MOUNTAIN EARTHQUAKE APR 8, 1968 - 1830 PST
IWA020 68.007.0 SAN DIEGO LIGHT AND POWER BLDG COMP VERT



FOURIER AMPLITUDE SPECTRUM OF ACCELERATION
BORREGO MOUNTAIN EARTHQUAKE APR 8, 1968 - 1830 PST
IVA020 68.007.0 SAN DIEGO LIGHT AND POWER BLDG COMP VERT



California Institute of Technology
Earthquake Engineering Research Laboratory

The following reports of the Earthquake Engineering Research Laboratory from 1970 on can be obtained from the National Technical Information Service, Springfield, Virginia 22151:

EERL 70-20	Strong-Motion Earthquake Accelerograms - Digitized and Plotted Data (Vol. I, Part A)	PB-187 847
EERL 70-21	" " (Vol. I, Part B)	PB-196 823
EERL 71-20	" " (Vol. I, Part C)	PB-204 364
EERL 71-21	" " (Vol. I, Part D)	PB-208 529
EERL 71-22	" " (Vol. I, Part E)	PB-209 749
EERL 71-23	" " (Vol. I, Part F)	PB-210 619
EERL 71-50	Strong-Motion Earthquake Accelerograms - Digitized and Plotted Data: Corrected Accelerograms and Integrated Ground Velocity and Displacement Curves (Vol. II, Part A)	PB-208 283
Joint Report:	Strong-Motion Instrumental Data on the San Fernando Earthquake of February 9, 1971	PB-204 198
EERL 71-01	P. C. Jennings <u>et al</u> , Forced Vibration of a 22-Story Steel Frame Building	PB-205 161
EERL 71-02	P. C. Jennings, ed., Engineering Features of the San Fernando Earthquake	PB-202 550
EERL 71-03	Randolph A. Adu, Response and Failure of Structures under Stationary Random Excitation	PB-205 304
EERL 71-04	Jacobo Bielak, Earthquake Response of Building-Foundation Systems	PB-205 305
EERL 71-05	M. D. Trifunac, F. E. Udawadia, A. G. Brady, High Frequency Errors and Instrument Corrections of Strong-Motion Accelerograms	PB-205 369
EERL 71-06	Knut Sverre Skattum, Dynamic Analysis of Coupled Shear Walls and Sandwich Beams	PB-205 267
EERL 71-07	John Brent Hoerner, Modal Coupling and Earthquake Response of Tall Buildings	PB-207 635
EERL 72-01	P. C. Jennings and J. Bielak, Dynamics of Building-Soil Interaction	PB-209 666